

# **Variations in magma composition in time and space along the Central Andes (13°S-28°S)**

**Dissertation**

zur Erlangung des Doktorgrades  
der Mathematisch-Naturwissenschaftlichen Fakultäten  
der Georg-August-Universität zu Göttingen

vorgelegt von

Mirian-Irene Mamani-Huisa  
aus Cuyocuyo (Peru)

Göttingen 2006

D 7

Referent: Prof. Dr. G. Wörner  
Koreferent: Prof. Dr. B.T. Hansen  
Tag der mündlichen Prüfung: 24. Oktober 2006

# Contents

Abstract.....	3
Zusammenfassung.....	5
Resumen.....	7
Acknowledgements.....	9
Preamble.....	10
1 Introduction.....	11
1.1 Variations in magma composition in time and space along the Central Andes (13°S-28°S): Facts and open questions.....	11
1.2 Working Hypothesis.....	11
1.3 Previous work.....	12
1.3.1 The Andes.....	12
1.3.2 Pre-Andean history.....	15
1.3.3 The Andean Cycle.....	17
1.3.4 Uplift of the Central Andes and subducting Nazca plate.....	18
1.3.5 Andean volcanism.....	20
1.3.6 Magma genesis.....	21
2 Geochemical variations in south Peruvian volcanic rocks (13°S-18°S): The role of crustal composition and thickening through time and space.....	25
2.1 Introduction.....	25
2.2 Tectonic Setting.....	26
2.3 Description of Cenozoic units and sampled volcanic centers.....	27
2.3.1 Middle Eocene - Lower Oligocene, ~ 45 to ~30 Ma (Lower Moquegua Formation, Anta Group).....	27
2.3.2 Upper Oligocene - Middle Miocene, ~30 to ~15 Ma (Upper Moquegua Formation, Tacaza Group).....	28
2.3.3 Upper Miocene – Lower Pliocene, ~10 to ~3 Ma (Lower Barroso Formation).....	29
2.3.4 Pliocene, ~3 to ~2 Ma (Sencca Formation).....	29
2.3.5 Upper Pliocene to Pleistocene, 3 to 0.8 Ma (Upper Barroso Formation).....	29
2.3.6 Holocene Volcanoes < 0.01 Ma.....	29
2.4 Results.....	30
2.4.1 Geochemistry.....	30
2.4.1.1 Temporal variations of element ratios.....	39
2.4.1.2 Isotopes.....	40
2.5 Discussion.....	45
2.5.1 Chemical isotopic composition of magmatic rocks in southern Peru and northern Chile.....	46
2.5.2 Lithospheric Cross Sections and the Tectonic and Magmatic History in southern Peru.....	52
2.6 Conclusions.....	56
3 Regional and temporal patterns in Meso-Cenozoic magmatic evolution in the Central Andes (13°S to 28°S).....	57
3.1 Introduction.....	57
3.2 Database.....	58

3.3 Geochemistry of Meso-Cenozoic magmatic rocks in the CA .....	60
3.3.1 Major and trace elements.....	60
3.3.2 Isotopes.....	66
3.4 Summary and Discussion: Implications for a tectonic model .....	71
3.4.1 Source or Processes? .....	72
3.4.2 Geochemical constraint in a Tectonic model .....	80
4 Geochemical variations in time and space of lead isotopic domains in the Central Andes (13°S -28°S): Implications of the crustal structure and metal sources.....	82
4.1 Introduction .....	82
4.2 Information systems and Pb isotope data .....	83
4.2.1 Lead isotope data.....	83
4.3 Results .....	84
4.3.1 Mapping of Pb isotopes and geochemical variations in Pb-domains .....	84
4.4 Discussion.....	87
4.4.1 Pb isotope mapping crustal domains .....	87
4.4.1.2 Isotopic framework of basement in the Central Andes .....	88
4.4.2 Crustal Contamination in the Pb domains .....	92
4.4.3 Isotopic domains constrained by 3D density model.....	94
4.4.4 The Nature of the Transition Zones.....	95
4.4.5 Segmentation of the Central Andes plateau related to the Pb-isotope domains.....	96
4.4.6 Rheological and structural identity of the Pb domains during Andean Orogeny....	97
4.4.7 Pb-isotopes of gold, silver copper and tin deposits, their relationship with the Pb- domains.....	98
4.5 Conclusions .....	103
5 Appendix .....	104
5.1 Sample locations.....	104
5.2 Analytical Methods .....	105
5.2.1 Sample Preparation.....	105
5.2.2 XRF (X-Ray Fluorescence Spectroscopy) analysis .....	106
5.2.3 ICP-MS (Inductively Coupled Plasma Mass Spectrometry) analysis.....	106
5.2.4 TIMS (Thermal Ionization Mass Spectrometer) analysis .....	107
6 References .....	108

## Abstract

This dissertation investigates the diversity of magma chemistry along and across the arc with time in the Central Andes, with emphasis in the Neogene magmatism. The main body of this thesis is formed by three independent chapters. The specific regions, results and conclusions of these individual works can be summarized as follow:

### *Chapter 2: Geochemical variations in south Peruvian volcanic rocks (13°S-18°S): The role of crustal composition and thickening through time and space*

Chemical and isotopic data from 36 volcanic centers (from Eocene to Holocene) of the northern Central Volcanic Zone (CVZ) in southern Peru. Volcanic rocks of these centers record the beginning as well as the peak of shortening and crustal thickening in the Upper Oligocene-Lower Miocene. Samples show systematic chemical and isotopic differences with age. The compositions of andesites erupted before and after crustal thickening are similar in terms of major elements. However, Post-Miocene andesites show enrichment in trace elements (Ba, Sr), LREE (La, Sm) as well as high  $^{87}\text{Sr}/^{86}\text{Sr}$  and low  $\epsilon_{\text{Nd}}$ . This indicates greater crustal contamination compared to the older equivalents. Pb-isotopic ratios behave differently, are mostly (25-0 Ma) independent of age, but change abruptly at 16°S, and in any given sector  $^{206}\text{Pb}/^{204}\text{Pb}$  ratios are similar. Comparison of contamination indicators with age show that contamination was low in the Tacaza arc (30 Ma to 15 Ma), increased sharply in the Lower Barroso arc (10 to 3 Ma), and remained at a high level up to the Present frontal-arc since then. These younger volcanoes (< 3 Ma) show large ranges of Sm/Yb ratios (e.g. Sara Sara, Huaynaputina).

I conclude that Y and HREE depletion from Miocene to Pleistocene volcanic rocks is caused by residual garnet of crustal assimilation after crustal thickening. Any involvement of slab melts in northern CVZ rocks to explain the “adakitic” signature is also excluded. The existing variations in lead isotopes in samples of similar age at 16°S support the notion that geochemical compositions in the magmas are controlled by the composition of the underlying basement.

### *Chapter 3: Regional and temporal patterns in Meso-Cenozoic magmatic evolution in the Central Andes (13°S to 28°S)*

Meso-Cenozoic magmatic arc systems of the Central Andes (CA) result from the subduction of the Nazca Plate beneath the South America plate since Jurassic time, the arc progressively shifted ~180 km from a western position in the Jurassic to the present Western Cordillera in the Oligocene time. These magmas formed prior, during and after crustal thickening. Present-day continental crust reaches a thickness of >70 km. Enhanced uplift between c. 30 and 15 Ma is documented by large clastic wedges in Western Andean Escarpment. The upper crust is formed by Precambrian to Paleozoic metamorphic rocks and sedimentary marine Mesozoic rocks, covered by mostly continental sediments of the Cretaceous and Tertiary.

Evolutionary pattern in geochemistry of rocks younger than mid-Tertiary show no evidence of crustal interaction involving garnet, in accordance with a thin crust at these times. While all older rocks are low in Sm/Yb, younger rocks (< 3 Ma) may be both, high and low in these ratios. Thus, high Sm/Yb in a particular rock cannot be simply taken as a proxy for thick crust.

Pliocene-Holocene volcanics north of 22°S show stronger indication of interaction with lower garnetiferous crust. To the South Sm/Yb is lower although crustal thickness is similar. This difference may then reflect the additional effect of variable crustal composition, north and south of 22°S. Significant isotopic and trace element differences are observed for rocks of the same age but at slightly different locations. Regional differences exist in other trace element ratios as well. This supports the notion that the crust not only controls the isotopes

composition of magmas but also their trace element patterns. Thus, caution needs to be applied when plotting geochemical data vs. age for rocks from a wide regional distribution as local basement control may be more important than age in controlling their composition.

*Chapter 4: Geochemical variations in time and space of Lead isotopic domains in the Central Andes (13°S -28°S): Implications of the crustal structure and metal sources*

Lead isotope compositions of 802 Pb isotope analysis (356 previously published, 446 new), Nd-Sr isotope values and trace elements (150 published data, 180 new) on Proterozoic to Holocene igneous, metamorphic, and sedimentary rocks as well as Jurassic to Mio-Pliocene arc-related ore deposits define - at high spatial resolution - distinct isotopic domains of the crust in the Central Andes. These domains correlate with crustal structure index ( $\Theta$ ) mapping based on geometries of the 3D density model. Pb isotopic boundaries thus correspond to variations in the intracrustal density structure that reflects distinct mafic and felsic crustal compositions. Our combined isotopic and geophysical mapping suggests that the variations in crustal composition must be old and that crustal evolution as reflected in its structure, age and composition had an important control on major element heterogeneity (mafic versus felsic), lead and Neodymium isotopes heterogeneity and Central Andean plateau segmentation.

## Zusammenfassung

Diese Dissertation untersucht die Diversität der Magmenchemie entlang sowie quer des magmatischen Bogens in Bezug auf die temporären Veränderungen in den zentralen Anden, mit Schwerpunkt auf dem Neogenen Magmatismus. Der Hauptteil dieser Arbeit ist in drei unabhängige Kapitel gegliedert. Die Spezifischen Regionen, Ergebnisse und Rückschlüsse dieser drei individuellen Kapitel können wie folgt zusammengefasst werden:

### *Chapter 2: Geochemical variations in south Peruvian volcanic rocks (13°S-18°S): The role of crustal composition and thickening through time and space*

Grundlage sind chemische und isotopische Analysen von 36 vulkanischen Zentren (vom Eozän bis Holozän) der nördlichen Central Volcanic Zone (CVZ) in Süd Peru. Die Vulkanite dieser Zentren spiegeln den Beginn und auch den Höhepunkt der Verkürzung und der damit assoziierten Krustenverdickung vom oberen Oligozän bis unteres Miozän wider. Die Proben zeigen systematische Veränderungen in der Chemie und Isotopie in Abhängigkeit von der Zeit. Die Zusammensetzungen von Andesiten die vor und nach der Krustenverdickung eruptiert wurden sind bezüglich der Hauptelemente ähnlich. Dahingegen zeigen post Miozäne Andesite Anreicherung an bestimmten Spurenelementen (Ba, Sr), LSEE (La, Sm) sowie auch hohe  $^{87}\text{Sr}/^{86}\text{Sr}$  und niedrige  $\epsilon_{\text{Nd}}$  Werte. Dies sind Indikatoren für größere krustale Kontamination im Vergleich zu den älteren Äquivalenten. Die Pb-Isotopenverhältnisse verhalten sich anders, sie sind zumeist (25-0 Ma) unabhängig vom Alter, verändern sich aber plötzlich bei 16°S und in bestimmten definierten Regionen sind die  $^{206}\text{Pb}/^{204}\text{Pb}$  Verhältnisse ähnlich. Vergleiche von Kontaminationsindikatoren in Bezug auf das Alter zeigen, dass die Kontamination gering war während des Tacaza Bogens (30 to 15 Ma), stark anstieg während des unteren Barroso Bogens (10 to 3 Ma) und auf einem hohen Level seit dieser Zeit blieb bis zum heutigen Frontalen Bogen. Diese jungen Vulkanite (< 3 Ma) zeigen ein großes Spektrum in Sm/Yb Verhältnissen (e.g. Sara Sara, Huaynaputina).

Ich schließe daraus, dass die Verarmung von Y und den SSEE in den Vulkaniten vom Miozän zum Pleistozän durch Granat im Residuum bei der Assimilation nach der Krustenverdickung entstanden ist. Des Weiteren lässt sich die „Adakit-Signatur“ von Gesteinen der nördlichen CVZ nicht durch Schmelzen aus der subduzierten Platte erklären. Die gefundenen Variationen in der Blei Isotopie in Proben gleichen Alters in der Region um 16°S erhärtet die Auffassung, dass die geochemische Zusammensetzung der Magmen durch die Zusammensetzung des darunter liegenden Grundgebirge kontrolliert wird.

### *Chapter 3: Regional and temporal patterns in Meso-Cenozoic magmatic evolution in the Central Andes (13°S to 28°S)*

Das Meso-Känozäne magmatische Bogen System der Zentralen Anden (CA) wird hervorgerufen durch die Subduktion der Nazca Platte unter die Südamerikanische Platte seit dem Jura. Der Bogen bewegte sich kontinuierlich ~ 180 km von einer westliche Position im Jura hin zur heutigen westlichen Gebirgskette im Oligozän. Diese Magmen wurden früher gebildet, während und nach der Krustenverdickung. Die heutige kontinentale Kruste erreicht eine Dicke von >70 km. Erhöhte Hebung zwischen ca. 30 und 15 Ma ist dokumentiert durch große klastische Keile in den Schichtstufen der westlichen Anden. Die obere Kruste besteht aus Präkambrischen und Paläozoischen Metamorphiten sowie Mesozänen marinen Sedimenten, die meist mit kontinentalen Sedimenten aus der Kreide und dem Tertiär bedeckt sind.

Die Entwicklungsmuster in der Geochemie der Gesteine jünger als mittel Tertiär zeigen keine Beweise für Krusteninteraktion mit Granateinwirkung, was in Übereinstimmung mit der dünnen Kruste zu dieser Zeit ist. Während alle älteren Gesteine ein niedriges Sm/Yb

Verhältnis haben, sind jüngere Gesteine (< 3 Ma) variabel und zeigen beides, hohe und niedrige Werte. Folglich können hohe Sm/Yb Verhältnisse in einzelnen Gesteinen nicht einfach als Indikatoren für eine mächtige Kruste herangezogen werden.

Pliozäne-Holozäne Vulkanite nördlich 22°S zeigen stärkere Anzeichen für Einwirkungen von tiefer granitischer Kruste. Im Süden ist das Sm/Yb Verhältnis geringer, obwohl die Krustendicke identische ist. Dieser Unterschied spiegelt dann den zusätzlichen Effekt der variablen Krustenzusammensetzung im Norden und südliche 22°S wider. Signifikante Unterschiede in Isotopen und Spurenelement werden in Gesteinen gleichen Alters beobachtet, unterscheiden sich aber etwas in den unterschiedlichen Regionen. Regionale Unterschiede existieren auch in anderen Spurenelementverhältnissen. Dies unterstützt die Annahme, dass die Zusammensetzung der Kruste nicht nur die Isotopenzusammensetzung sondern auch die Spurenelementmuster der Magmen kontrolliert. Folglich muss große Vorsicht gewährt werden wenn die geochemischen Daten gegen das Alter für bestimmte Gesteine mit einer großen regionalen Verteilung aufgetragen werden, denn das lokale Grundgebirge könnte die Zusammensetzung stärker beeinflussen als das Alter.

*Chapter 4: Geochemical variations in time and space of Lead isotopic domains in the Central Andes (13°S -28°S): Implications of the crustal structure and metal sources*

Die Blei Isotopen Zusammensetzung von 802 Pb-Isotopen Analysen (356 bereits veröffentlichte, 446 neue) sowie die Nd-Sr Werte und Spurenelementdaten (150 bereits veröffentlichte, 180 neue) an Proterozoischen bis Holozänen magmatischen, metamorphen und sedimentären Gesteinen wie auch an Jurassischen bis Mio-Pliozänen Bogen assoziierten Erzlager definieren - bei hoher räumlicher Auflösung – eindeutige Isotopendomänen der Kruste in den Zentral Anden. Diese Domänen korrelieren mit der Krusten-Struktur-Index (Θ) Kartierung welche auf den Geometrien einer 3D Dichte Modellierung basiert. Die Grenzen der Pb Isotope entsprechen den Variationen in den intrakrustalen Dichte Strukturen, welche mafische und felsische Krustenzusammensetzungen widerspiegeln. Unsere kombinierte isotopische und geochemische Kartierung weist darauf hin, dass die Variationen in der krustalen Zusammensetzung alt sind. Weiterhin hatten die Krustenentwicklung, die in diesen Strukturen festgehalten ist, sowie Alter und Zusammensetzung einen großen Einfluss auf die Heterogenität der Hauptelemente (mafisch gegen felsisch), die Heterogenitäten der Blei und Neodym Isotope, und die Segmentierung der Zentral Anden Hochebene.



## Resumen

Esta disertación investiga la diversidad de la química en espacio y tiempo de los magmas en los arcos de los Andes Centrales, con énfasis en el magmatismo del Neógeno. El principal contenido de esta Tesis está conformado por tres independientes capítulos. Las regiones específicas, resultados y conclusiones de estos trabajos individuales pueden ser resumidos como sigue:

### *Chapter 2: Geochemical variations in south Peruvian volcanic rocks (13°S-18°S): The role of crustal composition and thickening through time and space*

Datos químicos y isotópicos de 36 centros volcánicos (desde el Eoceno hasta el Holoceno) del norte de la Zona Volcánica Central (ZVC) en el sur de Perú. Las rocas volcánicas de estos centros registran el comienzo y el máximo acortamiento, y espesor cortical en el Oligoceno superior-Mioceno inferior. Las muestras indican diferencias en la sistemática de la química y isótopos con la edad. La composición de las andesitas eruptadas antes y después del espesamiento cortical son similares en términos de elementos mayores. Sin embargo, las andesitas post-Mioceno muestran enriquecimiento en elementos traza (Ba, Sr), LREE (La, Sm) así como también alto  $^{87}\text{Sr}/^{86}\text{Sr}$  y bajo  $\epsilon_{\text{Nd}}$ . Esto indica gran contaminación cortical comparado con los equivalentes antiguos.

Las relaciones de isótopos de Pb son diferentes, mayormente independientes de la edad (25-0 Ma), y cambian abruptamente a 16°S, y en determinados sectores las relaciones  $^{206}\text{Pb}/^{204}\text{Pb}$  son similares. Las comparaciones de indicadores de contaminación con la edad muestran que la menor contaminación fue en el arco del Tacaza (20 Ma to 10 Ma), incremento fuertemente en el arco del Barroso inferior (10 to 3 Ma), y permanece desde entonces a mayor nivel en el presente arco frontal. Estas lavas recientes (< 3 Ma) muestran amplios rangos en relaciones de Sm/Yb (e.g. Sara Sara, Huaynaputina).

Las depleciones de Y y HREE desde el Mioceno hasta el Pleistoceno fueron causados por granate residual de la asimilación cortical después del espesamiento de la corteza. Se excluye algún involucramiento de fusión de la corteza subductada en las rocas del norte de la ZVC para explicar las firmas de "adakitas". Las variaciones existentes de isótopos de plomo en las muestras de similar edad a 16°S soporta la idea que la composición geoquímica en los magmas fueron controlados por la composición del basamento infrayacente.

### *Chapter 3: Regional and temporal patterns in Meso-Cenozoic magmatic evolution in the Central Andes (13°S to 28°S)*

El sistema de arcos magmáticos Meso-Cenozoicos en los Andes Centrales resulta de la subducción de la placa de Nazca por debajo de la placa de Sud-América desde el Jurásico. El arco progresivamente se desplazó ~180 km desde una posición al oeste en el Jurásico hasta su posición actual en la Cordillera Occidental en el Oligoceno. Estos magmas se formaron antes, durante y después del espesamiento cortical. Actualmente el espesor de la corteza continental alcanza un espesor >70 km. El aumento del levantamiento entre c. 30 y 15 Ma está documentado por la larga sedimentación en la pendiente oeste de la Cordillera Occidental.

La corteza superior está formada por rocas metamórficas del Proterozoico y Paleozoico y sedimentos marinos del Mesozoico, cubiertos en su mayoría por sedimentos continentales del Cretácico y Terciario. El patrón evolucionario de la geoquímica de las rocas anteriores al Terciario-medio no muestra evidencia de interacción cortical envolviendo granate, en acuerdo con una corteza delgada en esos tiempos. Mientras que todas las rocas antiguas son menores en las relaciones de Sm/Yb, las rocas recientes (< 3 Ma) tienen ambos, mayores y menores.

Estas relaciones mayores de Sm/Yb en una roca particular no pueden ser tomada simplemente como una medida de corteza espesa.

Volcanicos del Plioceno-Holoceno al norte de 22°S muestran una indicación fuerte de interacción con corteza inferior granatífera. Hacia el sur Sm/Yb es menor a pesar de que el espesor de la corteza es similar. Esta diferencia al norte y sur de 22°S puede luego reflejar el efecto adicional en la variación de la composición de la corteza. Significantes diferencias en isótopos y elementos trazas son observados en rocas de igual edad pero en pequeñas locaciones diferentes. Diferencias regionales existen también en otras relaciones de elementos trazas. Esto soporta la idea que la corteza no solo controla la composición isotópica de los magmas, también controla sus patrones de elementos traza. Por eso, se necesita cuidado cuando se usan ploteos de datos geoquímicas vs. la edad de las rocas de una distribución regional extensa ya que el control del basamento local puede ser más importante que la edad en controlar su composición.

*Chapter 4: Geochemical variations in time and space of Lead isotopic domains in the Central Andes (13°S -28°S): Implications of the crustal structure and metal sources*

Composiciones de isótopos de Pb analizadas en 802 muestras (356 previamente publicadas, 446 nuevas) de rocas ígneas y sedimentarias del Proterozoico al Holoceno, así como también minerales de depósitos relacionados a arcos desde el Jurásico al Mio-Plioceno - definen a alta resolución - distintos dominios isotópicos de la corteza en los Andes Centrales. Estos dominios se correlacionan con discontinuidades de densidad dentro de la corteza mapeados sobre la base de la geometría en la estructura intracortical. Los límites de los isótopos de Pb corresponden a la variación en la estructura de la densidad cortical que refleja distintas composiciones corticales como máficas y félsicas. Nuestro mapeo combinado de isótopos y geofísica sugiere que las variaciones en la composición cortical deben ser antiguas, y la evolución intracortical como es reflejado en su estructura, edad y composición tienen un importante control en la heterogeneidad de elementos mayores (máficos versus félsicos), heterogeneidad en los isótopos de plomo y neodimio, y segmentación de las altiplanicies en los Andes Centrales.

## **Acknowledgements**

I wish to give my best thanks to my advisor Prof. Gerhard Wörner. He kindly opened the possibility to come to Germany, supported the application to the DAAD scholarship, gave from the beginning all that I needed to develop my work and scientific basis and skills he imparted to me to understand the geochemistry of the igneous rocks, its compositions, interpretation and relation with other geology branch. We spend many hours together discussing the multifarious aspects of my research, and he always made time for my questions.

I am grateful to the Deutscher Akademischer Austauschdienst (DAAD) for the scholarship I received to develop my doctoral thesis in Germany. The Geowissenschaftliches Zentrum Göttingen (GZG) at the Georg August Universität Göttingen welcomed me.

I am very grateful to Gerald Hartmann who introduced me to ion exchange column separation and carried out the TIMS analysis. I also thank Klaus Simon who spent many hours to make the ICP MS measurements.

I am grateful to the technical group of the Geochemistry Department, from which I received assistance during the laboratory work. From this group I wish to thank Ingrid Reuber, Erwin Schiffczyk and Angelika Reitz and essential tips in the handling of computer I thank Stefan Möller.

Occasional rich discussions, inspiring ideas on field trips or at congresses, with T. Sempere, D. Cassard, A. Tassara, F. Lucassen, M. Fornari and J.C. Thouret had a positive influence on the course of the present work and are gratefully acknowledged.

I would like to thank the people of the GIS Andes Project of the French Geological Survey (BRGM), for his helpful advice in the GIS programs. I also thank Yves Husson for help me with database management and processing.

I thank the members of the Peru Geological Survey (INGEMMET) for their cooperation.

I sincerely wish to acknowledge the generosity, friendly help, collaboration and constructive discussions of Philipp Ruprecht, Birgit Scheibner, Aneta Kiebała, Silvia Rosas, Wenke Wegner, Magdalena Banaszak, Silke Triebold, Andreas Kronz, Arnd Heumann, Janina Klaus and Sonja Pabst.

Finally, I wish to thank my mother Basilia Huisa, my father Carlos Mamani, my sisters Nora and Marisol, my brothers Carlos and Joel and the whole family in Peru. They have been the spiritual force that enabled me to meet this challenge, thus expanding my knowledge and skill to better research. Although we have not been physically close during my residence in Germany, I have always felt that they are by my side.

This dissertation and all the efforts that came along with it are dedicated to the “Pachamama”!

## Preamble

This dissertation studies the geochemistry and isotope composition of Meso-Cenozoic magmas formed before, during and after crustal thickening in the Central Andes that serves as a tool to analyse the causes of their variations in space and time. It consists of six chapters.

Chapter 1 is an introduction to the dissertation discussing the open questions related with the geochemical variation of volcanic rocks in the Central Andes that are intended to be addressed throughout this work.

This Chapter also summarises the main hypothesis driving the scientific work and previous work.

Chapter 2 is titled “Geochemical variations in south Peruvian volcanic rocks (13°S-18°S): The role of crustal composition and thickening through time and space”. I present the results of new geochemical analysis for 36 volcanic centers from southern Peru. In this chapter I explain in detail for each volcanic center the geochemical patterns, which allow me to observe abrupt geochemical variation at 16°S. This observation is compared to the northern Chile where previous works observed geochemical variations at 19°S. This chapter indicates me that for better understanding these geochemical variations in time and space in the Central Volcanic Zone is also necessary to compare this results with older rocks e.g. from Jurassic to early Tertiary volcanic arcs.

Chapter 3 has the title “Regional and temporal pattern in Meso-Cenozoic magmatic evolution in the Central Andes (13°S to 28°S)”. For this chapter I compiled the Göttingen Andes and selected published geochemical data of Meso-Cenozoic igneous rocks (>1500 samples) of the Central Andes, many ICPMS and Pb-Nd-Sr-isotope analysis of these samples were performed in order to provide an adequate framework for the geochemical pattern interpretation. The geochemical information in this database is the most complete for the study region. With this data I could observe that significant isotopic and trace element differences are observed for rocks of the same age but at slightly different locations. The spatial analysis of this data is presented in the following chapter.

Chapter 4 is “Geochemical variations in time and space of lead isotopic domains in the Central Andes (13°S -28°S): Implications of the crustal structure and metal sources”. For this chapter I used the compiled database of igneous rocks and data of ore deposits and sedimentary rocks under spatial analysis program at BRGM (French Geological Survey) in collaboration of GIS Andes Project to delineate the spatial isotopic variations boundaries in the Central Andes. This work is constrained by 3D model presented by Andres Tassara (under review). This result offers a new knowledge of the extension, structure and composition of the continental crust in the Central Andes.

Chapter 5 is the appendix with sample locations and explain the analytical methods.

Chapter 6 is a list of references cited throughout the previous chapters.

## 1 Introduction

### 1.1 Variations in magma composition in time and space along the Central Andes (13°S-28°S): Facts and open questions

Continued volcanic and plutonic magmatism due to subduction of the Nazca plate beneath the South American Continent in the Central Andes (CA) is active since the Jurassic (~180 Ma) until recent. During this time, referred to as the "Andean cycle" (Coira et al., 1982), the active volcanic arc shifted progressively eastwards by ~200 km, thus coupling temporal with spatial across-arc variations. Below the CA, the continental crust reaches a thickness of up to 70 km since crustal thickening started about ~25 m.y. ago (Isack, 1988).

The potential sources that would have contributed to create the geochemical characteristics of the magmas in the Central Volcanic Zone (CVZ) of the Andes would be: fluids from the subducted oceanic crust (Stern et al., 1989, 1991), asthenospheric mantle (Rogers and Hawkesworth, 1989), lower continental crust and upper continental crust (Hildreth and Moor bath, 1988; Wörner et al., 1988; Davidson et al., 1991), as well as melting of old subducted oceanic crust in the shallow subduction zones (Gutscher et al., 2000). These sources responsible for the geochemical characteristics of magmatic rocks observed in different areas of the CVZ have faced the geoscientific community since decades.

In order to have an adequate framework for this thesis, I found necessary to build a Central Andes metadata, which contains geochemical, geochronological, geological, metallogenic and geophysical information.

The open question is, at different sources and different processes can account for the observed diversity of magma chemistry along and across the arc with time. Apart from assessing contributions from different potential sources, the main interest is focused on the role of the continental crustal composition and thickening through time and space in magma genesis.

With the metadata this work will address the following questions:

- Do magmatic rocks chemistry and distribution reflect changes in the dip of the subducted Nazca plate and the thickness of the overlying lithospheric mantle and crust?
- In what way does crustal thickness affect the composition of magma?
- How is the dramatic increase of crustal thickness due to the recent uplift episode reflected in magma geochemistry, especially the REE?
- Do Neogene magma composition document contributions from different basement domains? and how is the real extension of these basements?

Further attention is given to ore deposits and their geological setting, the influence of basement rocks and to understand the regional control on ore deposits, based on Pb isotopes data of the mayor central Andean Neogene silver, gold, copper and tin deposits.

### 1.2 Working Hypothesis

The main hypothesis analysed throughout this dissertation is that igneous rocks of the central Central Volcanic Zone are contaminated by crustal material (e.g. Wörner et al., 1988; 1992; Davidson et al., 1990). Besides affecting Sr-Nd, and O-isotopic composition, the crustal component has a particularly strong impact on the Pb-isotope ratios of the erupted lavas (Tilton and Barreiro, 1980; Harmon et al., 1984; Barreiro, 1984; Mukasa, 1986; Aitchison et al., 1995; Wörner et al., 1992). This idea has been suggested for Cenozoic rocks, but never formally expressed for the entire Central Andes (Stern et al., 1989, 1991; Rogers and Hawkesworth, 1989) nor spacially and temporally explained in terms of its causes and consequences.

During this thesis I analysed the Meso-Cenozoic igneous rocks of southern Peru and I completed to analyse samples from northern Chile and also I analysed some new Proterozoic

and Paleozoic rocks for a better understanding the spatial and temporal variations of magmas along the entire Central Andes.

### 1.3 Previous work

#### 1.3.1 The Andes

The Andes is a mountain belt built along the western margin of the South American continent with a stretching over 8000 km from Venezuela to the Tierra del Fuego, a maximum width of 600 km and a maximum elevation of 7000 m a.s.l. This orogenic type has produced the highest non-collisional mountains in the world. However, when this chain is analyzed in detail it is evident that a great variety of processes has produced its present geology. Most of its length, the Andes consist of a magmatic arc flanked by a trench in the west and foreland Fold-Thrust Belt and Basin in the eastern. The geological history, as well as the present tectonic setting, is responsible for the unique geology of the Northern, Central, Southern and Austral Andes. The Northern Andes (10°N-3°S) are the result of Mesozoic and Cenozoic collision of oceanic terranes, prior to the present Andean-type setting (Bosch and Rodríguez, 1992). The central Andes (3°S-33.5°S) have a long history of subduction and volcanic arc activity (Sébrier and Soler, 1991, Isacks, 1988, Allmendinger, 1997), while the Southern Andes (33.5°S-46.5°S) record the closing of a back-arc oceanic basin (Ramos and Kay, 1992; Gorrington et al., 1997) and the Austral Andes (46.5°S-56°S) with volcanic activity (Stern, 2004). The Andean Chain borders the Caribbean Plate in the north. The Nazca and Antarctic Plate are in the west and the Scott Plate is in the south (Fig. 1.1).

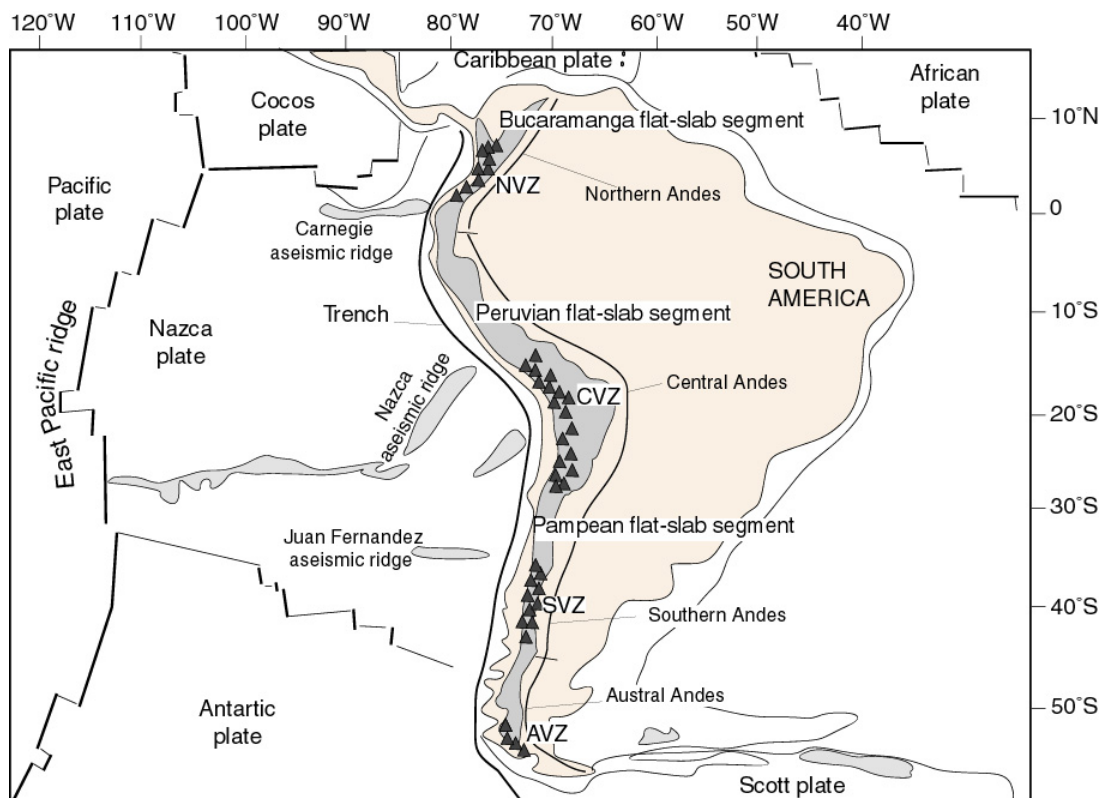


Fig.1.1. Plate-Tectonic setting of the Andes (based on the compilations of Wörner et al., 1988; Stern and Killian, 1996; Ramos 1999; Stern, 2004).

Eastward subduction of the Nazca and Antarctic oceanic plate beneath the South American Plate occurred since the Jurassic (Coira et al., 1982). The link between trench collision of

aseismic ridges and flat-slab segments play an important role in the volcanic activity. The distribution of the volcanic arc has been linked to the steepening of the subduction zone and influx of hot asthenosphere into the mantle wedge after a phase of flat-slab subduction, uplift and no magmatism (Isack, 1988; Wörner et al., 1994; Kay et al., 1999; James and Sacks, 1999). Thorpe and Francis (1979), Stern and Killian (1996) have shown a segmentation of the present-day active volcanism into four distinct segments with shallowly and steeply dipping Benioff zones based on spatial seismological variations.

- a) Northern Volcanic Zone (NVZ) extending from 2°S to 5°N
- b) Central Volcanic Zone (CVZ) extending from 15°S to 28°S
- c) Southern Volcanic Zone (SVZ) extending from 33°S to 46°S
- d) Austral Volcanic Zone (AVZ) extending from 47°S to 54°S

In the NVZ, SVZ and AVZ crustal thickness is < 45 km. The flat segments with absent volcanism and the foreland uplift correspond to the segments of Bucaramanga (north of 5°N), Peruvian (5°-14°S) and Pampean (28°-33°S) (Fig.1.1).

### **1.3.2 The Central Volcanic Zone (CVZ)**

The CVZ is widely developed between southern Peru, northwestern Bolivia, northern Chile and northwestern Argentina, along the Western Cordillera, which bounds the Altiplano-Puna plateau. Hundreds of volcanoes are widely spread along this region (Fig. 1.2). The most striking feature of the CVZ is its extraordinary thick crust, which reaches a thickness greater than 70 km since crustal thickening started about 25 m.y. ago (Isacks 1988). The CVZ is also the type region of a non-accreting continental margin, as an accretionary prism is missing opposite to the sediment-free trench along of the margin (Schweller et al., 1981). The most important normal subduction sector is between Arequipa and northern Argentina (16°-24°S), where the slab inclines 30° to the east. The subduction has an abrupt dip change between 14° and 16°S in southern Peru-Bolivia, and a smooth transition between 24° and 27.5°S in northern Argentina (Allmendigar et al., 1997). The present convergence rate is 10 cm/y (Pardo-Casas & Molnar, 1987)  $7.5 \pm 0.5$  cm/y in the direction N78°E (Norabuena et al., 1998; Angermann et al., 1999) and 7.5 cm/y (Somoza, 1998).

Paleomagnetic data indicate that a 30° clockwise rotation about a vertical axis of the area south of the bend and a 20° counterclockwise rotation north of the bend has occurred since the Miocene. Watts et al (1995) hold regional variations in flexural rigidity responsible for the along strike bending of the entire mountain belt.

The active volcanic front is situated 300 km east of the trench axis and 120 km above the Benioff zone and comprises 50 recently active volcanoes.

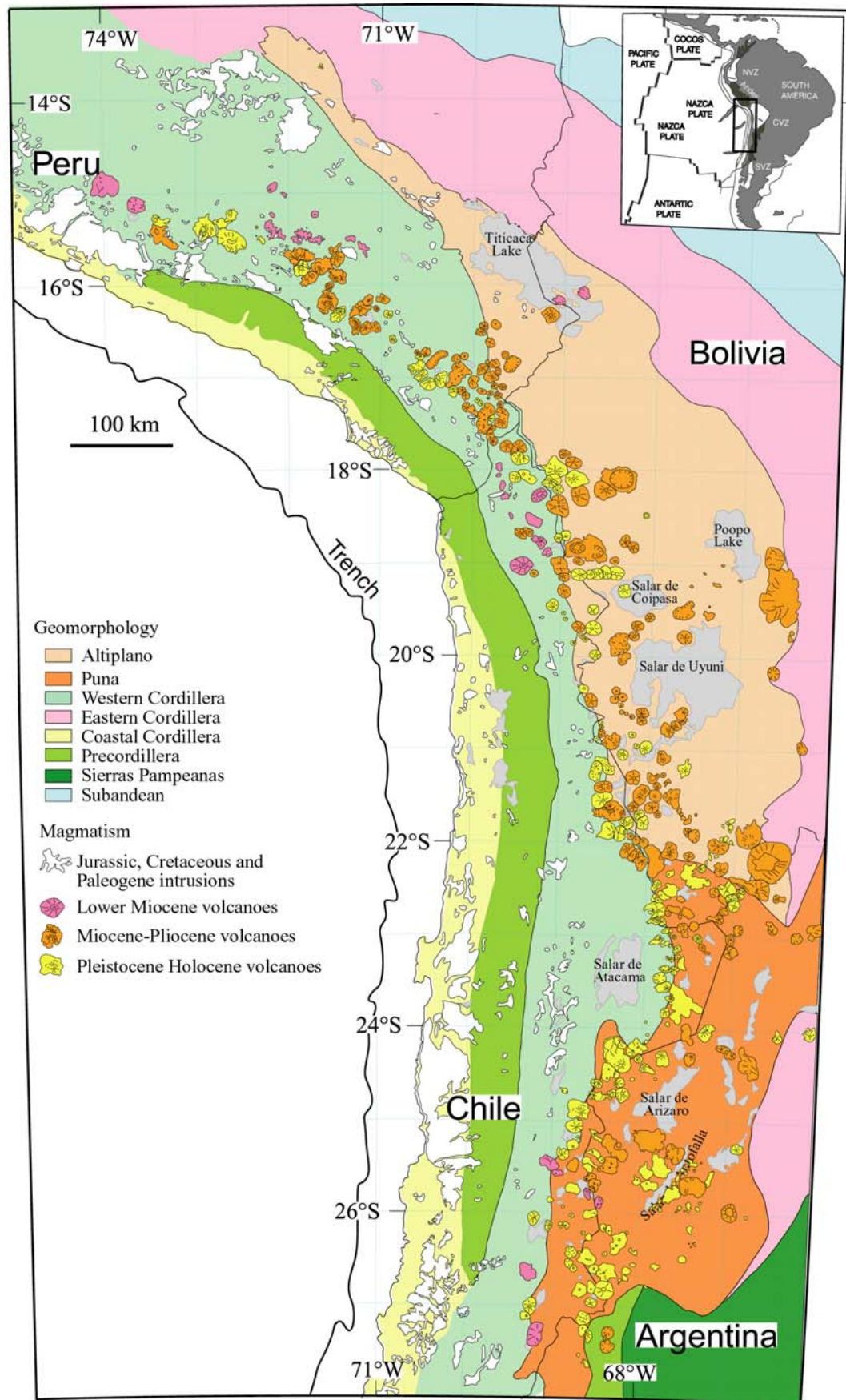


Fig. 1.2. Central Andean map showing principal Geomorphological Unites, locations of main Mesozoic and Early Cenozoic intrusions, and Neogene volcanism.



### 1.3.2 Pre-Andean history

#### Proterozoic basement

Some outcrops of Proterozoic rocks are exposed along the present-day Andean margin in southern Peru, western Bolivia and northern Chile. The major units are in the Fig. 1.3 and Table 1.1. These contain dissimilar rock type, previous workers cited a coherent whole-rock Pb isotopic signature throughout to define a single crustal block called Arequipa-Antofalla basement (Tilton and Barreiro, 1980; Barreiro and Clark, 1984; Wörner et al., 1992; Aitcheson et al., 1995; Tosdal, 1996; Wörner et al., 2000; Loewy et al., 2004).

According Wasteneys et al., 1995; Wörner et al., 2000 the oldest rocks are formed at ca. 2.0-1.9 Ga but there has been a debate over the timing of metamorphism of these rocks. Rb/Sr and early U/Pb studies implied granulite to amphibolite facies metamorphism between 1.9 and 1.8 Ga (Cobbing et al., 1977; Schakelton et al., 1979), but more recent U/Pb data from gneisses at Mollendo and Cerro Uyarani indicated high-grade metamorphism at ca. 1.2-1.0 Ga (Wasteneys et al., 1995; Wörner et al., 2000).

Tosdal (1996) and Wörner et al. (2000) propose that the Belén protoliths show a strong sedimentary contribution from the Arequipa Massif.

According precise U/Pb geochronology, group polarity, and the sequence of adjacent provinces Loewy et al. (2004) suggest that Arequipa-Antofalla basement was accreted, the docking occurred during Sunsás Orogeny at ca. 1.05 Ga.

Additional Proterozoic outcrops, apparently unrelated to the Arequipa-Antofalla basement, occur in northern and eastern of Cusco (Laubacher et al., 1984; Carlotto, 1998).

#### Paleozoic evolution

Paleozoic magmatism and metamorphism have been identified in the Coastal Cordillera in southern Peru, along the Eastern Cordillera and some outcrops are exposed across the western Cordillera and Altiplano-Puna (Damm et al., 1990; Wörner et al., 2000; Lucassen et al., 2001; Loewy et al., 2004) (Fig. 1.3 and Table 1.1).

During the Cambro-Ordovician (~500 to ~450 Ma) shallow to deep marine sediments were deposited in a large basin in southern Peru-Bolivia and northwestern Argentina with thickness increasing to the north (Bahlburg and Hervé, 1997). Syn-sedimentary intense volcanism transitionally changed from tholeiitic to calc-alkaline. Ordovician sedimentation and volcanism ended with the closure of the marine basin in the Ocluyic phase (Late Ordovician to Early Silurian) and its associated syn-cinematic granitic plutonism (Coira et al., 1982).

From Silurian-Devonian (~400 to ~350 Ma) two basins development, which were separated by the Altiplano-Puna. During the Silurian diamictite was deposited in the pampean and shallow-marine sandstones and Devonian shales were deposited to the east of the Eastern Cordillera and Subandean. They were uplifted during the Ocluyic phase (~450 to ~400 Ma) and deformed by the Chanic phase (Late Devonian to Early Carboniferous orogenesis occurred in the Andes). Calc-alkaline plutonism occurred syn-cinematically (Coira et al., 1982).

Carboniferous to Lower Permian (~350 to ~270 Ma) marine carbonates was deposited west and east of the Puna-Altiplano and continental red beds east of it (Coira et al., 1982).

During Triassic occur continental sedimentary rocks in local graben structures along northern Chile and southern Peru (Suarez and Bell, 1992; Sempere et al., 2004). Depositional conditions changed to shallow marine in the Late Triassic/Early Jurassic. The Jurassic sediments were deposited contemporaneously with Jurassic volcanic rocks in a north-south

oriented chain of basins located east of the Jurassic arc (Prinz et al., 1994; Sempere et al; 2004).

The Paleozoic evolution of the Central Andes has been and still is a subject of discussion. Current hypotheses on the geodynamic and tectonic processes that formed the pre-Andean basement can be summarized in the following three models (after Damm et al, 1994):

**Continuous subduction**, assumes a more or less uninterrupted eastward subduction beneath a stable active continental margin with varying plate geometries since Precambrian time (e.g. Coira et al, 1982; Pichowiak, 1994).

**Exotic terrane**, postulates crustal growth and consolidation during the pre-Mesozoic due to docking of various allochthonous terranes (Pampeana, Arequipa-Antofalla, Precordillera, Chilenia) to the stable margin of the Brazilian shield, causing deformational and metamorphic event (e.g. Ramos et al, 1988; Dalziel & Forsythe, 1985; Astini, 1995; Tosdal, 1996; Loewy et al., 2004).

**Ensialic margin**, states that the formation of the western margin of South America\Gondwana was complete by Late Proterozoic and remained autochthonous and tectonically passive until initiation of subduction by the break-up of Pangea in the Triassic. Precambrian to Paleozoic history is characterized by repeated closure and opening of the intracontinental basins (Damm et al, 1990, 1994; Dalziel & Forsythe, 1985; Lucassen et al., 1996, 2001).

Table 1.1. Proterozoic and Paleozoic ages. Data are from a=Loewy et al., 2004; b=Damm et al., 1990; c=Mpodozis et al., 1983; d=Lork and Bahlburg, 1993; e=Pacci et al., 1980; f=Cobbing et al., 1977; g=Wörner et al., 2000; h=Lehmann, 1978; I=Tosdal, 1996.

Outcrops	Rock type	Protolith age (Ma)	Metamorphic age (Ma)
San Juan	Banded Gneiss	1819+17/-16 <sup>a</sup>	1033±31 <sup>a</sup>
	Gneissic Tillite clast	1165 <sup>a</sup>	
	Granite	960 <sup>a</sup>	
Ocoña	Foliated Megacrystic granite	464+/- 4 <sup>a</sup>	
Mollendo	Banded Gneiss	1851+/- 5 <sup>a</sup>	935±14 <sup>a</sup>
	Granite	468+/- 4 <sup>a</sup>	
Arequipa Massif	Gneiss	1900 <sup>f</sup>	
Berenguela	Ortho-paragneiss clast	1158-1080 <sup>i</sup>	410-340 <sup>i</sup>
San Andres	Drill core	1050+/-100 <sup>h</sup>	530 <sup>h</sup>
Azurita	Granulite		650 <sup>g</sup>
Belén	Amphibole gneiss	1877+139/-131 <sup>g</sup>	366±3 <sup>g</sup>
	Biotite-gneiss	1745+/-27 <sup>g</sup>	456±4 <sup>g</sup>
	Amphibolite		444±14 <sup>e</sup>
	Granodiorite	1559±21 <sup>a</sup>	473±2 <sup>a</sup>
	Felsic dike intrudes muscovite schist	1866±2 <sup>a</sup>	227±17 <sup>a</sup>
	Amphibolite layers		1900 and 1000 <sup>b</sup>
Uyarani	Charnokite	2024+133/-11 <sup>g</sup>	1157+49/-62 <sup>g</sup>
Choja	Tonalite	1070 <sup>a</sup> and 1254+97/-94 <sup>b</sup>	450 <sup>a</sup>
	Orthogneiss	1067±4 <sup>a</sup> and 1213+28/-25 <sup>b</sup>	497±16 <sup>a</sup>
Limon Verde	Granodiorite	298±1.5 <sup>b</sup>	
Cordon de Lila	Granite	502±7 <sup>c</sup> and 450+12/-11 - 434±2 <sup>b</sup>	
Mejillones and Salar de Navidad	Granodiorite	561+12/-14 <sup>b</sup>	175±10 <sup>b</sup>
Puna	Monazite	476±1 <sup>d</sup>	

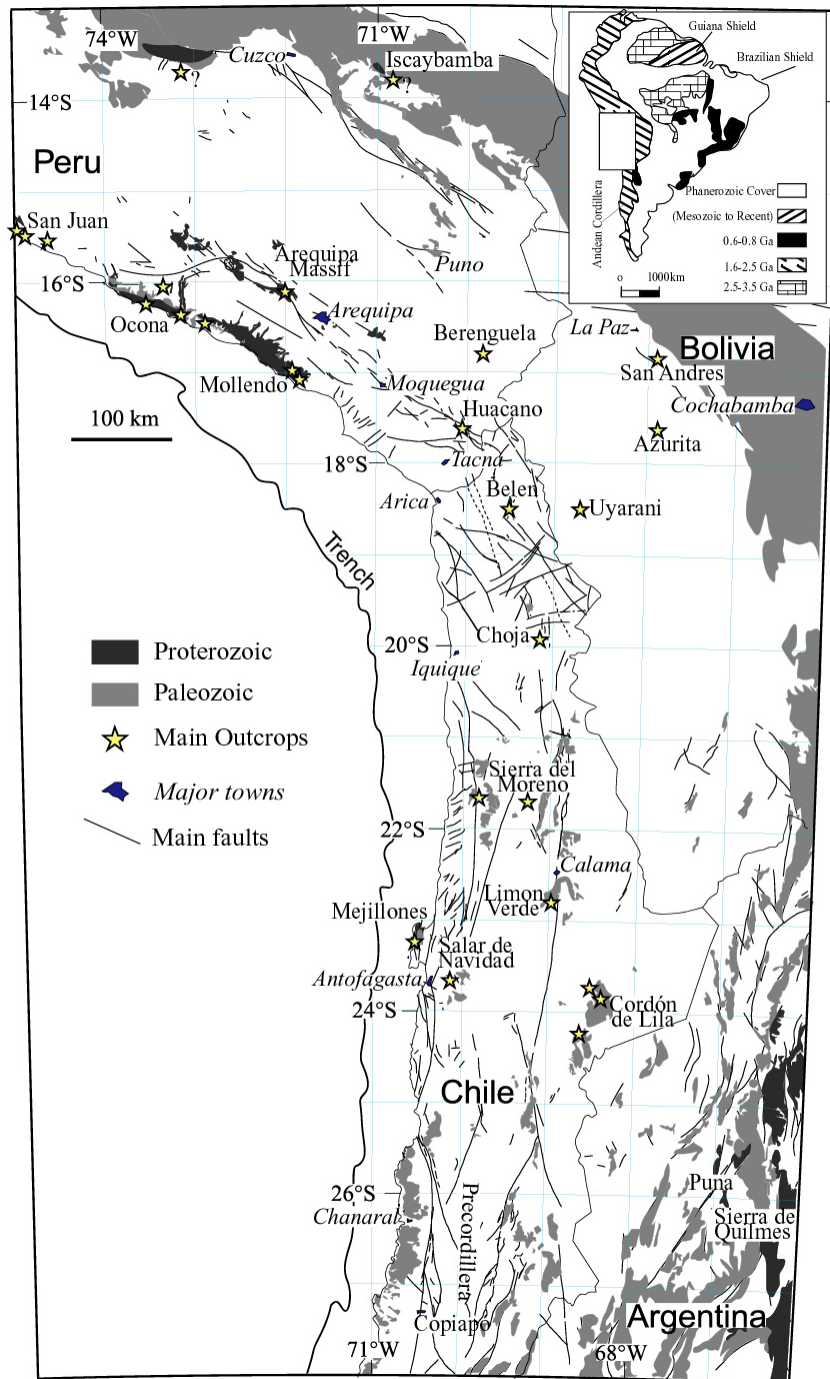


Fig. 1.3. Map of Proterozoic and Paleozoic Basement outcrops (after Damm et al., 1990; Worner et al., 2000; Lucassen et al., 2001; Loewy et al., 2004).

### 1.3.3 The Andean Cycle

The magmatic arc systems in the western continental margin of central South America developed from lower Jurassic to recent times due to the subduction of the Farallon-Nazca plate, the arc progressively shifted ~150 km from a western position in the Jurassic to the present Western Cordillera in the Oligocene time (Scheuber, 1994) (Fig. 1.2). Migration of the arc started before ~120 Ma and is attributed to crustal erosion and variable slab dip. This period is referred to as the Andean Cycle (Coira et al., 1982). Gradual eastward shift of magmatic activity was mainly restricted to plutonism, whereas volcanism occasionally paused and can be divided into periods of absent and abundant activity.

During the Lower Jurassic (~190 Ma), volcanism of the Precordillera shifted ~200 km westward into the region of the present Coastal Cordillera and formed the Jurassic to Early Cretaceous arc system. The great volumes of Jurassic igneous rocks in the Coastal Cordillera are mantle derived (Rogers and Hawkesworth, 1989; Pichowiak et al., 1990; Lucassen and Thirlwall, 1998).

Lower Cretaceous rift-related basins opened in a north-south corridor from northwestern Argentina (Salfety and Marquillas, 1994) to Bolivia and Peru (Sempere, 2004) and these were accompanied by small volumes of volcanism and alkaline intrusions (Lucassen et al., 1996b). The break-up of Gondwana in Middle-Cretaceous times increased spreading between South America and South Africa and enhanced the subduction rate at the western coast of the South American continent.

During the Late Cretaceous (~80 Ma) to Early Tertiary (~60 Ma) the magmatism arc was shifted eastward to the western foothills of the sub Western Cordillera. Several intramountain basins, partially interconnected, also developed in northern Chile, southern Peru (Bogdanic and Espinoza, 1994) and in northwestern Argentina were deposited in basins of Salta Rift System (Viramonte et al., 1999), these sedimentary rocks are characterized by carbonates and red beds.

Magmatic arc activity diminished after at ~40 Ma period during extensive red bed were deposited in the sub Eastern Cordillera.

During the Late Oligocene and Middle Miocene renewed alkaline magmatism activity occurred in the western border of the Altiplano-Puna. In the Late Miocene the main magmatic arc activity increased with the onset of the higher convergence rates. The modern subalkaline magmatic arc is 80 km broad and is located in the Western Cordillera (Coira, 1982; Wörner 1994) (Fig. 1.2 and 1.4).

### **1.3.4 Uplift of the Central Andes and subducting Nazca plate**

Uplift of the Central Andes (Fig. 1.4) since the Eocene without collision is considered a formidable geodynamic paradox. Uplift and the contribution of different processes are a matter of debate. Studies assumed that crustal thickening and correlative relief increase were caused by adding magmatic material from the mantle to the crust (Thorpe et al., 1981; Petford et al., 1996) due to changes in the rate and angle of convergence (Pardo-Casas and Molnar, 1987; Soler and Bonhomme, 1990), absolute plate motion (Somoza, 1998), the morphology of the subducting slab (Yañez et al., 2002) or the subduction of oceanic plateau or aseismic ridges (Gutscher et al., 1999; Yañez et al., 2002). Recent estimates show that magma addition would explain only a few percentages of the observed crustal thickness (Francis and Hawkesworth, 1994; Scheuber et al., 1994; Allmendinger et al., 1997; Giese et al., 1999). Nevertheless, magmatism has an influence on crustal rheology (Allmendinger et al., 1997) and might locally contribute to the thickness of active arc zones (Lamb et al., 1997). Other studies of the deformation of the upper crust and overlying sediments demonstrated that compressional shortening of the upper plate and thrusting of the Andean chain upon the Brazilian Shield are the driving mechanism of crustal thickening and the main phase of tectonic shortening took place in Miocene times, which accelerated the uplift (Jordan et al., 1983; Isacks, 1998; Sempere et al., 1990).

Estimates of shortening based on allegedly “balanced” cross sections and geophysical data (Schmitz, 1994; Baby et al., 1997; McQuarrie, 2002; Müller et al., 2002) appear too small to explain the present thickness of the whole Andean chain (Kley and Monaldi, 1998). However, possible lower crustal flow within the central Andes may be important in the mass transfer balance (Husson and Sempere, 2003; Hindle et al., 2005). James and Sacks (1999) developed a model suggesting that crustal shortening is a consequence of the steepening of the slab, caused by the heating and weakening of the crust. Models of Andean uplift consider that

uplift initiated ~60 m.y. ago in the Western Cordillera, developed later and slower within the Eastern Cordillera, and accelerated in both cordilleras starting ~25–20 Ma (Gregory-Wodzicki, 2000; Husson and Sempere, 2003). Wörner et al., 2000 concluded that crustal shortening in the Western Cordillera is very limited, not sufficient to explain the observed crustal thickening and the uplift is caused mainly by regional tilting between ~29 to 15 Ma rather by crustal shortening.

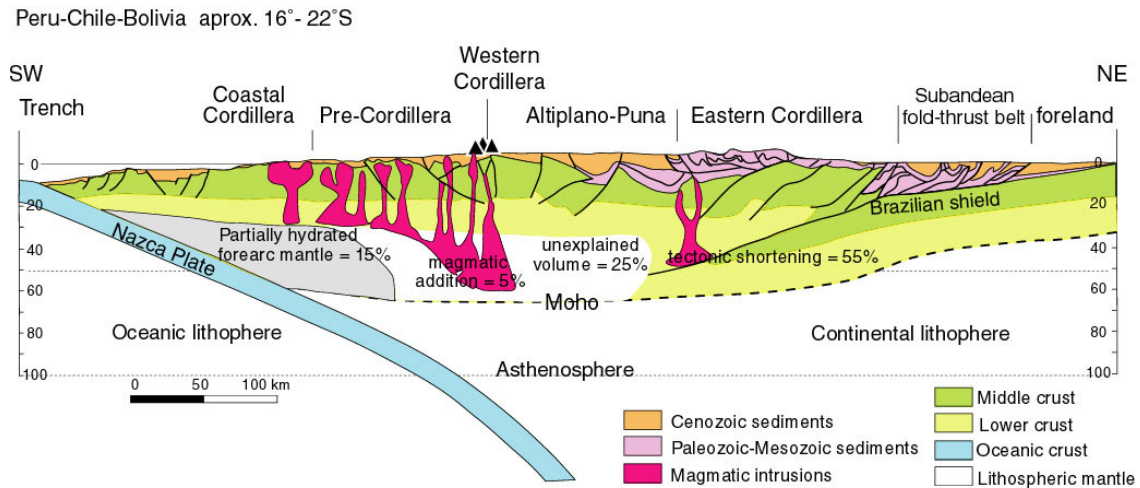


Fig. 1.4. Crustal-scale section of the Andes (16°-22°S) (Compiled from Allmendinger et al., 1997; Giese, 1999).

### Nazca Plate subduction

The East Pacific rise reached the North American subduction zone during Oligocene time, being progressively subducted beneath the continental lithosphere (Pardo-Casas and Molnar, 1978; Somoza, 1998).

This event appears to have led plate boundary reorganization in the Pacific basin. Outstanding Late Oligocene events are the breakup of the Farallon Plate into the Nazca and Cocos plate (Pilger, 1984; Pardo-Casas and Molnar, 1978; Tebbens and Cande, 1997; Somoza, 1998). In the western South America subduction zone the convergence during Late Oligocene-Early Miocene (28.3 – 25.8 Ma) appears to have been dextral and being slightly oblique in Peru and moderately oblique in Chile (Fig. 1.5b), these kinematic changes is likely related to this plate reorganization. The Nazca-South America reconstructions at 20 Ma suggest slight obliquity at the interplate boundary, being dextral in Chile and sinistral in Peru (Somoza, 1998) (Fig. 1.5b).

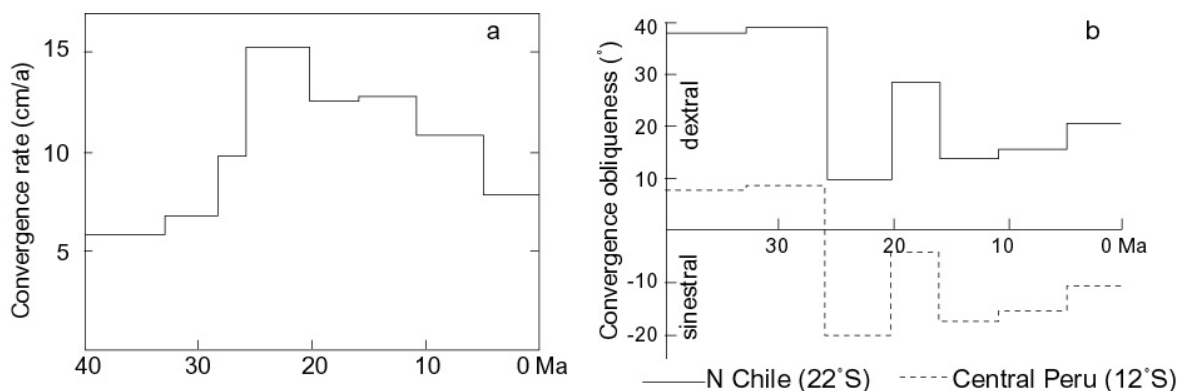


Fig. 1.5. a) Relation between the convergence rates of the Nazca plate during the last 40 Ma along Central Andes. b) Convergence obliquity in central Peru and in the northern Chile (After Somoza, 1998).

Early Cenozoic magmatism and deformation in the Central Andes were mainly concentrated in the present fore-arc region, although evidence of uplifted zones in the back-arc region has been reported (Kennan et al., 1995; Carlotto, 1998). The sudden change of the plate convergence kinematic during the Late Oligocene time (28 Ma) is coeval with a generalized eastward shift and widening of the locus of main tectonic activity, and beginning of formation of the modern Central Andes. Outstanding events are the establishment of the Late Cenozoic magmatic activity (Sébrier et al., 1988; Coira et al., 1982; Soler and Bohomme, 1990) and the onset of compressional failure in wide areas of the region (Sempere et al., 1994), suggesting that additional control, perhaps related to upper plate heterogeneities, may have existed. It could be considered, however, that strong acceleration of convergence during Late Oligocene time (28 Ma) was a factor contributing to mountain building in the Central Andean region. The slowdown of convergence rate since Late Miocene time (10.8 Ma) roughly correlates with the last deformation in the orogen. This deformation is characterized by the progressive end of internal deformation in the Altiplano-Puna region, acceleration of plateau uplift, and eastward jump of deformation to the Subandean and Sierras Pampeanas regions (James and Sacks, 1999; Sempere et al., 1990). The Pliocene-Pleistocene-Holocene (4.9-0 Ma) change in stress kinematics documented in the Puna region could be related to this slowdown of convergence rate, as Marrett et al. (1994) hypothesized.

### **1.3.5 Andean volcanism**

Neogene volcanism in the CVZ comprises stratovolcanoes and dome-cluster volcanoes with predominantly andesitic and dacitic lavas (de Silva, S.L. & Francis, P.W. 1991). Basalts are rare. Volcanic activity is frequently associated with deposition of pyroclastic flows. Large volume ignimbrites (e.g. Oxaya-Huaylillas-Cerrillos-Acay, Lauca-Peréz-Senca-Antofalla-Galan) with dacitic to rhyolitic compositions have been erupted from caldera complexes in a behind the arc, mainly in Late Oligocene, Mio-Pliocene times (Wörner et al., 2000; Tosdal et al., 1981; Coira et al., 1993). They cover areas up to 300 000 km<sup>2</sup> and these constitutes ones of the large ignimbrite provinces on earth (de Silva, 1989, Kay et al., 1999, Wörner et al., 2000, Siebel et al., 2001). Pleistocene and Holocene monogenetic cones comprising spatter cones, lava flows and proximal base surge deposits are found infrequently along the volcanic front (Wörner et al., 1994).

Back-arc Neogene volcanic activity behind the main magmatic arc is limited to the large fault, where rhyolitic ignimbrites to basaltic andesites flow have erupted (Soler et al., 1992; Kay et al., 1994a; Davidson and de Silva et al., 1992; Mamani et al., 2004; Carlier et al., 2005).

### **Petrography**

Most andesites, dacites from the arc and basalt andesites display a porphyritic texture with a fine grained to glassy matrix. The dominant phenocryst mineral phase is plagioclase. Hornblende is also abundant in many but not all rocks. Mafic phases like olivine, clinopyroxene and orthopyroxene are found in basaltic andesites, biotite, sanidine and accessory minerals such as magnetite, zircon, apatite or sphene are present in more evolved rocks. Quartz is abundant in ignimbrite samples and sometimes also found as xenocrysts in less evolved volcanics (Zbar, 1991).

The lavas from the back-arc are aphanitic to glassy volcanic rocks with less olivine and clinopyroxene phenocrysts. Shoshonites series rocks locally have phlogopite phenocrysts. Amphibole and orthopyroxene are present as microphenocrysts or resorbed phases in some samples. Plagioclase phenocrysts are scarce or absent (Schreiber and Schwab, 1991).

## Geochemistry

Most rocks of the main arc of the CVZ belong to the high-K calc-alkaline magma series. They are enriched in incompatible elements compared to tholeiitic low-K island arc rocks. However, the characteristic subduction zone trace elements pattern displaying relative enrichment of LILE (large ion lithophile elements) (Ba, K, Sr, Rb) and relative depletion of the HFSE (high field strength elements) Nb and Ta (e.g. Pearce 1983) is maintained. Concentrations of U, Th, Zr and K/Rb and Fe/Mg ratios are also elevated relative to island arc magmas (Wilson, 1989).  $^{87}\text{Sr}/^{86}\text{Sr}$  ratios are higher and  $^{143}\text{Nd}/^{144}\text{Nd}$  ratios are lower than in rocks erupted in most intra-oceanic setting (see Fig. 1.6). Pb isotopic compositions of CVZ are divided into three distinct values: A low  $^{206}\text{Pb}/^{204}\text{Pb} = 17.5$  to 18.3, middle  $^{206}\text{Pb}/^{204}\text{Pb} = 18.3$  to 18.7 and high  $^{206}\text{Pb}/^{204}\text{Pb} = 18.7$  to 18.9. These three isotopically different values reflect the composition of the underlying basement domains (Wörner et al., 1992; Aitchison et al., 1995).

$\delta^{18}\text{O}$  ratios of CVZ are consistently higher (6.8-14‰ SMOW) than those commonly observed from primitive lavas from oceanic regions (5.5-6.5‰ SMOW; Harmon, R.S. & Hoefs, J., 1984; Kyser et al., 1986).

Three geochemical group lavas in the back-arc are recognized: (1) a relative high volume intraplate group (high K; La/Ta ratio < 25), (2) an intermediate volume, high-K calc-alkaline group (La/Ta > 25), and a small-volume shoshonitic group (very high K). Shoshonitic group lavas have generally higher incompatible elements (Th, U, Cs, LREE (light rare earth elements)) concentrations than do intraplate and calc-alkaline group lavas. Generally these lavas have high Sr (> 0.7055) and lower Nd ( $\epsilon\text{Nd} < -0.4$ ) isotopic ratios (Kay et al., 1994).

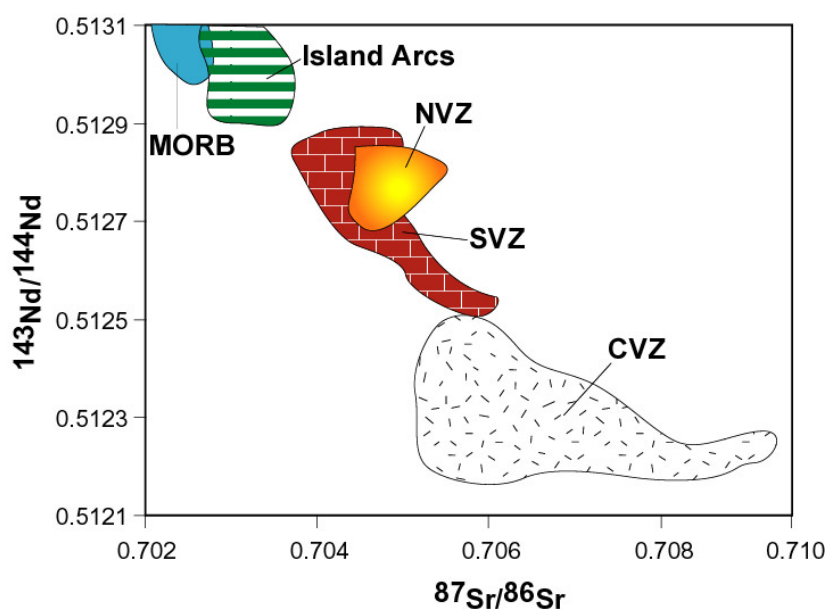


Fig. 1.6.  $^{143}\text{Nd}/^{144}\text{Nd}$  versus  $^{87}\text{Sr}/^{86}\text{Sr}$  from rocks of the NVZ, CVZ, SVZ compared to MORB and island arcs (from Davidson et al., 1991).

### 1.3.6 Magma genesis

Processes of magma genesis in the Central Andes (Fig. 1.2) have been and still are subject of debate. Question about the structure and composition of the lithosphere, the thermal structure beneath an arc or partitioning of elements between subducted slab derived fluids cannot be readily resolved. The following section summarizes fundamental processes, products and components in magma generation, which are widely agreed upon. Secondly, several contrasting models proposed by various authors are shortly discussed.

## General

The descending slab experiences increasing degrees of metamorphism, which leads to dehydration and/or partial melting. Both basaltic oceanic crust and entrained sediments are affected. The descending fluids derive from the subducted slab enrich the asthenospheric mantle wedge in mobile LILE, lower its solidus and trigger partial melting. However, partial melt can also be produced from the sub-continental enriched lithospheric mantle. While passing through the continental crust, the ascending magma may stagnate and induce partial melting of crustal material at various depths and may so be subject to contamination.

Thus, in an ocean-continent collision zone, the following components have to be considered as potential magma sources (see also Fig. 1.7).

- The subducted oceanic plate comprising variably altered and metamorphosed basalt with entrained pelagic or terrigenous sediments
- The sub-arc asthenospheric mantle wedge
- The sub-continental lithospheric mantle
- The continental crust

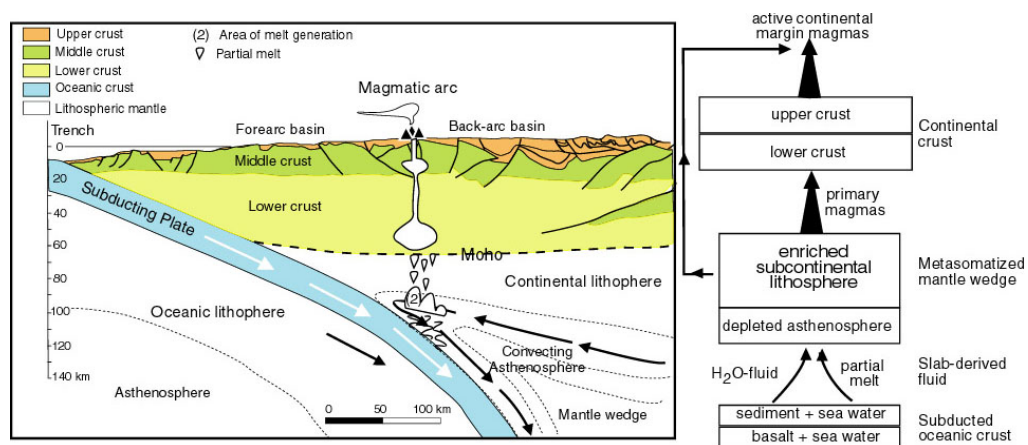


Fig 1.7. Schematic section of a subduction zones, showing the principal crustal and upper mantle components and their interactions, to the right side a flow diagram displaying potential components involved in magma genesis at active continental margins (after Wilson, 1989).

## Models

### *Tectonic erosion*

Stern et al., (1989, 1991) explain the elevated geochemical and isotopic characteristics of lavas of the SVZ with incorporation of carbonate sediment and tectonically eroded crustal material into the mantle source region by subduction. They based their conclusions on the lack of the accretionary prism along the Chilean coast and the eastward shift of the volcanic arc through Mesozoic to recent times. Variations in subduction geometry, type and amount of sedimentary input and/or margin basement, volume of mantle wedge, degree of partial melting are held responsible for geochemical and isotopic differences.

Davidson et al. (1991), however, doubt a significant contribution of subducted sediments to arc geochemistry, since most island arcs show very restricted Sr-, Nd-, and Pb-isotope compositions, independent of type and amount of sediments. Along the entire SVZ, sedimentary input remains constant, as shown by Morris et al. (1990) based on <sup>10</sup>Be isotopes. They additionally note the relative bareness of sediments in the trench outboard the CVZ and the relatively steep angle of subduction, which, following the Stern's model, would contradict the observed highly enriched geochemical characteristics of erupted lavas to be derived from sediment subduction. Further more, no CVZ lavas display Pb isotope compositions that might result from mixing between MORB and Nazca Plate sediments. Hildreth & Moorbath (1988)



argue that in SVZ in the segment (33-37.7°S) subduction geometry and sedimentary input are constant within analytical error and are thus implausible to explain the observed geochemical variability.

While no author questions the existence of tectonic erosion, its apparent constancy throughout the Andean margin seems unsuitable to explain the large observed variations in erupted lavas (Rogers & Hawkesworth, 1989).

#### *Enriched sub-continental lithospheric mantle*

Pearce (1983) postulated a significant role of enriched sub-continental lithospheric mantle in the genesis of active continental margin magmas, aided by a subduction zone component.

Rogers & Hawkesworth (1989) explain the enriched character of CVZ lavas with partial melting of the enriched sub-continental lithospheric mantle triggered by slab derived fluids. They observed an eastward increase of  $^{87}\text{Sr}/^{86}\text{Sr}$  ratios and incompatible element concentrations in magma along a W-E transect at 22°S and suggested an increasing involvement of Proterozoic lithospheric mantle beneath the Brazilian Shield. In intra-plate settings, lithospheric mantle is generally considered to produce incompatible element enriched magmas at a low degree of partial melting. Opposed to that, however, degrees of melting are commonly high in subduction zones (5-25%, e.g. Miller et al., 1994). In supporting their interpretation, Rogers & Hawkesworth (1989) argue that their observed increase in  $^{87}\text{Sr}/^{86}\text{Sr}$  ratios parallels increased abundance of Sr, which is inconsistent with contamination at crustal levels where plagioclase is stable. Fractionation of plagioclase should have lowered the Sr content with increasing differentiation and contamination, since  $D^{\text{plag}}_{\text{Sr}} > 1$ .

Davidson et al., (1991), however, suggest that plagioclase is not stable in deeper levels of the 70 km thick CVZ crust and Sr would behave incompatibly. Additionally, Sr is not expected to decrease with increasing contamination by bulk mixing of mantle derived magmas and lower-crustal melt, since plagioclase neither is a fractionating phase in mafic liquids, nor is it a residual phase of anatectic crustal melting at high pressure.

Rogers & Hawkesworth (1989) argument of eastward increasing of Ta/Sm and decreasing Th/Ta reflecting increasing involvement of enriched sub-continental lithosphere is poorly constrained: High Ta/Sm and low Th/Ta ratios are also estimated for crustal compositions (Taylor & MacLennan, 1985) and could thus well be a crustal signature that introduced by contamination.

#### *Crustal Contamination*

Leeman (1983) first describes the potential influence of crustal structures on geochemical composition of subduction related magmas with respect to their density driven ascent. Beneath oceanic crust, primitive melts may rise to shallow depths of only a few kilometers whereas at active continental margin settings, magmas stagnate at the mantle-crust boundary. The continental crust acts as a "density filter", magmas have to differentiate toward more acidic, less dense liquids prior to further ascent.

Hildreth & Moorbath (1988) postulate a large contribution of crustal contamination in Andean magma genesis, since they observed a good correlation of trace element and isotope composition with thickness of the continental crust in SVZ. The probability of contamination, that is interaction of primitive magma with the crust, increases with the increasing crustal thickness.

Moreover, as the depth of the stagnation zone increases, the easier the lowermost crust will melt. In their model, ascending asthenospheric mantle-derived magmas accumulate at the mantle-crust boundary due to the decreasing density differences. Low crustal assemblages start to melt, mix with sub-crustal magmas and slowly homogenize. In this zone of melting, assimilation, storage and homogenization (MASH), "base-level" isotopic and chemical values

of erupted lavas are established. Furthermore, ascending magmas can subsequently be modified by mid to upper-crustal AFC processes.

Strong evidence for crustal contamination is based on oxygen isotopic compositions: while mantle  $\delta^{18}\text{O}$ -values are restricted to  $6.0 \pm 0.5$  ‰ SMOW, crustal rock, which partially derive from rocks that may have been exposed to long term low-temperature alteration display higher and more variable values. CVZ lavas are characterized by significantly elevated  $\delta^{18}\text{O}$ -values ranging from 7.3 to 14‰ SMOW (Harmon et al., 1984) suggesting a notable amount of assimilated crust. On the other hand, crustal material could also have been incorporated into the mantle source by subducted terrigenous sediments or crustal erosion (Stern et al., 1990, 1991). To raise  $\delta^{18}\text{O}$  ratios from mantle values to 7-8‰ SMOW, more than 10% of sediments need to be incorporated into the magma source in the mantle. This is unrealistic since trace element abundances would have been extremely affected by that process (James et al., 1982). Davidson et al. (1991) estimate de sedimentary input into the arc source of the CVZ between 1 and 2%.

Good correlation of Pb isotope composition of erupted lavas with Pb isotope composition of underlying basement, through which the ascending magma passed, also indicates a significant amount of crustal assimilation.

Davidson et al. (1991) create a model for magma genesis in the CVZ, in which the most primitive magmas found are themselves considered to be differentiates from mantle derived magmas based on Mg#, Ni-content and isotopic composition. These "base-line" magmas are generated in deep crustal MASH zones. During further ascent, two possible processes of magma evolution are recognized: (1) a "closed system" trend characterized by constant isotopic composition from basalts to dacites (e.g. Nevados de Payachata), and (2) an "open system" trend characterized by increasing  $^{87}\text{Sr}/^{86}\text{Sr}$  and  $^{18}\text{O}$  ratios with higher degrees of differentiation (e.g. Cerro Galan). The first trend is assumed to result from fractional crystallization, recharge and mixing processes in the upper crust without contamination recorded in isotope composition. However, crustal contamination cannot be completely ruled out, if the isotopic contrast between crust and magma is small. The second trend is considered to result from upper crustal AFC with assimilation of high  $^{87}\text{Sr}/^{86}\text{Sr}$  and  $^{18}\text{O}$ -rich material.

## 2 Geochemical variations in south Peruvian volcanic rocks (13°S-18°S): The role of crustal composition and thickening through time and space

### Abstract

The past ~29 m.y. of geologic history in the northern (13°S-18°S: southern Peru) of the Central Volcanic Zone (CVZ) has seen increasing and decreasing magmatic production rates and temporadic westward relocation of arc segments accompanied by abrupt chemical changes in the magmas. These changes can be linked to underlying basement, to crustal thickening at times of uplift in the Western Cordillera and Altiplano plateau, to mantle lithosphere at times of frontal arc migration to the west.

The magmatic-tectonic coupling is well seen in the history: provided by new Ar-Ar ages, major and trace element analyses, and Sr-Nd-Pb isotope analyses from 36 volcanic centers are presented in this Chapter. Ages for the southern Peruvian centers range from Eocene (45-40 Ma) to Holocene (<0.01 Ma). Therefore, volcanic rocks of this volcanic centers record the beginning as well as the peak of shortening and crustal thickening in the Upper Oligocene – Lower Miocene.

The compositions of andesites erupted before and after crustal thickening are similar in terms of major elements. However, post Miocene andesites show enrichment in trace elements (e.g. Ba, Sr), LREE (e.g. La, Sm) and depleted in HREE (e.g. Yb).  $^{206}\text{Pb}/^{204}\text{Pb}$ ,  $^{87}\text{Sr}/^{86}\text{Sr}$  isotopic ratios and  $\epsilon_{\text{Nd}}$  values change abrupt at 16°S and they are similar at any given sector. Pb-isotopes are independent of age (25-0 Ma) and Sr-Nd change with time.

Comparison of contamination indicators with age show that contamination was low in the Tacaza arc (from 20 Ma to 10 Ma), increased sharply in the Lower Barroso arc (between 10 to 3 Ma), and remained at a high level up to the Present frontal-arc since then. These younger volcanoes (< 3 Ma) show large ranges of Sr/Y, Sm/Yb ratios (e.g. Sara Sara, Huaynaputina). “Adakite” magmas in southern Peru are attributed to shallow subduction of Nazca ridge. The timing over which could this occur show that the subduction of the Nazca ridge is not enough shallow and hot to melt.

Depletion of Y and HREE from Miocene to Pleistocene volcanic rocks is caused by residual garnet of crustal assimilation after crustal thickening. Any involvement of slab melts in northern CVZ rocks to explain the “adakitic” signature is also excluded. The existing variations in lead isotopes in samples of similar ages to the north and south in southern Peru like the well-documented Neogene volcanoes of the central CVZ in northern Chile, support the notion that geochemical compositions in the magmas are controlled by the composition of the underlying basement.

### 2.1 Introduction

The Central Andes (CA) are characterized by extremely thick continental crust (up to 75 km beneath the Altiplano plateau, Yuan et al., 2002). The main crustal thickening in the CA occurred between ~29 to 15 Ma (Wörner et al., 2000). This study was undertaken to discover what differences exist in the nature of the arc andesites erupted before and after crustal thickening and what these differences reveal about the processes of crustal evolution in the magmatic arc in southern Peru. It has been established that Recent andesites from the central and southern CVZ have compositional characteristic suggesting a high degree of crustal contamination compared with equivalent rocks erupted in regions with thinner crust (e.g. Hildreth and Moorbath, 1988; Davidson et al., 1991). I focus in this Chapter on andesites erupted between ~29 Ma and Recent, a time span which brackets the events of crustal thickening and uplift in the Western Cordillera, Altiplano plateau (Isacks, 1988, Wörner et al., 2000, Sempere et al., 2004). Sampling was restricted to the northern Central Volcanic Zone. The area is in southern Peru (13° to 18°S and 68.5°- 75°W). In this area an increasing number

of sequence-stratigraphical studies as well as mining and exploration in volcanics of the Neogene units (Tosdal 1981; Kaneoka & Guevara, 1984; Marocco et al., 1985; Fornari et al., 2002; Sempere et al., 2004; Acosta, 2004; Flores, 2004; INGEMMET Boletines) have welcome the debate about names conventions. Discrepancies exist between sedimentary and volcanology community for Neogene sediments, ignimbrites and lava flows of which stratigraphic positions are unknown and geochemical characterization is incomplete.

Studies of volcanic centers in the CVZ have concluded that contamination of arc magmas occurs within the crust (e.g. Wörner et al., 1988; Davidson et al., 1991), but alternative mechanism have been proposed such as “source contamination” by subduction erosion of the continental margin (Stern 1991) by the influence of enriched, subcontinental mantle lithosphere in the source region (Rogers and Hawkesworth, 1989) or by melting of old subducted oceanic crust in the shallow subduction zones (Gutscher et al., 2000).

In this light, the purpose of this study is threefold. Firstly, I summarize the Cenozoic stratigraphical sequence and combine Wörner’s Ar-Ar ages with other data previously reported for Neogene volcanic unit in southern Peru between 13 and 18.2°S to invoke a consistent naming convention. The second purpose is to present new whole rock chemical and isotopic data for Upper Oligocene to Recent arc rocks in the northern CVZ. And the last purpose is to define and interpret the chemical and isotopic trends in these data in the framework of a ~29 Ma tectonic interval. The case is made that younger magmas (< 10 Ma) over the shallow subduction of the Nazca ridge are linked to “adakites” or slab melting (Gutscher et al., 2000).

My goal is to better constraint the magmatic evolution in Cenozoic times and understanding how compositional changes in arc volcanics relate to the geodynamic evolution of the northern CVZ.

## 2.2 Tectonic Setting

The tectonic evolution of the Central Andes margin throughout the Tertiary has been strongly influenced by the changes in the plate convergence rate, obliquity and steepness of the subducting plate. In the western South American subduction zone the convergence during Late Oligocene-Early Miocene (28.3 – 25.8 Ma) appears to have been dextral and being slightly oblique in Peru and moderately oblique in Chile. These kinematic changes are likely related to the plate reorganization. The Nazca-South America reconstructions at 20 Ma suggest slight obliquity at the interpolate boundary, being sinistral in Peru and dextral in Chile (Somoza, 1998) (Fig. 1.5b).

Geological studies of the western Andean escarpment in the southern Peru have identified a discontinuous, punctuated history of uplift of the Western Cordillera. Sempere et al. (2004) proposed two major stages of sedimentation based on studies of Moquegua Group sediments and ignimbrites ages. The first stage of sedimentation was from 30 to 15 Ma and the second stage between ~10 and 2.7 Ma. Erosion has prevailed everywhere since 2.7 Ma. The age at which the present crustal thickness was established in southern Peru is hard to define directly. However, it is reasonable to assume that it corresponds to the cessation of the sedimentation in the western Andean escarpment.

Kay et al. (1999) suggested that the steep REE pattern in the younger volcanics of the southern CVZ indicate that garnet was stable in the crustal source region, and hence a thick crust (high pressure) was established in the Pliocene.

The timing of the subduction of the Nazca ridge is important because ridge subduction would induce flattening of the subduction angle, which in turn could lead to crustal thickening by increasing compression in the upper plate, and to migration or broadening of the zone of arc magmatism. Hampel (2002) proposed a model that the subduction of the northeastern end of the Nazca Ridge began ~11.2 Ma at 11°S. The Present “flat-slab” configuration north of the

CVZ is at 15°S (Fig. 2.1). Another piece of evidence in support of this model may be inferred from the correlation of the Nazca Ridge with the associated segment of low-angle subduction and the cessation of magmatic arc activity. At present, the boundary between active and ceased volcanism in the south and in the north, respectively, is located in the landward continuation of the ridge, but may have gradually propagated southward due to the lateral movement of the ridge.

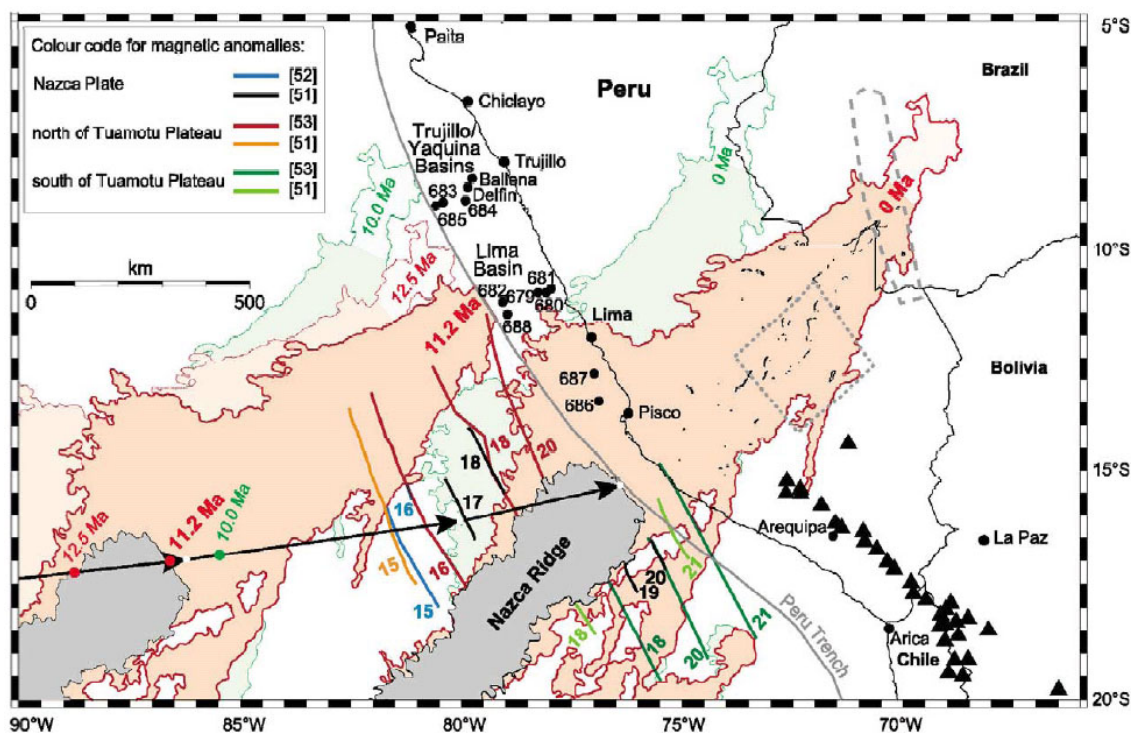


Fig. 2.1. Migration history of the Nazca Ridge (from Hampel, 2002)

### 2.3 Description of Cenozoic units and sampled volcanic centers

The volcanoes and volcanic units before, syn and after crustal thickening of southern Peru (Fig. 3.2) could be subdivided into different stratigraphic units using radiogenic age (e.g.  $^{40}\text{Ar}/^{39}\text{Ar}$  from Wörner unpublished data), bibliographic information, contact relations and morphological criteria observed in the field and satellite images (Fig. 2.3).

#### 2.3.1 Middle Eocene - Lower Oligocene, ~ 45 to ~30 Ma (Lower Moquegua Formation, Anta Group)

The Lower Moquegua Formation outcrops along the western Andean escarpment and is characterized by its reddish color sandstone and finer grain size sediments (mud, silt and clay). An ignimbrite layer close to the top of the sequence (in Moquegua) has been dated at ~30 Ma by Marocco et al. (1985) and ~27 Ma (Sébrier et al., 1988). To the top of this Formation near Cuno Cuno a marine section is exposed. These sediments were probably deposited during a marine transgression in the Late Eocene (Sempere et al., 2004).

While the Anta Group was deposited along the NE margin of the Western Cordillera, lithologically present alluvial and fluvial deposits; this sequence is synchronous with calc-alkaline andesitic and dacitic volcanism ~37-38 Ma toward the base, and alkaline toward the top ~29 Ma. This unit could be deposited in a compressive and transpressive deformation around 44-40 Ma (Carlotto, 1998).

### 2.3.2 Upper Oligocene - Middle Miocene, ~30 to ~15 Ma (Upper Moquegua Formation, Tacaza Group)

The Middle Moquegua Formation consists of sheet-and debris-flows of reworked volcanic material, lacustrine sediments, and ignimbrites also deposited on the western Andean escarpment. Within this Formation thick ignimbrites are intercalated with fine sediments called “Huaylillas Formation” (Tosdal et al., 1981). They have been dated in Moquegua at  $24.43 \pm 0.17$  Ma and in Puquio at  $22.2 \pm 0.34$  Ma (Wörner unpublished data). Similar ages of this ignimbrite are known in northern Chile (e.g. Oxaya ignimbrite, Wörner et al., 2000).

The Tacaza Group was developed along the Western Cordillera and particularly along its NE margin. It presents an intercalation of breccias, altered lava flows, alluvial and fluvial strata sequences and ignimbrites. Multiple intrusions of Tacaza time are observed along the Cusco-Lagunillas-Laraqueri-Abaroa faults system. The magmatic activity of this Group took place around 29-15 Ma (Clark et al., 1990a; Fornari et al., 2002, Mamani et al., 2004).

Some Tacaza volcanic centers of this age ~20 to ~15 Ma still form circular shield-like or amphitheater-shaped structures. Their central depression is often erroneously interpreted as caldera collapse. Erosion has leveled the structure to about 500-600 m above the base. Lava

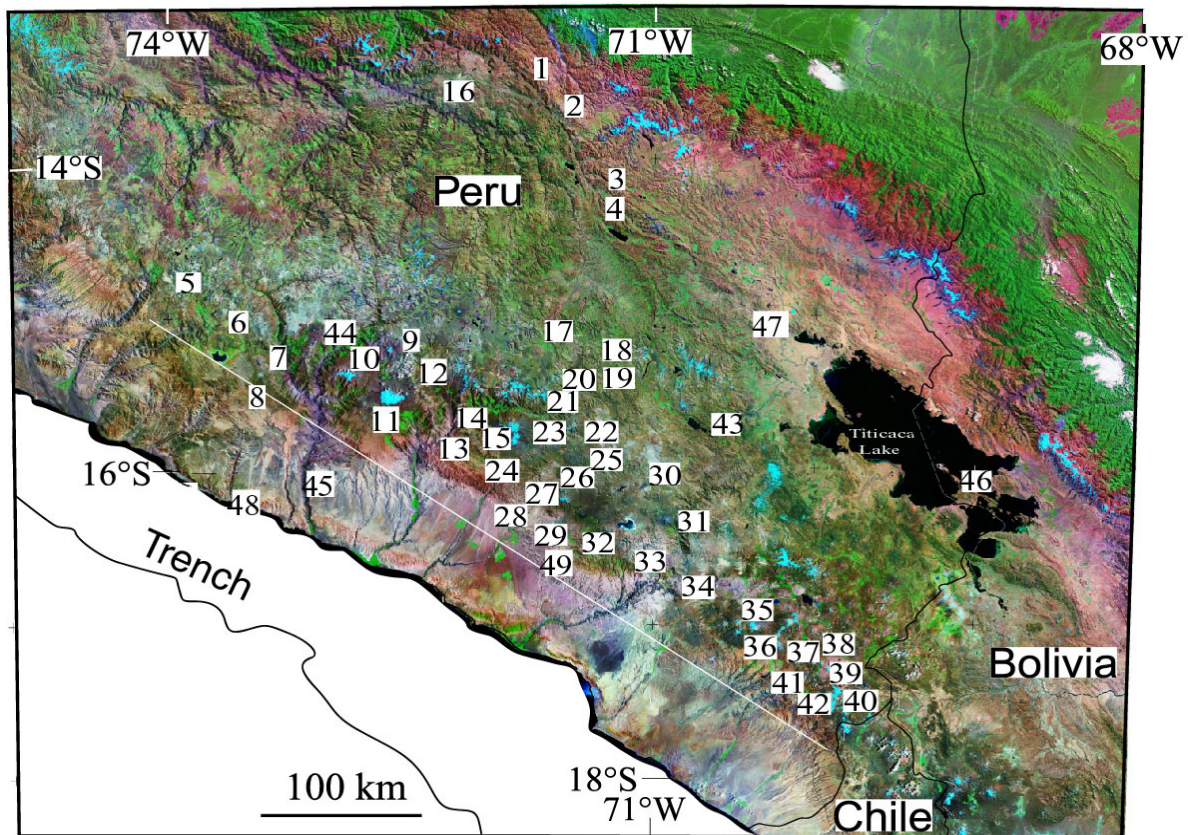


Fig. 2.2. Sample locations in southern Peru: **Active volcanic (0 - 0.8 Ma)** 7) Sara Sara, 12) Andagua, 13) Huambo, 45) Iquipi, 21) Chivay, 28) Nicholson, 15) Sabancaya, 27) Chachani, 29) El Misti, 31) Ubinas, 33) Huaynaputina, 34) Ticsani, 35) Tutupaca, 36) Yucamane, 37) Casiri, 38) Titiri, 39) Kere, 40) Purupurine. **Upper Barrosos (0.8 - 3 Ma)** 9) Firura, 10) Antapuna, 11) Coropuna, 14) Hualca Hualca, 26) Paquetane. **Lower Barrosos (3- ~10 Ma)** 8) Yarihuato, 20) Tuti, 22) Huarancante, 17) Morane, 23) Ananto, 24) Hualto, 25) Huacullani, 30) Salinas, 32) Pichu Pichu, 41) Tarata. **Tacaza (15- ~25 Ma)** 5) Puquio, 6) Cora Cora, 18) Condoroma, 19) Colca, 43) Sta. Lucia, 44) Cotahuasi. **Backarc (< 1 Ma)** 1) Pisaac, 2) Rumicolca, 3) Oroscocha, 4) Quinsachata. **(15 - 6 Ma)** 46) Lago Titicaca, 47) Chignaya. **Anta (~40 Ma). Proterozoic and Paleozoic basements** 42) Huacano, 49) Arequipa, 48) Pescadores. White line is the distance used in the chemical diagrams.

flows consist of aphanitic to porphyritic andesite. Many of the lavas are altered. However, samples collected for chemical analysis from Puquio, Cora Cora, Condoroma volcanoes were unaltered.

### **2.3.3 Upper Miocene – Lower Pliocene, ~10 to ~3 Ma (Lower Barroso Formation)**

Lower Barroso Formation developed along the western Cordillera and preserves the eroded stratovolcanoes structures with slightly erosion and hydrothermal alteration in the interior of the stratocones. The eroded lavas from such volcanoes intercalated with mud are observed toward the west of Lower Barrosos volcanoes (e.g. within Chili, Challahuaya valley). Tosdal et al. (1981) reported a plagioclase age for Cerro Barroso of  $5.3 \pm 0.3$  Ma and  $7.0 \pm 0.4$  Ma plagioclase age,  $3.3 \pm 0.1$  Ma whole rock age for andesites near Cerro Barroso. Bellón and Lefèvre (1976) reported ages of 4.45 and 4.10 Ma for stratovolcanoes northeast of Arequipa. Klinck et al. (1986) obtained ages: from Hualto volcano ( $6.1 \pm 0.6$  Ma), Ananto ( $9.5 \pm 0.6$  Ma), Huarancante ( $6.7 \pm 0.7$  Ma) and Tuti ( $5.3 \pm 0.7$  Ma). Kaneoka & Guevara (1984) reported an age of 7 Ma for Salinas volcano and 6 Ma for volcanoes near Lake Titicaca and between 6 and 3 Ma for volcanoes around Tarata.

Stratovolcanoes of Lower Barroso arc are comprised of flat shieldvolcanoes. Exposures suggest that most of the volcanoes are made up of andesites and dacites. They represent major volumes. Based on their state of erosion they fall into this group of stratovolcanoes and represent its largest examples of the Barroso arc. The samples collected correspond to Yarihuato, Huarancante, Morane, Ananto, Hualto, Huacullani, Pichu Pichu, Salinas, Tarata and many other deeply glaciated volcanoes.

Mio-Pliocene ignimbrite centers are not observed; pumices were taken from the ignimbrites units of the Lower Barroso Formation, these samples were collected in Condoroma, Pampa Cañahuas, Pausa, Caraveli, Cotahuasi, Ocoña, Yura, Sumbay, Chachani and Aguada Blanca (see on CD).

### **2.3.4 Pliocene, ~3 to ~2 Ma (Sencca Formation)**

The Sencca Formation is deposited between the Western Cordillera and NW of the Altiplano plateau, consist of lacustrine sediments and ignimbrite flows filling the incised valleys (e.g., Sencca, Yauri basins). We observed the Sencca ignimbrite on the top of Lower Barroso lavas near the Sencca village. This ignimbrite is correlated to the 2.72 Ma Lauca-Peréz ignimbrites of northern Chile (Wörner et al., 2000). For this study pumices of similar age were taken in Maure, Moquegua, Chuquibamba, Salamanca and Caraveli.

### **2.3.5 Upper Pliocene to Pleistocene, 3 to 0.8 Ma (Upper Barroso Formation)**

The Upper Barroso Formation represents recently active volcanoes along the Western Cordillera. Some of its stratocones (e.g. Coropuna, Hualca Hualca and Chachani) have been active up to the Pleistocene and Holocene. Kaneoka & Guevara (1984) reported ages for Antapuna volcano of 1.19 and 1.2 Ma. Klinck et al. (1986) obtained ages from Hualca Hualca lavas (1.1 Ma) and Chivay lavas (0.9 Ma). The typical evolution is characterized by continuous eruption of largely similar andesite or rhyo-dacite lava composition. Other volcanoes with such characteristic are Firura, Paquetane. Our sampling covers lavas from all volcanoes mentioned. The lavas are generally fresh andesites.

### **2.3.6 Holocene Volcanoes < 0.01 Ma**

The Recent volcanic arc groups the active volcanoes. They are ~230 km to the east of the Peru-Chile trench and ~150 km above the Benioff-Wadati plane (Cahill and Isacks 1992).

Most of the youngest and better known volcanoes: active with historical eruption <0.5 Ma (Sabancaya, El Misti, Ubinas, Huaynaputina, Ticsani, Tutupaca, and Yucamane); and

dormant < 0.8 Ma (Sara Sara, Ampato, Casiri, Purupurine, Titire, and Kere) are stratocones with symmetrical shape and central vent. The lavas from these volcanoes consist of hornblende-plagioclase andesites to dacites with a generally unaltered, glassy groundmass. The long lived (< 3 Ma) Chachani dormant volcano is a stratovolcano complex of dacitic domes, andesitic lavas and with pyroclastic surface.

Other Pleistocene to Recent volcanoes are:

#### *Shoshonites*

Glassy volcanic rocks (< 0.6 Ma) erupted from fissures associated with fault related to a change in the regional stress system in the back-arc, such as Quinsachata, Oroscocha, Rumicolca, and Pisaac volcanoes.

#### *Monogenetic*

Andesitic lavas (< 5000 yr B.P) erupted from small cinder cones, which produced steep-sided cones and sometimes ribbonlike flows (de Silva and Francis, 1991), such as Andaguas (Puca Mauras, Tischo, Jenchanya, Ninamama, Chilcayoc), Huambo, Cerro Nicholson, Chivay, Iquipi and many others.

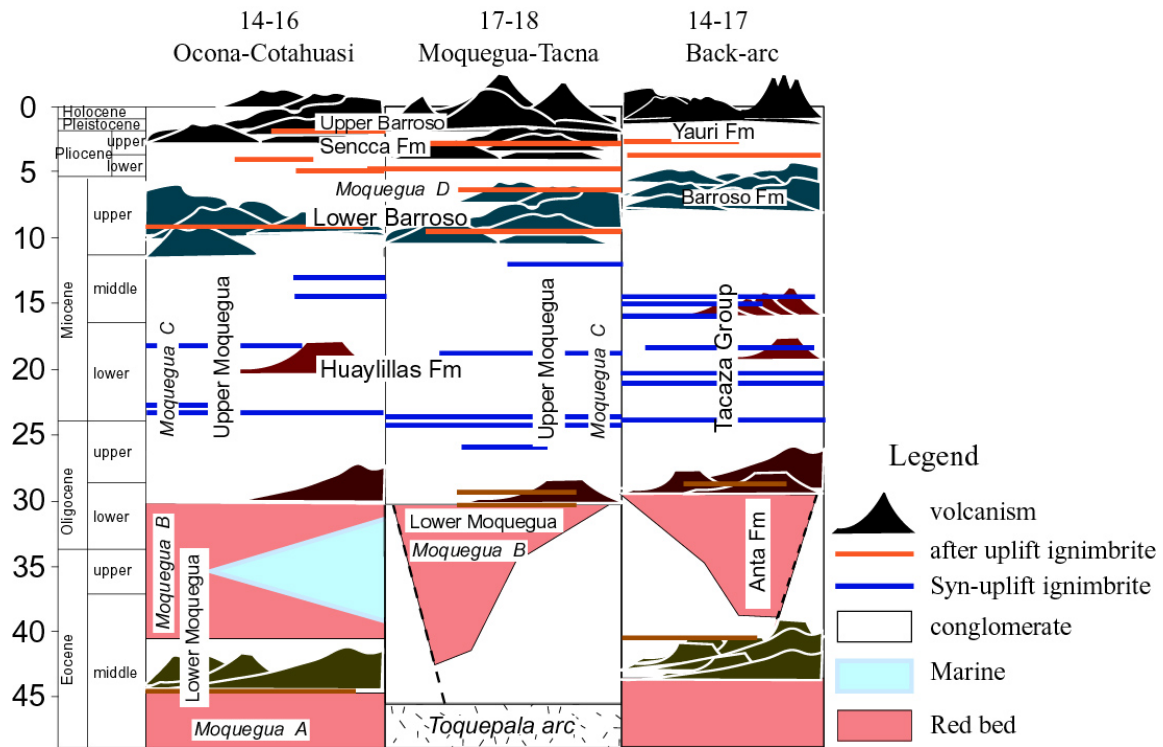


Fig. 2.3. Schematic profiles of Cenozoic stratigraphic units in southern Peru. After Tosdal et al. (1981), Kaneoka & Guevara (1984) and Sempere et al. (2004). In italic are the Moquegua stratigraphic units presented by Sempere et al. (2004).

## 2.4 Results

### 2.4.1 Geochemistry

The geochemical data set on which this discussion is based contains nearly 625 analyses from 36 volcanic centers and ignimbrites. Representative data from each center and the full data set is available on CD (opening: database and samples location).



## Major elements

All Neogene samples of this study in southern Peru plot in the calc-alkaline field of the AFM-diagram (Fig. 2.4). The vast majority of samples form a linear array displaying a typical calc-alkaline trend. However, this trend has two groups: lavas with more  $\text{FeO}_{\text{tot}}$  and  $\text{MgO}$ , and ignimbrites with higher content in alkalis.

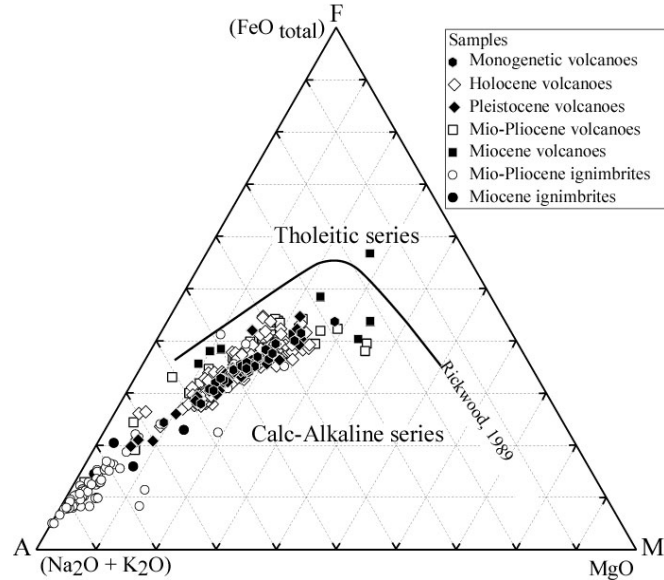


Fig. 2.4. AFM-diagram after Rickwood (1989) of southern Peru data

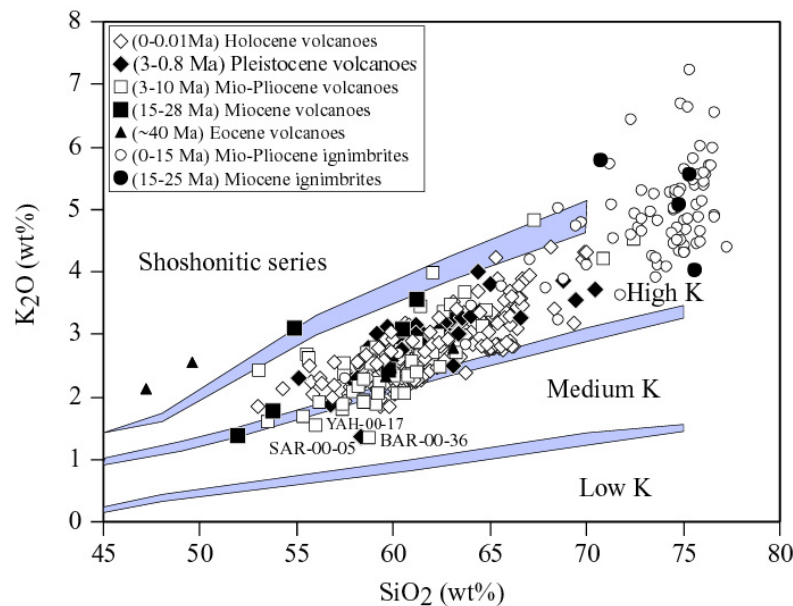


Fig. 2.5. The subdivision of subalkalic rocks diagram of volcanic rocks from southern Peru. After Rickwood et al. (1989).

The samples plot mainly in the “high K” field of the  $\text{K}_2\text{O}$  vs.  $\text{SiO}_2$  diagram (Fig. 2.5). Exceptions are Eocene lavas, which belong to the shoshonitic series. SAR-00-05 (Sara Sara), BAR-00-36 (Lower Barroso- near rio Tambo), YAH-00-17 (Yarihuato) fall into the “medium K” fields. A few Eocene samples plot in the shoshonitic field. The most basaltic lavas are rather rare and have  $\text{SiO}_2$  contents down to 54%. The Miocene lavas lack samples with silica

content higher than ~66 wt%. The ignimbrites display a very restricted silica range from 72-77 wt% SiO<sub>2</sub> and highly variable potassium content at a constant SiO<sub>2</sub> content. Total alkalis versus silica are plotted in the TAS diagram (Fig. 2.6). The main data define a more or less linear array from basalt to rhyolite. In contrast to the K<sub>2</sub>O vs. SiO<sub>2</sub> diagram, the ignimbrites do not deviate from this trend due to its lesser Na<sub>2</sub>O content at higher silica content.

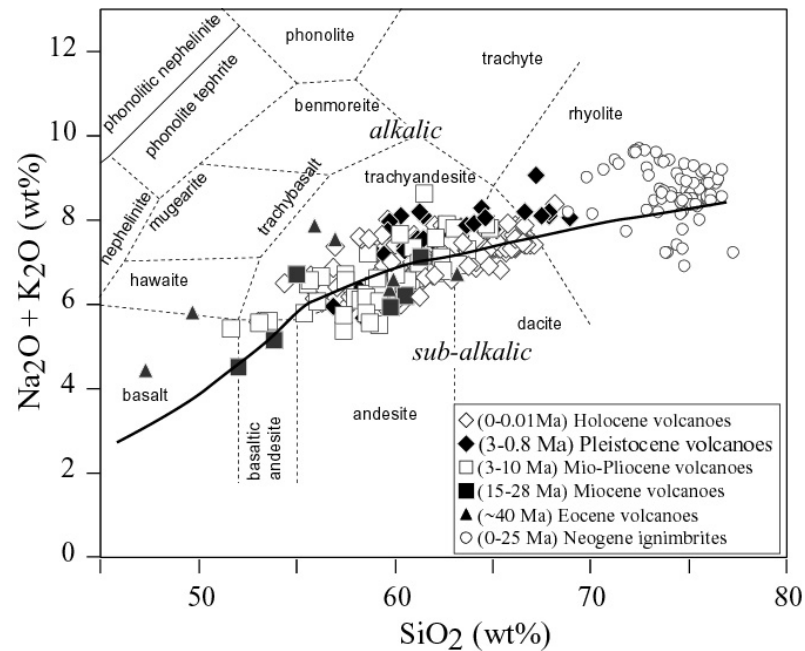


Fig. 2.6. TAS diagram after Wilson (1989) of southern Peru data.

There is little variation in major element composition with age. Figure 2.7 shows that Holocene, Pleistocene and Mio-Pliocene volcanoes are more variable in major elements contents and display the largest ranges than Miocene and Eocene volcanoes. No clear trend of TiO<sub>2</sub> and MgO are observed between the Neogene volcanoes.

### Trace elements

Spatial and temporal variations of selected trace elements are shown in Fig. 2.8. Elements have been analyzed by XRF (e.g. Rb, Sr, Ba, Y) and ICPMS (e.g. Nb and Zr). Concentration of the LIL elements Ba and Sr clearly increase with younger lavas. Contents of Zr and Nb do not change in the younger lavas. Y concentrations are highest in Miocene and Mio-Pliocene lavas and the minimum Y values decrease from Mio-Pliocene to present.

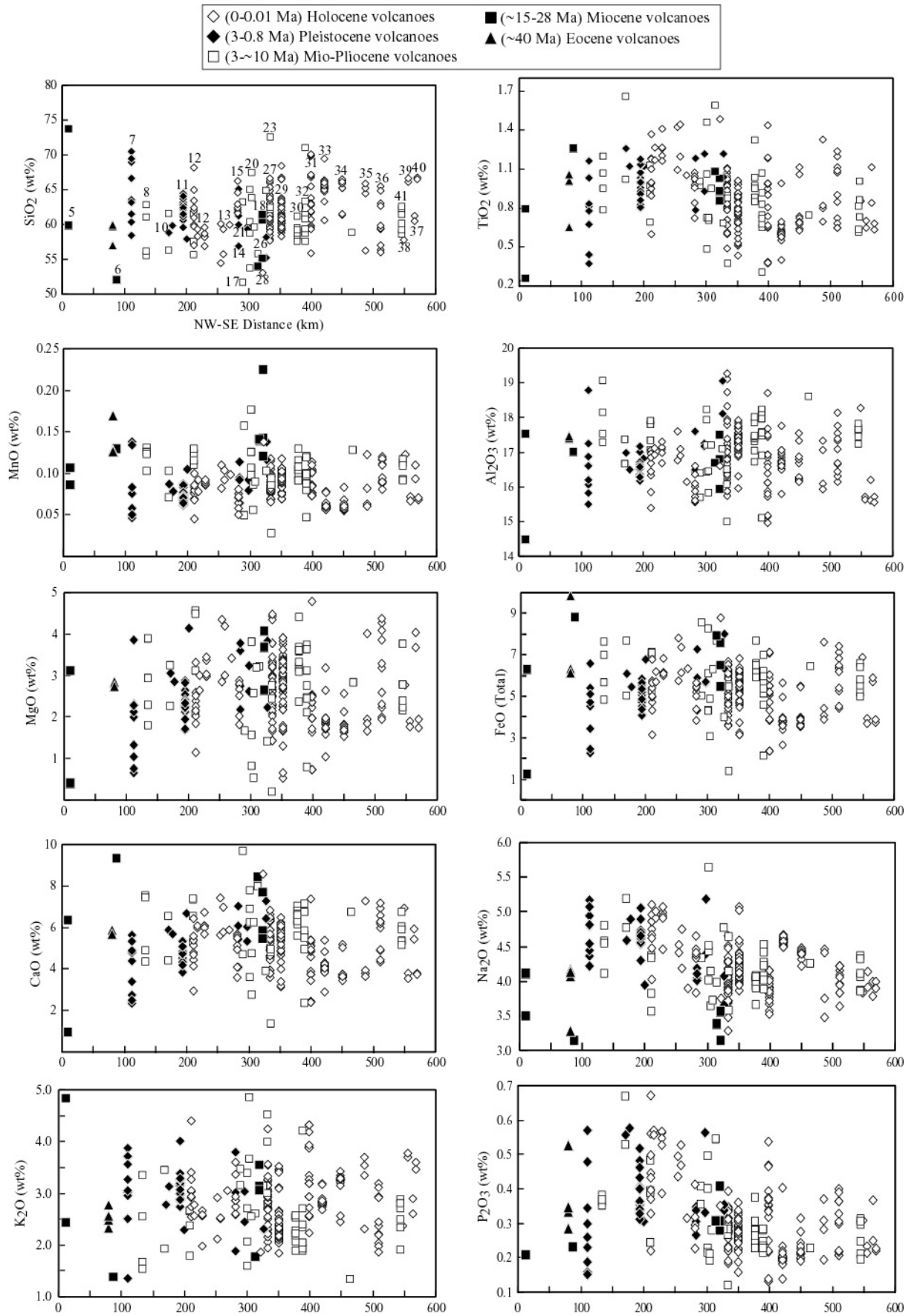


Fig. 2.7. Major elements of samples from southern Peru versus distance between volcanoes (see distance line in the Fig. 2.2). The numbers represent the volcanoes names (see Fig. 2.2).

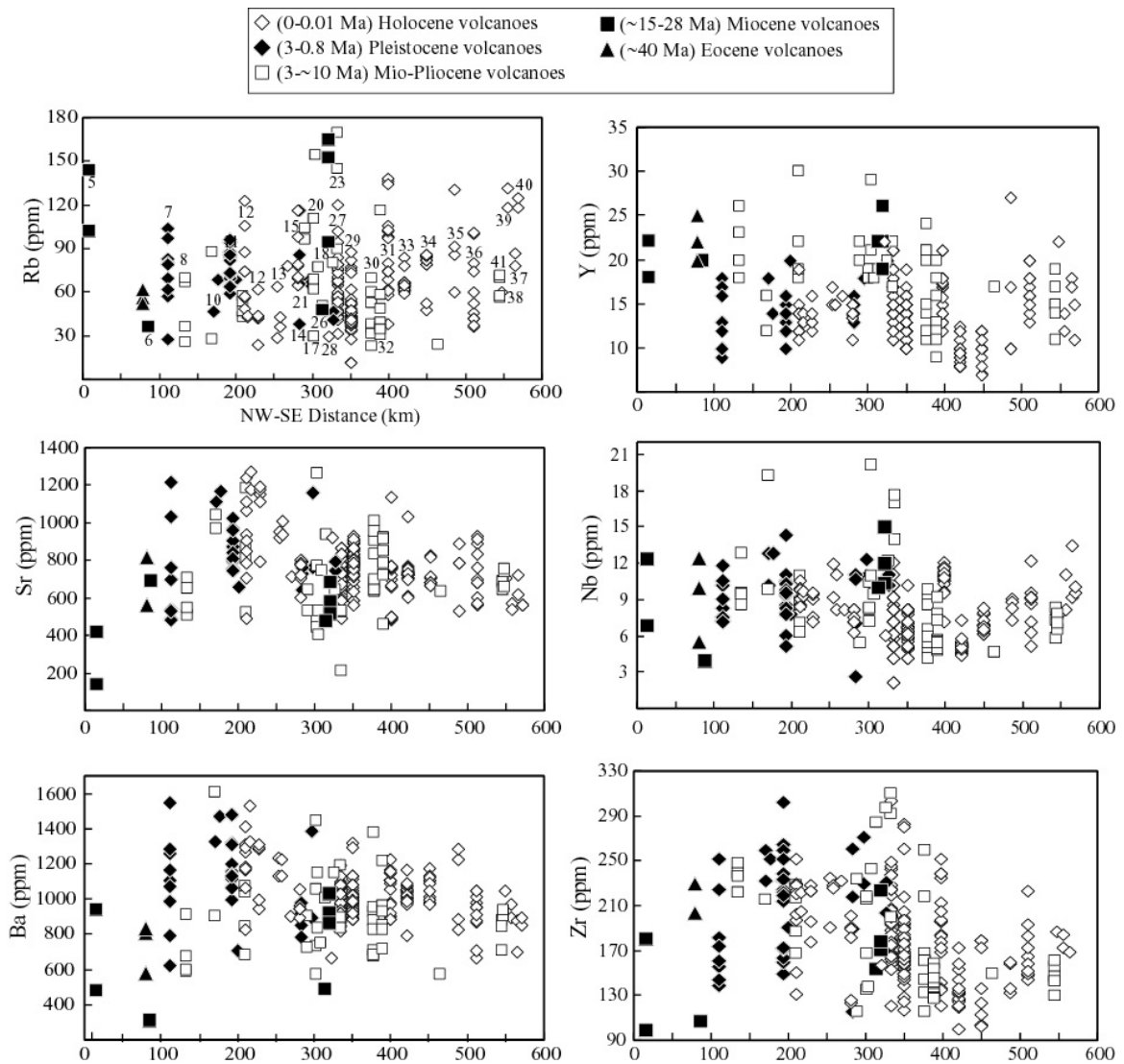


Fig. 2.8. Trace elements of samples from southern Peru versus distance between volcanoes.

### Spiderdiagrams

Primitive mantle normalized spiderdiagrams (primitive mantle values from McDonough et al., 1992) of trace elements plus potassium and titanium for Neogene volcanoes are shown in Fig. 2.9.

#### *Lavas*

The lavas display a relatively uniform typical arc signature characterized by strong enrichment of Rb, Ba, K and Th combined with a marked depletion at Nb and Ta (e.g., Pearce, 1983). U is also enriched, but shows highly variable concentrations. Samples from the Plio-Pleistocene to Holocene volcanoes display positive Sr anomalies. The Sr troughs occur within the Miocene and Eocene lavas (Fig. 2.9).

#### *Ignimbrites*

Similar to the lavas, both the Mio-Pliocene and Miocene ignimbrites display pronounced Nb-Ta depletion (see Fig. 2.10), probably reflecting the large amount of crustal material in their evolution. Negative Sr anomalies are strongly developed, especially in the younger ignimbrites. The ignimbrites also have marked Ba and Ti troughs.

### Shoshonites

Shoshonite backarc samples have positive Ba anomalies compared to the Pleistocene and Holocene lavas. Ta is not depleted as in the lavas from the arc. They are higher in La, Ce anomalies and lower in Y than the lavas from the arc.

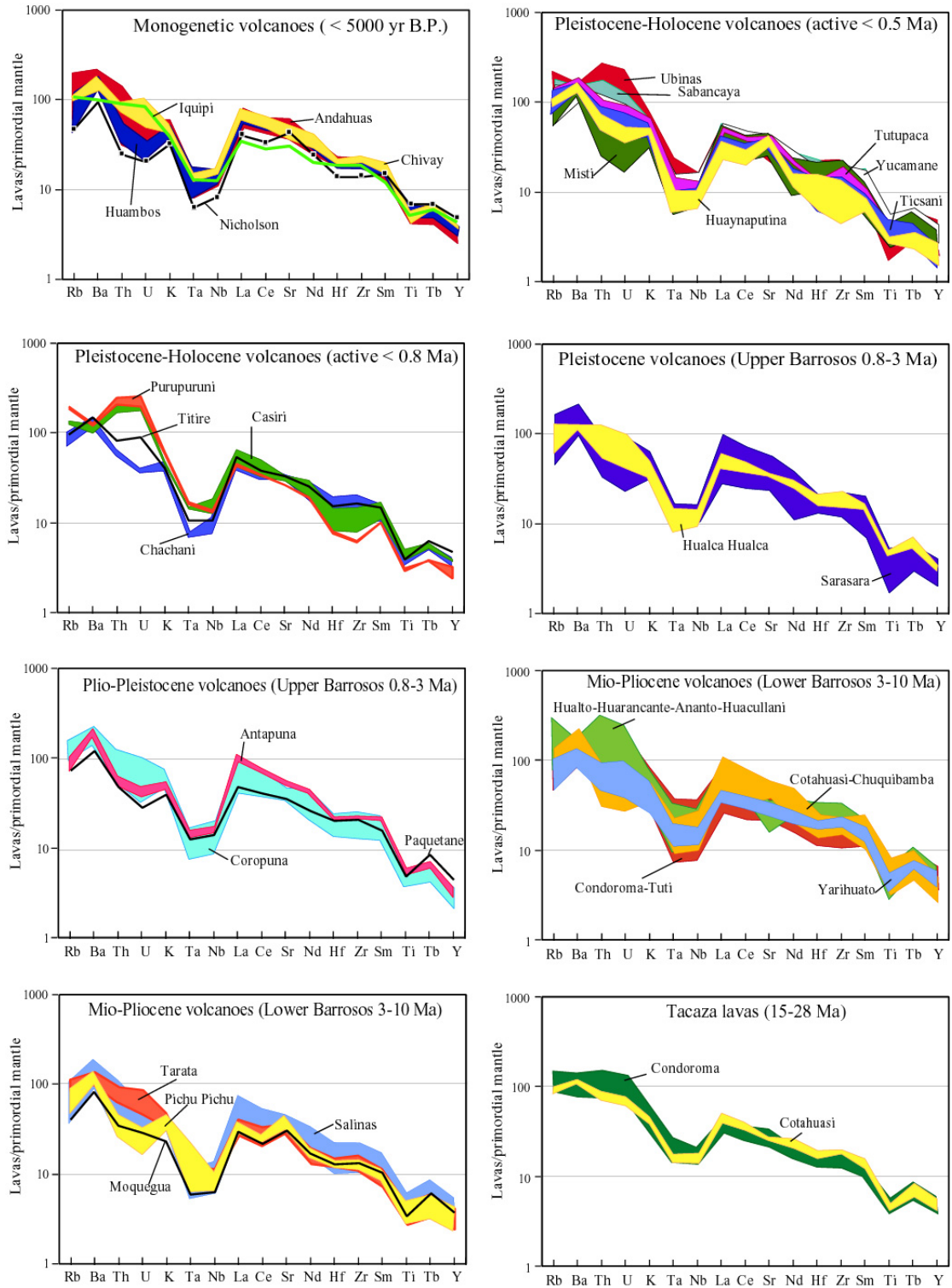


Fig. 2.9. Primitive mantle normalized concentrations of trace elements plus K and Ti of each volcano. Normalization factors are from McDonough et al. (1992).

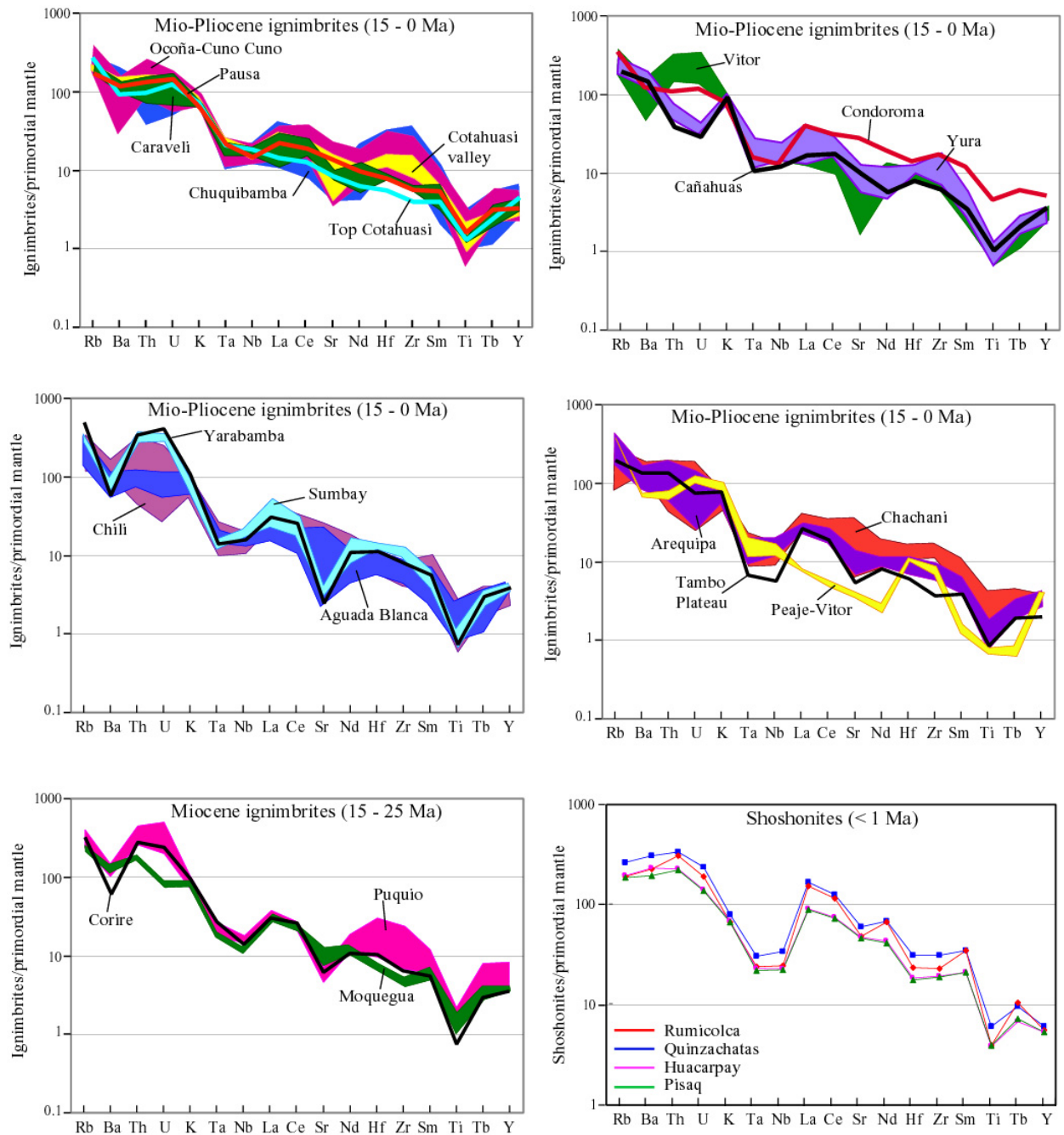


Fig. 2.10. Primitive mantle normalized concentrations of trace elements plos K and Ti of Neogene ignimbrites. Normalization factors are from McDonough et al. (1992).

### Rare earth elements (REE)

The overall shape of chondrite normalized (McDonough and Sun, 1995) REE element pattern of each volcano with respect to time and space will be described first in this section. Then, element ratios will be evaluated quantitatively.

#### Description of REE pattern

The slope of the REE patterns become steeper with decreasing age of the volcanoes (Fig. 2.10), as the HREE become more depleted and the concentrations of LREE are higher and more variable. No negative Ce anomaly or systematic trend in size and no Eu anomalies is observed in the lavas. A conspicuous feature of most samples is a flat HREE pattern (except

for Monogenetic, Huaynaputina and Ticsani volcanoes). All ignimbrites samples show marked negative Eu-anomalies and depletion in HREE (Fig. 2.11).

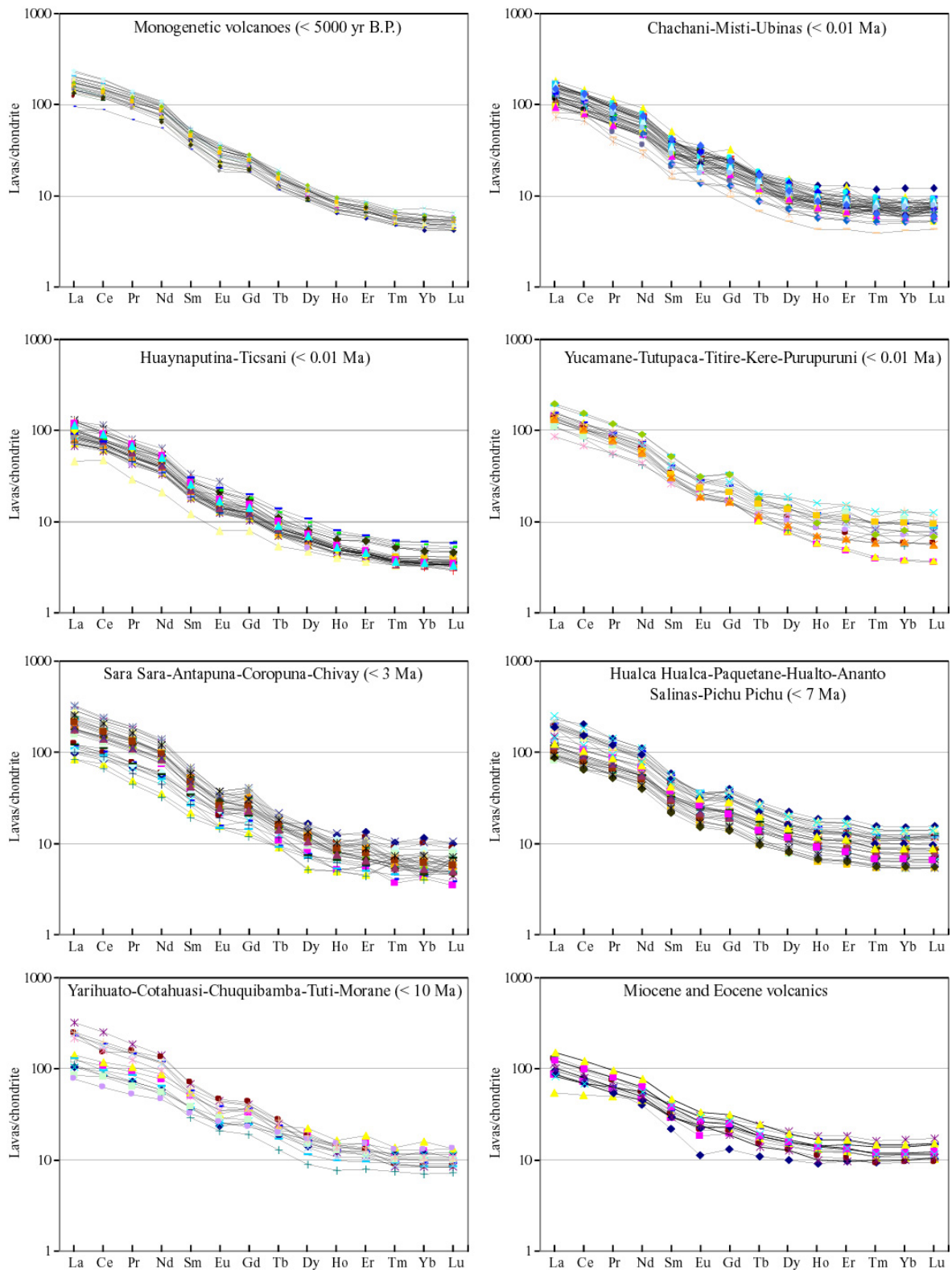


Fig. 2.11. Chondrite normalized REE-pattern of lavas. Normalized constant are taken from McDonough and Sun (1995). All samples have been analyzed by ICPMS.

*Eocene and Miocene volcanoes*

The Eocene and Miocene lavas display a relatively flat pattern with enrichment of LREE and a negative Eu-anomaly. They have the largest concentration of HREE (e.g. Ho, Er, Tm, Y) of all samples studied and the HREE also are parallel.

*Mio-Pliocene volcanoes*

The pattern of these volcanoes is very uniform, which display elevated pattern with LREE enrichments.

Lavas of Yarihuato, Cotahuasi, Chuquibamba, Tuti and Morane volcanoes have fixed HREE and variable LREE. Samples of Hualca Hualca, Paquetane, Hualto, Ananto, Salinas and Pichu Pichu volcanoes have parallel REE.

*Pliocene-Pleistocene-Holocene volcanoes*

The Pliocene to Holocene lavas show enrichment of LREE and depleted HREE concentrations compared to all samples.

Samples of Sara Sara, Antapuna, Coropuna, Chivay volcanoes have parallel LREE and fixed HREE. Lavas of Yucamane, Tutupaca, Titire, Kere, Purupuruni volcanoes show variable HREE. Ticsani and Huaynaputina lavas have parallel LREE, while Chachani, El Misti and Ubinas lavas have variable MREE and HREE.

*Mafic volcanoes (monogenetic)*

Mafic lavas show enrichment of LREE (principally La, Ce, Pr, Nd) and depleted HREE (Er, Tm, Yb, Lu) concentrations. They have fixed LREE and variable HREE.

*Ignimbrites*

Samples of Miocene and Mio-Pliocene ignimbrites show a trough at Dy-Er and elevated Yb and Lu concentrations, forming a dish-shaped pattern. Most ignimbrites of all ages display marked negative Eu anomalies.

*Shoshonites*

As seen in the Figure 2.12, REE pattern of shoshonites show LREE enrichment, variable LREE levels, small Eu anomalies. HREE elements are like the Mio-Pliocene lavas.



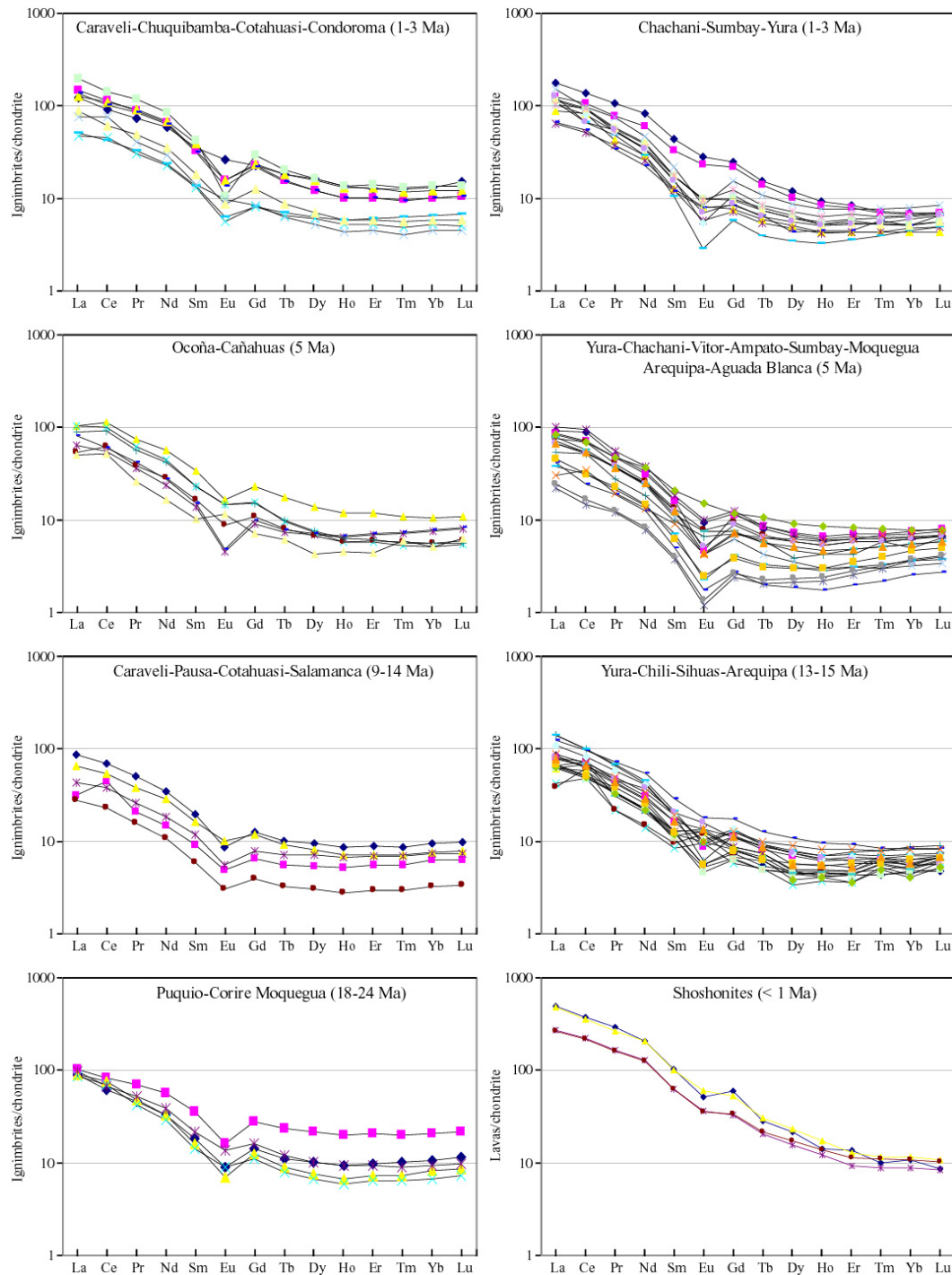


Fig. 2.12. Chondrite normalized REE-pattern of Neogene ignimbrites and Pleistocene shoshonites. Normalized constant are taken from McDonough and Sun (1995). All samples have been analyzed by ICPMS.

#### 2.4.1.1 Temporal variations of element ratios

In order to quantify the slope of REE pattern through time, selected chondrite normalized REE ratios are plotted versus age in Fig. 2.13. Along arc, maximum La/Yb ratios increase from Eocene to Holocene rocks. Also, ratios become more variable with younger ages. Sm/Yb ratios and La/Yb ratios resemble the same pattern in time. They show a pronounced increase with decreasing time.

La/Sm ratios have a base-line constant ( $La/Sm = 4$ ). The lavas display a trend that increase slightly with decreasing age. The ignimbrites exhibit high La/Sm ratios than the lavas.

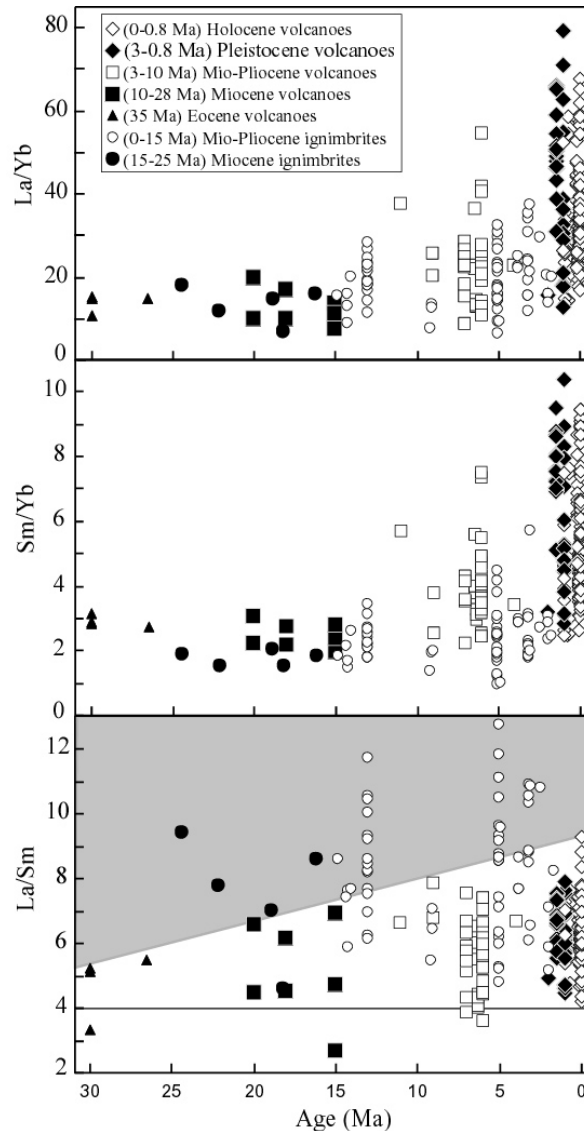


Fig. 2.13. REE ratios of lavas and ignimbrites of southern Peru.

### 2.4.1.2 Isotopes

#### Sr and Nd isotopes

Sr and Nd isotopes in igneous rocks can be used to determine the presence or absence of recycled continental crust. They are a powerful tool for constraining the age of magmatic sources and distinguishing between mantle, upper-crustal and lower-crustal sources (Hawkesworth and van Calsteren, 1984).

As shown in Fig. 2.14, variable  $^{87}\text{Sr}/^{86}\text{Sr}$  ratios and  $\epsilon_{\text{Nd}}$  values are observed in Peruvian volcanoes (PV). The Eocene (Anta lavas) and Miocene lavas from Cora Cora, Colca volcanoes have the highest  $\epsilon_{\text{Nd}}$  and lowest  $^{87}\text{Sr}/^{86}\text{Sr}$ . They overlap with data from the Southern Volcanic Zone (SVZ) of Neogene volcanoes. Nd-isotopes ratios decrease and Sr-isotopes ratios increase with time for volcanic centers between  $14^{\circ}\text{S}$  and  $16^{\circ}\text{S}$  (PV-A). High  $^{87}\text{Sr}/^{86}\text{Sr}$  ratios and low  $\epsilon_{\text{Nd}}$  ratios are observed between  $16^{\circ}\text{S}$  and  $18^{\circ}\text{S}$  (PV-B) with volcanoes toward the northeast of Arequipa city (El Misti, Salinas, Chachani, Pichu Pichu, Paquetane) having the highest Sr-isotopes and lowest Nd-isotopes ratios.

the Peruvian ignimbrites (PIG-A) around Puquio, Cotahuasi, Salamanca, Chuquibamba areas from 14°S to 16°S have high  $\epsilon_{Nd}$  values. Low Nd-isotope ratios are observed in PIG-B across the Moquegua region between 16.5°S and 18°S. The lowest  $\epsilon_{Nd}$  values have been analyzed for the Arequipa ignimbrites (Fig. 2.14).

Monogenetic volcanoes (e.g. Andagua and Huambo), and Shoshonite volcanoes (Rumicolca, Oroscocha, Quinzachata, Pisaq) have intermediate Sr-Nd isotopes ratios compared to all samples from southern Peru.

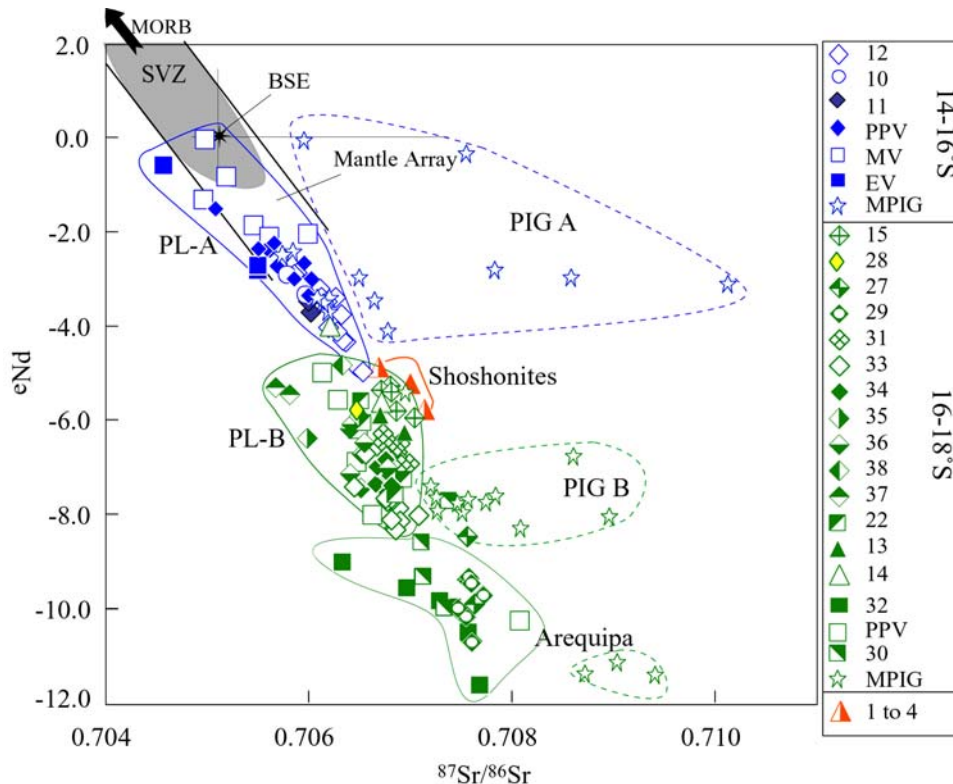


Fig. 2.14.  $^{87}\text{Sr}/^{86}\text{Sr}$  versus  $\epsilon_{Nd}$  of samples from southern Peru compared to Southern Volcanic Zone (SVZ) and Middle Oceanic Ridge Basalt (MORB). BSE is bulk silicate earth. Data of SVZ are taken from Kay et al. (2005). Lines mark the Mantle Array. PIG-A Peruvian Ignimbrites and PV-A Peruvian Volcanoes between 14°S and 16°S. PV-B Peruvian Volcanoes and PIG-B-Peruvian Ignimbrites between 16°S and 18°S. Number of the symbols in Fig. 2.2.

### Spatial and Temporal variations of Sr-Nd isotopes

$^{87}\text{Sr}/^{86}\text{Sr}$  and  $^{143}\text{Nd}/^{144}\text{Nd}$  analysis cover uniformly the area along the arc of southern Peru (see database).

In Fig. 2.15  $^{87}\text{Sr}/^{86}\text{Sr}$  ratios divides the arc into different groups. Further can be distinguished between lavas and ignimbrites. The northernmost groups of lavas (0 and 350 km of arc measured from NW tip) has a Sr-isotopes = 0.7045-0.707. Further south from 300 to 600 km arc distance, a decrease in  $^{87}\text{Sr}/^{86}\text{Sr}$  ratios 0.708-0.7065 to 0.707-0.706 is observed.

The ignimbrites have higher  $^{87}\text{Sr}/^{86}\text{Sr}$  ratios (up to 0.71) than the lavas and the lowest Sr-isotope ratio (0.7055) is observed between 0 and 300 km.

The  $^{143}\text{Nd}/^{144}\text{Nd}$  ratios display two groups independent of rocks type along the arc. The northern group (from 0 to 350 km) has higher ratios (0.5124 to 0.5127), while the second cluster further south (200 to 600 km) shows lower ratios (0.5124-0.5120). Monogenetic volcanoes lie in both groups and shoshonites display small differences for Nd-isotope ratios.

If plotted against age (Fig. 2.16)  $^{87}\text{Sr}/^{86}\text{Sr}$  ratios increase and  $^{143}\text{Nd}/^{144}\text{Nd}$  ratios decrease over time independent of spatial affiliation. The strongest variations of Sr-Nd isotopes ratios are

observed in Mio-Pliocene lavas (~7 Ma) and in Miocene ignimbrites (~15 Ma). Lavas between 10 and 0 Ma display more variable Sr-Nd isotope ratios than the older lavas (15 -30 Ma).

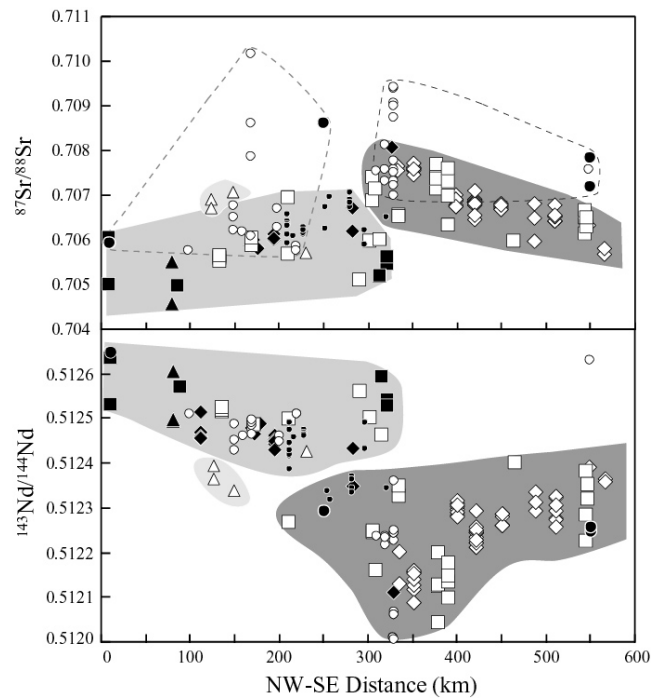


Fig. 2.15.  $^{87}\text{Sr}/^{86}\text{Sr}$  and  $^{143}\text{Nd}/^{144}\text{Nd}$  ratios versus distance. Legend as in Fig. 3.14.

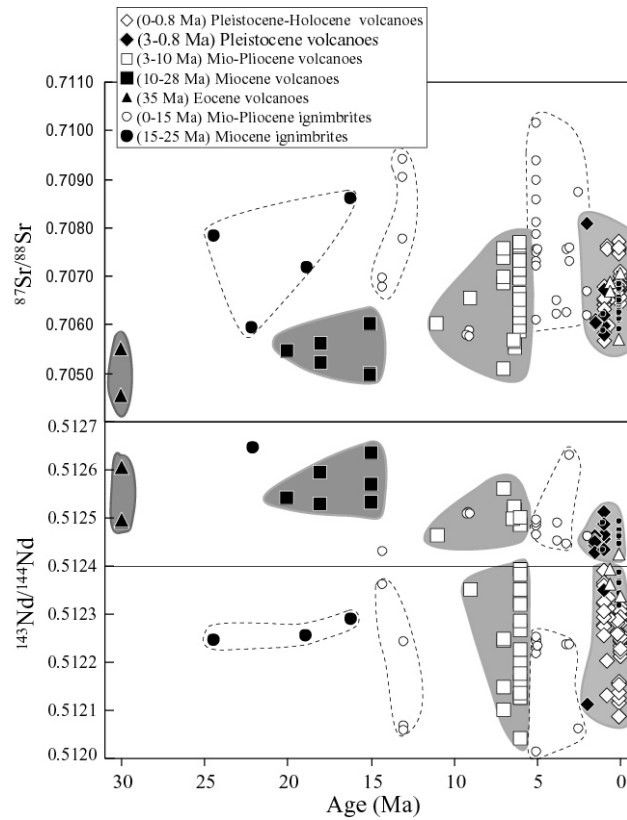


Fig. 2.16.  $^{87}\text{Sr}/^{86}\text{Sr}$  and  $^{143}\text{Nd}/^{144}\text{Nd}$  ratios versus Age.

## Lead isotopes

Lead isotopes data fall into two groups independent of age and rocks type: the most radiogenic samples range in  $^{206}\text{Pb}/^{204}\text{Pb}$  ratios ranging from 18.5 – 19. More unradiogenic samples show ratios of 17.8 to 18.5 (see Fig. 2.17, 2.18).  $^{207}\text{Pb}/^{204}\text{Pb}$  and  $^{208}\text{Pb}/^{204}\text{Pb}$  ratios increase slightly with increasing  $^{206}\text{Pb}/^{204}\text{Pb}$ .

Isotopic ratios observed in some volcanoes (e.g. El Misti, Huaynaputina, Huambo and Andaguas) have unusually low  $^{207}\text{Pb}/^{204}\text{Pb}$  ratios ranging from 15.50 to 15.55.

The samples of southern Peru in the  $^{207}\text{Pb}/^{204}\text{Pb}$  versus  $^{206}\text{Pb}/^{204}\text{Pb}$  diagram lie between the evolutions lines of an upper crustal lead and orogenic belt lead signature. In the  $^{208}\text{Pb}/^{204}\text{Pb}$  versus  $^{206}\text{Pb}/^{204}\text{Pb}$  diagram all samples plot above the orogenic belt lead line of Zartman and Haines (1988).

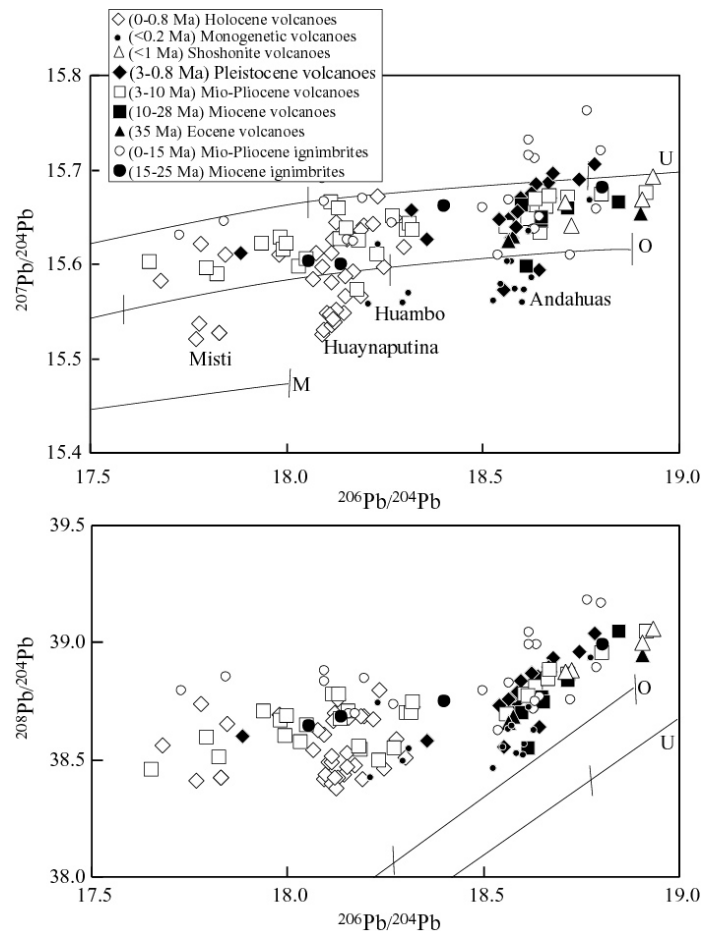


Fig. 2.17. Lead isotopic compositions of the Neogene rocks in southern Peru. Zartman & Heines (1988) lead evolution model: M. upper mantle lead; O. orogenic belt lead; U. upper crustal lead. The ticks of each curve are at 100 Ma interval.

## Spatial and Temporal variations of Pb-isotopes

Samples with higher  $^{206}\text{Pb}/^{204}\text{Pb}$  ratios (18.5 to 19) are located exclusively north of Huambo volcanoes. The low  $^{206}\text{Pb}/^{204}\text{Pb}$  ratios (17.8 to 18.5) are located to the south of Colca canyon. The lowest  $^{206}\text{Pb}/^{204}\text{Pb}$  (17.5-17.8) ratios have El Misti, Salinas and Paquetane volcanoes. Transitions between these groups are abrupt as seen in Figure 2.19.

Ignimbrites have the same Pb-isotope signature as the other volcanic products of their area. Neogene ignimbrites erupted around Moquegua and Arequipa regions have  $^{206}\text{Pb}/^{204}\text{Pb}$  ratios similar to Chachani, Pichu Pichu, Ubinas, Huaynaputina, Yucamane, Casiri, Tacora volcanoes. Ignimbrites erupted around Chuquibamba, Cotahuasi, Puquio, Caravelly, Cuno

Cuno, Pausa, Yauri have  $^{206}\text{Pb}/^{204}\text{Pb}$  ratios similar to Coropuna, Antapuna, Cora-Cora, Sara Sara and Condorama volcanoes.

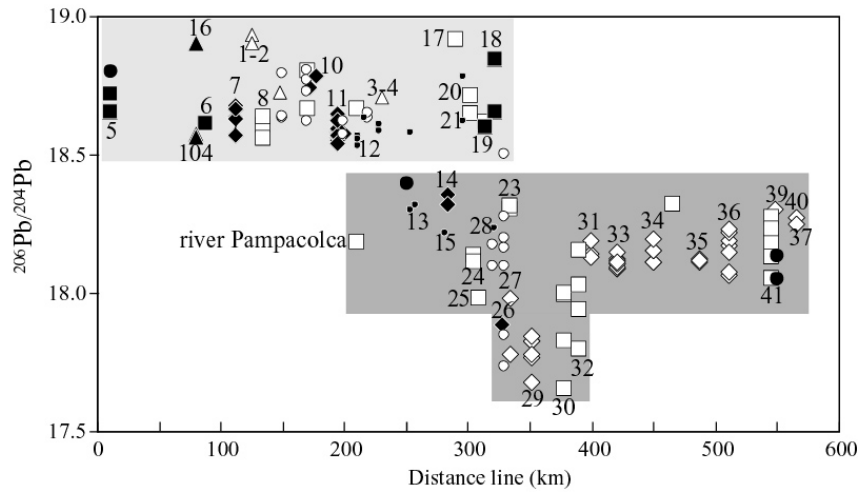


Fig. 2.18.  $^{206}\text{Pb}/^{204}\text{Pb}$  versus distance. Numbers represent the volcanoes positions (see Fig.2.2). Legend as in Fig. 2.17.

The  $^{207}\text{Pb}/^{204}\text{Pb}$  ratios change slightly with decreasing age of volcanic rocks. The unusually lowest ratios observed for Holocene lavas correspond to the El Misti, Huaynaputina Andaguas and Huambo volcanoes. The  $^{206}\text{Pb}/^{204}\text{Pb}$  ratios in both groups (radiogenic and unradiogenic) changed also with decreasing age of volcanic rocks (Fig. 2.19).

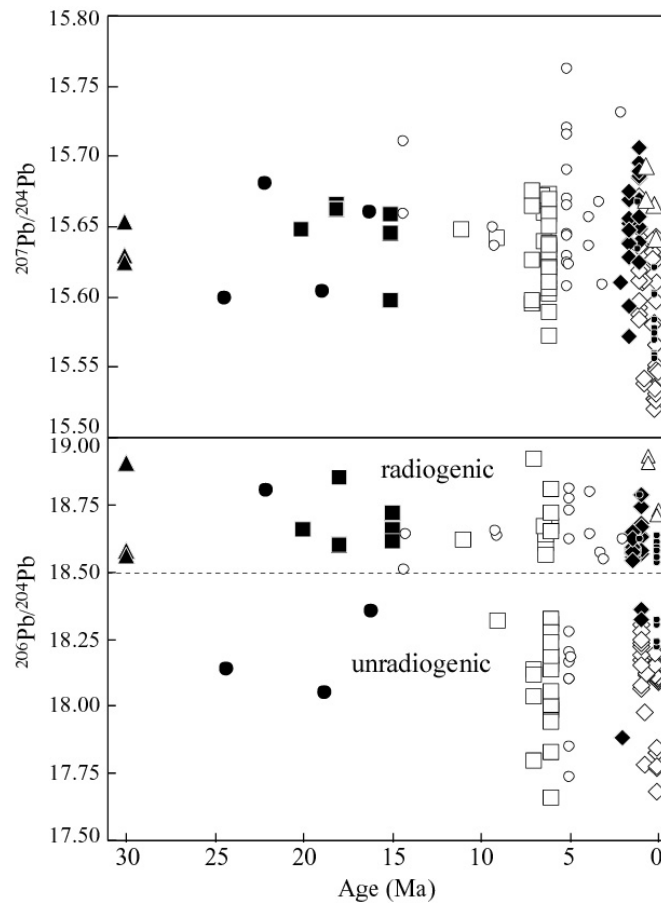


Fig. 2.19.  $^{207}\text{Pb}/^{204}\text{Pb}$  and  $^{206}\text{Pb}/^{204}\text{Pb}$  versus Age. Legend as in Fig. 3.17.

## 2.5 Discussion

This study has documented systematic spatial and temporal differences in trace element and isotope signature among lavas and ignimbrites rocks erupted at different ages and at different regions in the northern CVZ.

The compositional differences between MioPliocene-Recent and Eocene-Miocene lavas are observed in incompatible elements ratios (e.g. Sr/Yb, Sm/Yb, La/Yb). Compositional differences between Neogene lavas and ignimbrites exist for incompatible elements ratios of La/Sr, Sr/Y, La/Sm. Higher Sr/Y and Sm/Y or Sm/Yb between Miocene (Lower Barroso), Mio-Pliocene volcanic (Upper Barroso) and Frontal Arc volcanics in southern Peru is mostly controlled low Y and Yb in the younger rocks (<10 Ma) principally the volcanoes between 14 and 16°S. Thus rocks in southern Peru plot in the calc-alkaline field (Fig. 2.4), have a gradual slope to higher REE pattern (La/Yb = 70, Fig. 2.13) that reflect both light REE enrichment and heavy REE depletion (Fig. 2.11), small Eu anomalies and high La/Ta ratios. Andesites and dacites (SiO<sub>2</sub> = 57-67%) are distinguished by their high La/Ta ratios (to 160, Fig. 2.20), the steep REE pattern (La/Yb to 70) and high Sr/Y ratios (to 100, Fig. 2.21).

Other notable features are the less negative <sup>143</sup>Nd/<sup>144</sup>Nd values (0.5126-0.5124), high <sup>87</sup>Sr/<sup>86</sup>Sr values (0.705-0.7065) and high <sup>206</sup>Pb/<sup>204</sup>Pb (>18.5) ratios in the Upper Barroso and Recent volcanoes (e.g. Sara Sara, Yariahuato, Andaguas, Coropuna, Firura, Ananto) (Fig. 2.2, 2.14 and 2.18).

Magmas with chemical features like those in the andesites, dacites and young volcanics are now commonly called adakites (Defant and Drummond, 1990; Gutscher et al., 2000; Beate et al., 2001). However, the setting for the formation of adakites is related to the melting of the subducted hot and young oceanic crust, it is only during the early stages of flat subduction that the upper part and leading edge of the slab can melt, and prolonged flat subduction will cool both lithospheres and impede partial melting. In this sense Gutscher et al. (2000) presented a flat subduction slab melting model and the emphasis of their model is not on the initial temperature of the slab, but on its buoyancy and thus on the time spent at a relatively shallow (~80 km) depth, allowing the slab to heat up. Therefore, oceanic crust as old as 50 Ma can melt if it is given sufficient time to warm up.

In the discussion below, the regional setting, chemical and isotopic characteristic of the northern CVZ are compared to, and evaluated relative to, similar north and south trend in central CVZ (North Chile, Wörner et al., 1988). The chemical parallels seen in the northern and central CVZ and regional geologic observations, are used to argue that Miocene to Holocene trends in southern Peru magmas and northern Chile magmas have similar origins. The case is made that crustal contamination is needed to explain these trends and not slab melting. A simple geochemical parameter such as Sr/Y (Fig. 2.21) is clearly insufficient to make the case for slab melting (Kay, 2002; Garrison & Davidson, 2003).

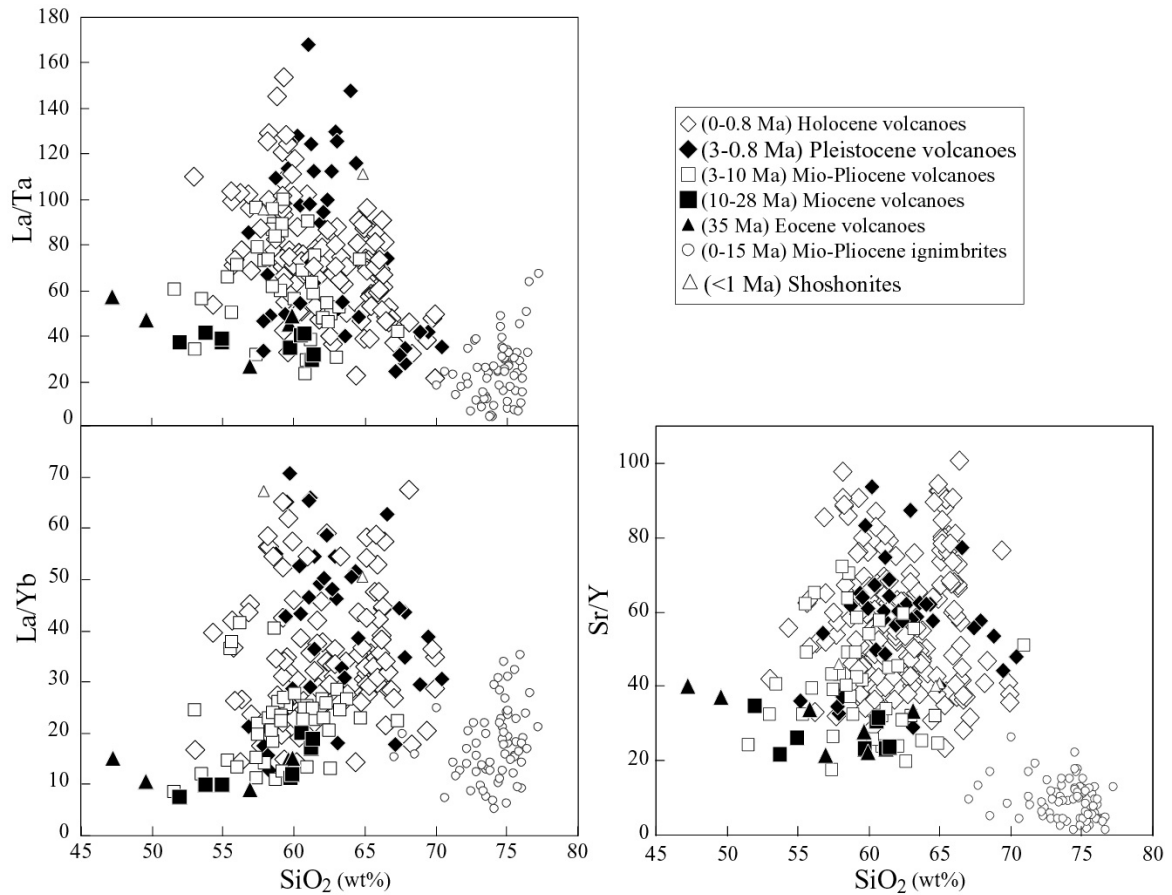


Fig. 2.20.  $\text{SiO}_2$  versus  $\text{La/Ta}$ ,  $\text{La/Yb}$  and  $\text{Sr/Y}$ .

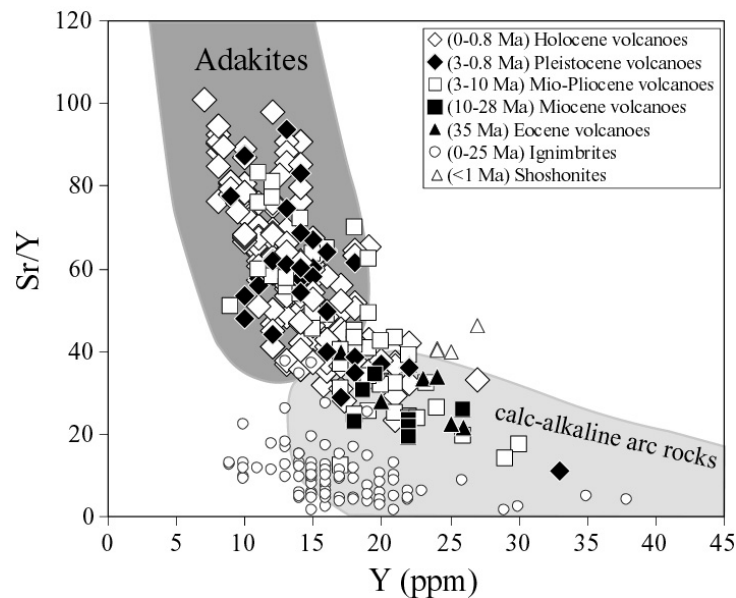


Fig. 2.21.  $\text{Y}$  versus  $\text{Sr/Y}$  diagram showing the evolution of the northern CVZ in southern Peru before, during and after crustal thickening. Adakite and calc-alkaline fields after Defant, M.J., & Drummond, M.S. (1990).

### 2.5.1 Chemical isotopic composition of magmatic rocks in southern Peru and northern Chile

The Temporal trends in northern CVZ (13-18°S) magmas discussed above are highlighted by calc-alkaline trace elements compositional have steepening REE patterns and isotopes varies



from north to south. On the basis of published data for central CVZ (18-22°S) magmas (Fig. 2.22, Wörner et al., 1988; 1992 and references therein), these trends are generally similar to those from south to north along the northern CVZ as shown by the following observations: (1) Neogene volcanic rocks between 16-18°S are like volcanics from 18-19.3°S; (2) samples from 14 to 16°S are like samples between 20.5 and 22°S; (3) in the transition zone in northern CVZ there is not a volcanic gap like in the transitional zone of the central CVZ.

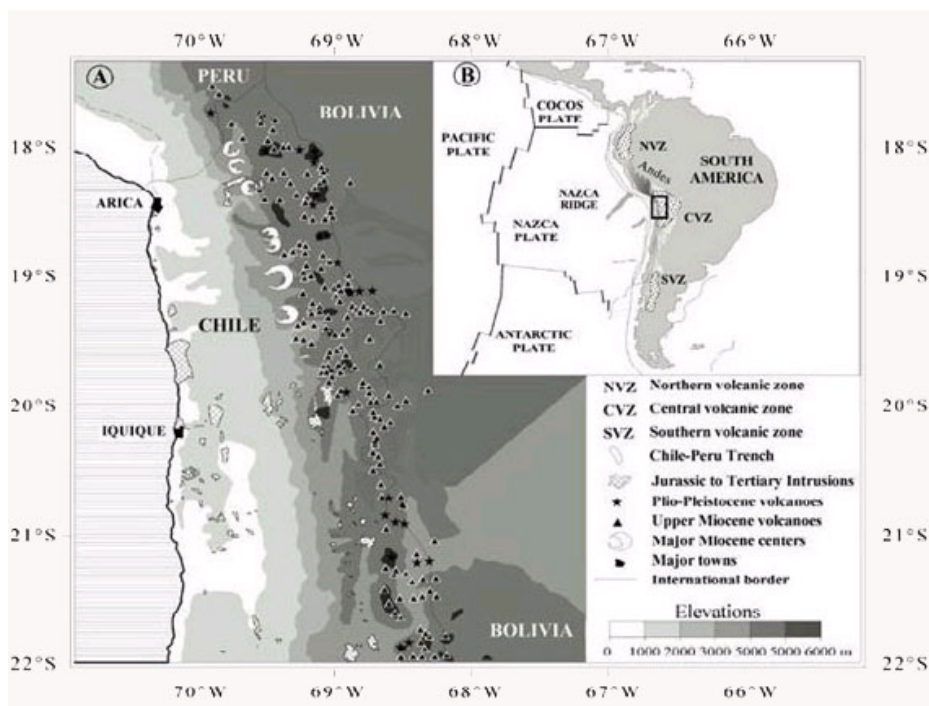


Fig.2.22. Morphological map of the area central CVZ between 18 and 22°S, with Plio-Pleistocene and Miocene volcanic centers, and outcrop areas of intrusive rocks after Wörner et al., 1988.

These broad regional comparisons of central CVZ and northern CVZ magmas are intended to emphasize their dominant characteristics in the long tradition of studies along the CVZ (Wörner et al., 1988, 1992; Davidson et al., 1991). On a finer scale, the composition of the magmas from some central CVZ centers have been shown to be quite diverse, as documented by detailed studies of the Nevados de Payachata (Pomerape and Paricota volcanoes, Wörner et al., 1988, Davidson et al., 1990).

The chemical variations in the northern CVZ magmas, like those along the central CVZ, can be attributed to first order changes in the chemistry of the magma source and the residual mineral assemblage that equilibrated with the magmas. Other modeling studies in the Andes (e.g. Kay et al., 1991, 1999; Hildreth and Moorbath, 1988; Davidson et al., 1991; Haschke et al., 2002) and elsewhere (e.g. Aleutians; Kay 1978) show that steep REE patterns that are with high Sr and high Na concentration can be explained by the last equilibration of these magmas with high-pressure plagioclase-poor, garnet-bearing residual mineral assemblages.

Changes in  $^{87}\text{Sr}/^{86}\text{Sr}$  ratios in the northern CVZ samples (Fig. 2.14) also show a Mio-Pliocene to Holocene progression similar to south and north trends along the central CVZ (Fig. 2.23; data summaries from Wörner et al., 1988, 1992, unpublished data and 30 new samples from this study).

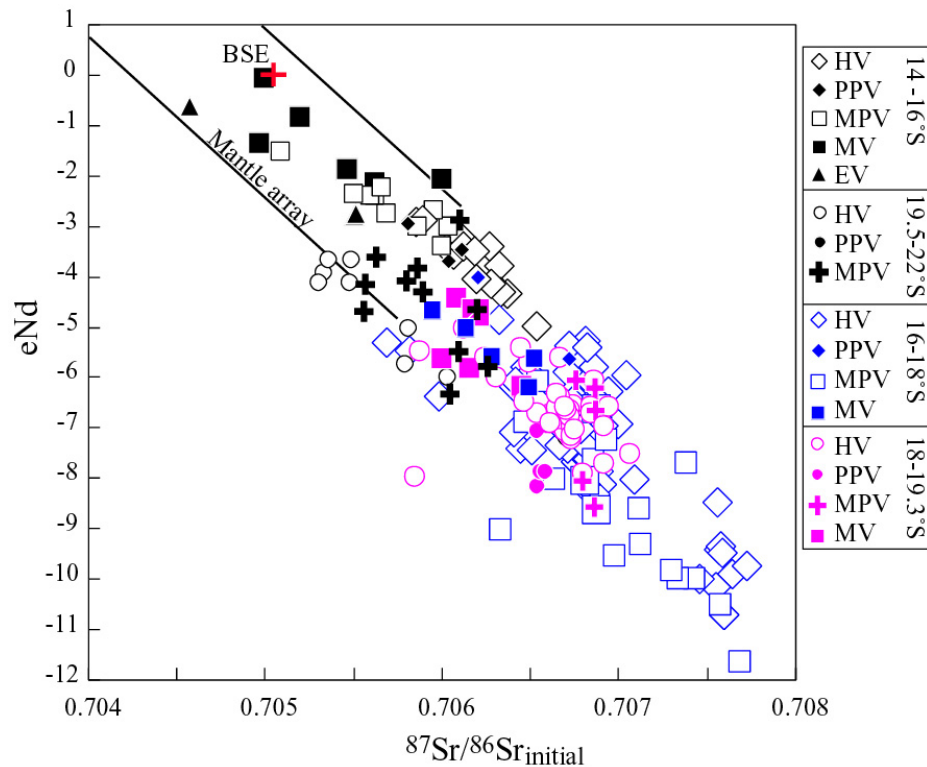


Fig. 2.23. Diagram of  $\epsilon_{Nd}$  vs.  $^{87}Sr/^{86}Sr$  for northern CVZ (14-18°S) and central CVZ (18-22°S). HV-Holocene volcanoes, PPV-Pliocene Pleistocene volcanoes, MPV-Mio-Pliocene volcanoes, MV-Miocene volcanoes, EV-Eocene volcanoes.

Especially,  $\epsilon_{Nd}$  values and  $^{87}Sr/^{86}Sr$  ratios in: 1) Miocene, Mio-Pliocene volcanoes (14-16°S), Mio-Pliocene volcanoes (19.5-22°S) samples either overlap or are depleted (higher  $\epsilon_{Nd}$  and lower  $^{87}Sr/^{86}Sr$ ) than those from Miocene, Mio-Pliocene volcanoes (16-18°S), Mio-Pliocene volcanoes (18-19.3°S); 2) Plio-Pleistocene to Holocene volcanoes samples from (16-18°S) overlap those from central CVZ centers (18-19.3°S); and 3) Plio-Pleistocene to Holocene volcanoes samples from (14-16°S) overlap those from central CVZ (19.3-22°S).

As with changes along the northern CVZ (14-16°S) and (16-18°S), distinct shifts to lower  $\epsilon_{Nd}$  values and higher  $^{87}Sr/^{86}Sr$  ratios between Eocene-Miocene samples and Mio-Pliocene-Pleistocene-Holocene volcanics after ca. 10 Ma (Fig. 2.24) are nearly independent of  $SiO_2$ , Nd, Sr contents (Fig. 2.24, 2.25). These shifts thus reflect differences in compositions and amount of crustal components. To maintain the narrow range in isotopic values seen across the broad range of  $SiO_2$  contents in each period and zone (Fig. 2.24), the evolution of the Tacaza magmas (~ 20-15 Ma, from 14-16°S) can be involve only minor subsequent crustal contamination or, less likely, only contaminants with low Sr and Nd contents and/or with isotopic ratios like those of the Anta lavas (Fig. 2.23).

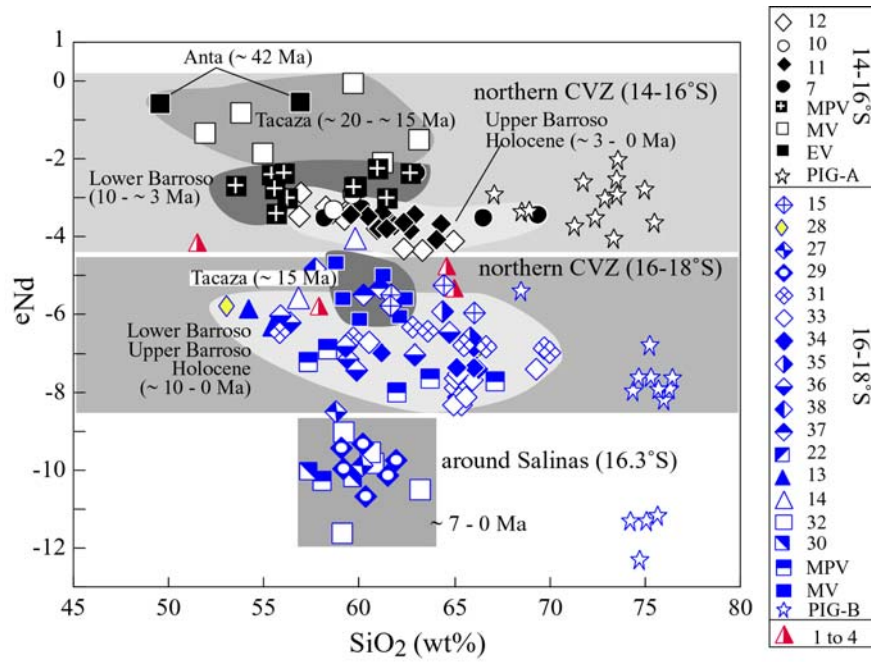


Fig. 2.24. Diagram of  $\epsilon_{Nd}$  vs.  $SiO_2$  for northern CVZ samples (number of samples as in Fig. 3.2).

Figure 2.25 shows that the Upper Barroso and Holocene lavas of both zones (14-16°S and 16-18°S) are enriched in incompatible trace elements (e.g. Ba, Sr). This reflects the response of increasing contamination in a thick continental crust (70 km), so that contaminated parent magmas may occur at depths between 50 and 70 km (lower crust) and at pressure between 15 and 20 kbar where plagioclase is unstable and Sr therefore behaves incompatible. Contrary Sr behaves compatible in Peruvian Ignimbrites indicating that contaminated parent magmas occur where plagioclase is stable, followed by upper crustal differentiation (fractionation and/or AFC).

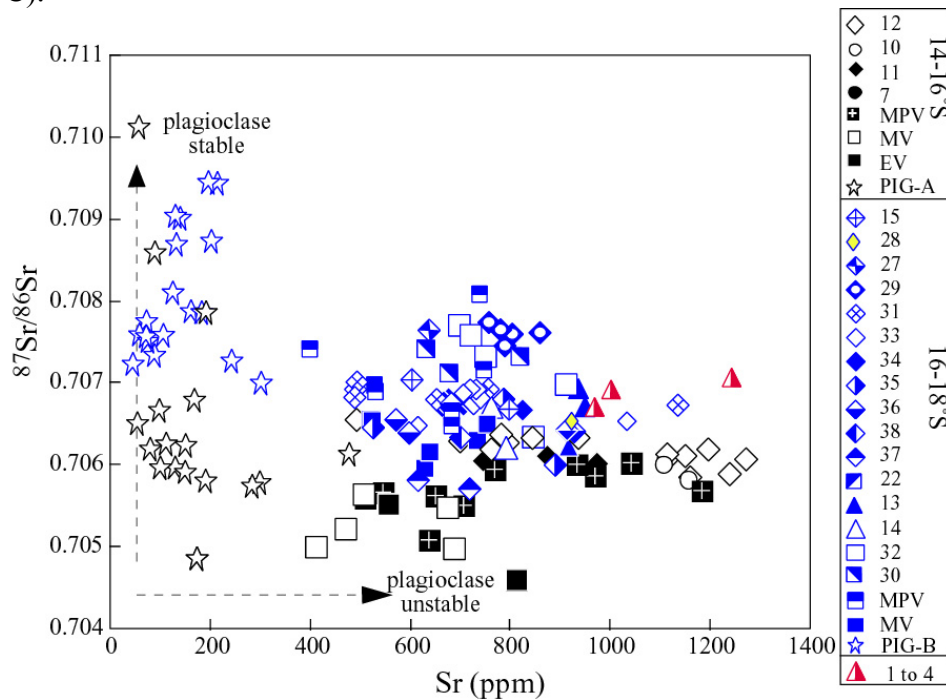


Fig. 2.25. Diagram of  $^{87}Sr/^{86}Sr$  versus Sr for northern CVZ samples (number of samples as in Fig. 3.2).

In contrast to Nd, and Sr isotope ratios in each zone, there is not obvious increase of  $^{206}\text{Pb}/^{204}\text{Pb}$  ratios with decreasing ages. The abrupt Pb isotope changes are at  $16^\circ\text{S}$  in the northern CVZ and at  $20.3^\circ\text{S}$  in the central CVZ (Fig. 2.26). Especially, the samples located between  $16$  and  $18^\circ\text{S}$  in southern Peru resemble the samples from  $18$  to  $19.3^\circ\text{S}$  in northern Chile. These samples have the lowest ratios, whereas volcanic samples from  $14$  to  $16^\circ\text{S}$  are like the volcanic samples between  $20.3$  and  $22^\circ\text{S}$ .

Wörner et al. (1992) and Aitchison et al. (1995) argued that Pb isotope ratios in central CVZ ( $18 - 22^\circ\text{S}$ ) centers strongly reflect contamination from the underlying basement, as ratios of volcanoes from ( $14-16^\circ\text{S}$ ) and ( $16-18^\circ\text{S}$ ) in southern Peru are like those in basement samples, or co-existing ignimbrites in the close vicinity (Fig. 2.27).

A local crustal contamination is consistent with mass-balance consideration, as Pb is strongly concentrated in feldspar-rich crust compared to peridotite mantle.

End-member model to explain Nd-Sr isotope variations along the northern CVZ agree well with models for trace elements. In the northern CVZ the MASH model can be applied (Hildreth and Moorbath, 1988). This model calls upon isotopic homogenization of mantle and crustal components at the base of the thicker crust, more radiogenic crust in the north ( $14-16^\circ\text{S}$ ) and unradiogenic crust to the south ( $16-18^\circ\text{S}$ ) like the central CVZ unradiogenic crust to the north ( $18-19^\circ\text{S}$ ) and more radiogenic to the south ( $20-22^\circ\text{S}$ , Wörner et al., 1992).

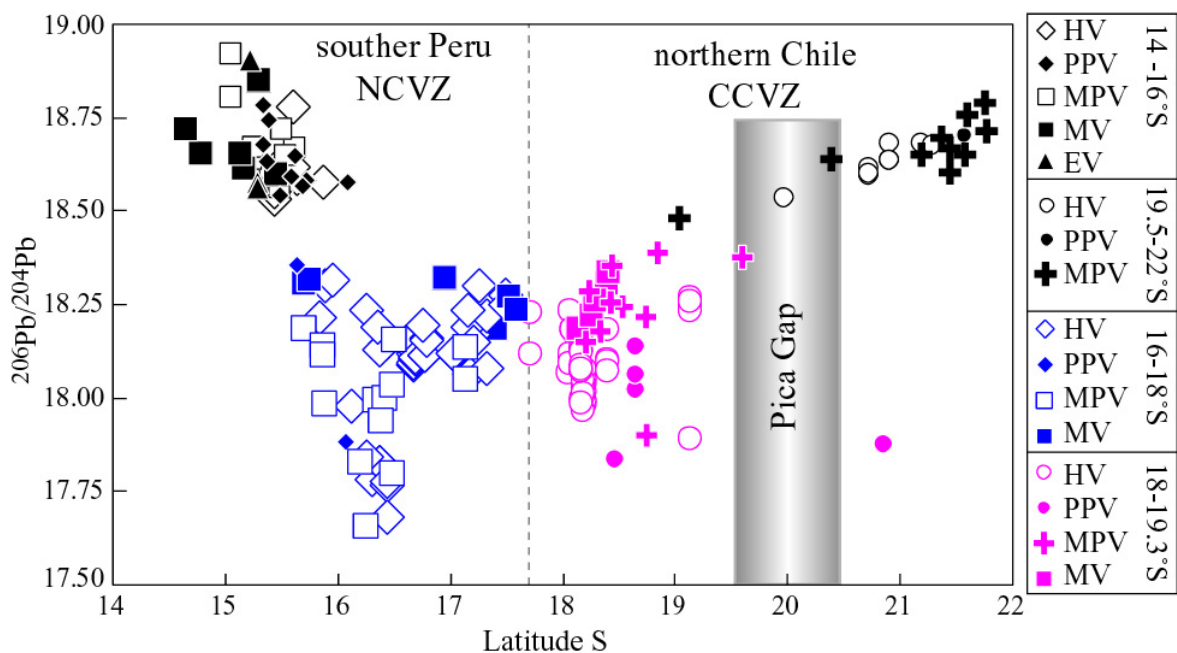


Fig. 2.26. Diagram of  $^{206}\text{Pb}/^{204}\text{Pb}$  versus Latitude S for northern central volcanic zone (NCVZ) and central volcanic zone (CCVZ) samples. HV-Holocene volcanoes, PPV-Pliocene Pleistocene volcanoes, MPV-Mio-Pliocene volcanoes, MV-Miocene volcanoes, EV-Eocene volcanoes, PIG-Peruvian ignimbrites.

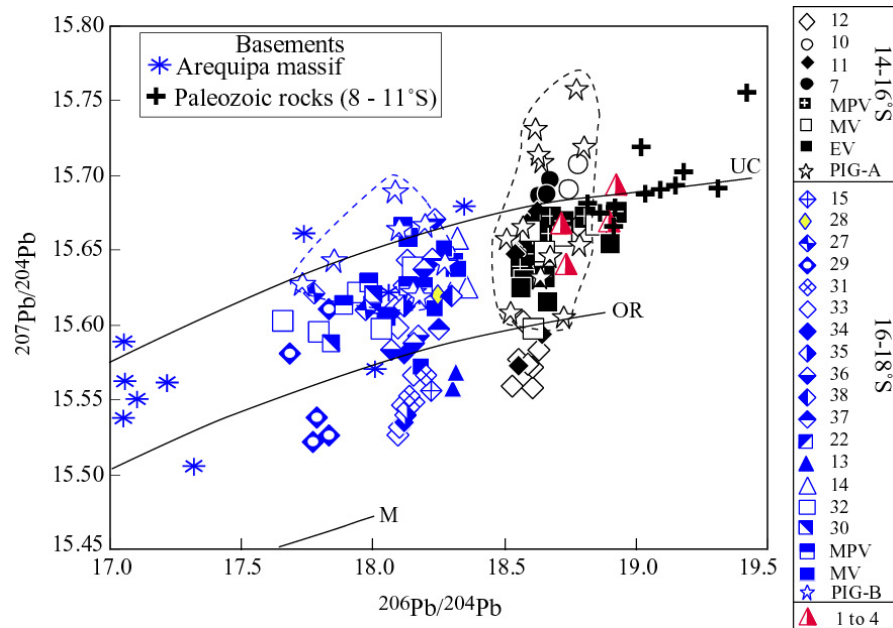


Fig. 2.27. Diagram of  $^{207}\text{Pb}/^{204}\text{Pb}$  versus  $^{206}\text{Pb}/^{204}\text{Pb}$  for northern CVZ volcanics. Number of samples as in Fig. 3.2. The upper crust (UC), orogen (OR) and mantle (M) evolution curves are from Zartman and Doe (1981).

The slab melting model of Gutscher et al. (2000) that calls for slab melting by flat slab subduction (e.g. Nazca ridge) is based on the geochemistry of erupted lavas (Fig. 2.21). Counter arguments against the slab melting model are based on geophysical, geological and detailed geochemical data, which show that regions of flat subduction in the Andes correspond to lack of volcanism (Cahill and Isacks, 1992). There is not an equally satisfying correlation between flat slab location and subducting seamount. Geometry of the slab angle shows that the dip of the Nazca ridge is steeper than Juan Fernandez and Carnegie ridges (Fig. 2.28, Gutscher et al., 2002).

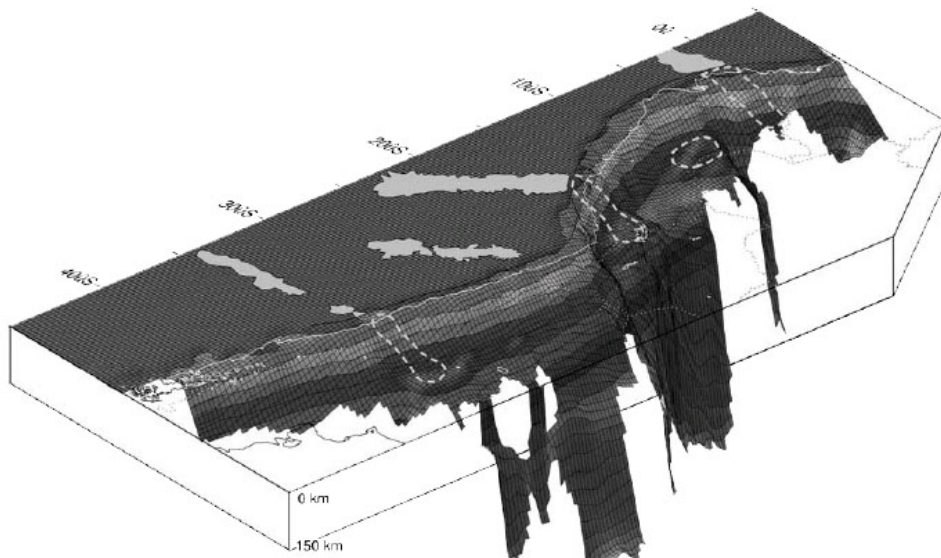


Fig. 2.28. 3D perspective image of the subducted Nazca plate (see Carnegie, Inka, Nazca, Iquique and Juan Fernández ridges) viewed from the southeast (from Gutscher, 2002).

Isotope and trace elements variations in volcanoes above the southern edge of the Nazca ridge are not from slab melting. These variations, which are reflected principally in Pb isotopes

show an assimilation of the underlying basement radiogenic to the north (14-16°S) and unradiogenic to the south (16-18°S, Fig. 2.27). Variation in the REEs, is due to the shift in the combined source and fractionating residual minerals assemblage from low-pressure anhydrous pyroxene-feldspar-dominant assemblage to a medium-pressure hydrous amphibole-feldspar-dominant assemblage to a finally higher-pressure garnet-bearing, feldspar poor assemblage (Kay et al., 1994). The thickness of the crust in southern Peru is > 70 km (Yuan et al., 2002) which correspond to pressures of ~21 kbar at the base of the crust, where garnet is stable. Plagioclase is the primary phase that incorporates Sr, any melt that forms in the absence of plagioclase will be enriched in Sr with respect to the residue. The presence of residual garnet, and to a lesser extent, amphibole, will decrease Y concentrations in the melt, because HREE and Y are highly compatible in garnet.

High Sr/Y signature (Fig. 2.21) is neither unique to slab melting nor insensitive to the residual minerals assemblage and fractionating phases.

### 2.5.2 Lithospheric Cross Sections and the Tectonic and Magmatic History in southern Peru

Questions of slab depth and crustal sources of 14-16°S (Section 1) and 16-18°S (section 2) regions are addressed below in relationship to the series of lithospheric sections in Fig. 2.29, 2.30 and 2.31. The frameworks of these sections are based on: 1) present-day CVZ analogues according to the premise that similar magmas and structures evolve in similar setting; 2) Geological constraint from an arc to backarc transect through southern Peru (Fig. 2.30). Crustal thicknesses, lithospheric asthenospheric boundaries and Moho in the CVZ analogues are based on geophysical models in Yuan et al. (2002), Tassara (2005), and Beck and Zandt, (2002) and subducting-plate geometries are from Cahill and Isack (1992), Gutscher (2002) and Hampel (2002). Time slices are chosen to depict sections during and after crustal thickening at ~29-15 Ma, 10-3 Ma and <3 Ma.

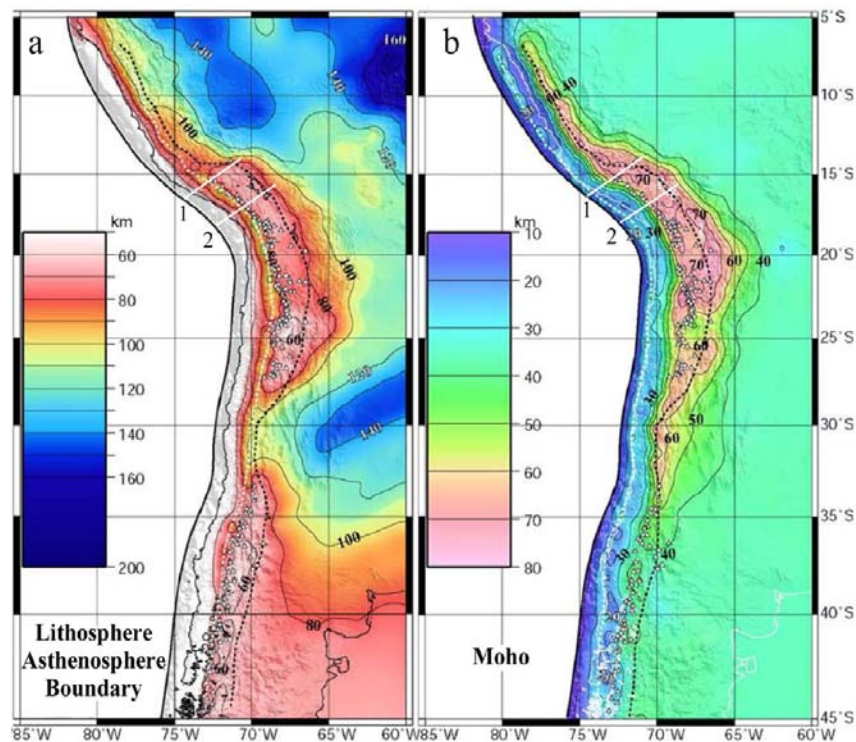


Fig. 2.29. Three dimensional density model of the Andean continental margin from Tassara et al. (2006). a) Lithosphere-asthenosphere boundary countoured every 20 km. b) Moho every 10 km. Dotted lines depict the intersection of the corresponding discontinuity with the subducted slab. White lines are section 1 and 2.

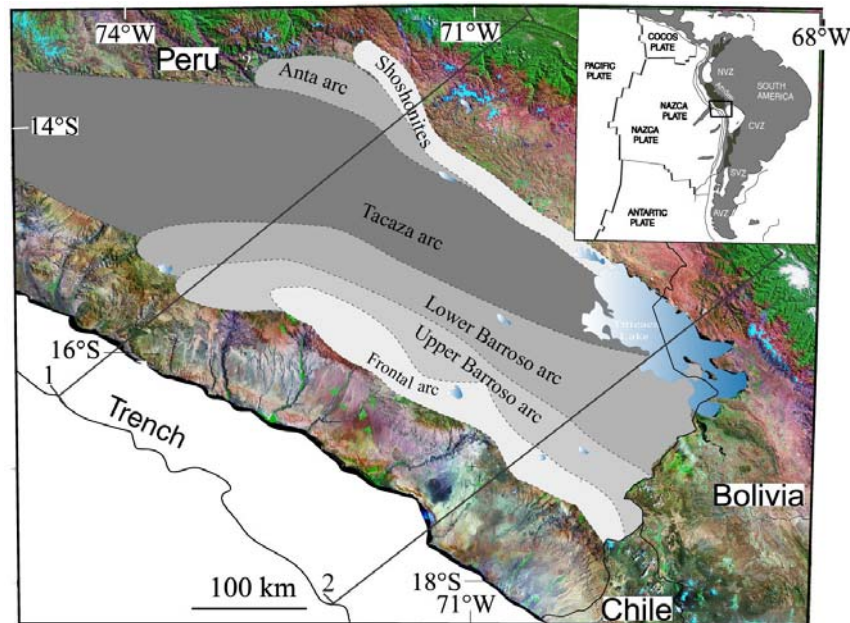


Fig. 2.30. Eocene, Oligocene and Neogene volcanic arcs in the Western Cordillera and northwestern Altiplano of south Peru. 1 and 2 are section lines.

#### Section for the Upper Oligocene to Lower Miocene (Tacaza arc ~29-15 Ma, Fig. 3.31 A)

Section 1, A (14-16°S)	Section 2, A (16-18°S)
<ul style="list-style-type: none"> <li>• Subducting Nazca plate relatively steep.</li> <li>• High Pb isotope compositions.</li> </ul>	<ul style="list-style-type: none"> <li>• Subducting Nazca plate steep.</li> <li>• Low Pb isotope compositions.</li> </ul>
<ul style="list-style-type: none"> <li>• The Uplift of the Western Cordillera began at about 28 to 15 Ma (Sempere et al., 2004; Wörner et al., 2000).</li> <li>• The foreland basin system is progressively driven by the uplift and the propagation of a newly formed Cordillera-the Eastern Cordillera (EC), which started at ~25 Ma (Lamb et al., 1997). This EC resulted from the west-dipping continental subduction of the Brazilian shield under the Altiplano.</li> <li>• Increased plutonic activity at ~20 Ma in the Altiplano (Colque massive, Mamani et al., 2004) fit with facilitation of magma storage in the crust in this contractional regimen.</li> <li>• The Tacaza arc has broadened eastward, volcanism has spread across the Western Cordillera and northwestern Altiplano as shown by the Huaylillas and Ocuvi ignimbrites, Cotahuasi-Tuti and Ayaviri lavas, Pinaya and Tacaza centers. The greater part of the metallic mineralization (Cu-Ag-Pb) is hosted by Tacaza volcanics rocks.</li> <li>• Increased ignimbrite activity at ~24 Ma and ~14 Ma in the frontal arc (e.g. Huaylillas, Tosdal et al., 1981) and in the backarc (e.g. Ocuvi, Mamani et al., 2004) indicate uplift of these areas. Thickening of the Asthenospheric wedge over the steepening subducted slab would have brought in hot asthenospheric melts, facilitating extensive melting of the previously hydrated continental lithosphere. Injection of these mantle-produced magmas into the hot, thickened crust would cause massive crustal melting, producing the magmas that subsequently erupted as large ignimbrite sheets.</li> <li>• Relative flat REE pattern in the Tacaza volcanic mafic magmas being due to partial melting of garnet-free mantle. Subsequent fractionation under low-pressure conditions is in accord with fractionating assemblages dominated by olivine, plagioclase, and pyroxene (Mamani et al., 2004).</li> <li>• Low <math>^{87}\text{Sr}/^{86}\text{Sr}</math> ratios high <math>\epsilon_{\text{Nd}}</math> values fit with minimal crustal contamination in a relative thin crust.</li> </ul>	

**Section for the Middle to Upper Miocene (Lower Barroso arc ~10 - 6 Ma, Fig. 3.31 B)**

Section 1, B (14-16°S)	Section 2, B (16-18°S)
<ul style="list-style-type: none"> <li>• Crust ~70 km thick.</li> <li>• Slab dip as somewhat shallower than in the Oligocene. Shallowing fits with waning of magmatism at 14°S as the arc broadened southeastward from ~10 Ma to 3 Ma.</li> <li>• The emplacement of the Shila, Orcopamapa silver and gold deposits (Fig. 3.32) is linked to magmatism processes at ~10-9 Ma (Tosdal et al., 1999; Cassard et al., 2000).</li> <li>• High Pb isotope compositions like the Tacaza arc.</li> </ul>	<ul style="list-style-type: none"> <li>• Crust ~70 km thick</li> <li>• Subducting Nazca plate steep</li> <li>• During 7 and 6 Ma andesitic to dacitic volcanism migrates into the Western Cordillera, period of widespread volcanism.</li> <li>• Small centers are preserved as small stocks and domes toward west of Titicaca Lake.</li> <li>• Low Pb isotope compositions like the Tacaza arc.</li> </ul>
<ul style="list-style-type: none"> <li>• Voluminous ignimbrite sheets, with ages ranging from 10 to 5 Ma, were erupted around Caravelly, Pausa, Aguada Blanca (Wörner unpublished data) indicating renovation of crustal thickening beneath the arc during Upper Miocene.</li> <li>• Intense shortening in the sub-Andean zone initiated in the mid- to late-Miocene (10–20Ma) with &gt;100 km of underthrusting of the Brazilian shield (Lamb et al., 1997). Deformation style is characterized by the development of a series of thrust imbricates involving Paleozoic sedimentary rocks (Gil, 2001).</li> <li>• Crustal thickening is also consistent with the high Sm/Yb ratios that reflect retention of middle and, to lesser extent, HREE could be in residual amphibol or garnet.</li> <li>• Relatively minor increase in <sup>87</sup>Sr/<sup>86</sup>Sr ratios and decreasing in ε<sub>Nd</sub> values in ca. 10-7 Ma (Fig. 3.23) such relatively small isotopic range require little change in the type or amount of crustal contaminat as the sub-Andean crust thickened in this period.</li> </ul>	

**Section for the Pliocene to Recent (Upper Barroso and Frontal arcs < 3 Ma, Fig. 3.31C)**

Section 1, C (14-16°S)	Section 2, C (16-18°S)
<ul style="list-style-type: none"> <li>• In the last ~3 Myr subducted slab is shown shallower than at ~11 Ma, due to the subduction of the Nazca ridge (Hampel, 2002). Shallowing fits with waning of the magmatism.</li> <li>• High Sr concentration and steep REE pattern (Fig. 3.21) in younger lavas “adakites” used as evidence for slab melting by Gutscher et al. (2000).</li> <li>• High Pb isotope compositions like the Tacaza and Lower Barroso arcs.</li> </ul>	<ul style="list-style-type: none"> <li>• The subducting slab is again steep in accord with the modern Benioff zone geometry under the CVZ (Cahill and Isack, 1992).</li> <li>• Frontal-arc migration to the westward from 3 to 0.08 Ma. The actual arc stabilized 30 km to the west by ca. 0.08 Ma, and is at 250 km distance from the trench.</li> <li>• Low Pb isotope compositions like the Tacaza and Lower Barroso arcs.</li> </ul>
<ul style="list-style-type: none"> <li>• Crust &gt;70 km thick (Yuan et al., 2000). The present-day configuration of the Central Andes was acquired at ~11 Ma (Lamb et al., 1997).</li> <li>• Major Pliocene to Recent volcanic activity is essentially restricted to the Western Cordillera. Using the geometry of Cahill and Isacks (1992) model, the Frontal arc are about 120 to 150 km above the slab and is underlain by a lithosphere thinner than 80 km. Backarc volcanic activity is limited to the shoshonites along the Vilcanota-Ayaviri lineament fault.</li> <li>• Sencca ignimbrites with ages from 2.7 to 3.2 (Wörner et al., 2000 and unpublished data) erupted principally in the Western Cordillera.</li> <li>• The particular high La/Yb and Sm/Yb ratios, and high Sr contents in the young volcanics</li> </ul>	



fit at least in part, with processes in which garnet residual of thick crust (Kay et al., 1999). Additional support for interaction of magmas with thickening garnet crust at high pressure comes from the flat REE pattern.

- Increases in  $^{87}\text{Sr}/^{86}\text{Sr}$  ratios and decreases in  $\epsilon_{\text{Nd}}$  values in Upper Barroso and Holocene magmas stand in marked contrast to large differences between Lower Barrosos and Tacaza magmas. Such isotopic range requires change in the amount of crustal contaminant. Geological evidence for crustal thickening correlate also with trace elements, high Sm/Yb and Sr/Y.

- Geophysical studies suggest that virtually all of the mantle lithosphere below the eastern Altiplano and western part of the Eastern Cordillera has been removed (Myers et al., 1998; Dorbath and Granet, 1996). The relatively strong Brazilian lithosphere is underthrusting as far west as the high elevations of the western part of the Eastern Cordillera (65.5°W) but does not underthrust the entire Altiplano. As the Brazilian craton underthrusts the subcrustal lithosphere (and possibly the mafic lower crust), the subcrustal lithosphere and the lower crust are decoupling from the upper crust and delaminating or subducting into the mantle. The subcrustal lithosphere is delaminating piecemeal and is not completely removed beneath the central Altiplano (Fig. 2.32: Beck and Zandt, 2002).

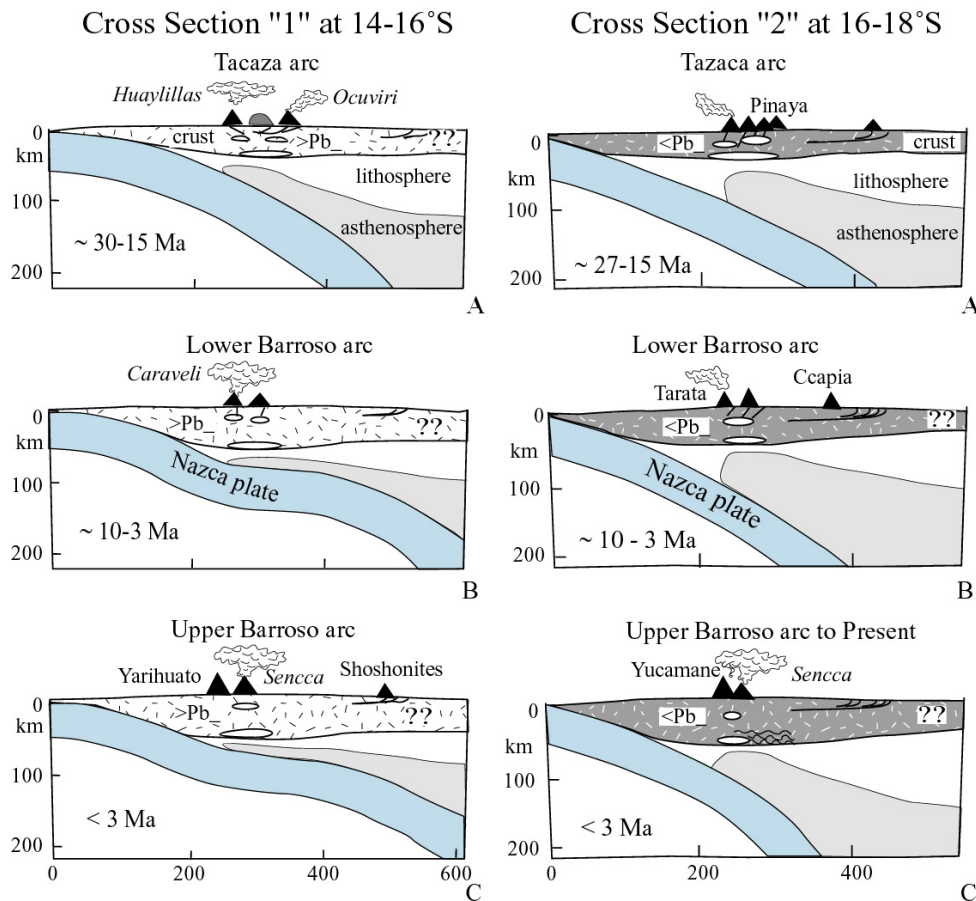


Fig. 2.31. Sequence of schematic lithospheric-scale cross sections showing the Tacaza to Recent magmatic arcs and tectonic evolution near 14-16°S (Cross Section 1) and 16-18°S (Cross Section 2). The framework of each section is based on a modern analogue along the northern CVZ. Frontal volcanic centers (triangles) active at the time shown in the section are plotted at their present distance relative to the modern trench (km 0 on the horizontal scale). Active volcanic centers, plutons, and faults are schematically shown for each time. The distributions of faults, foreland-basin sequences are based on GIS Andes (from BRGM). Fragment of crust and lithospheric mantle from the forearc are shown entering the mantle wedge under the arc at times of arc migration.

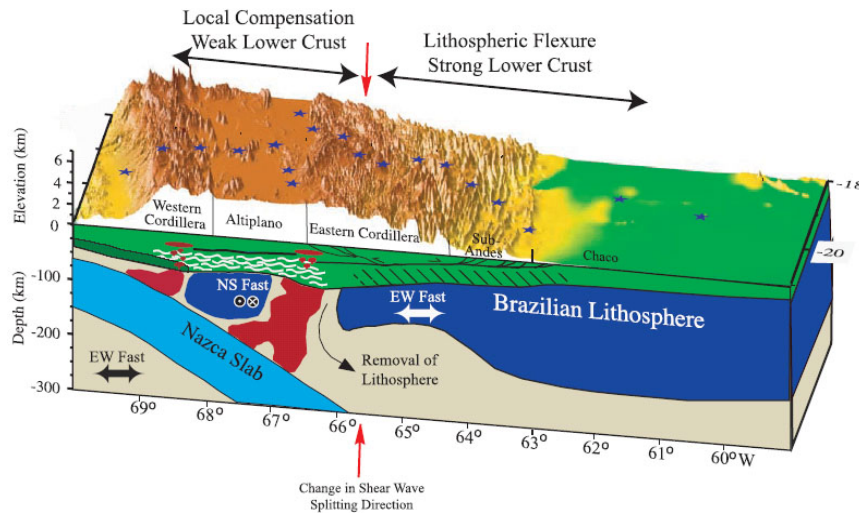


Fig.2.32. Schematic cross section showing interpretation of the lithospheric structure of the central Andes from geophysical and geological studies (Beck and Zandt, 2002). Red and blue indicate upper mantle P wave velocities that are slower and faster, respectively, than the reference IASPEI-91 model (Myers et al., 1998).

## 2.6 Conclusions

Oligocene to Recent volcanic centers in the northern CVZ (14-18°S) reveal systematic differences in trace elements and Sr-Nd isotope ratios with age, which reflect different degrees of crustal contamination. High-K, calc-alkaline andesites are the most common rock type in the 36 volcanic centers sampled. The major elements and most trace elements show no differences with age when andesites of the same degree of fractionation are compared. However Sr shows striking enrichments in the Upper Barroso to Recent andesites (<3 Ma) relative to their older equivalent (Lower Barroso and Tazaca rocks).

Regional differences exist: Barroso and Recent volcanic rock erupted north of 16°S have higher  $\epsilon_{\text{Nd}}$  values, low Sr isotope ratios and higher Pb isotope ratios than volcanic erupted to the south of 16°S (with lower  $\epsilon_{\text{Nd}}$  values, higher Sr isotope ratios and lower Pb isotope ratios). These support the notion that the magmas are controlled by the composition of the Andean crust in southern Peru.

All younger volcanoes in the northern CVZ have high Sm/Yb and Sr/Y ratios consistent with residual garnet in the source region. This excludes an “adakitic” signature and any involvement of slab melts of the volcanic rocks located between 16°S and 14°S.

The composition of andesites in the northern CVZ record a major change between 10 to 3 Ma after establishment of the thick crust and uplift of the Andes.

### 3 Regional and temporal patterns in Meso-Cenozoic magmatic evolution in the Central Andes (13°S to 28°S)

#### Abstract

Meso-Cenozoic magmatic arc systems of the Central Andes (CA) result from the subduction of the Nazca Plate beneath the South America plate since Jurassic time, the arc progressively shifted ~180 km from a western position in the Jurassic to the present Western Cordillera in the Oligocene time. These magmas formed prior, during and after crustal thickening. Present-day continental crust reaches a thickness of >70 km. Enhanced uplift between c. 30 and 15 Ma is documented by large clastic wedges in Western Andean Escarpment (Wörner et al., 2000; Sempere et al., 2004). The upper crust is formed by Precambrian to Paleozoic metamorphic rocks and sedimentary marine Mesozoic rocks, covered by mostly continental sediments of the Cretaceous and Tertiary.

Evolutionary pattern in geochemistry, initial Sr- Nd isotope and present day Pb-isotope characteristics of Central Andean (200 Ma to Present) magmatic rocks suggest that the pattern in Meso-Cenozoic magmatic evolution in this region was controlled by crustal thickness and the local basements.

#### 3.1 Introduction

Geochemical and isotopic variations of modern Andean magmatism arc and rocks tend to correlate with changing crustal thickness through time in the Central Andes (e.g. Kay et al., 1994, 1999; Davidson et al., 1991; Trumbull et al., 1999) and along the arc in the Southern Volcanic Zone (Hildreth and Moorbath, 1988). These correlations assume that melts equilibrated with and reflect the source mineralogy of a hydrous mafic melting assimilation storage homogenization (MASH) (Hildreth and Moorbath, 1988) crust-mantle boundary and not with variably enriched asthenospheric mantle due to contamination by subducted sediments or tectonic erosions suggested by Stern (1988, 1990) and/or partial melting of the enriched sub-continental lithospheric mantle triggered by slab derived fluids proposed by Rogers & Hawkesworth (1989). Crustal thickening result in increasingly higher pressures for the residual mineralogy of melts produced from this source region. Geochemically, most diagnostic of pressure-induced changes in the source mineralogy, from lower-pressure assemblages dominated by plagioclase and clinopyroxene to higher-pressure amphibole and garnet-bearing mineral assemblage passing through the garnet stability field at depths >12 kbar or crustal thickening >40 km (e.g. Kay et al., 1991, 1994, 1999; Petford et al., 1996; Haschke et al., 2003).

Since the beginning of subduction-related Andean magmatism some 200 m.y. ago, repeated stepwise eastward shifting of the main axis of arc magmatism generated a collage of four roughly parallel, eastward younging Andean magmatic arcs (Coira et al., 1982; Scheuber et al., 1994): 1) The Early Jurassic-Early Cretaceous arc along the present Coastal Cordillera; 2) The Middle Cretaceous arc aligning with Longitudinal Valley; 3) The Cretaceous-Eocene arc largely corresponding to the western edge of the Western Cordillera; and 4) The Late Oligocene-Late Miocene arc and modern CVZ composing the Western Cordillera and Altiplano-Puna plateau, where occur the greatest chemical variations. Each set of arcs have or no their magmatic backarc to ~120 km distance. These spatial and temporal variations make the Central Andes an ideal zone to studying long term (~200 Ma) crustal evolution and magmatic processes at subduction-related.

I compiled major and trace elements and isotope data for these successive arcs between 13°S and 28°S and found similar and different evolutionary pattern in geochemistry with time and space.

Each suite of arc magmatic rocks is characterized by increasing of Sr-Nd isotopic through time, Sm/Yb ratios increase with time, but with variable ratios along CVZ. Pb-Nd isotopes of rocks are not similar along the Central Andes, but are similar at any given area (e.g. in the central CVZ, Wörner et al., 1992; Aitcheson et al., 1995 and in the southern CVZ, Lucassen et al., 2001, and in northern CVZ, Chapter 2 of this thesis). Such patterns along the Central Andes were neglected and previous studies and discussions were concentrating in local areas (Fig. 3.1). To understand and use these patterns along the entire Central Andes require also study regionally in light of what control geochemical variations in time and space.

### **3.2 Database**

From the literature I compiled major and trace elements and Sr-Nd-Pb isotopic data (583 samples) for Central Andean magmatic arc rocks (200 Ma to present). Data for Jurassic to Early Tertiary rocks (Boily et al., 1989; Mukasa et al., 1986; Anthes, 1993; Guerra, 1993; Rogers and Hawkesworth, 1989; Haschke et al., 2002; Lucassen et al., 2002; Kay et al., 1994; Horn, 1992; Heumann, 1993). For late Oligocene to present magmatic rocks data come from Davidson et al. (1990), Horn (1992), Kay et al. (1994, 1999), Rogers and Hawkesworth (1989), Eusterhues (1993), Aitcheson et al. (1995), Wörner et al. (1988, 1994 and unpublished data), Mamani et al. (2004), Kohlbach (1999), Trumbull et al. (1999), Siebel et al. (2001). I also present 201 new analyses for major and trace elements as well as a large subset for Sr-Nd-Pb isotopes of volcanic and intrusive rocks with ages between 190 and 0 Ma, to fill spatial and temporal gaps and complete isotope analysis from earlier work and to establish the pattern along the Central Andes (Fig. 3.1). Sample locations, compiled data and representative new analyses are listed in database. The complete database for CA and map location of samples is available on CD.

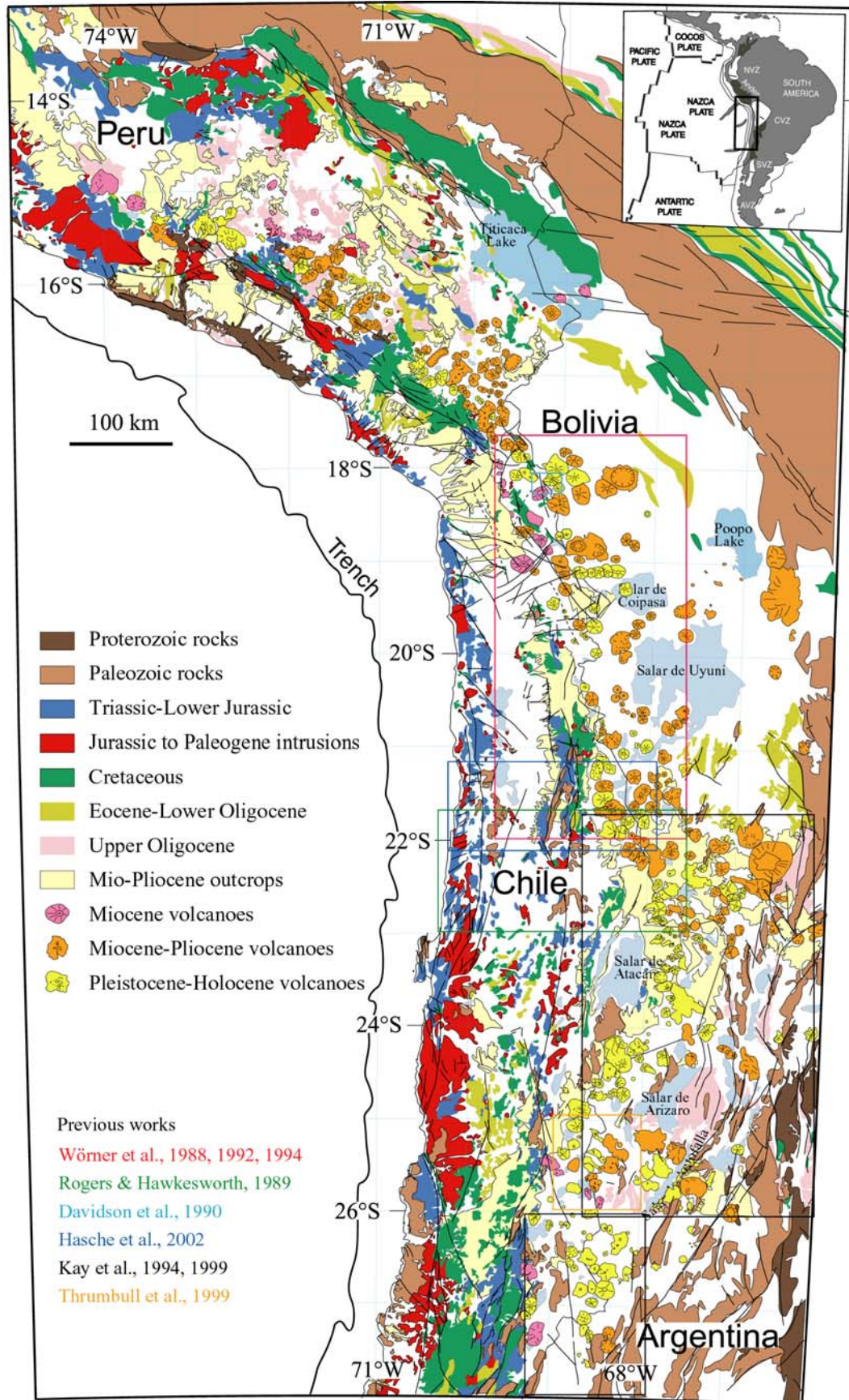


Fig. 3.1. Simplified geological map of the Central Andes. Different square colours indicate the zones of previous studies.

### 3.3 Geochemistry of Meso-Cenozoic magmatic rocks in the CA

#### 3.3.1 Major and trace elements

Volcanic and intrusive rocks from the Central Andes (CA) can be subdivided into members of two major magma series: alkalic and sub-alkalic. This distinction is presented in the Total Alkalis versus Silica (TAS) diagram. The alkalic serie is represented by backarc rocks, and the samples from Neogene arc and Jurassic-Early Tertiary intrusions plot in the transition zone between sub-alkaline and alkaline (Fig. 3.2).

In a TAS-diagram, compositional classification of the magmatic samples was done according to the international nomenclature (Wilson, 1989). Intrusive rocks of the area are also plotted into the diagram. Calc-alkaline samples are predominantly the Neogene lavas, varying in composition between basalt andesite, andesite, dacite and rhyolite. Backarc volcanic samples are “basanites”, a less alkalic suite ranges from basalt to basaltic-trachyandesite. Samples of the Jurassic and Early Tertiary rocks from the forearc are gabbros or basalts, andesites or diorite, granodiorites and granites.

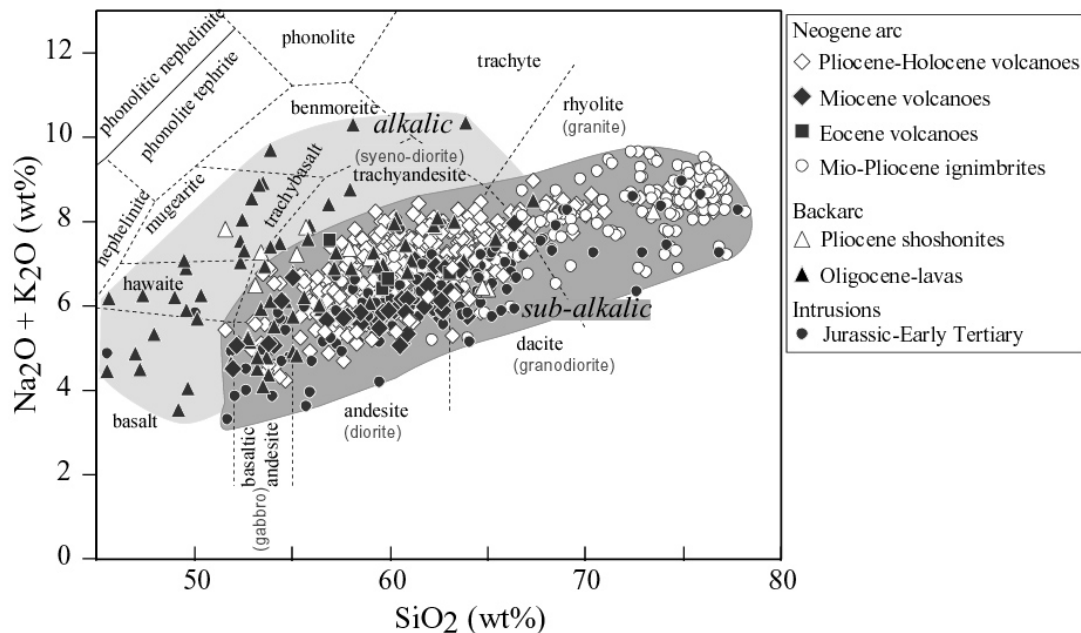


Fig. 3. 2. TAS diagrams from Wilson (1989) of own and compiled data from the CA.

Harker diagrams show the chemical differentiation or mixing trend of the CA rock series in respect of the major elements and some plots with trace elements are added. Besides trends due to fractional crystallisation of different mineral phases, mixing lines are also observed.

Samples of the Jurassic intrusions are the most primitive of the CA, i.e. they have undergone the least crystal fractionation. This is obvious from the element variation diagrams. The Oligocene alkaline rocks from the backarc are affected by some olivine and clinopyroxene fractionation. Few Jurassic intrusions show deep fractionations of these two minerals.

The most mafic rocks are Oligocene and Recent rocks from the backarc and some Jurassic rocks from the Coastal Cordillera with characteristically high MgO (> 4 wt %), Ni (> 30 ppm), and Cr (> 100 ppm) contents, but still lower MgO contents compared to primitive mantle basalt (Fig. 3.3).

Plots of CaO,  $\text{SiO}_2$ , and  $\text{Al}_2\text{O}_3$  versus MgO present a marked inflection in the liquid line of descent that is related plagioclase fractionation or the generalities of a mixing process. At high

MgO values only Ol and Cpx fractionation occurs (e.g. backarc samples), whereas around 4% MgO, plagioclase enters the fractionating assemblage. Samples of the Neogene lavas and Cretaceous intrusions have multiple mixing.

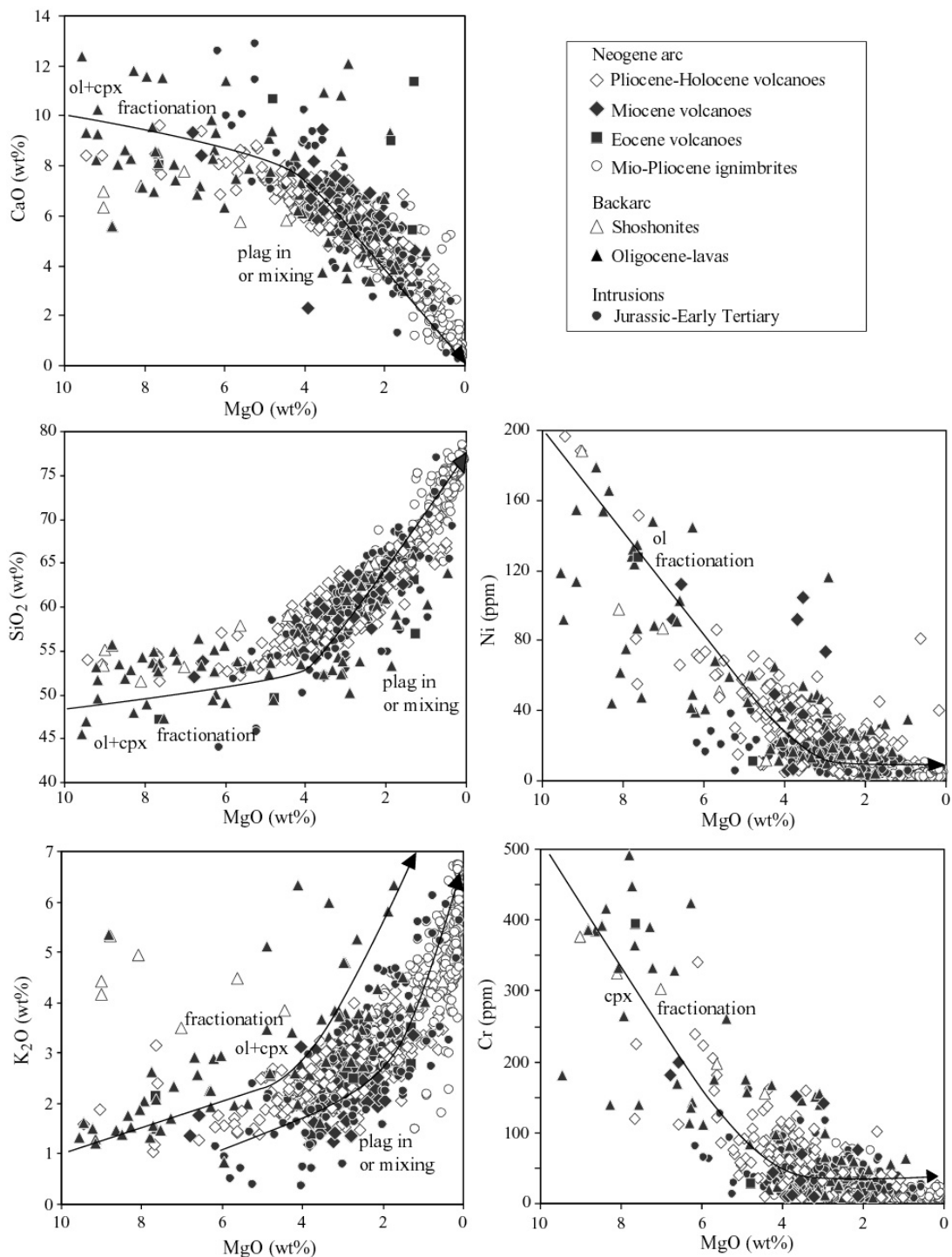


Fig. 3.3. Element variation diagrams for major and trace elements versus MgO. Folds in the liquid lines of descent report the start of crystal fractionation of a new mineral facies.

Harker diagrams of major element oxides versus  $\text{SiO}_2$  and some additional diagrams of trace elements versus  $\text{SiO}_2$  (Fig. 3.4) characterise the major fractionating phases olivine, clinopyroxene, plagioclase, as well as alkali-feldspar, magnetite/sphene and the accessory phases like apatite and zircon and mixing process.

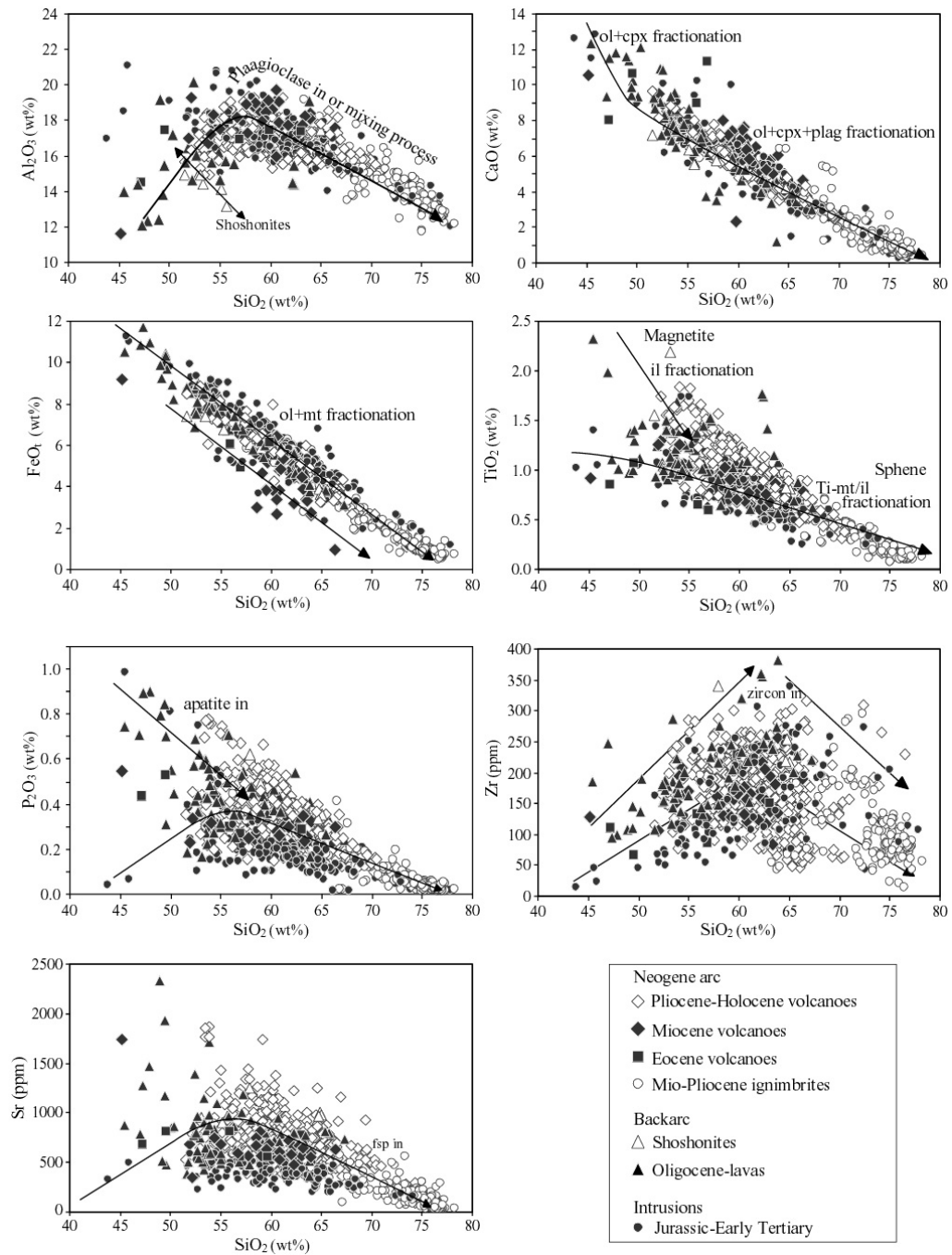


Fig. 3.4. Harker diagrams showing elemental variations of major elements and some trace elements versus  $\text{SiO}_2$ . The rock groups from the CVZ display liquid lines of descent with clear evidence for fractionation other straight lines due to mixing. ol=olivine, cpx=clinopyroxene, plag=plagioclase, mt=magnetite, il=ilmenite, fsp=feldspar.

In general ratios of major elements of rocks with  $>57\%$   $\text{SiO}_2$  are governed by multiple mixing between shallow magmas ( $<57\%$   $\text{SiO}_2$ ) and more evolved end of “deep” magmas as it showed in Rb versus Ni diagram (Fig. 3.5a).

In the  $\text{SiO}_2$  (wt%) versus U and Th diagrams is observed the ignimbrite fields (Fig. 3.5b, c), which indicate shallow level fractionation of accessories in this rocks. The trends follow the mixing between the deep fractionation magmas and more evolved magmas.



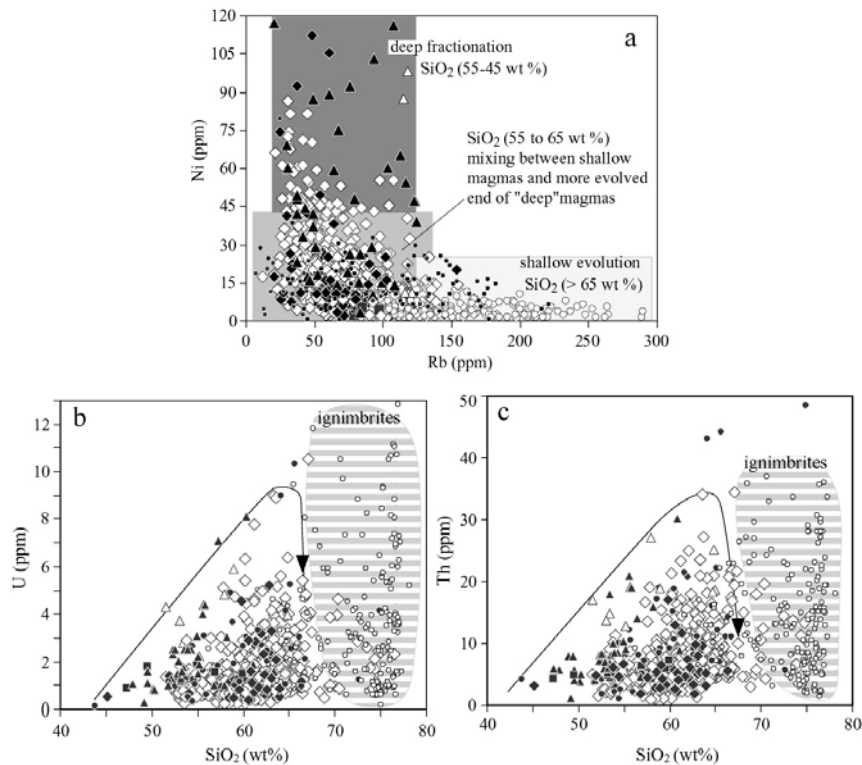


Fig. 3.5. a) Diagram Rb (ppm) versus Ni (ppm), b) and c) SiO<sub>2</sub> (wt%) versus U (ppm) and Th (ppm) to distinguish between deep and shallow fractionation and mixing process. Legend as in Fig. 3.4.

As we observed in the Figures 3.3, 3.4 and 3.5, geochemical data shows that arc lavas with SiO<sub>2</sub> (55 to 65 wt %, Fig. 3.5) content are product of mixing, this could explain why in the arc lavas there are no mafic lavas with ~50 % SiO<sub>2</sub> and most of the lavas have > 55% SiO<sub>2</sub> (Fig. 3.6).

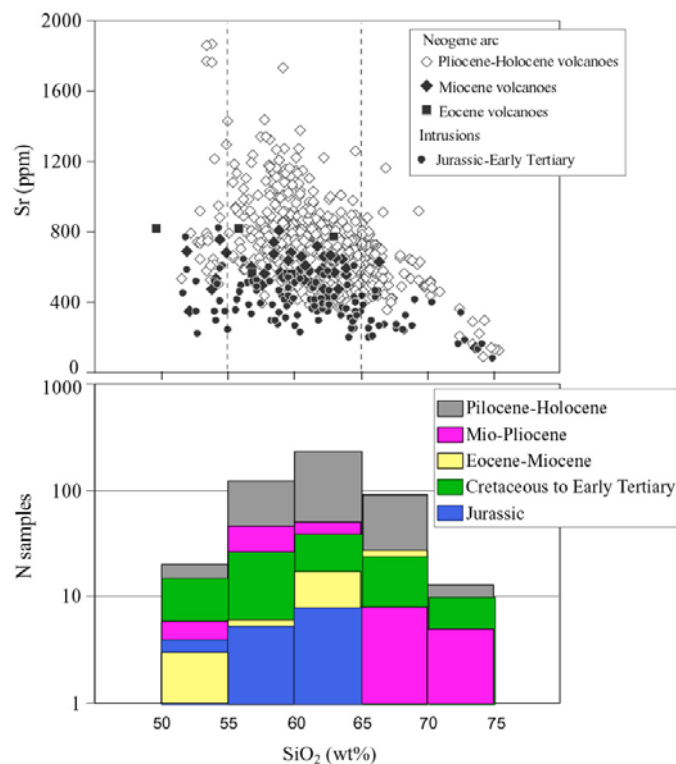


Fig. 3.6. Histogram of SiO<sub>2</sub> (wt %) concentration and Sr (ppm) content for samples from the CA.

### **Spider diagrams**

Mantle-normalised (McDonough et al., 1992) multi-element diagrams are illustrated for zones along the CVZ in (Fig. 3.7). The patterns show typical subduction signatures for almost all the samples. HFSE (Nb, Ta, Hf, Zr, Ti) depletion is a characteristic for this tectonic environment and most conspicuous with the Nb-Ta trough. This trough is most clearly visible in samples from the Jurassic-Tertiary intrusions and Neogene lavas.

The patterns of the Jurassic and Cretaceous are definitely distinct in that they show a more flat signature with almost flat REE.

Completely contrary is the pattern of the Neogene lavas. The pattern of the Mio-Pliocene to Holocene have a steep gradient from La to Y, in comparison Miocene are intermediate.

Sr concentrations in Neogene lavas are different e.i. high in zone 1 and 2, and low in zone 3.

The patterns of the backarc samples (shoshonites) show less depletion of the HFSE, enrichment of fluid-mobile elements (Ba, Th, U) and La, Ce, Sm, Tb in comparison with other rocks. Ba and La content are lower in backarc arc lavas, Ta are depleted as the Holocene lavas and not enriched as the backarc lavas. This is demonstrated in the diagram by comparison to the pattern of OIB (Fig. 3.7).

Different to the lavas, the Neogene ignimbrites do not display strong Ta-Nb depletions, but have strong negative Sr anomalies and Ba troughs due to intensive feldspar fractionation. The ignimbrites from the Zone 1 exhibit positive Ba anomalies and less negative Sr anomalies suggesting that no K-feldspar fractionation occurred. Depletion at Ti results from fractionation of accessory phases such as magnetite and sphene.

### **Rare earth elements (REE)**

A good tool for the distinctions of magmatic rocks from Central Andes is REE plots (Fig. 3.8). The REE contents of the samples are normalised to chondrite concentrations after McDonough & Sun (1995). For comparison, pattern from Jurassic to recent arc of the CVZ are shown in the diagrams.

The Jurassic samples display a pattern with little enrichment of the LREE (La/Sm), while the Cretaceous rocks pattern is to some respect comparable but shows in most cases a negative Eu anomaly due to plagioclase fractionation, and higher LREE concentrations.

The REE pattern of the Neogene lavas is definitely distinct: the Miocene samples show a signature with moderate gradients from LREE to HREE. Completely contrary is the REE pattern of the Mio-Pliocene to Holocene samples, because their patterns are steeper. The gradient variations of the Neogene rocks change from zone 1 (steeper) to zone 3 (lest steep).

LREE pattern for the ignimbrites from the three zones are similar and characterized by a large range. Eu and HREE patterns are different, the marked negative Eu anomalies and HREE contents are lower in the ignimbrites from the Zone 2 (Fig. 3.8).

The Shoshonites LREE patterns are different from the other samples of CVZ. These young backarc volcanics display a generally steeper LREE pattern than arc and forearc and the HREE pattern are relatively flat.

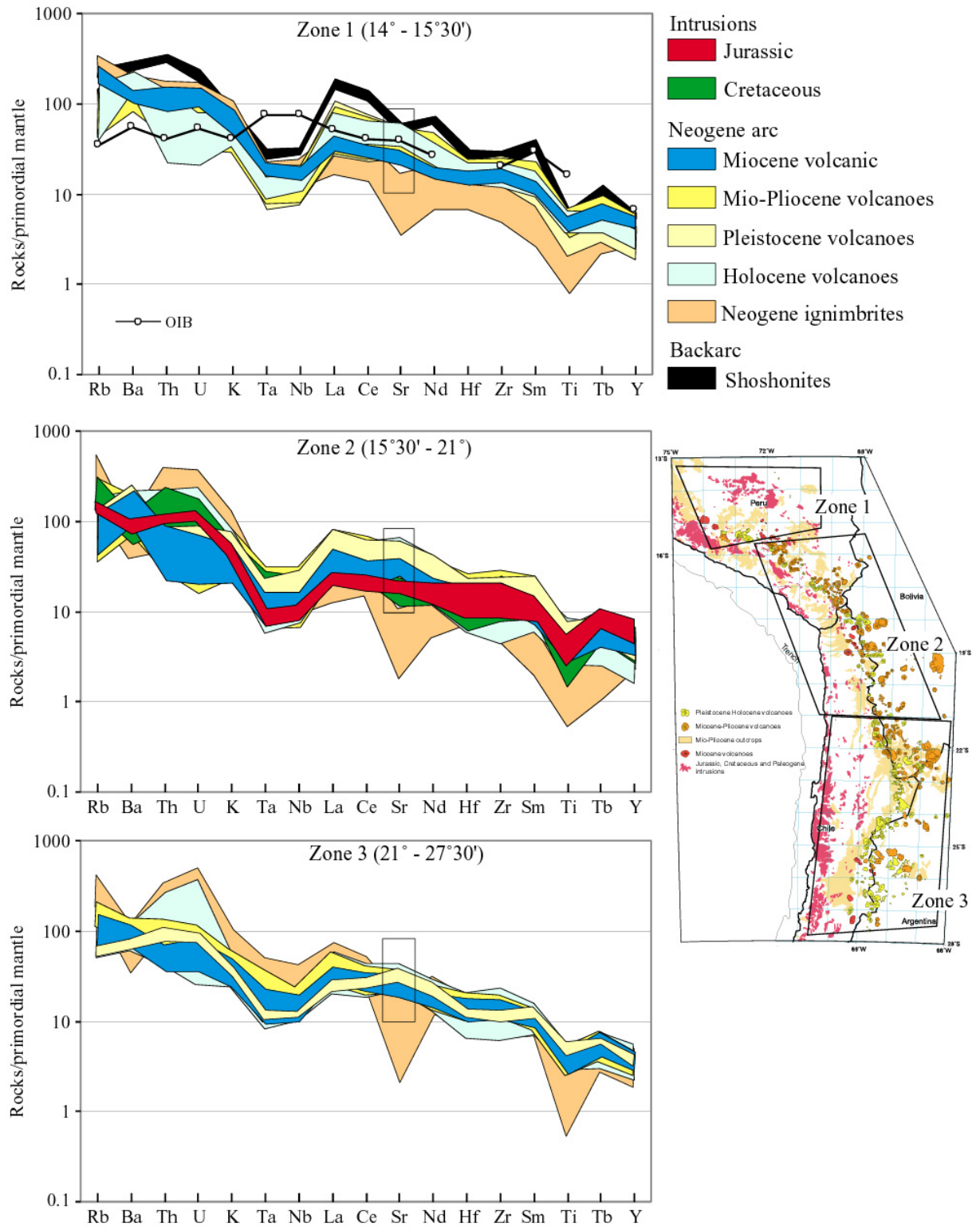


Fig. 3.7. Primordial mantle normalized concentrations of trace elements plus K and Ti from northern, central and southern part of the Central Volcanic Zone. Normalization factors are from McDounough et al. (1992). The OIB pattern (Sun, 1980) is shown for comparison.

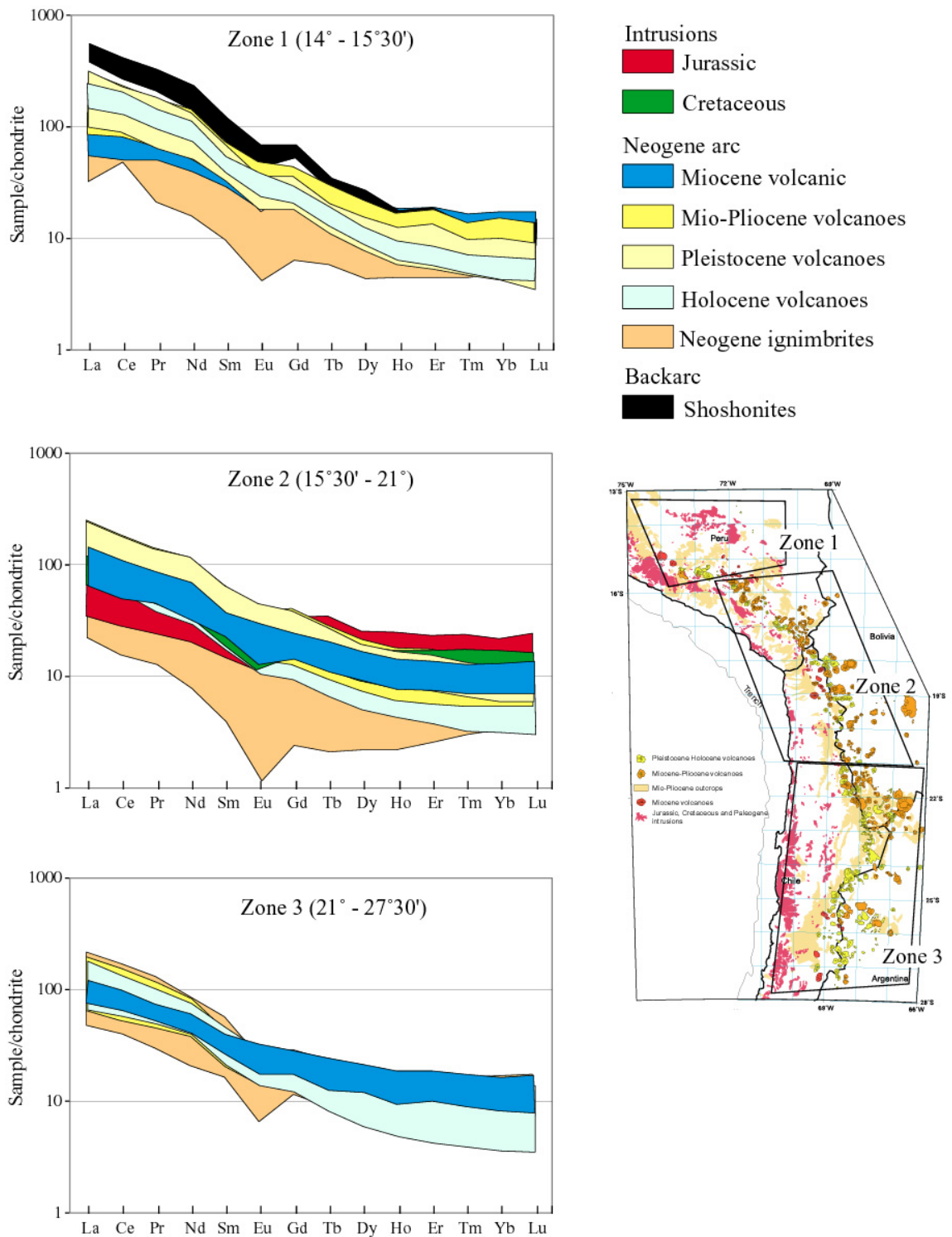


Fig. 3.8. REE diagrams for the CVZ. Normalization factors are from McDonough & Sun (1995).

### 3.3.2 Isotopes

#### Sr- and Nd-isotopes

The initial isotopic composition of the rocks provides information about the (mantle-) sources of the magmatic rocks as well as about processes by which their chemical and isotopic compositions are modified (e.g. crustal contamination).

When the age of the rock is known, its initial isotopic ratios can be calculated by using the basic geochronological equations:

$$\frac{{}^{87}\text{Sr}}{{}^{86}\text{Sr}} = \left( \frac{{}^{87}\text{Sr}}{{}^{86}\text{Sr}} \right)_{\text{initial}} + \frac{{}^{87}\text{Rb}}{{}^{86}\text{Sr}} (e^{\lambda t} - 1)$$

which are transformed to:

$$\left( \frac{{}^{87}\text{Sr}}{{}^{86}\text{Sr}} \right)_{\text{initial}} = \frac{{}^{87}\text{Sr}}{{}^{86}\text{Sr}} - \frac{{}^{87}\text{Rb}}{{}^{86}\text{Sr}} (e^{\lambda t} - 1)$$

The epsilon notations (DePaolo & Wasserburg 1976) are calculated by using the following equations:

$$\epsilon_{\text{Nd}} = \left[ \frac{({}^{143}\text{Nd}/{}^{144}\text{Nd})_{\text{initial}}}{I'_{\text{CHUR}}} - 1 \right] * 10^4$$

Jurassic and Early Tertiary intrusions (data from Boyle et al., 1989; Mukasa et al., 1986; Hawkesworth et al., 1989; Clark et al., 1990; Anthes, 1993; Lucassen et al., 2002) show distinctly positive  $\epsilon_{\text{Nd}}$  and lower  ${}^{87}\text{Sr}/{}^{86}\text{Sr}$  than younger samples, most of the intrusions overlap with the ratios reported from NVZ, SVZ and AVZ.

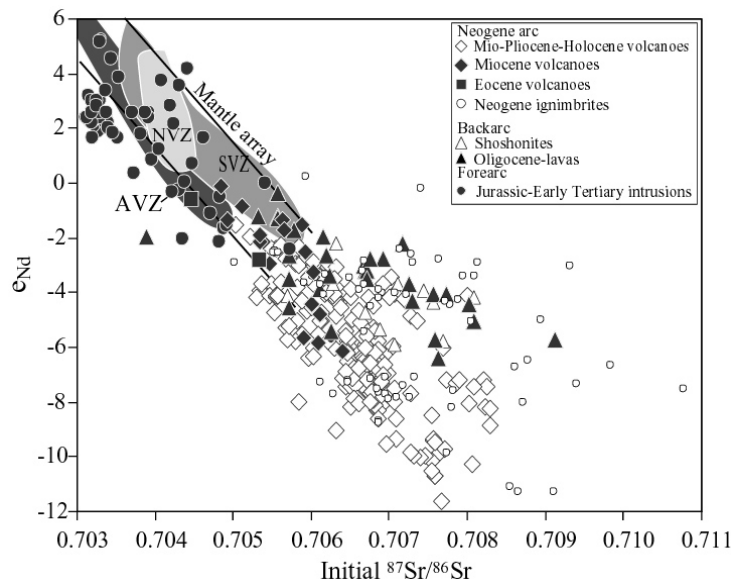


Fig.3.9. Diagram of  $\epsilon_{\text{Nd}}$  vs. Initial  ${}^{87}\text{Sr}/{}^{86}\text{Sr}$  presenting the data set from the CVZ in comparison to data fields from NVZ (Bourdon et al., 2002), SVZ (Kay et al., 2005), AVZ (Stern and Killian, 1996). BSE is bulk silicate earth.

The isotopic variability of the Neogene magmatic rocks have values ranging between  ${}^{87}\text{Sr}/{}^{86}\text{Sr} = 0.705$  to  $0.7085$  and  $\epsilon_{\text{Nd}} = 0$  to  $-12$ . Jurassic, Cretaceous, Eocene rocks are more depleted (e.i., higher  $\epsilon_{\text{Nd}}$  and lower  ${}^{87}\text{Sr}/{}^{86}\text{Sr}$ ) than those of the Neogene arcs, and overlap the ratios reported from SVZ and NVZ.

Shoshonite samples display less negative  $\epsilon_{\text{Nd}}$  and middle  ${}^{87}\text{Sr}/{}^{86}\text{Sr}$  ratios compared with cluster formed by all volcanic rocks of the CVZ.

Oligocene lavas are less depleted in  $\epsilon_{\text{Nd}} = 0$  to  $-7$  than Neogene lavas.

The ignimbrites show a wide range of  $\epsilon_{\text{Nd}}$  and higher  ${}^{87}\text{Sr}/{}^{86}\text{Sr}$  ratios, some of them overlap the Neogene lavas.

### Spatial and Temporal variation of Sr-Nd isotopes

As seen in Fig. 3.9  $^{87}\text{Sr}/^{86}\text{Sr}$  ratios increase with decreasing age from Jurassic to Miocene. During Mio-Pliocene until present, Sr-isotopic compositions remain nearly constant with most ratios falling within a range of 0.705-0.7085. Mio-Pliocene to Holocene volcanoes displays more variable values than Miocene, probably simple reflecting the larger number of available data.

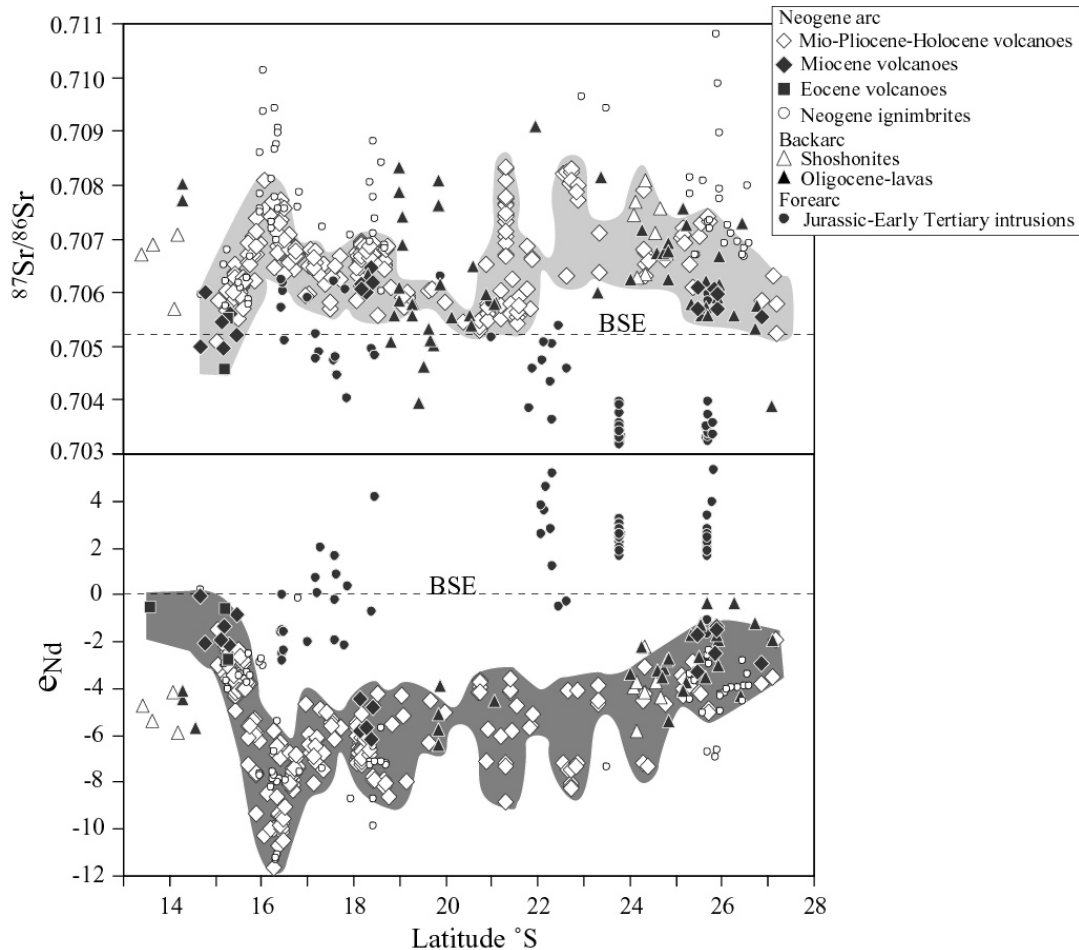


Fig. 3.10.  $^{87}\text{Sr}/^{86}\text{Sr}$  and  $\epsilon_{\text{Nd}}$  ratios versus Latitude  $^{\circ}\text{S}$ .

Increasing  $^{87}\text{Sr}/^{86}\text{Sr}$  from the coast to Western Cordillera with decreasing age has been observed by Rogers & Hawkesworth (1989) at  $22^{\circ}\text{S}$ , Kay et al. (1994) at  $26-29^{\circ}\text{S}$  and Haschke et al. (2002) at  $21-26^{\circ}\text{S}$ . In all work cited, Mio-Pliocene to recent samples show drastically elevated and variable Sr-isotope ratios, probably reflecting increased crustal thickness and assimilation resulting from the recent uplift episode.

Nd-isotopes ratios decrease with decreasing ages. Jurassic and Early Tertiary rocks drop from  $\epsilon_{\text{Nd}}$  5 to  $\epsilon_{\text{Nd}}$  -2.

The Eocene, Oligocene and Neogene rocks delineate three groups for Nd-isotope ratios. In the central sector between  $15^{\circ}\text{S}$  and  $\sim 25^{\circ}\text{S}$ ,  $\epsilon_{\text{Nd}}$  ranges from -4 to -9. The notable low  $\epsilon_{\text{Nd}}$  values from -9 to -12 are around  $16^{\circ}\text{S}$  (Arequipa). The northern sector ( $13^{\circ}\text{S}$  -  $16^{\circ}\text{S}$ ) and southern sector ( $24^{\circ}\text{S}$ - $28^{\circ}\text{S}$ ) have similar values of  $\epsilon_{\text{Nd}}$  from 0 to -6. Transitions between these groups are relatively abrupt.

The Mio-Pliocene to Holocene volcanoes between 16 to  $22^{\circ}\text{S}$  show notably high  $^{87}\text{Sr}/^{86}\text{Sr}$  ratios and low  $\epsilon_{\text{Nd}}$  values (Fig. 3.9) than the volcanoes from ( $13-16^{\circ}\text{S}$  and  $22-28^{\circ}\text{S}$ ), and high

Sr contents (400 to 1600) are observed between 22 and 14°S (Fig. 3.11), although crustal thickness is similar along these latitudes.

Concentration between 0 and 400 Sr (ppm) is conformed only by ignimbrites ( $\text{SiO}_2 > 60\%$ ), Jurassic and Cretaceous rocks.

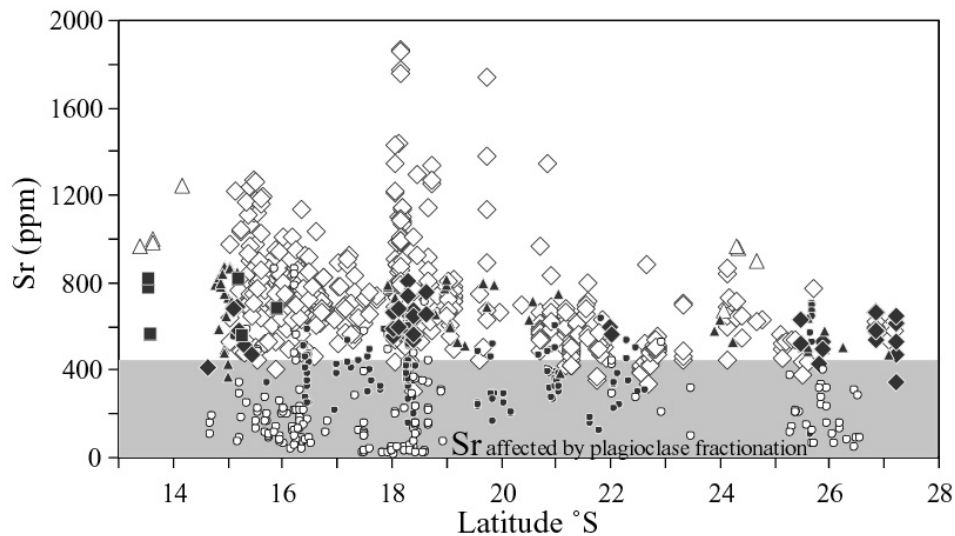


Fig. 3.11. Sr contents along the central volcanic zone. Legend as in Fig. 3.10.

### Spatial and Temporal variation of Pb- isotopes

New lead isotopic compositions (68 samples) were determined on carefully selected whole rock and were combined with published data.

The majority of the analyses are Neogene lavas. En general the Meso-Cenozoic samples show two groups that are distinct in their  $^{206}\text{Pb}/^{204}\text{Pb}$  ratios (Fig. 3.12). The low  $^{206}\text{Pb}/^{204}\text{Pb} = 17.5-18.5$  and the high  $^{206}\text{Pb}/^{204}\text{Pb} = 18.5-19$ . The rocks from the basements also show two groups: Paleozoic rocks have the highest  $^{206}\text{Pb}/^{204}\text{Pb} > 18.5$  and plot in the radiogenic site, and Proterozoic samples show the lowest  $^{206}\text{Pb}/^{204}\text{Pb} < 18$  (unradiogenic site).

In the diagram  $^{207}\text{Pb}/^{204}\text{Pb}$  versus  $^{206}\text{Pb}/^{204}\text{Pb}$ , the data set plot between to the upper crustal lead and orogenic belt lead of Zartman and Haines (1988).

Jurassic intrusion plot near the Nazca plate basalts field and Nazca plate sediments in the diagram  $^{208}\text{Pb}/^{204}\text{Pb}$  versus  $^{206}\text{Pb}/^{204}\text{Pb}$ .

The different Pb-isotope ratios observed in the Cenozoic rocks derivate from the isotopic compositions of the underlying basements, the low Pb ratios overlap the Proterozoic points, while the high lead isotope overlap the Paleozoic samples (Fig. 3.12). Such tendency of the  $^{206}\text{Pb}/^{204}\text{Pb}$  found in volcanic rocks has been interpreted as a result of mixing between mantle-derived Pb and Pb crustal by various authors (e.g. Tilton & Barreiro, 1980; Barreiro, 1984; Mukasa et al., 1986; Wörner et al., 1992; Aitchison et al., 1995).

Based on assimilation model for some volcanoes of the CVZ, crustal input about 12 and 20% into mafic mantle magmas through melting in the middle or lower crust prior to differentiation in the upper crust (Aitchison et al., 1993 and Entenmann, 1994).

Some Jurassic and Early Tertiary intrusion are interpreted to reflect either variations from a more radiogenic mantle source or assimilation of rarely more radiogenic or unradiogenic crustal components.

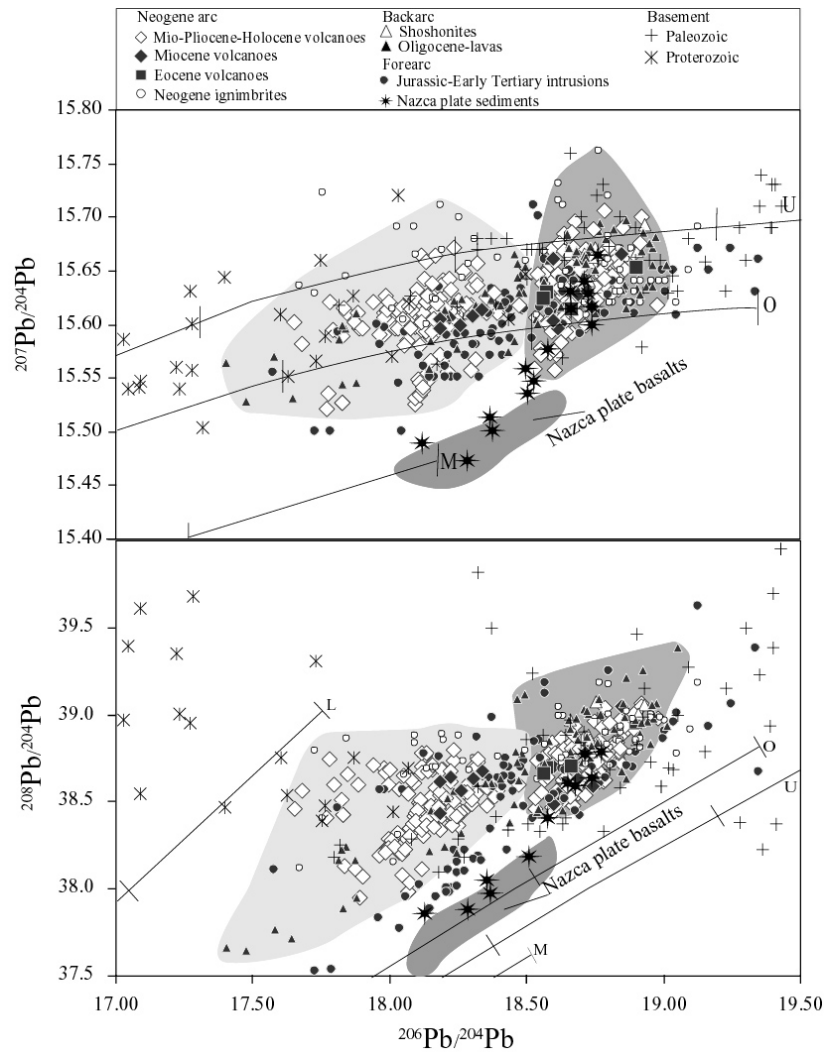


Fig. 3.12. Pb-isotope diagrams of the Meso-Cenozoic rocks from the CVZ, compared with the lead isotope composition from the Proterozoic and Paleozoic basement (outcrops in Fig. 1.3), Nazca Plate sediments and basalts (Dash, 1981). Zartman and Haines (1988) lead evolution model: M. upper mantle lead; O. orogenic belt lead; U. upper crustal lead; L. lower crust lead. The ticks on each curve are at 100 Ma intervals.

Although the overlapping of all samples along the CVZ (Fig. 3.13), three groups independent of age and  $\text{SiO}_2$  contents, show abrupt transition at 18.5 to 18.7 ratios in the diagram  $^{206}\text{Pb}/^{204}\text{Pb}$  versus Latitude  $^\circ\text{S}$ . In the central part between  $15.30^\circ\text{S}$  and  $20.8^\circ\text{S}$   $^{206}\text{Pb}/^{204}\text{Pb}$  varies from 17 to 18.50. The high  $^{206}\text{Pb}/^{204}\text{Pb}$  ratio of 18.5 to 19.5 is found in  $13\text{--}16^\circ\text{S}$  and  $20\text{--}28^\circ\text{S}$ . Such variations are correlated with Nd-isotopes variations along the CVZ (see Fig. 3.10) and with Sr-isotopes are not clear the correlation.

In the diagrams  $^{207}\text{Pb}/^{204}\text{Pb}$  and  $^{208}\text{Pb}/^{204}\text{Pb}$ , the ratios show no steep transitions as the  $^{206}\text{Pb}/^{204}\text{Pb}$  along the arc.



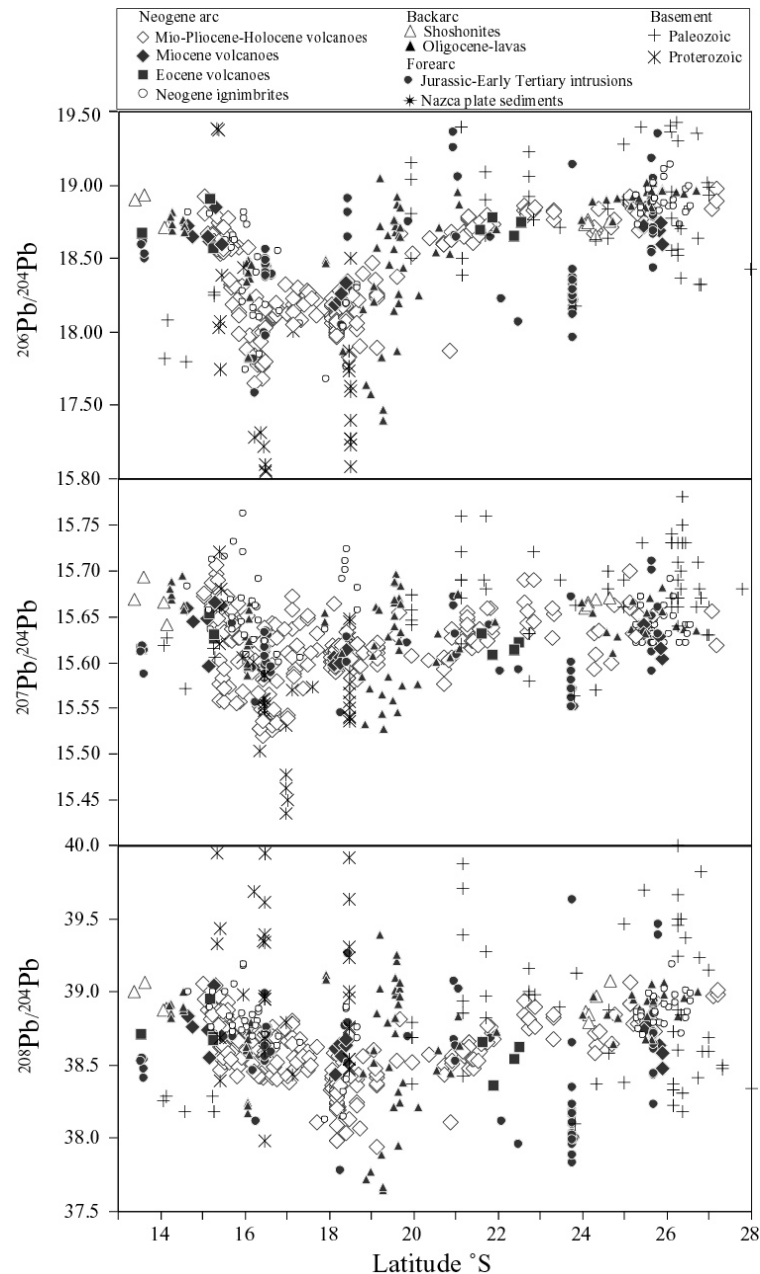


Fig. 3.13. Regional variation in Pb isotope compositions along the CA.

### 3.4 Summary and Discussion: Implications for a tectonic model

#### Summary

Following observations have been made along the CA.

- Mesozoic intrusions and Cenozoic lavas from the arc are classified calc-alkaline and Cenozoic rocks from the backarc are alkaline. These rocks display signatures characterized by LILE enrichment and HFSE depletion. The ignimbrites do not show a marked Nb-Ta depletion.
- Concentrations of,  $P_2O_5$ ,  $K_2O$ ,  $Na_2O$ , Sr, Ba, Zr, Nb increase from Jurassic to present, whereas abundances of, CaO,  $Fe_{tot}$  and MnO decrease. Content of Y are highest in Cretaceous-Eocene rocks and remain at constantly low values from Mio-Pliocene to Present.
- The slope of REE patterns increase from Jurassic to Holocene rocks, as Yb contents decrease and Sm contents increase and become more variable with time.

- $(^{87}\text{Sr}/^{86}\text{Sr})_{\text{initial}}$  ratios increase from Jurassic until present.
- $^{143}\text{Nd}/^{144}\text{Nd}$  ratios decrease from Jurassic until present.
- Pb isotope compositions of igneous rocks clearly reflect a contribution of the underlying basement.

### Discussion

Geochemical variations across or along the active continental Andean margin have been investigated by numerous authors (Fig. 3.1, Kay et al., 1994, 1999, 2005; Stern, 1990, 1991; Hildreth & Moorbath, 1988; Roger & Hawkesworth, 1989; Wörner et al., 1988, 1992; Davidson et al., 1990; Haschke et al., 2002, 2003). The uncertainties about the nature of this complex subduction setting characterized by an interplay of many components (such as descending slab, sediments, fluids, asthenospheric mantle, lithospheric mantle lower and upper crust) by various processes (partial melting, assimilation, fractional crystallization) led to the development of conflicting models on Andean Petrogenesis.

The following discussion try to assess debate different sources or different processes are responsible for the observed variations in major, trace elements and isotope geochemistry along the CVZ.

#### 3.4.1 Source or Processes?

As described in Chapter 1 and in the Introduction, the large number of conflicting models can be split into two major groups: One group proposes that the geochemical characteristics of erupted lavas simply reflect heterogeneity of the source. A heterogeneous source either represents variably enriched asthenospheric mantle due to contamination by subducted sediments or tectonic erosions (Stern, 1988, 1990) or ancient enriched lithospheric mantle (Roger & Hawkesworth, 1989).

The second group postulates that all primary magmas produced at subduction zones are essentially similar (since they have been derived by similar mechanisms from a similar source, the asthenospheric mantle wedge) and inherit their diverse geochemical features by interaction with the crust during ascent (Hildreth & Moorbath, 1988; Wörner et al., 1988, 1992; Davidson et al., 1990).

#### Subducted sediments & Tectonic erosion

Although Stern (1988) holds variable subduction geometry and sedimentary input responsible for along arc variations in magma geochemistry between 33°S - 38°S, Hildreth & Moorbath (1988) have demonstrated that rather varying amounts of crustal contributions can account for the observed diversity. The question is, despite of apparent constancy of sedimentary input along arc today, whether changes in subduction geometry and/or sedimentary input through time have influenced magma geochemistry across arc. Seyfried et al. (1995) recognized crucial changes in the drainage system and humidity regime at 18°S from Miocene until present: in contrast to the present extremely arid climate impeding intense erosion, over 1000 m of alluvial sediments were deposited in the Longitudinal valley (Fig. 1.2) during the Miocene times. Flores et al. (2005) suggested increasing subsidence and synsedimentary activity in the Longitudinal valley of southern Peru during the Early and Middle Miocene. Allmendinger et al. (2005) concluded that it is doubtful that significant amounts of terrigenous sediments reach the Peruvian-Chilean trench as the Coastal Cordillera scarps prevents high sedimentary input.

A strong influence of pelagic sediments is also not observed in the rocks of this study as no sample displays negative Ce-anomalies or Pb-compositions resulting from hypothetical mixing of primitive island arc basalt with Nazca plate sediments (Davidson et al., 1990). Entenmann (1994) however, demonstrated that mixing of MORB with ~1% pelagic Pacific

sediments can account for the variable LILE content of CVZ basaltic andesites. On the other hand he argued that elevated  $\delta^{18}\text{O}$  values are caused by intra-crustal assimilation and are not source effects resulting from sediment subduction and tectonic erosion, or derivation from ancient subcontinental mantle lithosphere.

Plots of Rb/Cs and Ba/La versus age (Fig. 3.14) underlie the apparently conflicting evidences for or against source contamination: whereas maximum Rb/Cs ratios (low ratios indicate involvement of Cs-rich pelagic sediments, Plank & Langmuir, 1988) decrease from Miocene to present, Maximum Ba/La ratios (high ratios indicate involvement of subducted sedimentary components, Kay, 1977) also decrease or remain constant, contradictory to what one would expect, if these features were established only by increasing amounts of a slab component. Rb/Cs ratios have their maximum and largest scatter in Miocene times exactly when the uplift event occurred. As Hildreth & Moorbath (1988) proposed that intra-crustal contamination is the dominating process in establishing Ba/La ratios, high Rb/Cs and Ba/La ratios might reflect the onset of large scale crustal involvement in the 20 Ma to Recent rocks. However, Ba/La ratios are very sensitive to K-feldspar fractionation, as we see in the Neogene ignimbrites ratios (Fig. 3.14). Thus, the Ba/La ratios have to interpret with caution.

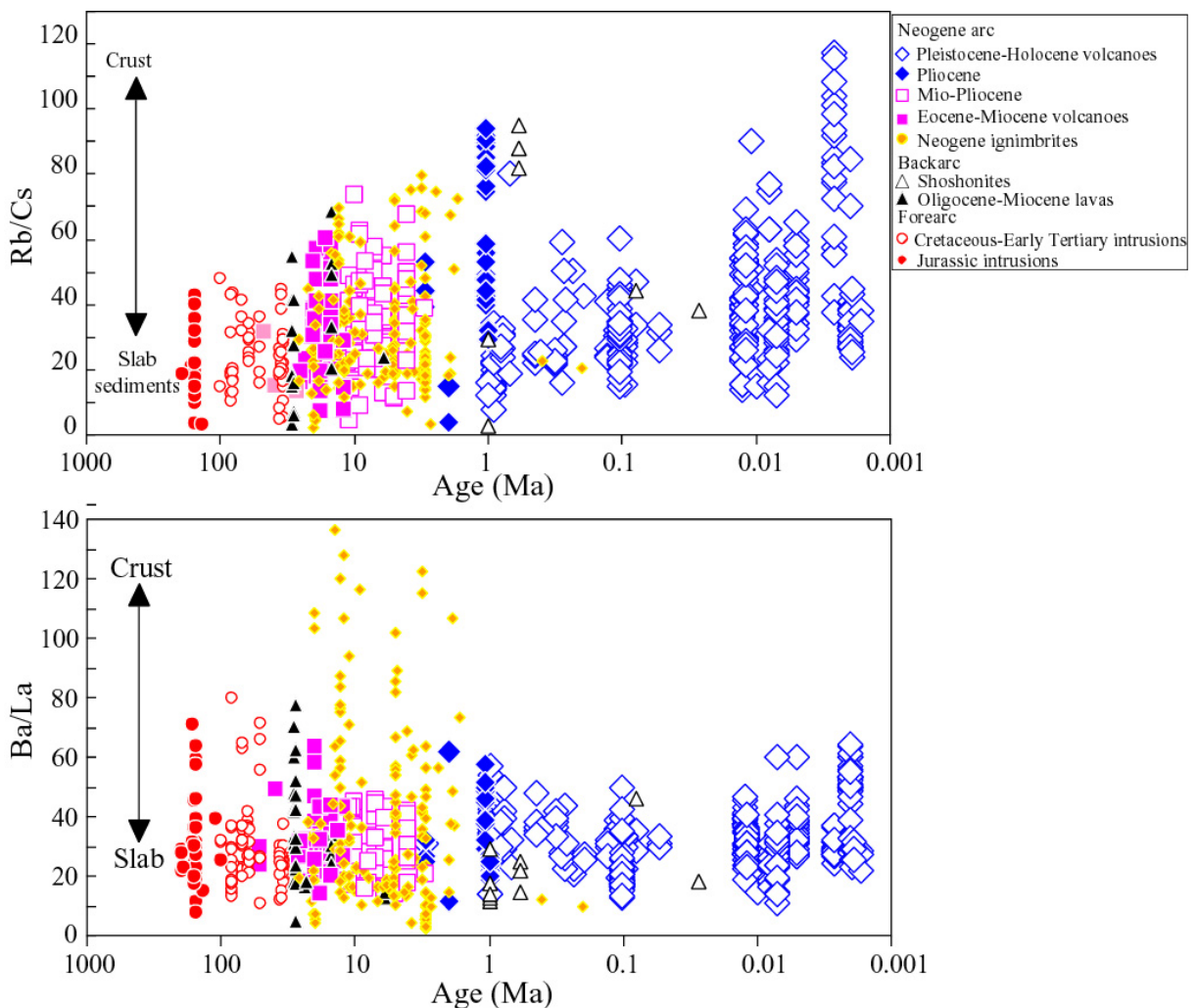


Fig. 3.14. Rb/Cs and Ba/La versus age diagrams of samples from the CA.

In the light of the obviously contradictory indications above, it is hard to assess the role of source contamination in Andean Petrogenesis. With respect to strong evidence from Pb isotopes data, the influence of source contamination is considered to be small.

### Enriched subcontinental lithosphere

Roger & Hawkesworth (1989) postulated the ancient enriched subcontinental lithosphere to be the main site of magma production, as both incompatible elements abundances (including Sr concentration) and  $^{87}\text{Sr}/^{86}\text{Sr}$  ratios increase from west to east at 22°S. In contrast to Roger & Hawkesworth (1989)  $\epsilon_{\text{Nd}}$  values decrease and Sr contents increase with time and are independent of Ta/Sm ratios, Th/Ta ratios does not unequivocally decrease with higher Ta/Sm ratios and younger ages (Fig. 3.15), indicating that no large contribution of subcontinental lithosphere occurred with time.

Nevertheless, Stern et al. (1991), reported highly variable bulk compositions from upper mantle xenoliths in Patagonian basalts at 52°S thus demonstrating the potential heterogeneity of subcontinental lithospheric mantle (at least for the SVZ).

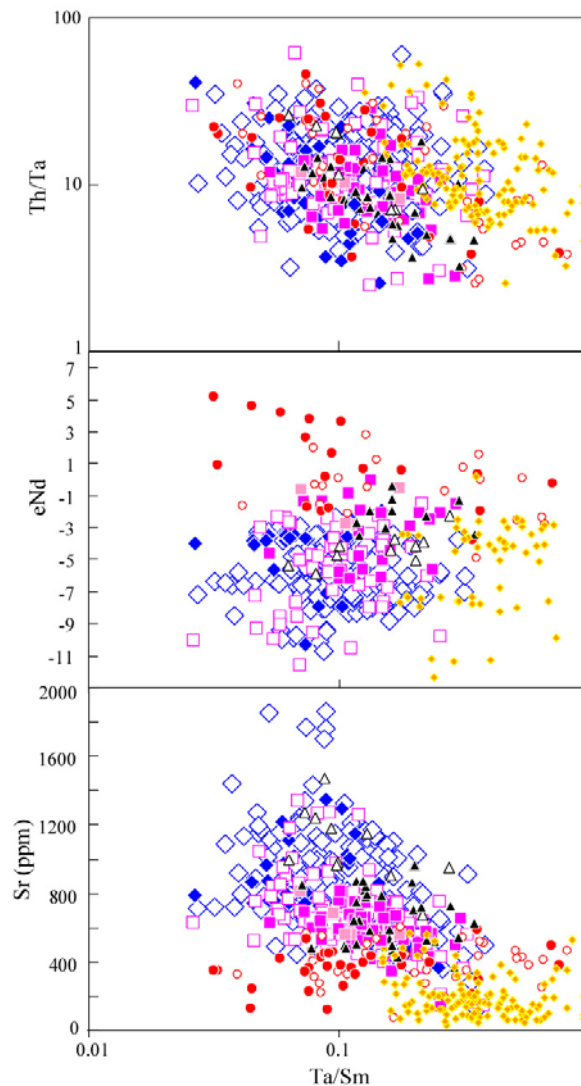


Fig. 3.15. Diagrams of Th/Ta,  $\epsilon_{\text{Nd}}$  and Sr versus Ta/Sm of samples from the CVZ similar to those from Roger & Hawkesworth (1989). Legend as in Fig. 3.14.

However, as discussed in Davidson et al. (1991), in the Figure 3.16 Mio-Pliocene to recent lavas trend show high pressure (where garnet is stable) during depth assimilation, in agreement with a 70 km thick crust after Andean uplift. Contrasting are the Jurassic, Cretaceous, Early Tertiary, and Miocene samples, which display much lower Sr contents. The lower Sr-isotope ratios probably reflect a lesser degree of crustal assimilation involving no

garnet, in accordance with a thin crust at these times. The Neogene ignimbrites trend show higher  $^{87}\text{Sr}/^{86}\text{Sr}$  ratios and low Sr contents indicating that they added additional crustal component by contamination of low Sr and high  $\text{SiO}_2$  magmas late in the differentiation process with plagioclase stable at low pressure.

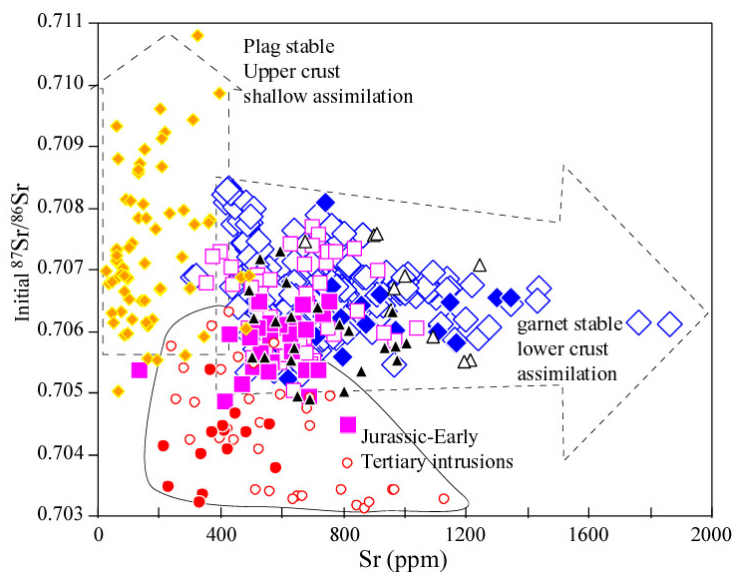


Fig. 3.16. Initial  $^{87}\text{Sr}/^{86}\text{Sr}$  versus Sr of samples from the CA. Symbols and data sources as in Fig. 3.14

Oxygen and Pb isotopes data provide convincing evidence against a dominant role of enriched mantle lithosphere in Andean rocks at  $18^\circ\text{S}$  (Davidson et al., 1991, Fig. 3.1).

### Crustal Contamination

Although many uncertainties about composition and structure of the continental crust exist, all data presented here are most consistent with models involving intra-crustal assimilation in MASH-zones as proposed by Hildreth & Moorbath (1988), Wörner et al. (1988, 1994), Davidson et al. (1990, 1991). Geochemical trends and Nd-Sr isotope indicate an increase of crustal thickness with time and clearly document the Andean uplift event which started  $\sim 25$  m.y. ago.

Constraint on the amount and timing of crustal thickening and on the source region come from the temporally changing REE signatures of magmatic arcs formed before, during and after crustal thickening. In simple terms, the REEs are guides to the pressure-sensitive residual mineral and melting percentage of the source. These correlations assume that the melts equilibrated with and reflect the source minerals of a hydrous mafic crust-mantle boundary region showing melting-assimilation-storage-homogenization (Hildreth and Moorbath, 1988) processes.

Increasing La/Yb ratios in magma across arcs (with decreasing ages) is widely observed phenomenon (e.g. Gill, 1981; Torpe, 1979; Kay et al., 1991, 1994, 1999; Hawkesworth, 1988; Haschke et al., 2002, 2003). Hildreth and Moorbath (1988) also observed an increase of La/Yb along at  $33\text{-}37.7^\circ$ . In all cases, La/Yb ratios are higher on thicker and more mature crust, thus crustal thickness seems to play an important role in processes that fractionate HREE from LREE.

Haschke et al., 2002, 2003 observed increasing La/Yb ratios and increasing Sr-Nd isotopic enrichment with time are characteristic of Neogene magmatic rocks and Pre-Neogene magmatic episodes between latitudes  $21^\circ\text{S}$  and  $22^\circ\text{S}$  (Fig. 3.17, Fig. 3.1). These temporal

geochemical changes reflect a progressive transfer of melting zone from the upper mantle into variably thickened garnet-bearing (lower) crust.

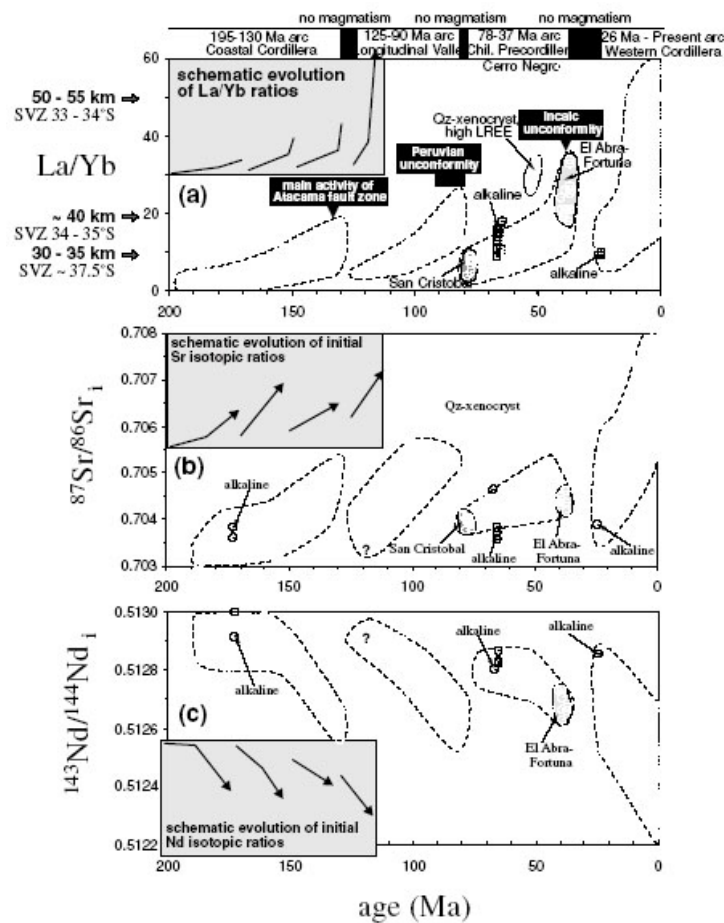


Fig. 3.17. Plot of age of Central Andean magmatic rocks vs. La/Yb ratios, showing steepening rare earth element (REE) patterns within each arc system and with thickening of arc crust (from Haschke et al., 2003).

Our compiled data of different magmatic arcs in the CA show dramatic change in the values of Sr-Nd isotopes and REE ratios from Jurassic to Recent times (Fig. 3.18).

To quantify the general slope of REE pattern through time along the CA (principally during the “Andean Cycle”), La/Yb, La/Sm, and Sm/Yb ratios are plotted versus age in Figure 3.18.

As was observed by Haschke et al. (2003) La/Yb ratios increase with time in the CA (Fig. 3.18c). However, LREE ratios (La/Sm) show that they are sensitive to plagioclase fractionation (see ratios of Neogene ignimbrites in Fig. 3.18d and Fig. 3.19) and HREE ratios (Sm/Yb) are less affected by plagioclase fractionation (Fig. 3.18e). HREE ratios is signal to changes in pressure and residual crustal mineralogy and high Sm/Yb ratios is the best indicator of garnet-bearing in residual mineralogy and because garnet preferentially fractionates the HREE.

Jurassic rocks (50-70 wt % SiO<sub>2</sub>) show fractionated but largely overlapping REE pattern (Fig. 3.8). Evolution of Sm/Yb ratios of these rocks shows less increase (Sm/Yb from 1 to 3). Cretaceous-Early Tertiary before-uplift rocks are characterized by LREE-enriched patterns (Fig. 3.8 and 3.18d) and Sm/Yb (1-3.5). Eocene lavas show Sm/Yb ratios (from 1 to 3.5).

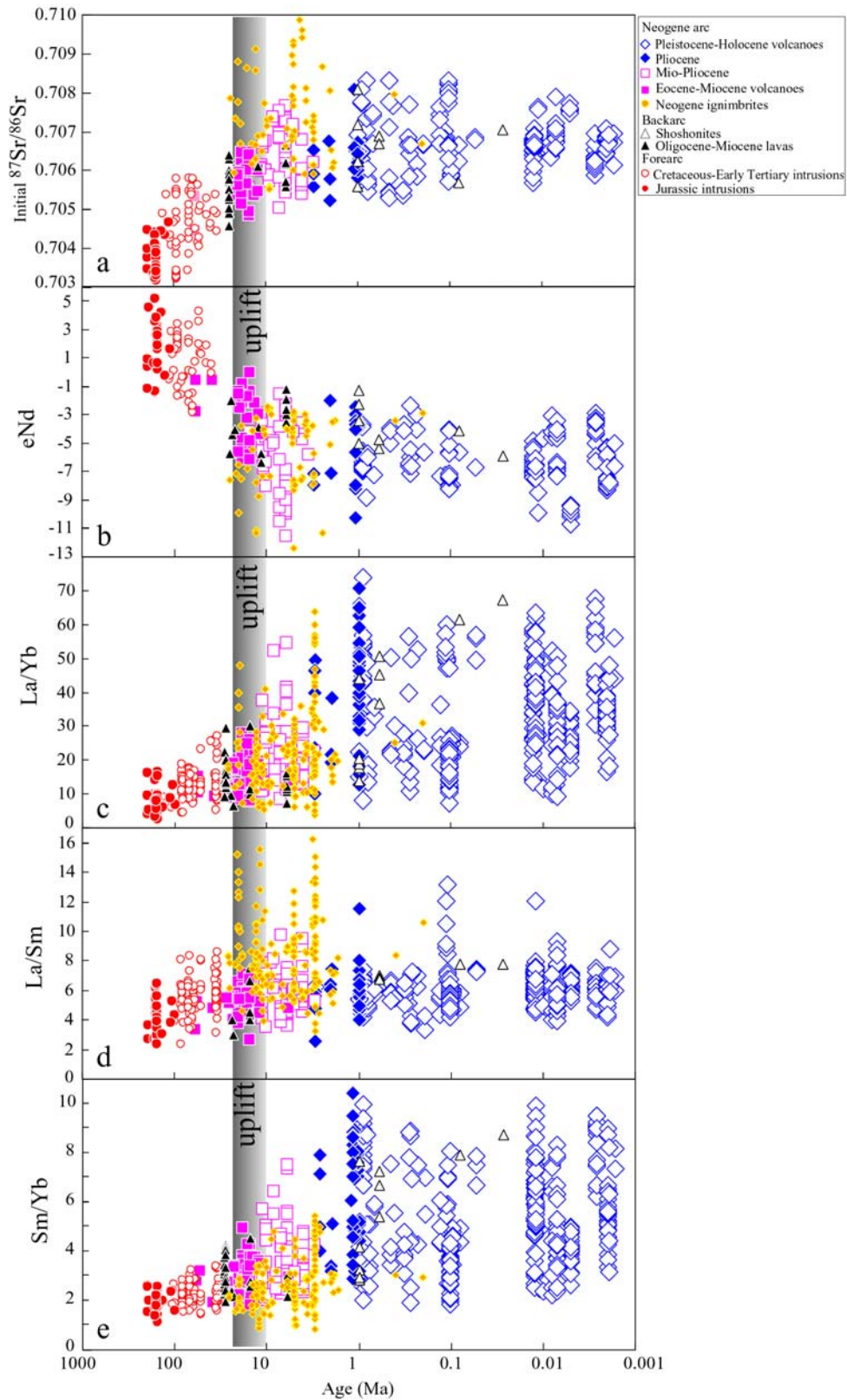


Fig.3.18. Semilog scale plotting the Age (Ma) for CA rocks versus Sr-isotope, eNd values, La/Yb, La/Sm, and Sm/Yb ratios.

Miocene syn-uplift andesitic and dacitic composition (55-65 wt % SiO<sub>2</sub>, Fig. 3.19) exhibit fractionated REE pattern with steeper HREE patterns (Fig. 3.8). Sm/Yb ratios of these rocks increase through time from mostly low Sm/Yb (1-3) to high Sm/Yb (1.5-5) ratios.

Mio-Pliocene after-uplift andesites and dacites (53-68 wt % SiO<sub>2</sub>, Fig. 3.19) show fractionated REE pattern (Fig. 3.8) and have higher Sm/Yb (2-7) ratios.

Pleistocene to Recent andesites and dacites (53-68 wt % SiO<sub>2</sub>, Fig. 3.19) show extremely fractionated REE pattern (Fig. 3.8) with strongly steepening HREE pattern at this time. Sm/Yb ratios vary from 2 to 10.

Oligocene-Miocene and Quaternary rocks in the backarc (47-65 wt % SiO<sub>2</sub>) show also increasing HREE pattern with decreasing age (Fig. 3.19 and 3.18e).

These systematic changes are due to progressively decreasing Yb (from 3.7 to 0.4 ppm) with decreasing age (Fig. 3.20).

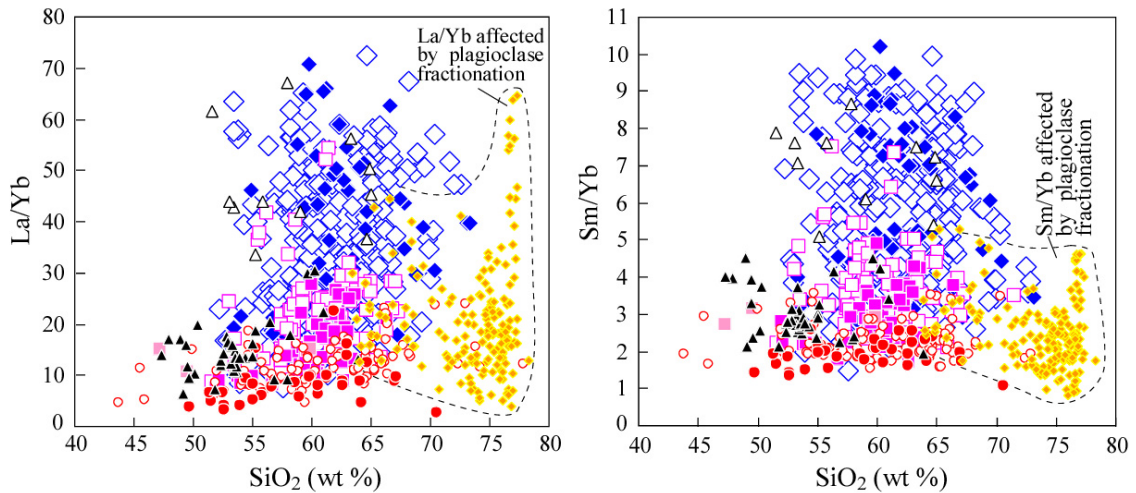


Fig.3.19. Plot of La/Yb, Sm/Yb versus SiO<sub>2</sub> (wt %), rocks with more than 68% are affected by plagioclase fractionation. Legend as in Fig. 3.18.

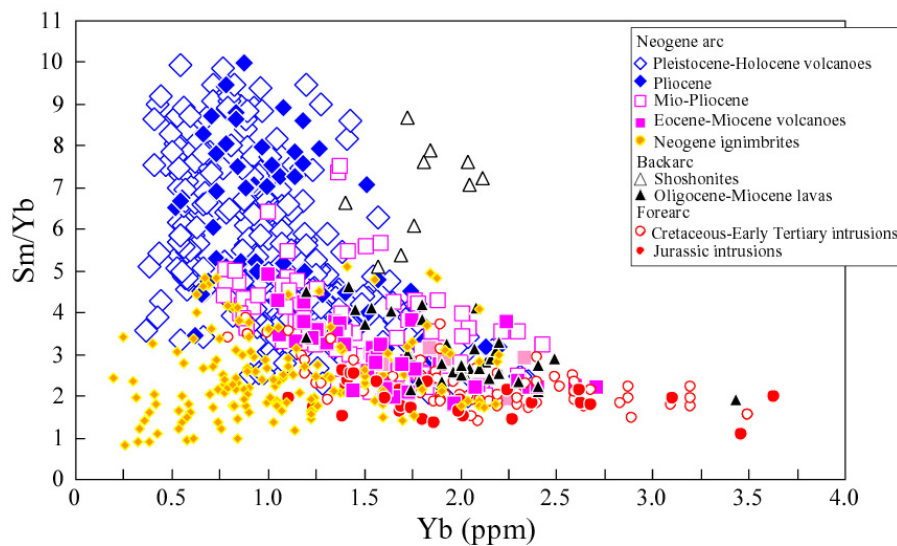


Fig. 3.20. Sm/Yb ratios versus Yb (ppm).

Many of these characteristics of the youngest lavas Mio-Pliocene to Recent andesites-dacites match those of adakites (e.i. primary dacite melts from subducted young oceanic crust (Defant and Drummond, 1990)). However, geophysical, geologic, isotopic, and age data from our study suggest that partial melting of the base of thick orogenic crust (~40 km during Mesozoic time, and ~70 km during Neogene).



Sm/Yb ratios not increases similar along the CA even they have the same age and cross the same thick crust, the highest ratios are between latitudes 14°S and 22°S (Fig. 3.21). However, there is an obvious decoupling between the tectonic development and its reflection in geochemistry of erupted rocks: while elevated crustal thickness (~70 km) may have been established by ~10 Ma, the rapid increase in Sm/Yb ratios occurred some ~3 Ma later. Observed Sm/Yb ratios of 2-10 associated with 70 km thick crust along the CA correspond well with Sm/Yb ranging 2-8 reported from Kay et al. (1999) associated with ~60 km crust at 28°S-33°S and Sm/Yb ratios of 3-9 at 34°S -36°S.

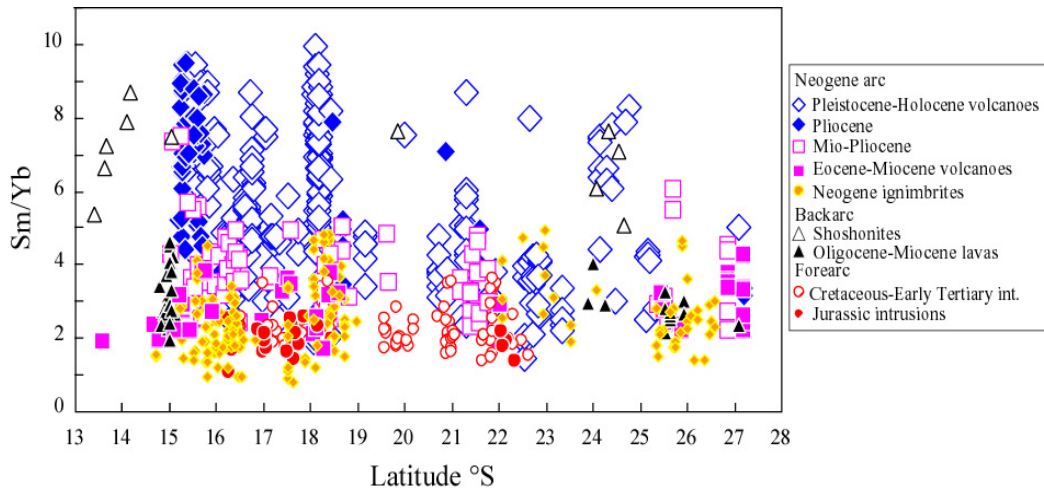


Fig. 3.21. Sm/Yb ratios along the Central Volcanic Zone.

Dostal et al. (1977) proposed an alternative model in which steeper REE patterns are produced by smaller (<5%) degrees of partial melting of an enriched upper mantle source across an arc which also results in the increase of incompatible element abundances. Lopez-Escobar et al. (1977) modeled the steep REE pattern of a silicic andesite as a product of 3% melting of a garnet peridotite. However, these processes are not capable of explaining the elevated Sr isotope ratios, unless subsequent crustal assimilation has occurred. Hildreth and Moorbath (1988) show that the steeper REE pattern, elevated abundances of incompatible elements, and increased Sr and Oxygen isotope ratios can be accounted for by assimilation of lower crust. Furthermore, they do not see evidence why melting of garnet peridotite beneath thick crust should be a more effective sink for HREE than beneath thin crust.

Sr-Nd isotopic data of arc magmatic rocks show isotopic enrichment with decreasing age (Fig. 3.18a, b and 3.19), overall there is contrast between Jurassic-Early Tertiary ( $^{87}\text{Sr}/^{86}\text{Sr} = 0.703-0.705$  and  $\epsilon_{\text{Nd}} = 6$  to  $-2$ ) and Neogene rocks ( $^{87}\text{Sr}/^{86}\text{Sr} = 0.703-0.705$  and  $\epsilon_{\text{Nd}} = 0$  to  $-12$ ). The major change is seen before and after crustal uplift (Fig. 3.22).

Pb isotope signatures reflect different crust (Wörner et al., 1992; Aitchison et al., 1995) and the increasing of Sm/Yb of Pliocene to Recent lavas is observed in the radiogenic and unradiogenic groups (Fig. 3.22).

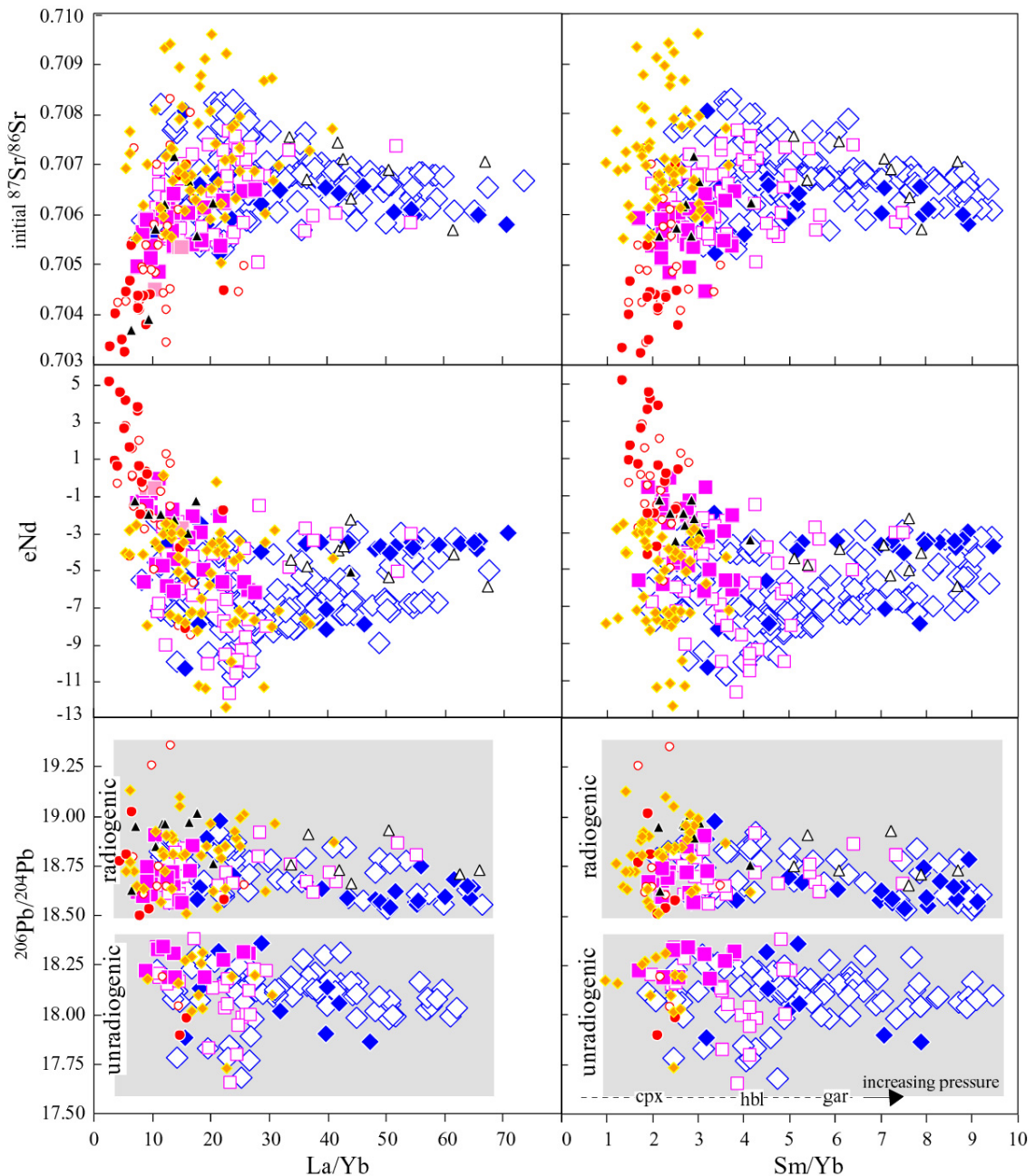


Fig. 3.22. Plot of  $^{87}\text{Sr}/^{86}\text{Sr}$  ratios,  $\epsilon_{\text{Nd}}$  values (indicator of degree of assimilation) and  $^{206}\text{Pb}/^{204}\text{Pb}$  ratios (indicator of different crustal contaminant) versus Sm/Yb ratios (indicator of depth of assimilation). cpx = clinopyroxene, hbl = hornblende, gar = garnet. Legend as in Fig. 3.21.

### 3.4.2 Geochemical constraint in a Tectonic model

During Jurassic time, the arc developing at the South American Continent margin immature, as is documented by the geochemical and isotope characteristic of Jurassic samples. Either the crust was juvenile characterized by low  $^{87}\text{Sr}/^{86}\text{Sr}$  ratios and positive  $\epsilon_{\text{Nd}}$  values, or the degree of assimilation of mature crust was very small (e.g. along Coastal Cordillera). Accordingly, the distinct Pb-isotope composition indicates either derivation from a more radiogenic mantle source or contamination with basement from the Arequipa basement (Proterozoic) or other basement (Paleozoic). For the Jurassic arc there is not evidence for crustal shortening or significant crustal thickening, consistent with overall Sm/Yb (1 to 2.5) ratios.

In the Cretaceous there are evidences that indicate some shortening and thickening of the crust between 90 and 80 Ma (Peruvian unconformity, Scheuber et al., 1994) and the temporal evolution pattern is constrained in Cretaceous-Early Tertiary rocks with Sm/Yb from 1 to 3.5 ratios. Either increasing degree of crustal assimilation or contamination by more mature crustal material raised  $^{87}\text{Sr}/^{86}\text{Sr}$  ratios and lowered  $\epsilon_{\text{Nd}}$  values along Longitudinal Valley. The Pb isotope composition of samples from Linga Yarabamba, Punta Coles, Murmantani suggest contamination of Arequipa basement (Proterozoic). The geochemical character of samples from Ocoña, Quebrada Blanca, Cerro Colorado, Cerro Ceusis suggests contamination of Paleozoic basement.

At about ~25 Ma, uplift rates at the Andean margin accelerate and Neogene arc was established on thickened continental crust as indicating Sm/Yb (1.5–5) ratios in Miocene lavas. Ignimbrites flare-up at ~24 Ma characterized by eruption of voluminous ignimbrites (e.g. Oxaya, Huaylillas) mark episode of major crustal melting.  $^{87}\text{Sr}/^{86}\text{Sr}$  ratios,  $\epsilon_{\text{Nd}}$  values and Pb-isotope ratios of younger lavas (Mio-Pliocene to Recent) indicate increase in the assimilation of their basements. Sm/Yb ratios (1.5 to 8) of the 10-3 Ma lavas document crustal thickening during Mio-Pliocene times, as the MASH zone probably had no thermally equilibrated yet (see REE pattern).

As the MASH zone approaches thermal equilibration, more fertile rocks are partially molten in the Mio-Pliocene times.

The younger lavas (<3 Ma) north of 22°S shows dramatically elevated Sm/Yb ratios and higher incompatible element abundances, which is a stronger indication of interaction with lower garnetiferous crust. To the South Sm/Yb is lower although crustal thickness is similar. This difference may then reflect the additional effect of variable crustal composition, mafic in the north (13°S-22°S) and may be more felsic in the south (22°-28°). Regional differences exist in other trace element ratios as well.

### **Perspectives**

While the influence of increasingly thick crust and different basement rocks on magma genesis has been fairly well documented and had compiled an extensive geochemical and isotopic database of the Central Andes (13°-28°S and 75°- 66°W) are needed a spatial analysis of the data to better constraint the regional variation of Meso-Cenozoic magmatic arcs. Geographic Information System (GIS) could help to show the exact locations where the geochemical variations are. Especially Pb-isotope data would be useful to investigate the nature and extention of the contaminat basements in the Central Andes.

## **4 Geochemical variations in time and space of lead isotopic domains in the Central Andes (13°S -28°S): Implications of the crustal structure and metal sources**

### **Abstract**

Boundaries of the Pb-isotope domains in the Central Andes of southern Peru, northern Chile, northwestern Argentina and Bolivia are presented based on 356 selected published data and 446 new Pb-isotope analyses of rocks and ores from the Central Andes. A GIS database contains further geochemical, isotopic, geological, metallogenic, geochronological and geophysical information that constrain the chemical compositions of rocks, large structural trends, main mining districts and provinces, as well as, the depth of the Moho and the subducted slab. Combining Pb isotopes with Sr, and Nd isotopes further allows to characterize and distinguish these domains. These data are combined with a 3D density model of the continental margin of the Central Andes. Crustal domains are thus constrained much more precisely as previously has been possible boundaries in the Central Andes. Geochemical and isotopic data in Jurassic to Recent volcanic rocks from these different domains show increasing crustal assimilation of local basement through time. Combining the isotopic domains map with 3D density model shows a surprising correlation between the average of crustal densities and isotopic compositions of the domains. Some domain boundaries are also enhanced by large crustal scale tectonic structures. Occurrence and type of Cu-Au-Ag-Sn deposits also appear to be correlated to certain crustal domains.

This evidence suggest that several crustal compositions construes density, crustal structure, Central Andean plateau segmentation, ore formation and the composition of emplaced magmas through crustal assimilation.

### **4.1 Introduction**

The Central Andes contain most dense outcrops of Meso-Cenozoic magmatism and concentrations of ore deposit in South America. Here, the magmatic rocks and ore deposits were formed on different basement with different geological histories and isotopic characteristics (James, 1982; Barreiro, 1984; Barreiro and Clark, 1984; Puig, 1988; Gunnesch et al., 1990; Kontak et al., 1990; Macfarlane et al., 1990; Mukasa et al., 1990; Aitcheson et al., 1995; Tosdal, 1996; Wörner et al., 1992).

We evaluate >1100 rock samples for mayor and trace elements as well as a large subset for Pb-Nd and Sr isotopes from the Central Andes, which we combine with selected published data. The basement in southern Peru, western Bolivia and northern Chile, northwestern Argentina (13° to 28°S and 75° to 66°W) is heterogeneous: Felsic from 21° to 27°S (Lucassen et al., 2001). Mafic the northern part of the Arequipa terrane (Tosdal, 1996). The basement below Altiplano-Puna at 22°S is felsic to the depth of 50-55 km but has more mafic composition below this depth (Yuan et al., 2002). The only significant juvenile additions to the crust are confined to the Mesozoic magmatic arcs mainly in the Peruvian and Chilean coastal range (Mukasa, 1986; Lucassen et al., 1996).

Various studies suggest that lead isotopic compositions of igneous rocks and ores in the Central Andes reflect the compositions of the underlying basement and thus can be used to map out crustal domains (MacFarlane et al., 1990; Wörner et al., 1992; Aitcheson et al., 1995) and for evaluating plate reconstructions (Tosdal 1996; Loewy et al., 2004).

Here, I use a large geochemical and isotopic data (published and new data) to redefine crustal boundaries at much higher spatial resolution by combining Pb-Nd-, and Sr isotopes and geochemical trace element data with a 3D density model. This geophysical model (The geometry of the crustal structure index =  $\Theta$ , Tassara et al., 2006), which constrain the crustal domains defined in this thesis.

## 4.2 Information systems and Pb isotope data

I have compiled an extensive geochemical data on the Central Andes (13°-28°S and 75°-66°W) using a GIS, which contains data and metadata grouped into thus categories:

*Geochemistry*: a database with >1500 whole rock analysis (major elements, trace elements, Sr-Nd-Pb isotopes) covering an age range from the Proterozoic to the Present and encompassing intrusive and volcanic rocks, metamorphic basement and (limited) sedimentary rocks.

*Geology*: a geological synthesis at 1:2,000,000 scale and the distribution of Jurassic-Cretaceous-Paleogene intrusions, Neogene volcanic rocks, and active centers. The compiled geological map also contains major crustal-scale tectonic lineaments.

*Geophysic*: gravimetry (Bouguer anomalies), gravity model for the Nazca Plate and the intracrustal density discontinuity (IDC) geometry and crustal structure index ( $\Theta$ ). Also based on geophysical data I included depth of Moho and depth contours of the downgoing Nazca Plate.

*Metallogeny*: Pb isotope data on 120 Andean ore deposits combined with metadata on location, main metallogenic features of the mining districts and provinces.

The Principal analytical methods of major elements, trace elements and Sr-Nd-Pb isotopes carried out on my samples are described in the Appendix.

### 4.2.1 Lead isotope data

Pb isotope data (Fig. 4.1) are available for Proterozoic basement rocks in only a few scattered localities in the Central Andes (Fig. 1.3) from the Arequipa basement of southern Peru, northern Chile and western Bolivia (36 samples from Tilton & Barreiro, 1980; Tosdal, 1996; Wörner et al., 2000; Loewy et al., 2004 and 16 new samples). Pb isotopes of the Arequipa basement are unradiogenic with low  $^{206}\text{Pb}/^{204}\text{Pb} = 16.083\text{-}18.45$ ,  $^{207}\text{Pb}/^{204}\text{Pb} = 15.606\text{-}15.636$ ,  $^{208}\text{Pb}/^{204}\text{Pb} = 36.712 - 38.625$  typical of ancient, high-grade terranes. Outcrops of Paleozoic rocks of the Eastern Cordillera, some across the Western Cordillera and Altiplano-Puna (Fig. 1.3) have a lower metamorphic grade and contain more radiogenic  $^{206}\text{Pb}/^{204}\text{Pb} > 18.5$  than the Arequipa basement (100 samples from Damm et al., 1990; Bock et al., 2000; Lucassen et al., 2001). Jurassic rocks from the Coastal Cordillera (30 samples data from older igneous rocks from Mukasa, 1986; Lucassen et al., 1996; 20 new samples) have  $^{206}\text{Pb}/^{204}\text{Pb}=17.5\text{-}18.8$ . To these and 30 published Rogers and Hawkesworth (1989), Haschke et al. (2002), 74 own new data of Cretaceous igneous rocks were combined with 406 Pb-isotope ratios of Cenozoic igneous rocks (70 samples from Trumbull et al., 1999; Kay et al., 1999; Siebel et al., 2001 and 336 own new data). Ore deposits (80 samples from GIS Andes BRGM; Macfarlane et al., 1990, 1999; Puig, 1988; Tosdal, 1993; Vivallo et al., 1998). All data combined fall into two groups: a low  $^{206}\text{Pb}/^{204}\text{Pb}=17.5\text{-}18.5$  in the central part (16°S-21°S) and high  $^{206}\text{Pb}/^{204}\text{Pb}=18.5\text{-}18.9$  in the northern part of the Arequipa basement (16°S-13°S) and to the south (21°S-28°S). The samples from the Eastern Cordillera (10 samples from Macfarlane, 1990; Aitchison et al., 1995 and 10 new samples) have highest  $^{206}\text{Pb}/^{204}\text{Pb} > 18.904$ ,  $^{207}\text{Pb}/^{204}\text{Pb} > 15.667$ ,  $^{208}\text{Pb}/^{204}\text{Pb} > 38.944$ .

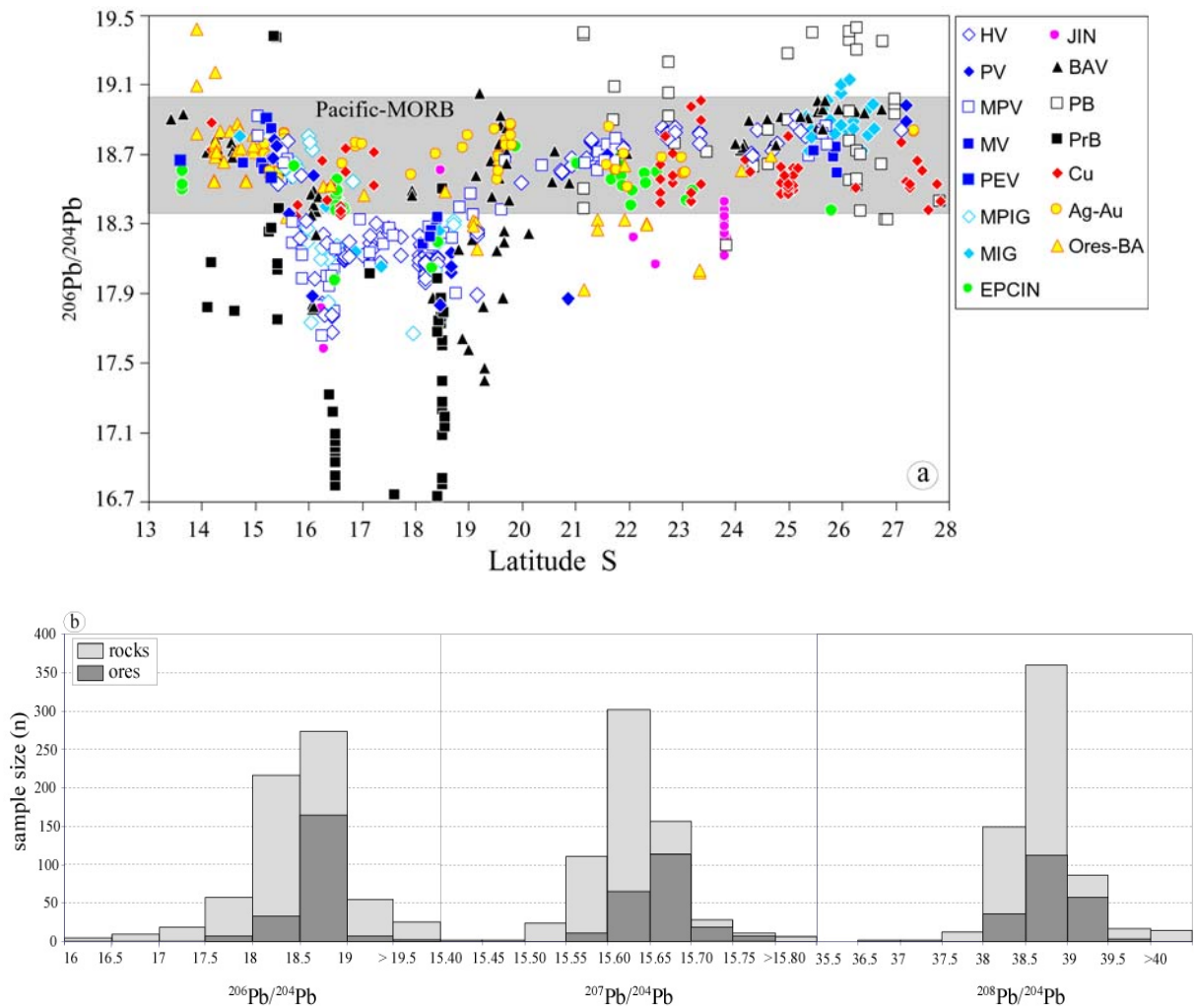


Fig. 4.1. a) Diagram of  $^{206}\text{Pb}/^{204}\text{Pb}$  ratios versus Latitude  $^{\circ}\text{S}$  in the Central Andes. Holocene volcanoes (HV), Pleistocene volcanoes (PV), Mio-Pliocene volcanoes (MPV), Miocene volcanoes (MV), Paleocene-Eocene volcanoes (PEV), Mio-Pliocene ignimbrites (MPIG), Miocene ignimbrites (MIG), Eocene-Paleocene-Cretaceous intrusions (EPCIN), Jurassic intrusions (JIN), Back-arc volcanoes (BAV), Paleozoic basement (PB), Proterozoic basement (PrB), Copper sulfurs (Cu), Silver-Gold sulfurs (Ag-Au) and ores along the back-arc (Ores-BA). Field of Pacific mid-ocean ridge basalt are from Hergt and Hawkesworth, 1994. b) Histogram of Pb-isotope compositions. Data sources of samples plotted here are explained in section 3.2 and 4.2.1.

### 4.3 Results

#### 4.3.1 Mapping of Pb isotopes and geochemical variations in Pb-domains

The large number of Pb-isotope measurements of Andean rocks (Fig. 7.1) now available allow to delineate crustal domains much more precisely than previously possible and to construct present-day Pb isotope maps using GIS.

Spatial analysis of lead isotope data established different domains and transitional zones, which have special geochemical characteristics (Fig. 4.2 to 4.7):

**The Arequipa domain** presents lowest  $^{206}\text{Pb}/^{204}\text{Pb}$  ratios (from 16.083 to 17.846),  $^{207}\text{Pb}/^{204}\text{Pb}$  ratios (15.435 to 15.612),  $^{208}\text{Pb}/^{204}\text{Pb}$  ratios (35.625 to 38.491) in Proterozoic and Paleozoic rocks. Slightly higher in  $^{206}\text{Pb}/^{204}\text{Pb}$  from 17.846 to 18.551 ratios are found in Neogene arc volcanoes and early Tertiary intrusions.

The Neogene volcanics in this domain have low  $\epsilon_{\text{Nd}}$  values (-5 to -9), Sr isotope between 0.7051 and 0.7073 and higher Sm/Yb (2 to 10) ratios.

**The Transition zones** with  $^{206}\text{Pb}/^{204}\text{Pb} = 18.551$  to  $18.727$ ,  $^{207}\text{Pb}/^{204}\text{Pb} = 15.612$  to  $15.652$ ,  $^{208}\text{Pb}/^{204}\text{Pb} = 38.491$  to  $38.767$  between the Arequipa and Cordillera domain.

The Neogene lavas in this domain have intermediate  $\epsilon_{\text{Nd}}$  values from  $-0.9$  to  $-5$ , Sr isotope ratios from  $0.705$  to  $0.7065$ , high Sm/Yb ratios (2 to 10) in southern Peru, and low Sm/Yb ratios (1.5 to 5) in northern Chile-southwestern Bolivia.

**The Clemesi domain** is defined by Mesozoic rocks of Coastal Cordillera. Lead ratios  $^{206}\text{Pb}/^{204}\text{Pb} = 18.7$  to  $18.4$  of Mesozoic rocks are generally higher than the Proterozoic basements ( $^{206}\text{Pb}/^{204}\text{Pb} = 16.7$  to  $18.4$ ), and lead compositions  $^{207}\text{Pb}/^{204}\text{Pb}$ ,  $^{208}\text{Pb}/^{204}\text{Pb}$  like the basement on which they are located. Their higher  $\epsilon_{\text{Nd}}$  values (5 to  $-0.9$ ) and low  $^{87}\text{Sr}/^{86}\text{Sr}$  ratios ( $0.703 - 0.705$ ) are representative of a juvenile magma addition to the crust in Jurassic and Cretaceous times. These rocks have low Sm/Yb ratios ( $< 3$ ).

**The Cordillera domain** occurs to the south and north of Transition zones and has the highest  $^{206}\text{Pb}/^{204}\text{Pb} > 18.727$ ,  $^{207}\text{Pb}/^{204}\text{Pb} > 15.652$ ,  $^{208}\text{Pb}/^{204}\text{Pb} > 38.767$ . Neogene volcanoes in this domain have low  $\epsilon_{\text{Nd}}$  values ( $-0.9$  to  $-9$ ), Sr isotope between  $0.7029$  to  $0.7051$  and high Sm/Yb ratios (5 to 9).

**The Mejillonia domain** with lead compositions  $^{206}\text{Pb}/^{204}\text{Pb} = 18.375$  to  $18.551$ ,  $^{207}\text{Pb}/^{204}\text{Pb} = 15.573$  to  $15.652$ ,  $^{208}\text{Pb}/^{204}\text{Pb} = 38.170$  to  $38.767$ . The Jurassic rocks of la Negra Formation have high  $\epsilon_{\text{Nd}}$  values (5 to  $-0.9$ ), low  $^{87}\text{Sr}/^{86}\text{Sr}$  ratios ( $0.703 - 0.705$ ) and low Sm/Yb ratios (1.5-2.5).

**The Chilenia domain** has similar  $^{206}\text{Pb}/^{204}\text{Pb}$ ,  $^{207}\text{Pb}/^{204}\text{Pb}$ ,  $^{208}\text{Pb}/^{204}\text{Pb}$  ratios to the Mejillonia domain. Mejillonia and Chilenia domain are separated by a Transitional zone at  $25^\circ\text{S}$ .

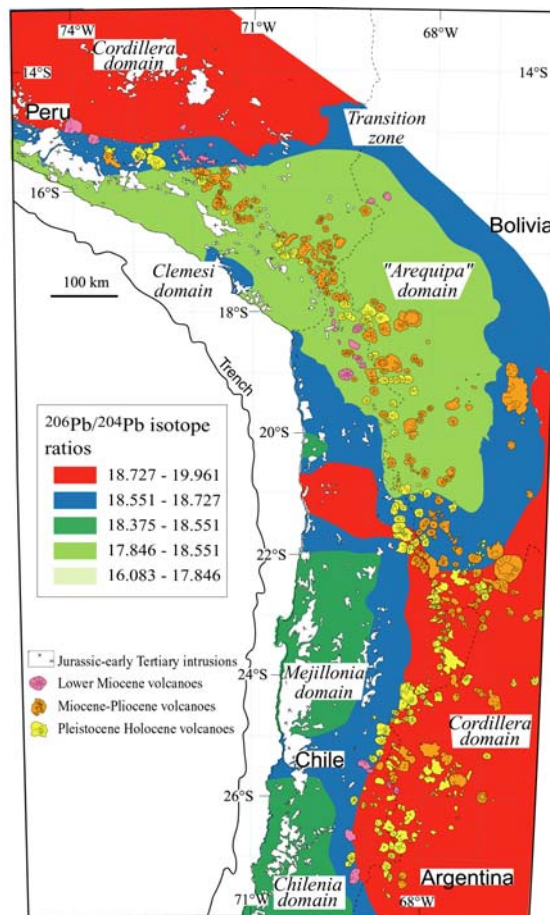


Fig. 4.2.  $^{206}\text{Pb}/^{204}\text{Pb}$  isotope map in the Central Andes ( $13^\circ\text{S}$  -  $28^\circ\text{S}$ ).

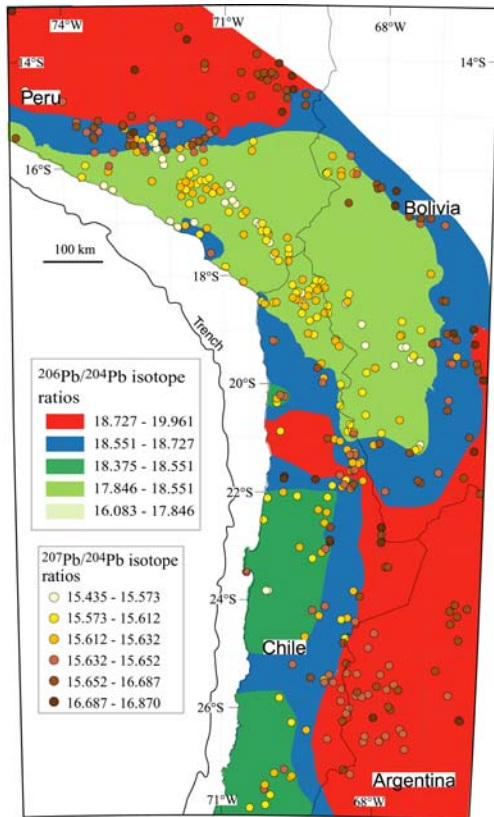


Fig. 4.3. Map of present-day  $^{206}\text{Pb}/^{204}\text{Pb}$  ratios and  $^{207}\text{Pb}/^{204}\text{Pb}$  ratios of rocks from Central Andes.

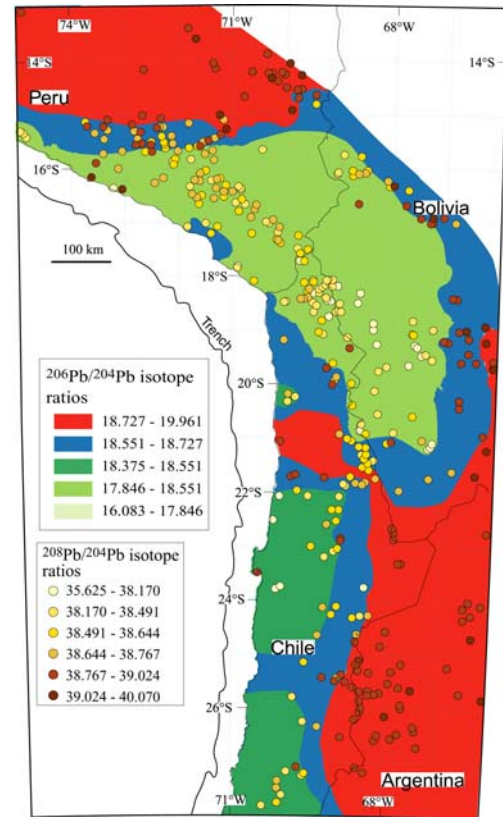


Fig. 4.4. Map of present-day  $^{206}\text{Pb}/^{204}\text{Pb}$  ratios and  $^{208}\text{Pb}/^{204}\text{Pb}$  ratios of rocks from Central Andes.

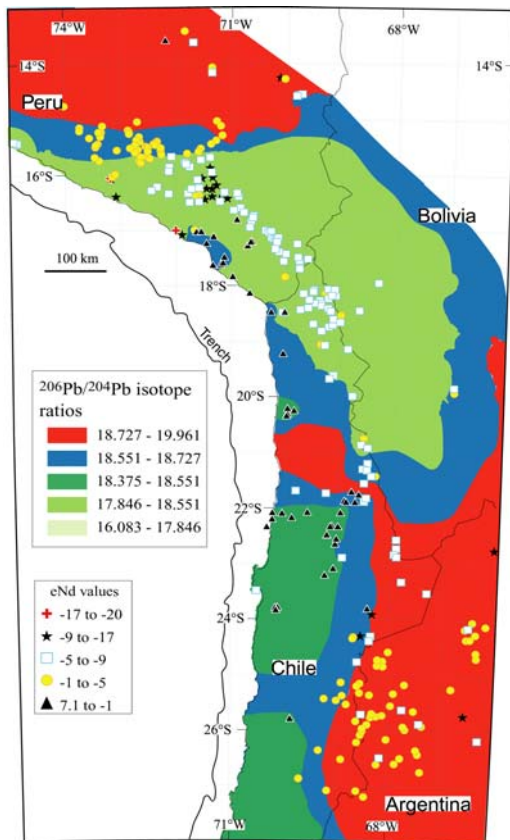


Fig. 4.5. Map of present-day  $^{206}\text{Pb}/^{204}\text{Pb}$  ratios and  $\epsilon_{\text{Nd}}$  values of rocks from Central Andes.

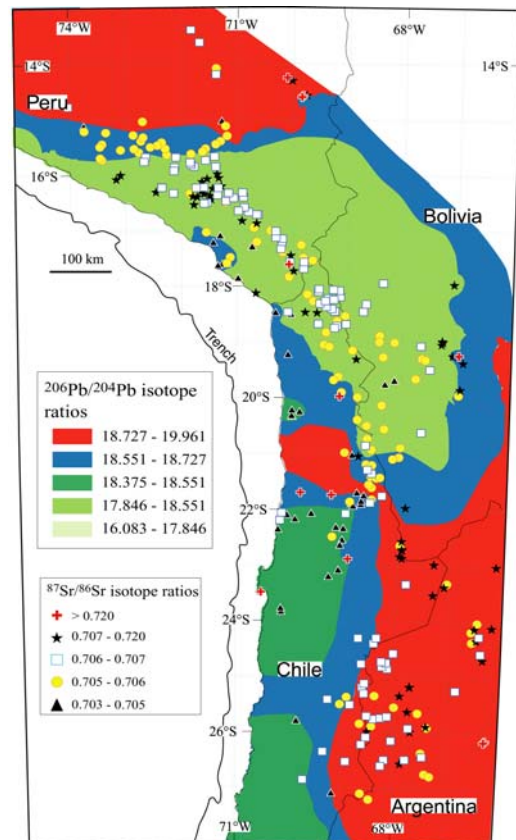


Fig. 4.6. Map of present-day  $^{206}\text{Pb}/^{204}\text{Pb}$  ratios and  $^{87}\text{Sr}/^{86}\text{Sr}$  isotope ratios of rocks from Central Andes.



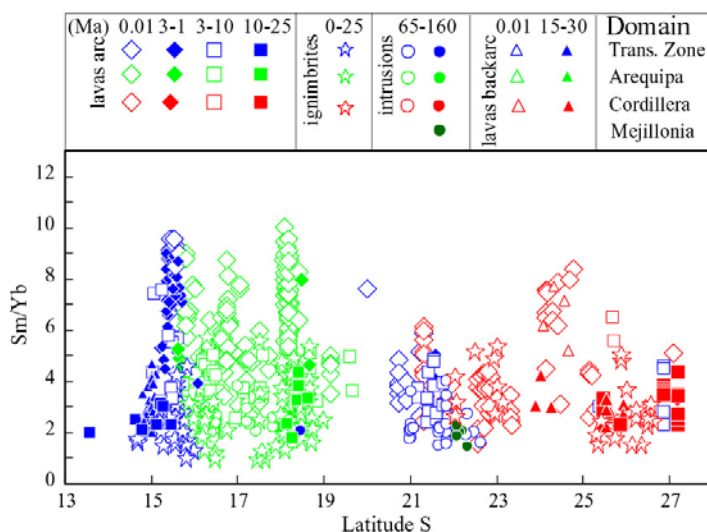


Fig. 4.7. Diagram Sm/Yb ratios versus Latitude. Colors of the symbols are according to the Pb domains (see illustration of Neogene volcanoes in Fig. 4.2).

## 4.4 Discussion

### 4.4.1 Pb isotope mapping crustal domains

The nature and timing of, and processes involved with, crust formation and the extraction of the crust from the Earth's mantle remain subjects of much debate. The Pb isotopic system is one of several isotopic systems that have been used to help understand the processes of crust formation and has the advantage of being based on 3 parent-daughter systems with very different decay rates and 2 elemental pairs (U/Pb and Th/Pb) with different geochemical properties. Early studies of crustal Pb isotopic systematics (e.g. Oversby, 1978) established that by the late Archean, crustal provinces existed with distinct Pb isotopic signatures. Additional work has confirmed these distinctions and emphasized that igneous rocks inherit geochemical characteristics from crustal sources, their isotope composition can “fingerprint” basement terranes and provided useful information for delineated crustal domains/mapping (Ayuso and Bevier 1991; MacFarlane et al., 1990; Aitchison et al., 1995; Wörner et al., 1992) and for evaluating plate reconstruction (Tosdal et al., 1996 and Loewy et al., 2004). Examples are illustrated from the cordilleras of southwestern North America, Greenland, Antarctica, Northern Andes and Central Andes.

In the western United States, Wooden et al. (1988), Wooden & DeWitt (1991) used present-day Pb isotope compositions of Proterozoic rocks, and Mesozoic and Cenozoic plutonic, volcanic rocks and ores to define distinct Proterozoic crustal-scale Pb provinces characterized by different U-Th-Pb histories that broadly, but not precisely, correlate with known geologic provinces (Fig. 4.8). Proterozoic Pb isotope provinces and Nd isotope provinces (DePaolo et al., 1991) are similar in their geographic extent, but they are not the same. One area of disagreement is the extent of the Mojave Pb province in Nevada, Utah, and Arizona. Given that there are fundamental differences in the geochemical basis of the Pb and Nd isotope systems, these differences in extent of crustal provinces may be real and/or rooted in sample distribution and types. In contrast, the Pb isotope and Sr isotope provinces, particularly the edge of significant Precambrian crust marked by the initial Sr ( $Sr_i$ ) equal to 0.706 (Fig. 4.8, Kistler, 1990), correlate well (Wooden et al., 1998). Elison et al. (1990) showed that the  $Sr_i = 0.706$  line also correlate with the shelf-slope break defined by Paleozoic and Triassic strata. Pb isotopic mapping in Nevada, coupled with geophysical information (Rodriguez, 1998) demonstrates that these boundaries are crustal scale faults.

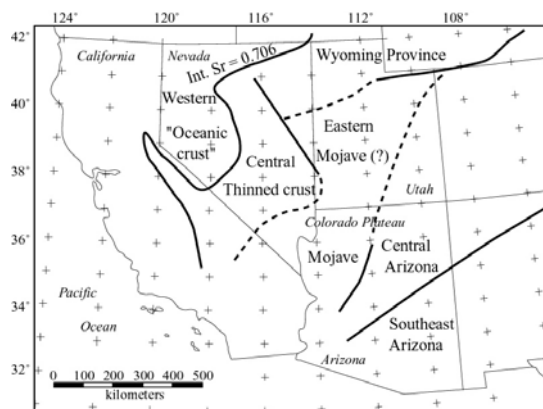


Fig. 4.8. Pb isotope provinces in the western United States. From Wooden & DeWitt (1991).  $Sr_i = 0.706$  line from Elison et al., 1990.

#### 4.4.1.2 Isotopic framework of basement in the Central Andes

The Central Andes is underlain by a complex geology (Fig. 3.1). However, unlike western United States, Pb, Sr, Nd isotope frame work of the rocks were not well established because an extensive cover by young volcanic rocks.

Macfarlane et al. (1990) used Pb isotope compositions of rocks and ore deposits of differing ages over a broad geographic area to map out crustal provinces along and across the arc, and they divided the Central Andean arc into three geological provinces (I, II, III) and six Pb isotope subprovinces (Fig. 4.9a; Ia, Ib, Ic; II, IIIa, IIIb).

Aitcheson et al. (1995) documented a Pb subdivision in detail for the area in the Central Andes from lat  $16^\circ$  to  $24^\circ$ S and from long  $64^\circ$  to  $70^\circ$ S and they differentiated in the northern Altiplano a unradiogenic Pb isotope domain in ores and igneous rocks (Fig. 4.9b), and they were not sure if this domain is part of the Arequipa massif. However, they noted that Nd crustal extraction ages of  $\sim 1.9$  Ga from northern Altiplano basement samples are similar to the Protolith age inferred by Dalmayrac et al. (1977) for Arequipa massif granulites from U-Pb zircon upper-intercept ages.

Tosdal (1996), based upon U-Pb geochronologic and Pb isotopic study, concluded that Middle Proterozoic rocks in the Arequipa craton in western Bolivia and northern Chile are not reworked Early Proterozoic rocks of Arequipa massif (Fig. 1.3). They are however, related by similar unradiogenic  $^{206}\text{Pb}/^{204}\text{Pb} < 18.2$  reservoirs and be haved as a coherent block since the Middle Proterozoic (Fig. 4.9c). Tosdal (1996) also proposed that parts of the Arequipa craton are allochthonous with respect to Amazon craton.

Loewy et al. (2004) however, interpreted the Arequipa Antofalla craton as a single basement block, which comprises three domains based mainly on geochronology: a northern domain (2.02-1.79 Ga), a Central domain (1.2 – 0.94 Ga) and a southern domain dominated by Ordovician metasediments derived partially from Proterozoic crust (Fig. 4.9e). Using integrated data set that includes U-Pb geochronology, and the sequence of adjacent provinces they suggested that the Arequipa Antofalla craton was accreted at ca. 1.05 Ga.

Lucassen et al. (2001) compiled from extensive geological and geochemical studies of exposed pre-Mesozoic basement rocks in the Central Andes and presented an important constraints on the compositional evolution of the crust in the Central Andes from  $21^\circ$  to  $27^\circ$ S from the Early Paleozoic onwards (Fig. 4.9d). They also concluded that in terms of its Nd and Sr isotope composition, the crust in this part of the Andes was already rather homogeneous at the time Early Paleozoic metamorphism and granitic magmatism in the Paleozoic served to increase this homogeneity. The geological and sedimentary record of the area indicates that the crust that formed in the Early Paleozoic orogen was largely entire at the beginning of the Cenozoic crustal thickening of the Central Andes.



Based on tectonostratigraphic analysis of southern South America Ramos et al. (1988, 1986), Bahlburg and Hervé (1997) presented a simplified terrane distribution maps. These terranes define a mosaic of old continental crust (e.g. Arequipa-Antofalla, Mejillonia, Chañaral, Chilenia, Pichidangui, Cuyania-Precordillera, Pampia terranes) amalgamated during the Late Proterozoic to early Paleozoic times (Fig. 4.10a, b).

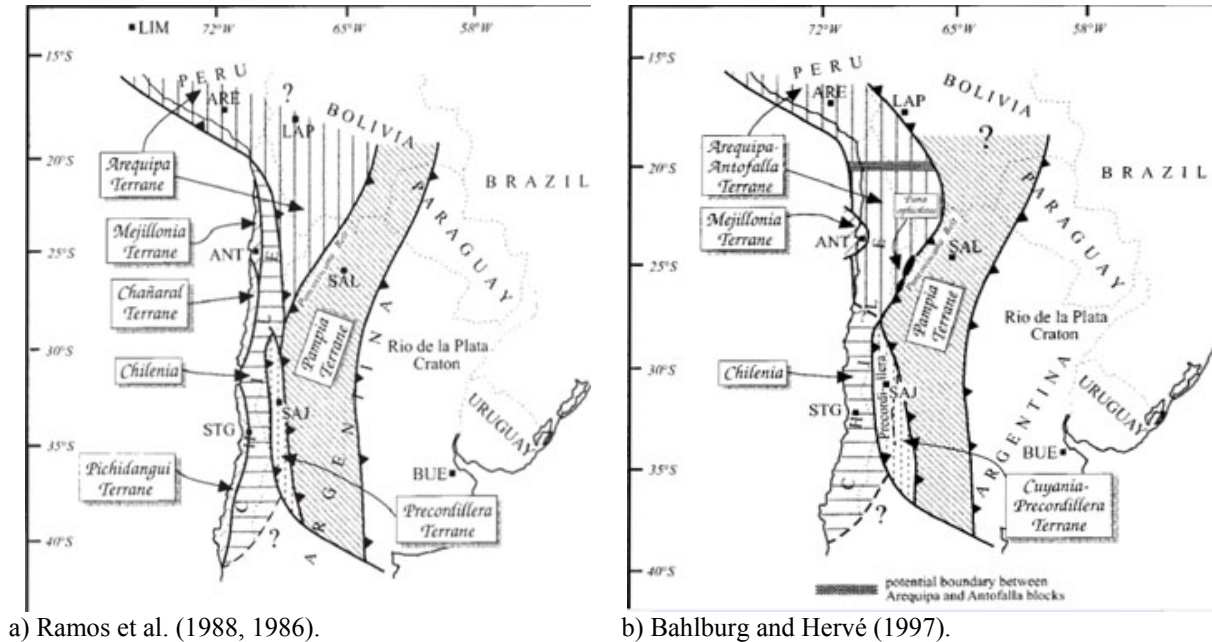


Fig. 4.10. Maps of accreted terranes in the southern of South America.

In all these works mentioned above based on lead isotopes and tectonostratigraphic analysis, and radiometric ages in the Central Andes is not well defined the real extension and locations of terranes, mafic or felsic crust and transition zones between terranes. The crucial for the reconstruction of the terrane assemblage of the Central Andes is the Arequipa terrane.

For the most part, boundaries for the Pb isotope provinces and terrane distribution presented by Macfarlane et al. (1990), Aitchison et al. (1995), Tosdal (1996), Loewy et al. (2004), Lucassen et al. (2001), Ramos et al. (1988, 1986), Bahlburg and Hervé (1997) are similar in their gross geographic location but differ significantly in their exact geographic position and shapes. Differences in the exact locations of the boundaries in previous works are in function of sampling density and interpretation.

The data set (Fig. 7.1) of this thesis is the most extensive used so far to delineate crustal domain boundaries. Therefore the crustal boundaries are much better defined than in all previous models.

Nd isotope analyses along these domains presented for the first time (Fig. 4.5, 4.12) further support our crustal domain distinctions and corroborate the domain boundaries defined here. Nevertheless, boundaries of crustal domains are not necessarily constrained by Sr isotopes variations (Fig. 4.6) due to the effect of mixing of magmas, fractional crystallization, and assimilation (see section 3.3).

High Sm/Yb (Fig. 4.7, 4.13, 4.14, 4.15) on thick crust implies a garnet residue, probably in intermediate to deep crust in mafic to intermediate crustal rocks (Kay et al., 1999) as is the case of younger volcanoes in the Arequipa domain and volcanoes in the Transition zone between 16 and 14°S. Indeed most of the Proterozoic rocks of Arequipa terrane are mafic and unradiogenic (Loewy et al., 2004; Aitchison et al., 1995; and Tosdal, 1996).

Low Sm/Yb even on thick crust may imply either felsic crust as is the case of volcanoes in the Cordillera domain between 22 and 28°S (Fig. 4.7) or assimilation occurred only in the upper crust, which is unlikely. Lucassen et al. (2001) also agree that the crust in this region is felsic (Fig. 4.9e and 4.12).

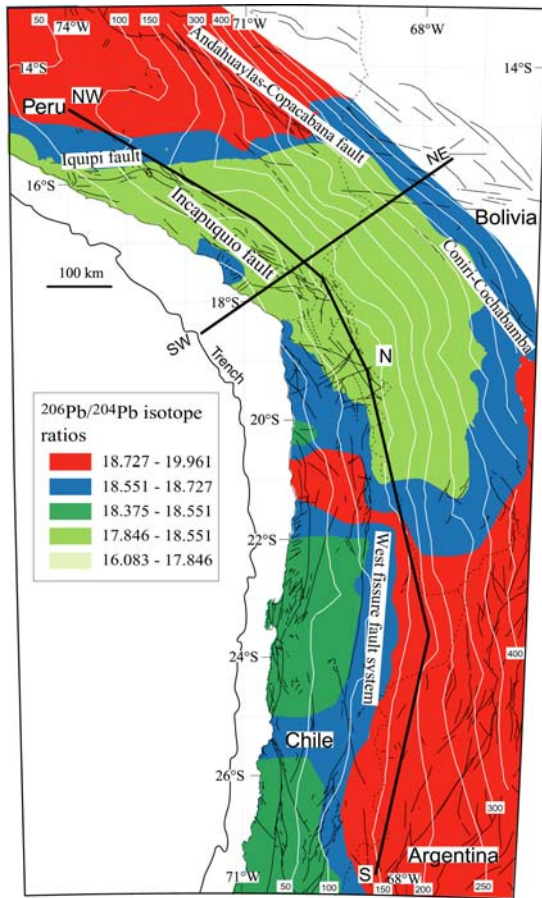


Fig. 4.11. Pb isotope domains and large-scale structural trends in the Central Andes. The Contours to the Wadati-Benioff zone with depths in km.

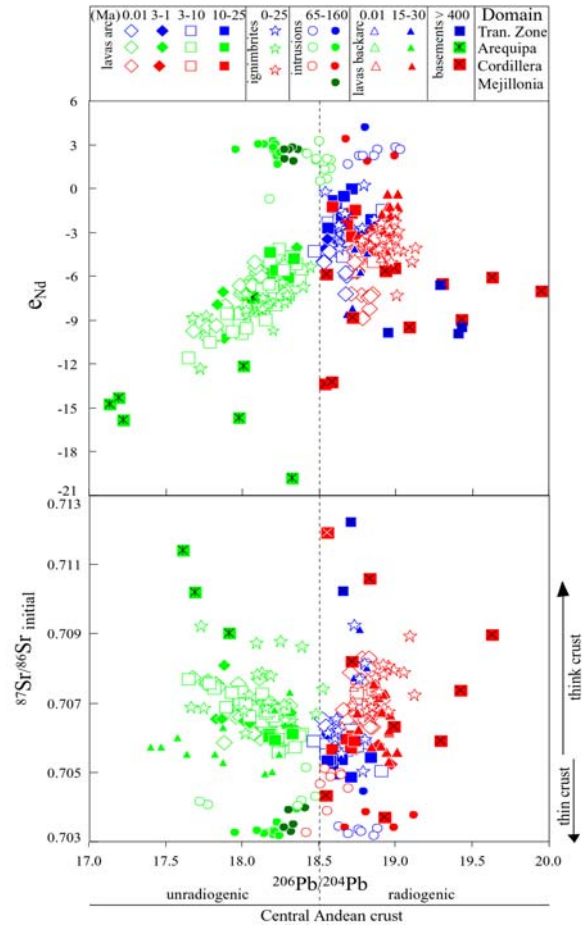


Fig. 4.12. Diagram of initial  $\epsilon_{Nd}$  and Sr isotope versus Pb isotope domains.

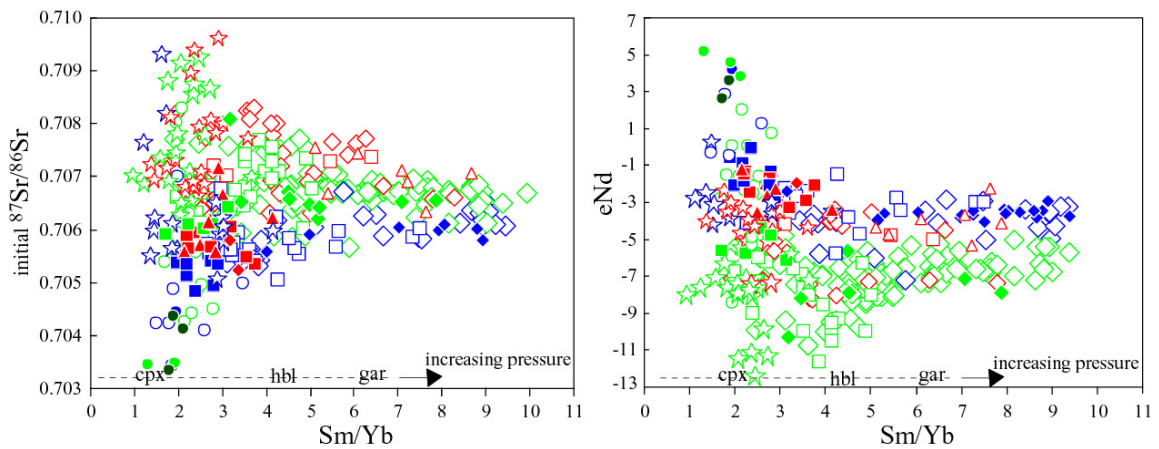


Fig. 4.13. Diagram initial  $^{87}\text{Sr}/^{86}\text{Sr}$  and  $\epsilon_{Nd}$  versus Sm/Yb of rocks from the different Pb domains. Legend as in Fig. 4.12

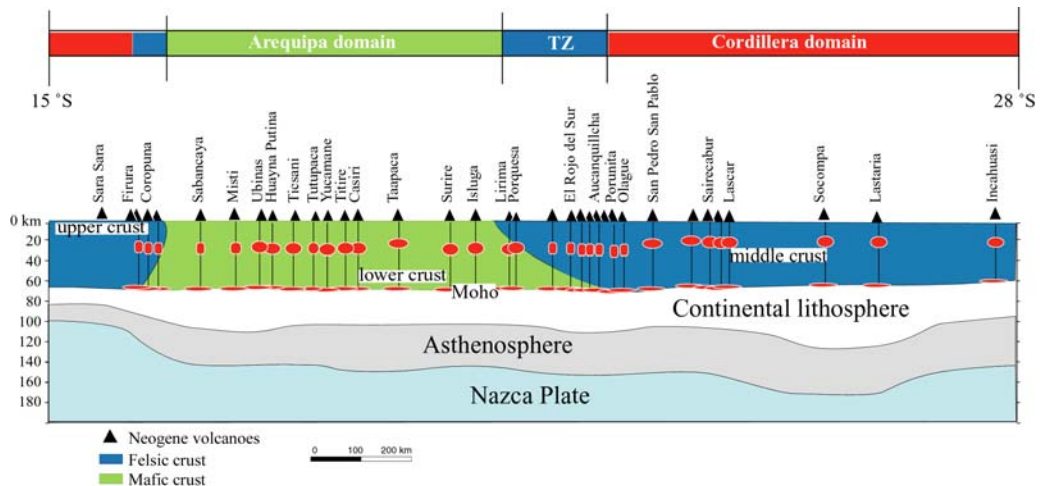


Fig. 4.14. Crustal Pb-domain scale section (NW14°S – N18.5°S – S28°S). (after Wörner et al., 1992; Kay et al., 1999).

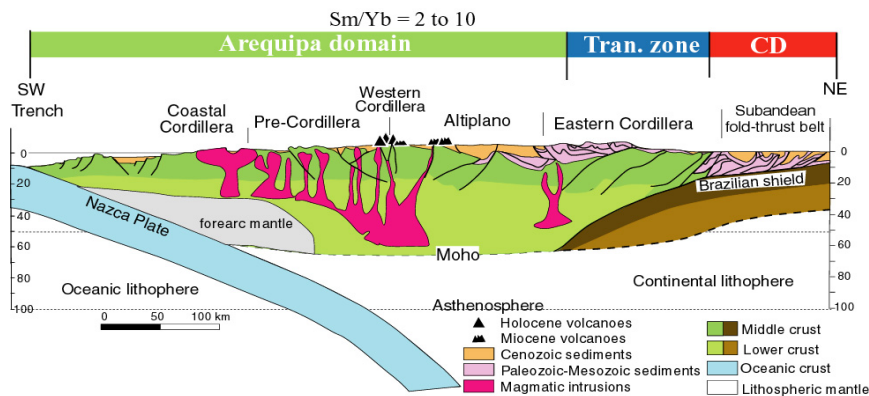


Fig. 4.15. Crustal-scale section of Arequipa domain (NW17°S – NE15°S). Superimposed on crustal profile of Allmendinger et al. (1997). Section line in Fig. 3.13.

The boundaries of these blocks reflect the positions and character of real geologic boundaries between the different crustal blocks and these follow large-scale structural trends (Fig. 4.11). The abrupt boundary between Arequipa domain and Transition zone at  $\sim 16^\circ\text{S}$  coincides with the Iquique fault and with the Colca Canyon. Toward the East between the Transition zone and Cordillera domain could be a major fault parallel to the Andahuayllas-Copacabana fault system. The transition of Arequipa domain to the east may be related to the Copacabana-Coniri fault system. The boundaries to the west of Arequipa domain and the east boundary of Clemesi domain coincide with Incapuquio fault system. The transition zone between the Cordillera domain and Mejillonia – Chilena domains coincides with West fissure fault system in northern Chile.

#### 4.4.2 Crustal Contamination in the Pb domains

It is mostly accepted for Central Andean Miocene to Recent magmas that Nd-Sr isotope mostly variations reflect the process and degree of crustal contamination (Davidson et al., 1992). There is a general pattern of decreasing  $\epsilon_{\text{Nd}}$  and increasing  $^{87}\text{Sr}/^{86}\text{Sr}$  with time for rocks of each Pb domain. Jurassic rocks and early Tertiary intrusions are less contaminated than Neogene volcanoes.

The lowest  $\epsilon_{\text{Nd}}$  values and low  $^{87}\text{Sr}/^{86}\text{Sr}$  ratios have the Neogene volcanoes in Arequipa domain. The low  $\epsilon_{\text{Nd}}$  values and high  $^{87}\text{Sr}/^{86}\text{Sr}$  ratios have the volcanoes of the Transition zones and Cordillera domain.

Figure 4.16 shows a simple mixing model using the parameters of the Table 4.1. Mixing curve for Arequipa domain between Cretaceous granite (67 Ma) and Proterozoic gneiss (2 Ga), and for Cordillera domains in northwestern Argentina between Miocene andesite (19.6 Ma) and Paleozoic orthogneiss (460 Ma).

Table 4.1. Values used in the mixing model. Data are from a-Boily et al. (1989), b-James (1982), c-Thrumbull et al. (1999), d-Lucassen et al. (1999b).

Samples (Long.°W, Lat.°S)	Age (Ma)	Sr	Nd	$^{87}\text{Sr}/^{86}\text{Sr}_{\text{initial}}$	$^{144}\text{Nd}/^{143}\text{Nd}$
Arequipa domain (70.70, 17.29) <sup>a</sup>	67	401	24.4	0.7049	0.512739
Arequipa domain (71.5, 16.5) <sup>b</sup>	2000	150	36.0	0.720	0.511500
Cordillera domain (63.38, 25.9) <sup>c</sup>	19.6	414	21.9	0.7050	0.512634
Cordillera domain (57.5, 24.6) <sup>d</sup>	460	143	32	0.7235	0.511810

The mixing model result are two curves, which show that the smallest amounts of crustal contamination in Early Tertiary intrusions ( $\leq 10\%$ ). In Arequipa domain Miocene lavas have  $\leq 25\%$  and the maximum crustal contamination (40 %) is modeled for the Mio-Pliocene to Recent lavas. In Cordillera domain Miocene lavas have  $\leq 15\%$  and the Mio-Pliocene to Recent lavas have 40% (Fig. 4.14).

The simple mixing curve (dashed line) for ignimbrites in the Cordillera domain and Transitional zone shows that  $(^{87}\text{Sr}/^{86}\text{Sr})/\epsilon_{\text{Nd}}$  ratios of their magmas are lower than  $(^{87}\text{Sr}/^{86}\text{Sr})/\epsilon_{\text{Nd}}$  ratios of crust.

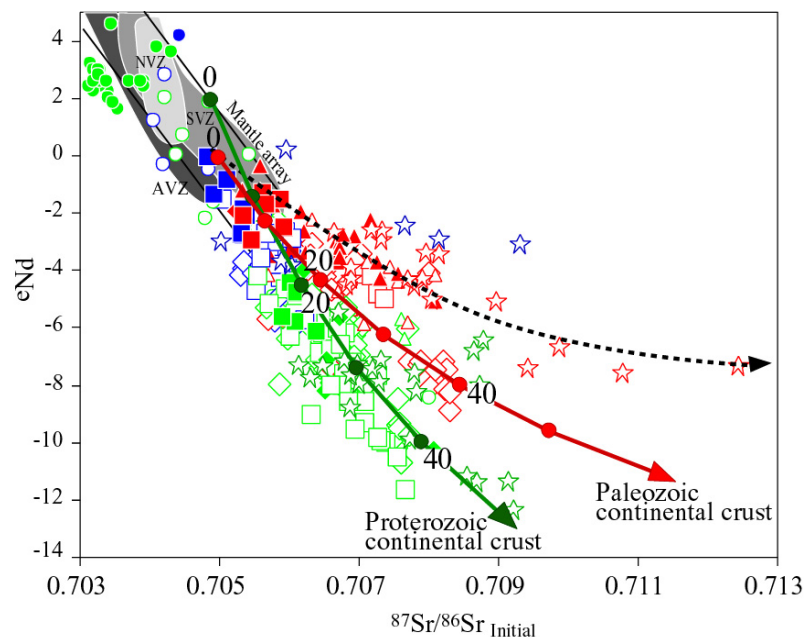


Fig. 4.16. Diagram of  $\epsilon_{\text{Nd}}$  versus  $^{87}\text{Sr}/^{86}\text{Sr}_{\text{Initial}}$  for rocks of the Central Andes. Circles mark percentages of crustal contamination of specific domain. NVZ=north volcanic zone (Bourdon et al., 2002), SVZ=south volcanic zone (Kay et al., 2005) and AVZ=austral volcanic zone (Stern and Killian 1996). Legend as in Fig. 4.12.

It have presented a simple mixing model because is a regional analysis, advances models of open system magmatic processes like AFC (Assimilation Fractional Crystallization: after DePaolo, 1981; O'Hara and Mathews, 1981), EC-AFC (Energy-Constrained Assimilation Fractional Crystallization: Spera and Bohron, 2001), MASH (Mixing Assimilation Storage Homogenization; Hildreth and Moorbath, 1988), RAFT (Recharge, Assimilation,

Fractionation, Tapping: Aitchison and Forrest, 1994) need estimate values of local parameters such as  $F$  (mass of remaining magma, mass of original magma) and  $r$  (rate of assimilation/rate of fractional crystallization), O-isotopes ratios,  $T_m$  (magma temperatures),  $T_a$  (assimilant temperature). These models are more useful in individual volcanoes or local areas and previous studies of volcanic complex have calculated for Parinacota volcano (Bourdon et al., 2000), Taapaca volcano (Kohlbach, 1999), El Misti volcano (Kiebalá in preparation). However, we cannot just explain by fractional crystallization the large variability in trace elements of volcanic in the Central Andes.

#### 4.4.3 Isotopic domains constrained by 3D density model

The three-dimensional density model of Tassara et al. (2006) was designed to represent the current distribution of mass along the Andean margin ( $5^\circ$ - $45^\circ$ S) at continental and lithospheric scales. The structure of the model is formed by a number of bodies simulating the subducted slab, the sub-continental mantle and the continental crust. Each body has one value of density that was selected in accordance to its position into the model and after studying the dependency of this physical parameter on chemical composition, metamorphic pressure-temperature conditions, water content and degree of partial melting. To reduce the degrees of freedom during the forward modelling of the Bouguer anomaly, the geometries of the slab, lithosphere-asthenosphere boundary, and continental Moho were fixed, as far as available geophysical data allow (for location and sources of data see Tassara et al., 2006). The existing geophysical database for the Central Andes constrains the subcrustal and Moho geometry. The one remaining degree of freedom is the geometry of intracrustal density discontinuity (ICD), separating an upper-crustal body of density  $2.7 \text{ g/cm}^3$  from a lower-crustal body of density  $3.1 \text{ g/cm}^3$ . Following empirical relationships between density and silica content of crystalline, anhydrous crustal rocks (Tassara, 2006), the former simulates a granitic upper crust of ca. 70 wt%  $\text{SiO}_2$ , whereas the dense lower-crustal body represents a garnet-pyroxene granulite of 55-58 wt%  $\text{SiO}_2$ . If the lower crust below the Central Andean orogen is accepted to be partially hydrated and containing some degrees of molten material, then the selected bulk density of  $3.1 \text{ g/cm}^3$  represents even more basic compositions (55-48 wt%  $\text{SiO}_2$  following Tassara, 2006).

The geometry of the ICD is a proxy to regional-scale (several tens to some hundred kilometers) lateral density variations occurring inside the crust. The main factor controlling such variations is the bulk compositional structure of the crust, i.e. the vertically-integrated proportion of felsic to mafic crust, whereas spatial variations of lower crustal temperature, hydration and partial melting could have a secondary effect (Tassara, 2006; Tassara et al., 2006).

Using the final geometries of the 3D density model in their electronic version (Tassara et al., 2006), we computed a grid covering the study area for what we call the “crustal structure index  $\Theta$ ”, i.e. the ratio between the thickness of the upper-crustal body and the total crustal thickness. Low (high) values of  $\Theta$  indicate a predominance of mafic (felsic) material in the crust.

For this study we combined the result of crustal structure index ( $\Theta$ ) mapping and our Pb isotope analysis, and they show a good correlation (Fig. 4.17):

- Low  $\Theta < 0.2$  coincides with Pb isotopes of Arequipa domain.
- High  $\Theta > 0.2$  correlates with Pb isotopes of Transitional zones and Cordillera domain.

This correlation between 3D density model and Pb domains indicate that the age and proportion between felsic and mafic crust are the factors controlling the density structure inside the crust and isotopic and geochemical variations along the Central Andes.

The highest Sm/Yb ratios (2 to 10) in the youngest volcanoes ( $< 3 \text{ Ma}$ ) typically occur on more mafic crust (Arequipa domain) and the Transition zone in southern Peru. On more felsic



crust (Cordillera domain in northern Chile and northwestern Argentina) Sm/Yb ratios (2 to 6) increase with time but never reach these high levels obtained in Arequipa domain. This confirms that bulk crustal composition is another control of the garnet signature in addition to crustal thickness. Petrophysical modelling (i.e. Sobolev and Babyeko, 1994; Tassara, 2006) demonstrated that mafic rocks are able to form more garnet than felsic rocks for the same pressure-temperature conditions (i.e. crustal depth), explaining why the garnet-effect (high Sm/Yb ratios) is apparently stronger in the Arequipa domain compared to the Cordillera Domains.

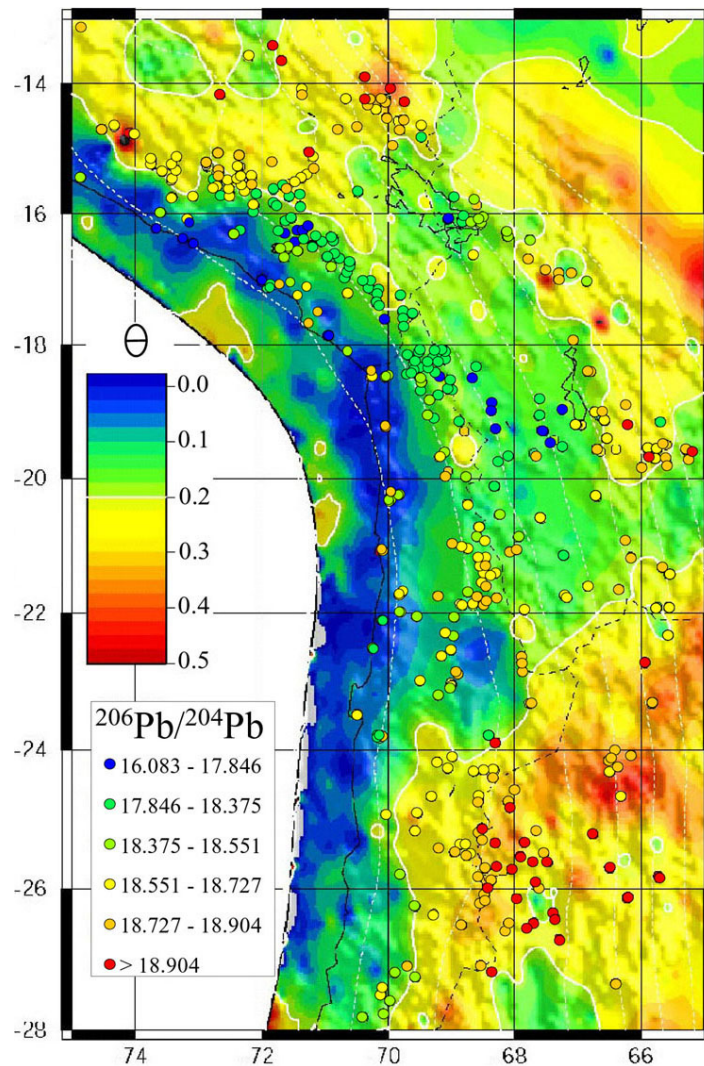


Fig. 4.17. Map of crustal structure index  $\Theta$ , (Tassara et al., 2006). Circles are locations of the different  $^{206}\text{Pb}/^{204}\text{Pb}$  ratios.

#### 4.4.4 The Nature of the Transition Zones

The Transitional Zone to the N of the Arequipa domain was traversed by magmas, which have high Sm/Yb ratios indistinguishable from those of the Arequipa domain, yet their Pb (and Nd) isotopic character is distinctly different for all young volcanic rocks. Thus, the boundary between the Arequipa Domain and the northern Transition Zone should be abrupt and possibly near-vertical within the crust, because the Pb-signature is the same (within a domain) for mafic and silicic rocks that probably sample preferentially the lower and upper crust. This suggests that the boundary may be a deep transversal crustal fault (e.g. Iquique fault, Fig. 4.11), unlike the southern boundary of the Arequipa Domain (Wörner et al., 1992). In

addition, a high-P garnet signature is present in the northern Transition Zone near the boundary even where the crustal structure index  $\Theta$  is high, indicating the absence of a thick mafic lower crustal layer. This apparent contradiction to the general pattern predicted above may be due to the poor lateral resolution of the crustal structure index  $\Theta$  and the poorly-known physical nature of the crustal boundary.

From 21 to 22°S is located the Transitional zone between Arequipa and Cordillera domain (Fig. 4.18). Seismic studies by Zandt et al. (1996), Swenson et al. (2000) beneath this area have concluded that the average velocity of the crust is low ( $V_p = 5.9$  to  $6.2$  km/s, see e.g. Zandt et al., 1996), and its average Poisson's ratio is about 0.25 ( $V_p/V_s = 1.73$ ) and this was interpreted as an evidence for the felsic composition of the crust.

However, Yuan et al. (2002) showed that the average correlation between topography and Moho depth changes at 21° to 22°S. They suggest that in this region the crust contains a thick lower crustal mafic component below the Altiplano. They suggested a less proportion of mafic crust further to the S as a consequence of the delamination and detachment of high-grade mafic metamorphic lower crust. Lower crustal delamination below the Puna plateau was also suggested by Kay et al. 1994. Recent studies (e.g. Lucassen et al., 2001; Swenson et al., 2000) confirm that the lower crust below the Puna region may be felsic- rather than mafic-dominated.

Our geochemical and isotopic data for igneous rocks between 21° and 22°S (Fig. 4.3, 4.4, 4.5, 4.6 see also Wörner et al., 1992) also suggests the presence of mafic crust at depth beneath this area. Apparently the southern margin of the Arequipa mafic terrane extends toward 22°S and is covered the Phanerozoic felsic rocks (Fig. 4.14)

#### **4.4.5 Segmentation of the Central Andes plateau related to the Pb-isotope domains**

In the last decades several authors have discussed the role of inherited pre-Andean crustal structures in the upper plate on the Cenozoic evolution and segmentation of the Central Andes (Allmendiger and Gubbels, 1996). Jordan (1988) suggested that the Altiplano formed across the western margin of a thick and stabilized cratonic lithosphere or "Tectosphere" and that the thick Paleozoic sedimentary sequences may have localized thin-skinned tectonics during shortening (Sclater et al., 1980; McQuarrie and DeCelles, 2001). The Puna segment, its morphological characteristics and the thick-skinned tectonics of the Sierras Pampeanas was proposed to have developed over a thermally thinned continental lithosphere and that this segmentation is controlled by the internal crustal structure and delamination in this segment (Kay et al., 1994 and reference therein).

The crustal domain boundaries newly defined here should help to further constrain the role of pre-existing crustal heterogeneities in the evolution and deformation pattern of the Central Andes:

Figure 4.18 shows that the segmentation of the Central Andean plateau and its adjacent foreland is in fact spatially related to the Pb-isotope domains: The Arequipa domain is coincident with the broad high Altiplano plateau (3.8 km high and 300 km wide). The largest amount of shortening in the Eastern Cordillera and Subandean belt during Andean Orogeny is located to the E and NE of the Arequipa domain. The Transition Zone (between 21°S and 22°S) coincides with the transition between the Altiplano and Puna segments. In the region of the southern Cordillera Domain, the Puna plateau is higher (4.4 km) than the Altiplano and is much narrower. The foreland structure is dominated by thick-skinned Laramide-style basement uplift on steeply E- and W- dipping reverse faults (Santa Barbara System; Allmendiger and Gubbels, 1996). Therefore I argue that the nature, i.e. the bulk composition and thus the different rheologies of the crust are an important factor that controlled the deformation pattern of the Central Andes and the localization of the Andean plateau.

#### 4.4.6 Rheological and structural identity of the Pb domains during Andean Orogeny

Crustal architecture and evolution are also different with respect to the sedimentary cover: The thickness of Paleozoic to Cenozoic sediments is small, if at all present in the Arequipa domain. Outcrops of metamorphic basement occur below a relatively thin cover of Jurassic and Tertiary sediments. By contrast, significant thicknesses of older sediments, which are strongly deformed by the Andean orogeny, are observed predominantly in areas surrounding the Arequipa domain. Conversely, erosion products deposited during uplift of the Central Andes (e.g. Moquegua and Azapa Formations and equivalents, e.g. Semperé, 2000, Roperch et al., 2006) appear to be much thicker on the Western Andean Escarpment (Fig. 3.1 and Fig. 4.18) in the area of the Arequipa domain. Furthermore paleomagnetic study combined with stratigraphic analysis of Neogene basin on the Altiplano plateau (e.g. Rouse et al., 2005) suggested that the Huacochullo and Corque basins (Fig. 4.18) are deformed and rotated more or less coherently, while the region directly east (e.g., the Copacabana-Coniri-Cochabamba fault system: Fig. 4.11) accommodated the bulk of the shear component associated with the large block rotation. These differences attest to the rheological and structural identity of the Arequipa domain during Andean Orogeny.

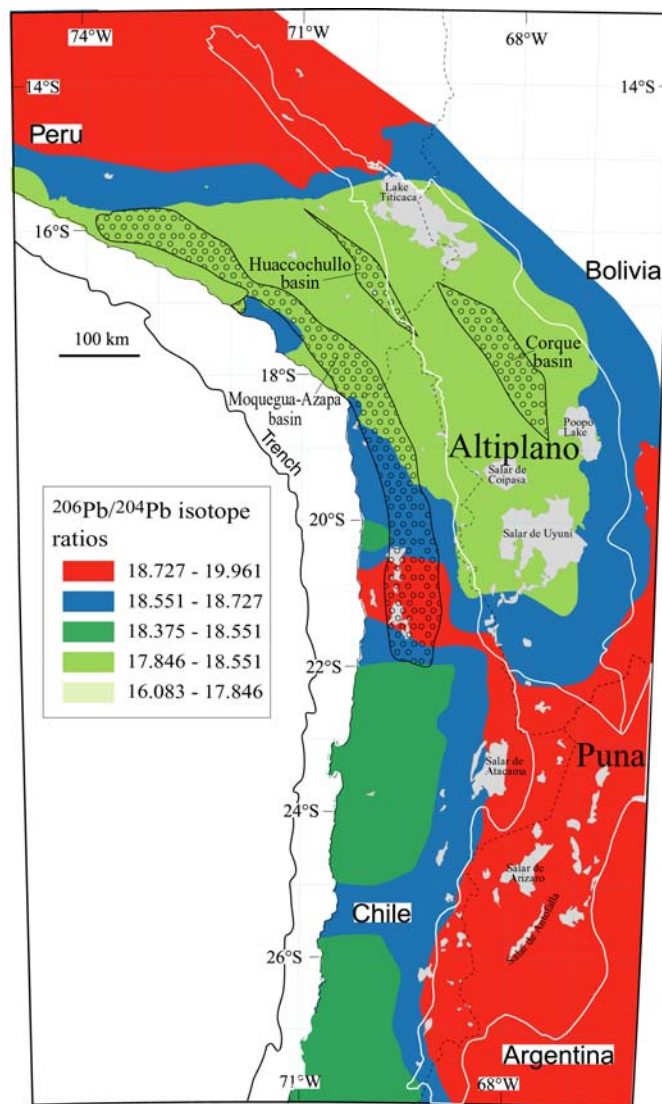


Fig. 4.18. Central Andean plateau and its adjacent foreland related to the Pb-isotope domains. Extensions of Huacochullo and Corque basins from Rouse et al. (2005), Moquegua-Azapa basin from Roperch et al. (2006) and Inner Arc from Clark et al. (1990).

#### 4.4.7 Pb-isotopes of gold, silver copper and tin deposits, their relationship with the Pb-domains

Lead isotopes tell us about the influence of basement rocks and tectonic setting on (Pb-) sources of ore deposits in magmatic arcs. Thus, the application of crustal scale Pb isotope variation contributes to an understanding of regional controls on ore deposits (Tosdal et al., 1999).

The geology and geochemistry of the mayor ore districts in the Central Andes have been described by Tilton and Barreiro (1980), Barreiro and Clark (1984), Puig (1988), Boric et al. (1990), Macfarlane et al. (1990), Mukasa et al. (1990), Vivallo et al. (1998), Clark et al. (1990a and b), Tosdal (1995), Richard et al. (2001), Kamenov et al. (2002), and BRGM GIS Andes Project (see <http://gisandes.brgm.fr>).

Economic copper deposits are hosted in Jurassic and early Tertiary rocks in the Arequipa, Mejillonia, and Chilenia domains and they have transitional Pb isotope compositions. Silver-gold deposits are hosted in a variety of rocks across several Neogene volcanoes in Transitional zone and Cordillera domain boundary with Pb isotope ratios comparable to that of the Paleozoic basement (Fig. 4.1, 4.19).

As is observed in Figure 4.20, there are no abrupt Pb-isotope distinctions among Jurassic (La Negra Formation;  $^{206}\text{Pb}/^{204}\text{Pb} = 18.1-18.5$ ) and Early Tertiary igneous rocks (Toquepala and Cerro Verde complexes;  $^{206}\text{Pb}/^{204}\text{Pb} = 18.3-18.7$ ) that host the copper deposits. However, there are Pb isotope distinctions between Pb-isotopes of these copper deposits and Neogene silver-gold deposits with  $^{206}\text{Pb}/^{204}\text{Pb} > 18.5$ . This implies that the Cu ores and Ag-Au ores may have significantly different sources.

Lead isotope compositions ( $^{206}\text{Pb}/^{204}\text{Pb} > 18.5$ ) of Neogene volcanoes that host the silver-gold deposits form trends similar of those of the local Paleozoic basement rocks. Lead isotope compositions of Jurassic and Early Tertiary rocks ( $^{206}\text{Pb}/^{204}\text{Pb} = 18.7-18.4$ ) generally have higher ratios than the Proterozoic basements ( $^{206}\text{Pb}/^{204}\text{Pb} = 16.7-18.4$ ) on which or near to which they are located (Fig. 4.1). This is also true from Cenozoic volcanoes emplaced on Proterozoic rocks.

This difference is in part the result of the time integrated growth of Pb isotope compositions in response to widely different U/Pb and Th/U in Proterozoic rocks.

Jurassic and Early Tertiary tectonics in southern Peru and northern Chile were dominated by large-scale faults, extension and crustal thinning that was accompanied by wide-spread tholeiitic and cal-alkaline magmatism (Mukasa et al., 1990; Lucassen and Thirlwall, 1998). In contrast, Neogene volcanic were emplaced during and after crustal thickening (James and Sacks, 1999; Kay et al., 1999).

Jurassic, Early Tertiary rocks and sulfide minerals of Arequipa, Mejillonia domains are also isotopically distinct from Neogene rocks and sulfide minerals of Transition zone and Cordillera domain (Fig. 4.21). The Jurassic and Early Tertiary sulfide minerals in porphyry deposits are lower in  $^{206}\text{Pb}/^{204}\text{Pb} < 18.7$  (Vivallo et al, 1998; Tilton and Barreiro, 1980; Puig, 1988) as most of the igneous rocks with which the sulfides are associated.

In the Precordillera arc (northern Chile) Late Cretaceous–Eocene (68 Ma, Wörner et al., 2000 to 38.5 Ma, Scheuber et al., 1994) alkalic magmatism occurred in an extensional tectonic arc and backarc setting (Scheuber et al., 1994, Charrier and Reutter, 1994), the Pb isotope compositions ( $^{206}\text{Pb}/^{204}\text{Pb} = 18.65$ ) of these rocks are distinct from the Jurassic plutons and the difference reflect extensional tectonic setting and derivation from the mantle source without crustal assimilation (Fig. 4.21).

Of note is the fact that Pb isotope compositions of other some Jurassic rocks of the Coastal Cordillera are devoid of porphyry copper deposits (e.g., Morro de Arica with  $^{206}\text{Pb}/^{204}\text{Pb} =$

18.8 and Punta Coles with  $^{206}\text{Pb}/^{204}\text{Pb} = 17.58$ ) and these rocks were formed with less crustal interaction.

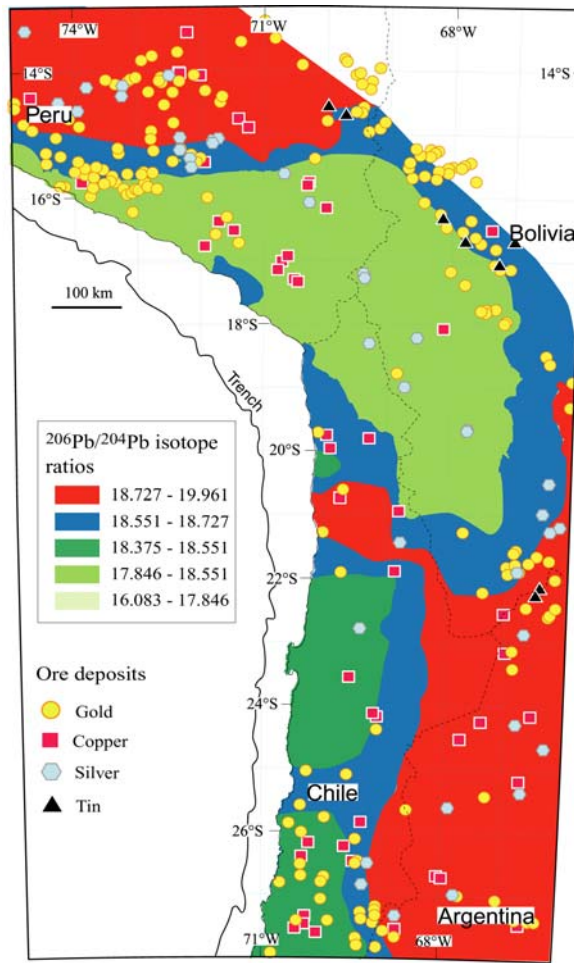


Fig. 4.19. Distribution of mineral deposits and Pb isotope domains.

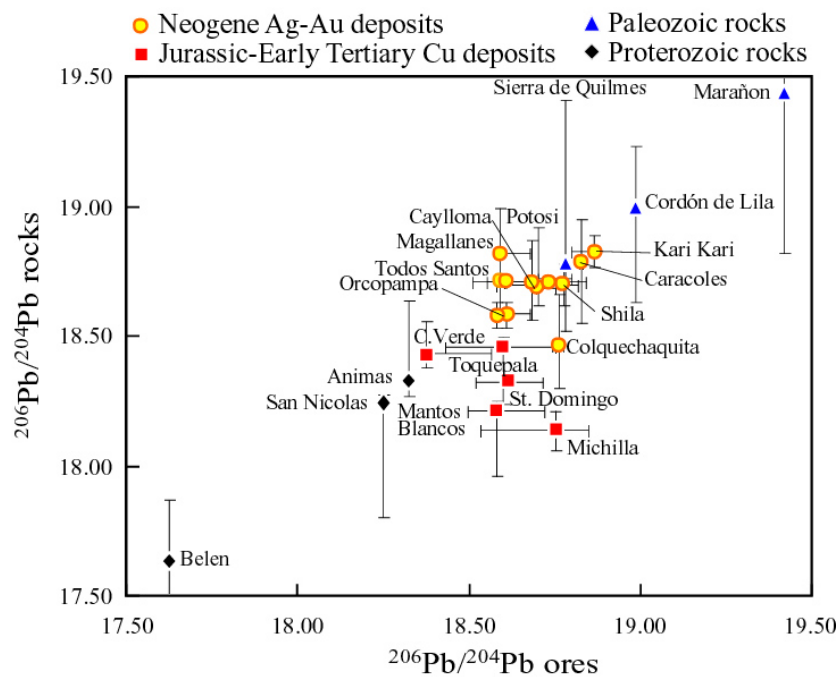


Fig. 4.20.  $^{206}\text{Pb}/^{204}\text{Pb}$  of Proterozoic, Paleozoic, Jurassic, Early Tertiary and Neogene crustal rocks versus  $^{206}\text{Pb}/^{204}\text{Pb}$  of sulfide minerals from different domains.

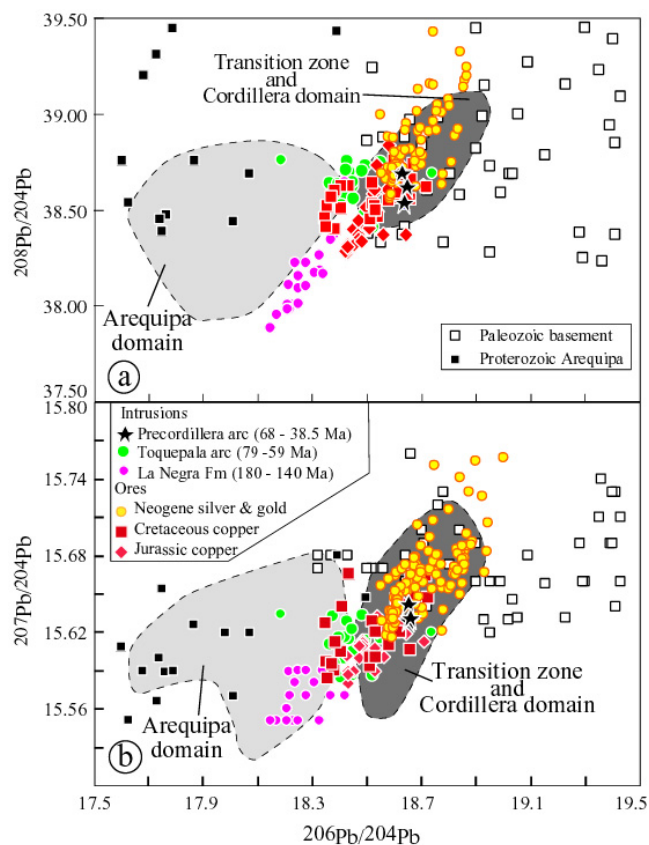


Fig. 4.21. a)  $^{208}\text{Pb}/^{204}\text{Pb}$  versus  $^{206}\text{Pb}/^{204}\text{Pb}$ , b)  $^{207}\text{Pb}/^{204}\text{Pb}$  versus  $^{206}\text{Pb}/^{204}\text{Pb}$  diagrams for Proterozoic, Paleozoic, Jurassic, Early Tertiary rocks and sulfide minerals. Fields with dashed lines represent Pb isotope values of Neogene volcanoes in different Pb domains.

Crustal interaction is important for Jurassic and Early Tertiary porphyry-copper deposits (Santo Domingo, Mantos Blancos, Michilla, Cerro Verde, Toquepala) and principally for Neogene epithermal-silver-gold deposits (Shila, Colquechaquita, Potosi, Caylloma, Magallanes, Todos Santos, Orcopampa).

The gradual increase of Pb isotope ratios with time within productive Jurassic and Early Tertiary igneous rocks and ore minerals in the Arequipa domain suggest progressively involvement of Proterozoic Arequipa crust material with lower U/Pb and a less assimilation of high U/Pb crust in magma genesis. A scenario where mantle-derived magmas underplate, assimilate lower mafic crust with lower U/Pb and in the upper part is added high U/Pb crust seems to best explain the evolution of Pb isotope composition from Jurassic to Early Tertiary times (Fig. 4.22).

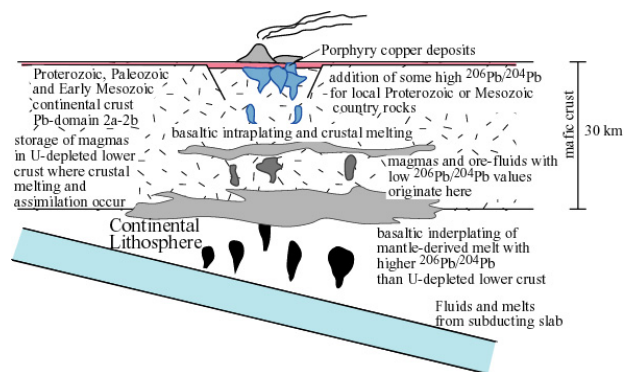


Fig. 4.22. Model of Jurassic and Early Tertiary rocks and porphyry copper formation in the Arequipa domain.

Neogene crustal thickening accompanied by emplacement of magmas leads to a progressively warmer crust, consequent lessening of the density contrast between those magmas and crust, and stalling the magmas in the lower crust. Ponding magma further heat the crust, causing melting of lower crust rocks and either the rise of a separate magma or the assimilation of these partial melting into the ponded magma (Babeyko and Sobolev, 2002). Additional partial melting, fractionation, assimilation of thick Paleozoic and Meso-Cenozoic crust with high U/Pb can modify the chemical characteristic of the magma prior to or at site of emplacement (Fig. 4.23). This is also constrained by Nd-Sr isotope of the volcanoes in the Transition zones (Fig. 4.16). I propose thicker crust during Miocene time may have promoted ponding magmas at upper levels in the crust and extensive assimilation of felsic rocks (section 4.4.2).

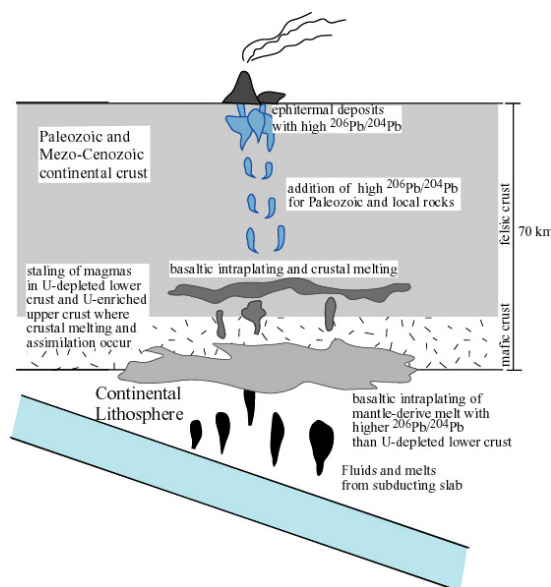


Fig. 4.23. Model of Neogene and Epithermal silver and gold formation in the Transition zone.

The Pb isotope results of this study concur with Kamenov et al. (2002) study and their identification to the east of the Arequipa basement (Fig. 4.24a) and in the notion that the degree of incorporation of ore metals from the basements appears to depend on the timing and/or location of the mineralization event. My domain map defines the margins of the Arequipa domain more clearly (Fig. 4.2).

I disagree with Chiaradia and Fontbote (2002) in the notion that mantle heterogeneity is an important factor responsible for Pb isotope variability of the Andean provinces at the continental scale (Fig. 4.24b). This may be true for the Northern Andes and thinner crust, but in the Central Andes the heterogeneity of the crust (mafic and felsic) dominates.

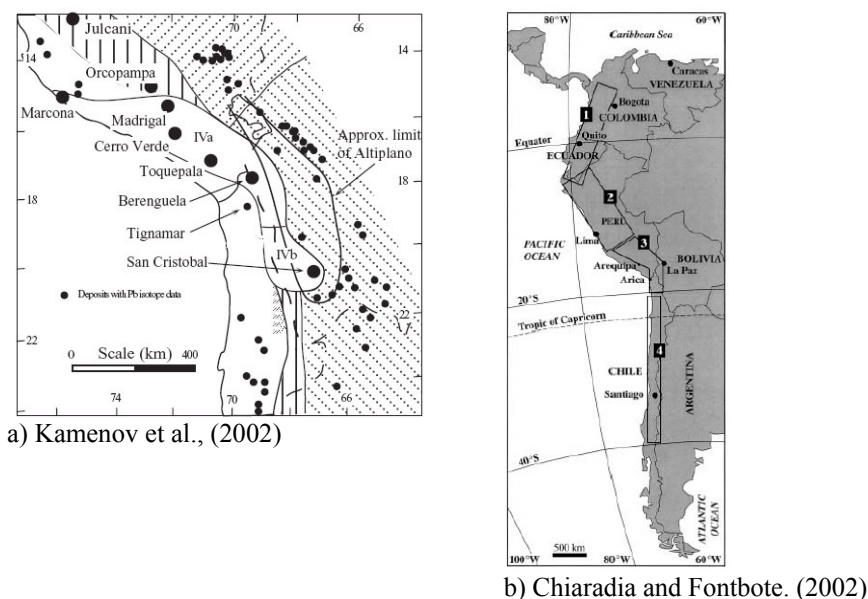


Fig. 4.24. a. Geographic distributions of ore lead isotope provinces in the Central Andes (Kamenov et al., 2002). b. Map of Western South America showing the four lead isotope provinces of the Andean Cordillera defined by Chiaradia and Fontbote. (2002), 1=Ecuador–Colombia, 2=Northern Peru, 3= Southern Peru, 4=Chile.

Different to the Copper, Silver and Gold deposits, the Tin deposits are restricted to the central section between 14°S and 22°S (Fig. 4.19). This belt, referred to as the Inner arc (Clark et al., 1990), is restricted to the Eastern Cordillera of the centermost Andes, and lies to the east of the zone of high Altiplano plateau (Fig. 4.18).

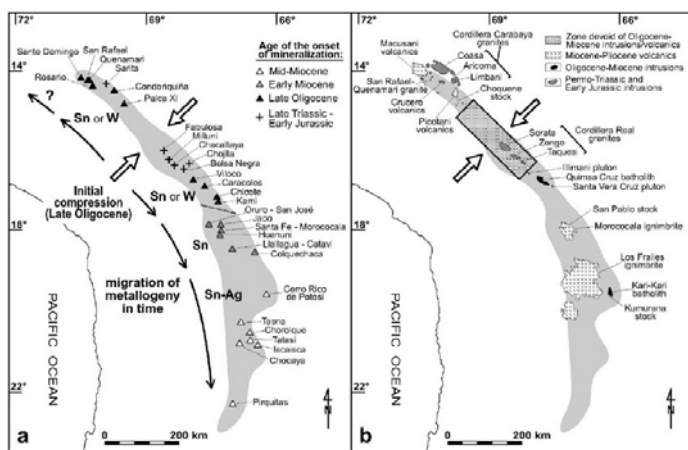


Fig. 4.25

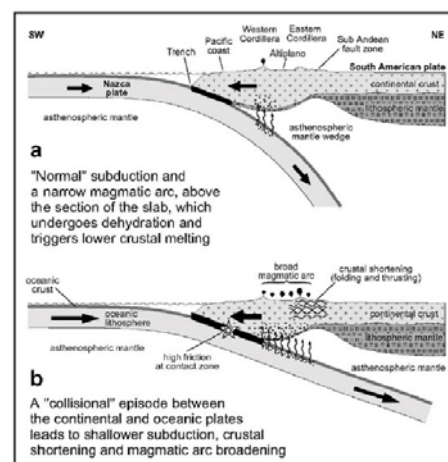


Fig. 4.26

Fig. 4.25. The inner arc with tin belt metallogeny in the Central Andes (from Mlynarczyk and Williams-Jones, 2005). (a) Migration of mineralized centers with time (b) Permo-Triassic, early Jurassic and Tertiary plutons and volcanics in the Central Andean tin belt.

Fig. 4.26. Schematic cross-section of the Andean continental margin, showing the relationships between the rate of convergence, the corresponding retreat of the subducted slab, the angle of subduction, and the width of the magmatic arc (from Mlynarczyk and Williams-Jones, 2005).

Studies by Mlynarczyk and Williams-Jones (2005, Fig. 4.25, Fig. 4.26) concluded that Tertiary magmatism in the Inner arc of the Central Andes and the associated world-class tin mineralization are directly related to discrete episodes of “collisional” interaction between the Nazca slab and the South American plate. During these geodynamic events, the asthenospheric mantle wedge, undergoing intense melting, was shifted eastward by a



shallowing of subduction and caused the underplating of thick continental crust by hot mafic melts. This, together with shear heating generated by crustal thrusting, radiogenic heat from crustal thickening, and the depression of the lower crust into the mantle caused an extensive anatexis of the thick sequences of metasedimentary rocks and the gneissic basement, which underlie the Inner Arc. Voluminous, tin-rich magmas of peraluminous composition were produced and upon emplacement gave rise to large deposits of high grade tin mineralization. They infer that this process has taken place repeatedly since the onset of the Andean orogeny and, therefore, concluded that it may also be responsible for the earlier episodes of tin mineralization in the Central Andes.

If it is as Mlynarczyk and Williams-Jones (2005) concluded why the tin belt don't extend along all "colisional" zone e.g. south of 22°S under the Puna plateau and north of 14°S under the Altiplano plateau?

I observe that the Tin deposits and the high heat flow region of the inner arc coincide spatially with the eastern boundary of Arequipa domain (Fig. 4.18, 4.19). Thus appear that the Tin belt are related to the eastern Transition zone between the Arequipa domain and Cordillera domain (see Fig. 4.15).

#### 4.5 Conclusions

- The trace elements and Sr-Nd-Pb isotope ratios of Cenozoic lavas and ignimbrites formed during and after crustal uplift follow patterns consistent with their basement: volcanics erupted through Arequipa domain are affected by assimilation of mafic basement. Lavas and ores on Mejillonia and Chilenia domains have received mafic crust contribution. Volcanics in northern and southern Transitional zones were contaminated by less mafic basement and more felsic basement. Lavas from Cordillera domain are affected by assimilation of felsic basements. Clemesi domain contain more juvenile component.
- Caution needs to be applied when plotting geochemical data vs. age for rocks from a wide regional distribution as local basement control is more important than age in controlling their geochemical composition.
- The correlation between the present-day Pb-isotope domains and crustal structure index variations strongly supports an intracrustal control of the lead isotope compositions of igneous rocks and ore deposits. The main control on Pb isotope compositions is clearly the time-integrated trace element compositions of mafic and felsic basement.
- Bulk crustal composition is another control of the garnet signature in addition to crustal thickness. Garnet-effect (high Sm/Yb ratios) is higher in the mafic domains and low in felsic domains.
- The relative abundance of ore deposits that fall into boundary of the mafic domains with which they share their Pb-isotope compositions suggest that this crustal structure and composition (as expressed also in the index model) are may be more favorable to the formation of porphyry copper deposits. By contrast, The Transitional zones and The Cordillera domain (felsic crust) are may be more favorable to the formations of epithermal silver-gold deposits, and the east Transitional zone between Arequipa and Cordillera domains are may be favorable to the formation of tin deposits.
- On the basis of the geochemical and isotopic parameters discussed in this chapter and geophysical model, the crustal rheology is peculiar in each basement domain.

## 5 Appendix

### 5.1 Sample locations

Data of 1545 samples rock analysis from the Central Andes were used in this study (Fig. 7.1). The vast majority of the samples represent lavas and ignimbrites from the Miocene, Mio-Pliocene, Pleistocene and Holocene arcs rocks. Additional samples are Proterozoic and Paleozoic metamorphics rocks, Jurassic, Cretaceous and Paleogene intrusions, and ores. For better graphical display, the samples are grouped in 18 groups (Table 7.1 and on CD).

Table 7.1. Table of age groups and numbers of samples.

Frontal arc	Age (Ma)	Mamani work samples	Wörner et al. and unpublished samples	Literature samples	Total of samples
HV= Holocene volcanoes	0 - 0.3	46	380	8	434
PV= Pleistocene volcanoes	0.8 - 3	26	19	2	47
MPV= Mio-Pliocene volcanoes	3 - 15	67	39	10	116
MV= Miocene volcanoes	15 - 25	12	14	18	44
EOV= Eocene-Oligocene volcanoes	> 25	9			9
MPIG= Miocene to Recent ignimbrites	0 - 15		149	38	187
MI= Miocene Ignimbrites	15 - 25		17	6	23
<b>Back Arc</b>					
HVBA=Holocene volcanoes	> 0.7	6		7	13
MPVBA=Miocene-Pliocene volcanics	3 - 15			72	72
OVBA=Oligocene volcanics	28 - 30		28	29	57
MPIGBA=Mio-Pliocene Ignimbrites	5 - 21			17	17
MINBA=Miocene intrusions	~ 13 -15	1		8	9
INBA=Oligocene Intrusions	28 - 30			17	17
<b>Intrusion</b>					
CPIN=Cretaceous-Paleocene intrusions	90 - 33	8	80	80	168
JIN=Jurassic intrusions	100 - 190	7	3	37	47
<b>Basement</b>					
PB=Paleozoic	502 - 298	4	21	90	115
PR=Proterozoic	561-2000	8	11	24	43
Ores	8 - 120	7		120	127

Description of the volcanoes from the CVZ listed in the database can find on a website listed in Table 7.2.

Table 7.2. Volcanoes Website.

	Website
Peru volcanoes	<a href="http://www.igp.gob.pe/vulcanologia/">http://www.igp.gob.pe/vulcanologia/</a>
Central Volcanic Zone volcanoes	<a href="http://volcano.space.edu/cvz/volcindx.html">http://volcano.space.edu/cvz/volcindx.html</a>
Globalvolcanism (Holocene volcanoes)	<a href="http://www.volcano.si.edu/world/allvolcs.htm">http://www.volcano.si.edu/world/allvolcs.htm</a>

The Figure 7.1 shows all Andes Project samples, which have been taken during 1988-2004, while the Figure 7.2 on CD is located only those samples with complete analyses (XRF-ICPMS-TIMS). Samples with just XRF and ICPMS data from the campaigns 1999 to 2004 are not illustrated on the Fig. 7.2.

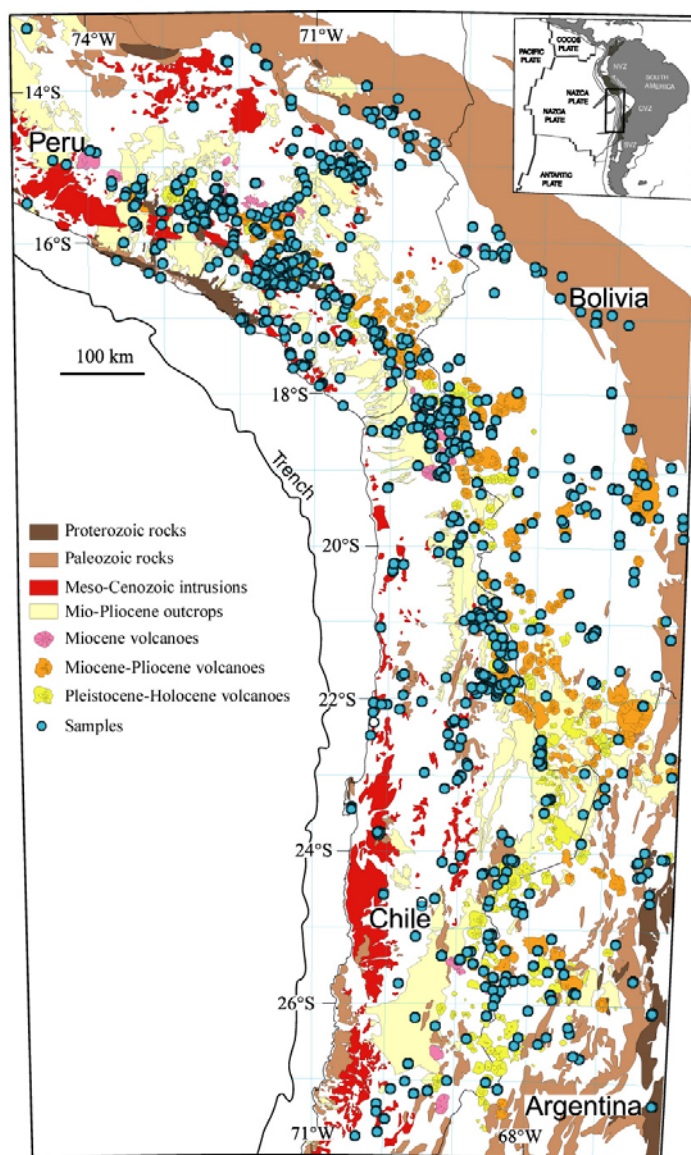


Fig. 7.1. Samples locations.

## 5.2 Analytical Methods

In this section I describe the analytical methods used in this work and in Wörner et al. after 1993 and unpublished data, which have been done at the Geowissenschaftliches Zentrum Göttingen (GZG).

Samples from Wörner et al. before 1993 were analyzed by Atomic Absorption Spectrometry and Instrumental Activation Analysis. Some samples of this group were analyzed again by ICP-MS in this study in order to obtain a complete set of HFSE and REE.

### 5.2.1 Sample Preparation

Representative samples from CVZ were collected, analyzed by XRF and ICP-MS and TIMS. The most unaltered rocks were selected in the field to minimize contamination of the samples, removal of alteration rims and crushing up into chips of ~5 cm in diameter was done directly at the sampling location. About 1-3 kg of each sample was collected and a hand-specimen was kept from all samples.

The chips were then disintegrated with the small jaw crusher down to fragments of less than 1 cm in diameter. About 100 g of samples material was separated from the remaining fragments

with a mechanical splitting device. This 100 g were then ground to powder (65  $\mu\text{m}$ ) in agate mills for about 30 and 40 min. The rest of the samples not used to ground, some of which were used to mineral separation.

### 5.2.2 XRF (X-Ray Fluorescence Spectroscopy) analysis

XRF spectroscopy uses characteristic x-rays (secondary fluorescence), generated by excitation of inner shell electrons with primary X-Rays to specify elements and concentration. This analytical method was used to determine major- and minor elements (Si, Ti, Al, Fe, Mn, Mg, Ca, Na, K, P) of the rocks as well as some trace elements (Nb, Zr, Y, Sr, Rb, Ga, Zn, Cu, Ni, Co, Cr, V, Ba, Sc). 700 mg of powder sample were thoroughly mixed with 4200 mg Spectroflux 100 (Dilithiumtetraborate [ $\text{Li}_2\text{B}_4\text{O}_7$ ]) and automatically fused and transformed to a glass disc by an automatic fusion device (Labor-Schoeps SGE 20).  $\text{Fe}_2\text{O}_3$  was determined titrimetrically with  $\text{KMnO}_4$  and the loss on ignition (LOI) by weight difference at heating to  $1100^\circ\text{C}$ . Analytical error for major elements are around 1% (except for Fe and Na, 2%; and LOI,  $\sim 10\%$ ) and for trace elements around 5%. Measurements were carried out on a Philips PW 1480 and the data processing is controlled by the Philips X40 software package. For the calibration of major and trace element determination were used about 50 reference materials: a wide variety of international geochemical reference samples from the US Geological Survey, the International Working Group "Analytical standards of minerals, ores and rocks", the National Research Council of Canada, the Geological Survey of Japan, the South African Bureau of Standards, the National Institute of Standards & Technology, etc.

### 5.2.3 ICP-MS (Inductively Coupled Plasma Mass Spectrometry) analysis

The ICPMS technique provides the advantage of simultaneous determination of a wide range of trace elements from Li to U, low detection limits and good analytical precision especially for masses  $>80$ . Fundamentals of this method are described in Potts (1987), Garbe-Schönberg (1993). For the present purpose, trace elements like REE (La – Lu), HFSE (Nb, Ta, Zr, Hf), LILE (Rb, Sr, Ba, Cs), and others (Li, Sc, Cu, V, Cr, Co, Ni, Zn, Y, Pb, Th, U) of selected samples were analyzed on an ICPMS Perkin Elmer SCIEX (Elan DRC II).

Sample preparation to ICPMS: About 100 mg of sample powder was weighed into Teflon beakers after Heinrichs & Herrmann (1990) and dissolved under pressure in a mixture of acids composed of 3 ml HF, 3 ml  $\text{HClO}_4$ , and 1 ml  $\text{HNO}_3$ . After cessation of gas formation, the beakers were tightly closed and heated in a muffle oven at  $200^\circ\text{C}$  for 14 hours. After cooling to ambient temperatures, the beakers were opened and placed on a hot plate for evaporation at  $180^\circ\text{C}$ . The dried sample was re-dissolved in 2 ml  $\text{HNO}_3$  and once again put onto the hot plate. After the second stage of evaporation, 2 ml  $\text{HNO}_3$ , 5 ml de-ionised water and the internal standard were added to the sample. This solution was rinsed into a 100 ml quartz-glass flask and the remaining volume was filled with de-ionised water. The resulting solution contained the sample in a dilution 1:1000 in 2 %  $\text{HNO}_3$  with 20 ppb Rh, Re, In as internal standard. It was kept in polyethylene bottles and measured within two days to minimize the risk of precipitation or interchange with the plastic container. For each batch of fifteen samples a blank solution and a lab-intern or international standard were prepared. All reagents used were three times distilled to suppress blank values.

Selection of respective isotopes was done on criteria of abundance and exclusion of isobaric interference. Calibration of the intensities against concentration values for each element is provided by measuring multi-element calibration solutions prior to sample acquisition. These calibration solutions were prepared from stock solutions by aiming to span the total range of expected concentrations and by the attempt to keep the elemental ratios close to natural conditions. A control for contaminations due to dissolution processes is obtained by measurement of simultaneously prepared blank solutions, a correction for the machine drift is

provided by repeated measurement of one of the calibration solutions and by the internal standards of Rh, Re, In. Co-processed lab-internal and international standards JB3 (n= 19) and JA2 (n = 8) were measured as unknowns in the experiments. From this the  $2\sigma$  error of the method is estimated to be <20% for Nb and Ta, <10% for Be, Cs, Cu, Hf, Li, Y, Pb, Rb, Tl, Th and U and ~5% for the rare earth elements (REE).

#### 5.2.4 TIMS (Thermal Ionization Mass Spectrometer) analysis

The isotope ratios of Sr, Nd and Pb on corresponding 194 whole rocks were measured at a Finnigan MAT262-RPQII plus in Göttingen (Abteilung Radiogene Isotope).

For Sr and Nd isotopic determination 100 mg of sample powder was dissolved in 6 ml HF: HNO<sub>3</sub> (1:1) for 16 hours at 200°C baked within Savillex vials. The solution was evaporated to complete dryness at 140°C on a hot plate, dissolved and evaporated two times again in 4 ml 6N HCl, and evaporation for the last time, it was re-dissolved in 2.5 ml 2.6 N HCl, stored in PE vials and centrifuged. For separation the sample solution was rinsed with 2.6 N HCl through columns containing ion exchange resin BIORAD AG 50W-X8 Resin, 200-400 mesh. The strontium rich elution fraction was caught in a vial, evaporated to dryness and stored until measuring. For Nd separation, the REE rich fraction gained from the above separation sequence was separated in a second set of columns containing Teflon powder which is impregnated with ion-exchanging HDEHP Bis-(2-ethylhexy)-Phosphate. Elution of Nd was done with 0.18 N HCl.

For measurement, Sr was dissolved in 0.5 N H<sub>3</sub>PO<sub>4</sub> and mounted on Re-double filaments (~1 µg), and Nd was dissolved in 2 N HCl and mounted on Re-double-filaments (~1 µg). The Sr and Nd isotope ratios were corrected for mass fractionation to  $^{87}\text{Sr}/^{86}\text{Sr} = 0.1194$  and  $^{143}\text{Nd}/^{144}\text{Nd} = 0.7219$  and normalized to values for NBS987 (0.710245), and La Jolla (0.511847), respectively. Measured values of these standards over the period of the study were  $0.710262 \pm 24$  (21 analyses) and  $0.511847 \pm 20$  (12 analysis). External error  $2\sigma$  are estimated at < 0.004% for Sr and Nd. Total procedural blank: Sr (0.26 ng) and Nd (< 0.14 ng). For Pb isotopic determination about 100 mg of sample powder was dissolved in 4 ml HF: HNO<sub>3</sub> (1:1) in Savillex beakers at 200°C for 24 hours. After dilution in 1 ml 0.5 N HBr and subsequent evaporation, it was diluted again in 0.5 N HBr and centrifuged. Lead was separated on anion exchange columns containing 100 µl resin (Biorad AG1-X8, 200-400 mesh). The samples were dissolved in 0.3 ml 2 N HCl and washed into the columns, afterward rinsed with 1ml 0.5N HBr and finally eluted with 1 ml 6N HCl. To get rid of alkalis and earth-alkalis, the separation process was repeated. The entire processing was carried out within a laminar flow box to exclude contamination by lead which is bound to dust particles. Pb was mounted on Re double filament using silica-gel. Lead isotopes were corrected to NBS 981. Normalization of our data to recommended values was performed using a mass fractionation factor of 0.122%. From measurements of twenty one standards gave a mean of  $^{206}\text{Pb}/^{204}\text{Pb} = 16.90 \pm 0.01$ ,  $^{207}\text{Pb}/^{204}\text{Pb} = 15.44 \pm 0.02$ ,  $^{208}\text{Pb}/^{204}\text{Pb} = 37.53 \pm 0.05$ , total error ( $2\sigma$ ) < 0.1% were determined. Total blank were 0.29 ng. Ionisation temperature for Pb measurement was held constant at 1200°C.

## 6 References

- Acosta, J., 2004, Facies y ambientes sedimentarios de la formacion Moquegua superior en los alrededores de la ciudad de Tacna: In: J. Jacay & T. Sempere (eds.), Nuevas contribuciones del IRD y sus contrapartes al conocimiento geológico del sur del Perú, Sociedad Geológica del Perú, Publicación Especial n° 5, p. 183-186.
- Aitchison, S.J., Forrest, A.H., 1994, Quantification of crustal contamination in open magmatic systems: *Journal of Petrology*, v. 35, p. 461-488.
- Aitchison, S.J., Harmon, R.S., Moorbath, S., Schneider, A., Soler, P., Soria, E.E., Steele, G., Swainbank, I., Wörner, G., 1995, Pb isotopes define basement domains of the Altiplano, Central Andes: *Geology*, v. 23, p. 555-558.
- Allmendinger, R., Gonzalez, G., Yu, J., Hoke, G., Isacks, B., 2005, Trench-parallel shortening in the northern Chilean forearc; tectonic and climatic implications: *Geological Society of America Bulletin*, v. 117, p. 89-104.
- Allmendinger, R.W., Gubbels, T., 1996, Pure and simple shear plateau uplift, Altiplano-Puna, Argentina and Bolivia: *Tectonophysics*, v. 259, p. 1-13.
- Allmendinger, R.W., Jordan, T.E., Kay, S.M. and Isacks, B., 1997, The evolution of the Altiplano-Puna plateau of the Central Andes: *Annual Reviews of Earth and Planetary Sciences*, v. 25, p. 139-174.
- Angermann, D., Klotz, J., Reiber, C., 1999, Space-geodetic estimation of the Nazca-South American Euler vector: *Earth and Planetary Science Letters*, v. 171, p. 329 - 334.
- Anthes, G., 1993, Haupt-, Spurenelement und Isotopengeochemie an den Oberkretazischen und Tertiären Granitoiden der Präkordillere Nordchiles zwischen 10° und 22°S, MS Thesis (Unpublished) Universität Mainz.
- Astini, R.A., Benedetto, J.L., Vaccari, N.E., 1995, The early Paleozoic evolution of the Argentine Precordillera as a Laurentian rifted, drifted and collided terrane: a geodynamic model: *Geol. Soc. Am. Bull.*, v. 107, p. 253-273.
- Ayuso, R.A., Bevier, M.L., 1991, Regional differences in Pb isotopic compositions of feldspars in plutonic rocks of the northern Appalachian Mountains USA, and Canada: A geochemical method of terrain correlation: *Tectonics*, v. 10, p. 191-212.
- Babeyko, A.Y., Sobolev, S.V., Trumbull, R.B., Oncken, O., Lavier, L.L., 2002, Numerical models of crustal scale convection and partial melting beneath the Altiplano-Puna plateau: *Earth Planet. Sci. Lett.*, v. 199, p. 373- 388.
- Baby, P., Rochat, P., Mascle, G., Herail, G., 1997, Neogene shortening contribution to crustal thickening in the back arc of the Central Andes: *Geology*, v. 25, p. 883-886.
- Bahlburg, H., Hervé, F., 1997, Geodynamic evolution and tectonostratigraphic terranes of northwestern Argentina and Northern Chile: *Geological Society of America Bulletin*, v. 109, p. 869-884.
- Barreiro, B.A., 1984, Lead isotope and Andean magmagenesis in Harmon, R.S., and Barreiro, B.A., eds., *Andean magmatism, chemical and isotopic constraints*: Cheshire, UK, Shiva, p. 21-30.

- Barreiro, B.A., Clark, A.H., 1984, Lead isotopic evidence for evolutionary changes in magma crust interaction, Central Andes, southern Peru: *Earth Planet. Sci. Lett.*, v. 69, p. 30-42.
- Beate, B., Monzier, M., Springs, R., Cotton, J., Bourdon, E., Eissen, J. P., 2001, Mio-Pliocene adakite generation related to flat subduction in southern Ecuador: Quinsacocha Volcanic center: *Earth Planet. Sci. Lett.*, v. 192, p. 561-570.
- Beck, S.L., Zandt, G., Myers, S.C., Stephen, C., Wallace, T.C., Silver, P.G., 1996, Crustal thickness variations in the central Andes. *Geology*, v. 24, p. 407-411.
- Beck, S.L., Zandt, G., 2002, The nature of orogenic crust in the Central Andes: *J. Geophys. Res.*, v. 107 doi:10.1029/2000JB000124.
- Bellon, H., Lefèvre, C., 1976, Données géochronométriques sur le volcanisme andin dans le sud du Pérou, v. Implications volcano-tectoniques C.R. Acad. Sci. Paris 238, Ser. D, 1-4.
- Bock, B., Bahlburg, H., Wörner, G., Zimmermann, U., 2000, Tracing crustal evolution in the southern Central Andes from Late Precambrian to Permian using Nd and Pb isotopes: *Journal of Geology*, v. 108, p. 515- 535.
- Bogdanic, T., Espinoza, S., 1994, Tectono-sedimentary evolution of the Cretaceous-Early Tertiary and metallogenic scheme of Northern Chile: In: Salfity, J. (ed.) *Cretaceous Tectonics of the Andes*. Braunschweig: Vieweg, p. 213-265.
- Boily, M., Brooks, C., Ludden, J.N., 1989, Chemical and Isotopic Evolution of the Coastal Batholith of Southern Peru: *Journal of Geophysical Research*, v. 94, p. 483-498.
- Boric, R., Díaz, F., Maksaev, V., 1990, Geología y yacimientos metalíferos de la Región de Antofagasta: Servicio Nacional de Geología y Minería, Boletín, p. 246, 2 mapas escala 1:500.000.
- Bosch, M., Rodriguez, I., 1992, North Venezuelan collisional crustal block; the boundary between the Caribbean and South American plates: *Journal of South American Earth Sciences*, v. 6, p. 133-143.
- Bourdon, B., Wörner, G., Zindler, A., 2000, U-series evidence for crustal involvement and magma residence times in the petrogenesis of Parinacota Volcano, Chile: *Contributions to Mineralogy and Petrology*, v. 139, p. 458-469.
- Bourdon, E., Eissen, J.P., Monzier, M., Robin, C., Martin, H., Hall, M.L., 2002, Adakite-like lavas from Antisana Volcano (Ecuador): evidence for slab melt metasomatism beneath the Northern Andean Zone: *J. Petrol.*, v. 43, p. 199-217.
- Cahill, T., Isacks, B.L., 1992, Seismicity and shape of the subducted Nazca plate: *Journal of Geophysical Research*, v. 97, p. 17, 503-17, 529.
- Carlier, G., Lorand, J.P., Liegeois, J.P., Fornari, M., Soler, P., Carlotto, V., Cardenas, J., 2005, Potassic-ultrapotassic mafic rocks delineate two lithospheric mantle blocks beneath the southern Peruvian Altiplano: *Geology*, v. 33, p. 601-604.
- Carlotto, V., 1998, Evolution andine et raccourcissement au niveau de Cusco (13°-16°S, Pérou), Thèse de doctorat, Université de Grenoble, France, p. 159.
- Cassard, D., Chauvet, A., Bailly, L., Llosa, F., Rosas, J., Marcoux, E., Lerouge, C., 2000, Structural control and K/Ar dating of the Au-Ag epithermal veins in the Shila Cordillera, southern Peru: *C. R. Acad. Sci. Paris*, v. 330, p. 23-30.

Charrier, R., Reutter, K.J., 1994, The Purilactis Group of Northern Chile: Boundary Between Arc and Backarc from Late Cretaceous to Eocene In: Reutter, K.J., Scheuber, E. & Wigger, P. (eds.): *Tectonics of the Southern Central Andes*: Springer Verlag, Berlin, p. 189-202.

Chiaradia, M., Fontboté, L., 2002, Lead isotope systematics of Late Cretaceous – Tertiary Andean arc magmas and associated ores between 8°N and 40°S: evidence for latitudinal mantle heterogeneity beneath the Andes: *Terra Nova*, v. 14, p. 337–342.

Clark, A.H., Farrar, E., Kontak, D.J., Langridge, R.J., Arenas, M.J., France, L.J., McBride, S.L., Woodman, P.L., Wasteneys, H.A., Sandeman, H.A., Archibald, D.A., 1990a, Geologic and geochronologic constraints on the metallogenic evolution of the Andes of southeastern Peru: *Economic Geology*, v. 85, p. 1520-1583.

Clark, A.H., Tosdal, R.M., Farrar, E., Plazolles, A., 1990b, Geomorphologic environment and age of supergene enrichment of the Cujone, Quellaveco, Toquepala Porphyry Copper deposits, southeastern Peru: *Economic Geology*, v. 85, p. 1604-1628.

Cobbing, E.J., Ozard, J.M., Snelling, N.J., 1977, Reconnaissance geochronology of the crystalline basement rocks of the Coastal Cordillera of southern Peru: *Geol. Soc. Am. Bull.*, v. 88, p. 241-246.

Coira, B., Davidson, J., Mpodozis, C., Ramos, V., 1982, Tectonic and magmatic evolution of the Andes of northern Argentina and Chile: *Earth Sci. Rev.*, v. 18, p. 303-332.

Coira, B., Kay, S.M., Viramonte, J., 1993, Upper Cenozoic magmatic evolution of the Argentine Puna\_ A model for changing subduction geometry: *International Geology Review*, v. 35, p. 677-720.

Dalmayrac, B., Laubacher, G., Marocco, R., 1977, *Géologie des Andes Péruviennes, Caracteres Generaux de L'évoution géologique des Andes Péruviennes*, Thèse Université des Sciences et Techniques du Languedoc. p. 361.

Dalziel, I.W.D., Forsythe, R.D., 1985, Andean evolution and the terrane concept: In *Tectonostratigraphic Terranes of the Circum-Pacific Region*; Circum-Pacific council for Energy and Mineral Resources, *Earth Sci. Series*, v. 1, p. 565-581.

Damm, K.W., Pichowiak, S., Harmon, R.S., Todt, W., Omaniri, R., Niemeyer, H., 1990, Pre-Mesozoic evolution of the Central Andes-the basement revisited: *Geol. Soc. Am. Spec.*, v. 241, p. 101-126.

Damm, K.W., Harmon, R., Kelley, S., 1994, Some isotopic and geochemical constraints on the origin and evolution of the Central Andes basement (19°-24°): In Reutter, KJ, Scheuber E & Wigger PJ (eds) *Tectonic of the Southern Central Andes*. Springer Verlag, Berlin, p. 263-276.

Dasch, J., 1981, Lead isotopic composition of metalliferous sediments from Nazca plate: *Geological Society of America Memoir*, v. 154, p. 199-210.

Davidson, J.P., McMillan, N. J., Moorbath, S., Wörner, G., Harmon, R.S., Lopez-Escobar, L., 1990, The Nevados de Payachata Volcanic Region (18°S/69°W, N. Chile) II: Evidence for Widespread Crustal Involvement in Andean Magmatism: *Contributions to Mineralogy and Petrology*, v. 105, p. 412-432.

Davidson, J.P., Harmon, R.S., Wörner, G., 1991, The source of the Central Andes magmas: some considerations: *Geol. Soc. Am. Andean magmatism and its tectonic setting*, v. 265, p. 233-244.

Davidson, J.P., de Silva, S., 1992, Volcanic rocks from the Bolivian Altiplano: Insights into crustal structure, contamination, and magma genesis in the central Andes: *Geology*, v. 20, p. 1127-1130.



- De Silva, S.L., 1989, Altiplano-Puna volcanic complex of the central Andes: *Geology*, v. 17, p. 1102-1106.
- De Silva, S.L., Francis, P.W., 1990, Potentially active volcanoes of Peru - Observations using Landsat Thematic Mapper and Space Shuttle imagery: *Bulletin of Volcanology*, v. 52, p. 286-301.
- , 1991, *Volcanoes of the Central Andes*: Heidelberg, Springer-Verlag, 232 p.
- Defant, M.J., Drummond, M.S., 1990, Derivation of some modern arc magmas by melting of young subducted lithosphere: *Nature*, v. 347.
- DePaolo, D.J., Wasserburg, G.J., 1976, Nd isotope variations and petrogenetic models: *Geophys. Res. Lett.*, v. 3, p. 249-252.
- DePaolo, D.J., 1981, Trace element and isotopic effects of combined wallrock assimilation and fractional crystallization: *Earth and Planetary Science Letters*, v. 53, p. 189-202.
- DePaolo, D.J., Linn, A.M., Schubert, G., 1991, The Continental crustal age distribution: Methods of determining mantle separation ages from Sm-Nd isotopic data and application to the southwestern United States: *Journal of Geophysical Research*, v. 96, p. 2071-2088.
- Dorbath, C., Granet, M., 1996, Local earthquake tomography of the Altiplano and Eastern Cordillera of northern Bolivia: *Tectonophysics*, v. 259, p. 117-136.
- Dostal, J., Zentilli, M., Caelles, J.C., Clark, A.H., 1977, Geochemistry and origin of volcanic rocks of the Andes (26-28°S): *Contrib. Mineral. Petrol.*, v. 63, p. 113-128.
- Entenmann, J., 1994, Magmatic evolution of the Nevados de Payachata Complex and the petrogenesis of basaltic andesites in the Central Volcanic Zone of northern Chile, PhD Thesis, Universität Mainz, p. 184.
- Eusterhues, K., 1993, *Geochemie miokaener Vulkanite Nordchiles (18°-20°S)*, MS Thesis (Unpublished) Universität Mainz.
- Flores, A., Sempere, T., Fornari, M., 2004, Síntesis actualizada de la estratigrafía del Cenozoico en el extremo sur del Perú: XII Congreso Peruano de Geología. Resúmenes Extendidos. Sociedad Geológica del Perú.
- Flores, A., Acosta, J., Bedoya, C., Sempere, T., 2005, Oligocene-Neogene tectonics and sedimentation in the forearc of southern Peru, Tacna area (17.5°-18.5°S): in VI International Symposium on Andean Geodynamics, September, Barcelona, Spain, p. 269-262.
- Fornari M., B.E., Espinoza F., Ibarra I., Jiménez N., Mamani M., 2002, Ar-Ar Dating of Late Oligocene-Early Miocene Volcanism in the Altiplano: V International Symposium on Andean Geodynamics, Toulouse-French, p. 223-226.
- Francis, P.W., Hawkesworth, C.J., 1994, Late Cenozoic rates of magmatic activity in the Central Andes and their relationships to continental crust formation and thickening: *J. Geol. Soc. (London)*, v. 151, p. 845-854.
- Garbe-Schönberg, C.D., 1993, Simultaneous determination of 37 trace elements in 28 international rock standards by ICP-MS: *Geostandards Newsletter*, v. 17, p. 81-93.
- Garrison, J.M., Davidson, J.P., 2003, Dubious case for slab melting in the Northern volcanic zone of the Andes: *Geology*, v. 31, p. 565 - 568.

- Giese, P., Scheuber, E., Schilling, F., Schmitz, M., Wigger, P., 1999, Crustal thickening processes in the Central Andes and the different natures of the Moho-discontinuity: *J. South Am. Earth Sci.*, v. 12, p. 201-220.
- Gil, W., 2001, Evolution latérale de la déformation d'un front orogénique: Exemple des Bassins subandins entre 0° et 16°S: Toulouse, Phd Thesis, Université Paul Sabatier. p.150.
- Gill, J., 1981, *Orogenic andesites and plate tectonics*: Springer Verlag, Berlin, p. 330.
- Gorring, M.L., Kay, S.M., Zeitler, P.K., Ramos, V.A., Rubiolo, D., Fernández, M.I. and Panza, J.L., 1997, Neogene Patagonian plateau lavas: continental magmas associated with ridge collision at the Chile Triple Junction: *Tectonics*, v. 16, p. 1-17.
- Gregory-Wodzicki, K.M., 2000, Uplift history of the central and northern Andes: A review: *Geol. Soc. Am. Bull.*, v. 112, p. 1091-1105.
- Guerra, E., 1993, Petrographie und Geochemie der magmatischen Gesteine und Petrographie der Sedimentgesteine des Murmutani Escarpment in the Präkordillere Nordchiles: Diploma Tesis (Unpublished), Universität Mainz, p. 115.
- Gunnesch, K.A., Baumann, A., Gunnesch, M., 1990, Lead isotope variations across the central Peruvian Andes: *Economic Geology*, v. 85, p. 1384-1401.
- Gutscher, M.A., Olivet, J.L., Aslanian, D., Eissen, J.P., Maury, R., 1999, The "lost Inca Plateau": Cause of flat subduction beneath Peru?: *Earth Planet. Sci. Lett.*, v. 171, p. 335-341.
- Gutscher, M.A., Maury, R., Eissen, J.P., and Bourdon, E., 2000, Can slab melting be caused by flat subduction?: *Geology*, v. 28, p. 535-538.
- Gutscher, M.A., 2002, Andean subducting styles and their effect on thermal structure and interplate coupling: *J. South Am. Earth Sci.*, v. 15, p. 3-10.
- Hampel, A., 2002, The migration history of the Nazca Ridge along the Peruvian active margin; a re-evaluation: *Earth and Planetary Science Letters*, v. 203, p. 665-679.
- Harmon, R.S., Hoefs, J., 1984, Oxygen isotope ratios in Late Cenozoic Andean volcanics: in Harmon, R.S. & Barreiro, B.A. (eds.), *Andean magmatism, chemical and isotopic constraints*. Shiva Publishing Ltd, p. 9-21.
- Harmon, R.S., Barreiro, B.A., Moorbath, S., Hoefs, J., Francis, P.W., Thorpe R.S., Déruelle, B., McHugh, J., Viglino, J.A. , 1984, Regional O-, Sr- and Pb relationships in Late Cenozoic calc-alkaline lavas of the Andean Cordillera: *J. Geol. Soc. London*, v. 141, p. 803-822.
- Haschke, M., Günther, A., 2003, Balancing crustal thickening in arcs by tectonic vs. magmatic means: *Geology*, v. 31, p. 933-936.
- Haschke, M.R., Siebel, W., Günther, A., and Scheuber, E., 2002, Repeated crustal thickening and recycling during the Andean orogeny in north Chile (21°-26°S): *Journal of Geophysical Research*, v. 107.
- Heinrichs, H., Herrmann, A.G., 1990, *Praktikum der Analytischen Geochemie*: Springer, Berlin.
- Heumann, A., 1993, *Geochemistry and Petrology of Upper Cretaceous and Tertiary Granitoids in northern Chile 18°-22°S*, MS Thesis (Unpublished), Universität Mainz.

Hildreth, W., Moorbath, S., 1988, Crustal contributions to arc magmatism in the Andes of central Chile: Contributions to Mineralogy and Petrology, v. 98, p. 455-489.

Hindle, D., Kley, J., Oncken, O., Sobolev, S., 2005, Crustal balance and crustal flux from shortening estimates in the central Andes: Earth Planet. Sci. Lett., v. 230, p. 113-124.

Horn, S., 1992, Intra- und intervulkanische Variationen entlang der Zentralen Vulkanzone in Nordchile 17-22°S. Petrographische und geochemische Untersuchungen: MS Thesis (Unpublished), Universität Mainz, p. 145.

Husson, L., Sempere, T., 2003, Thickening the Altiplano crust by gravity-driven crustal channel flow: Geophys. Res. Lett., v. 30 (5), 1243, doi: 10.1029/2002GL016877.

Isacks, B.L., 1988, Uplift of the Central Andean plateau and bending of the Bolivian Orocline: J. Geophys. Res., v. 93, p. 3211-3231.

James, D.E., 1982, A combined O, Sr, Nd and Pb isotopic and trace element study of crustal contamination in central Andean lavas, I. Local geochemical variations: Earth Planet. Sci. Lett., v. 57, p. 47-62.

James, D.E., Sacks, I. S., 1999, Cenozoic formation of the central Andes: a geophysical perspective in Geology and Ore Deposits of the Central Andes: (Special Publication no. 7), B. J. Skinner, ed., Littleton, Society of Economic Geologists, p. 1-25.

Jordan, T.E., Isacks, B.L., Allmendinger, R.W., Brewer, J.A., Ramos, V.A., Ando, C.J. , 1983, Andean tectonic related to the geometry of the subducted Nazca Plate: Geol. Soc. Am. Bull., v. 94, p. 341-361.

Jordan, T.H., 1988, Structure and formation of the continental tectosphere: J. Petrology, special lithosphere issue, Menzies, M.A. (Ed.), p. 11-37.

Kamenov, G., Macfarlane, A.W., Riciputi, L.R., 2002, Sources of lead in the San Cristobal, Pulacayo, and Potosi mining districts, Bolivia, and a reevaluation of regional ore lead isotope provinces: Economic Geology, v. 97, p. 573-592.

Kaneoka, I., Guevara, C., 1984, K-Ar age determinations of late Tertiary and Quaternary Andean volcanic rocks, southern Peru: Geochemical Journal, v. 18, p. 233-239.

Kay, R.W., 1977, Geochemical constraints on the origin of Aleutian magmas: In Talwani, M. Pittman III W.C. (eds) Island Arcs, Back-arc Basins, and Deep-sea Trenches. Amer Geophys Union, Maurice Ewing Series v. 1, p. 229-242.

Kay, S.M., Coira, B., Viramonte, J., 1994, Young mafic back arc volcanic rocks as indicators of continental lithospheric delamination beneath the Argentine Puna Plateau, Central Andes: American Geophysical Union, v. 99, p. 24,323-24,339.

Kay, S.M., Mpodozis, C., Coira, B., 1999, Neogene magmatism, tectonism, and mineral deposits of the Central Andes (22°S to 33°S): in Skinner, B. et al., eds, Geology and Mineral Deposits of Central Andes, Society of Economic Geology Special Publication, v. 2, p. 1-35.

Kay, S.M., Mpodozis, C., Coira B., 1999, Neogene magmatism, tectonism and mineral deposit of the Central Andes (22° to 33°S Latitude): In Skinner B.J. (ed) Geology and Ore Deposit of the Central Andes. Soc. Econ. Geol. Spec. Pub. 7, p. 27-59.

- Kay, S.M., 2002, Andean Adakite from slab melting, crustal thickening, and forearc subduction erosion: in V International Symposium on Andean Geodynamics, September, Toulouse, France, p. 405-408.
- Kay, S.M., Godoy, E., Kurtz, A., 2005, Episodic arc migration, crustal thickening, subduction erosion, and magmatism in the south-central Andes: *Geol. Society of America*, v. 117, p. 67-88.
- Kay, S.M., Mpodozis, C., Ramos, V.A., and Munizaga, F., 1991, Magma source variations for mid-late Tertiary magmatic rocks associated with a shallowing subduction zone and a thickening crust in the central Andes (28 to 33°S): in Harmon, R.S., and Rapela, C.W., eds., *Andean magmatism and its tectonic setting: Geological Society of America Special Paper*, v. 265, p. 113-137.
- Kennan, L., Lamb, S., Rundle, C., 1995, K-Ar dates from the Altiplano and Cordillera Oriental of Bolivia: Implications for Cenozoic stratigraphy and tectonic: *Journal of South American Earth Sciences*, v. 8, p. 163-186.
- Kistler, R.W., 1990, Two different lithosphere types in the Sierra Nevada: *Geologic Society of America Memoir*, v. 174, p. 271-281.
- Kley, J., Monaldi, C.R., 1998, Tectonic shortening and crustal thickness in the Central Andes: How good is the correlation?: *Geology*, v. 26, p. 723 - 726.
- Klinck, B.A., Ellison, R.A., Hawkins, M.P., 1986, The geology of the Cordillera Occidental and Altiplano, West of the Lake Titicaca, southern Peru. Instituto de Geología Minería y Metalurgia, Preliminary report: Lima, p. 353.
- Kohlbach, I., 1999, Spatial and temporal variations in magma geochemistry along a W-E traverse at 18°-19°S, North Chile, MS Thesis (Unpublished), Universität Göttingen.
- Kontak, D.J., Cumming, G.L., Krstic, D., Clark, A.H., Farrar, E., 1990, Isotopic composition of lead in ore deposits of the Cordillera Oriental, southeastern Peru: *Economic Geology*, v. 85, p. 1584-1603.
- Kyser, T., 1986, Stable isotopic variations in the mantle: In Valley, J.W., Taylor, H.P.Jr., O'Neil, J.R. (eds.) *Stable isotopes in high temperature geological processes*. *Rev. Mineral.*, v. 167, p. 41-164.
- Lamb, S., Hoke, L., Kennan, L., Dewey, J., 1997, Cenozoic evolution of the Central Andes in the Bolivia and Northern Chile. In: Burg, J.p., Ford, M. (Eds), *Orogeny through time*. *Geol. Soc. Spec. Publ.*, v. 121, p. 3237-264.
- Laubacher, G., Bonhomme, M., Fornari, M., Herail, G., Vivier, G., 1984, Le bassin d' Ananea-Ancocala, témoin de l'évolution plio-quaternaire des Andes sud-orientales du Pérou: In *Dixième RAST*, Bordeaux, p. 336.
- Leeman, W.P., 1983, The influence of crustal structure of compositions of subduction- related magmas. *Arc Volcanism: J. Volc. Geotherm. Res.*, v. 18, p. 561-588.
- Lehmann, B., 1978, A Precambrian core sample from the Altiplano/Bolivia: *Geologische Rundschau*, v. 67, p. 270-278.
- Loewy, S.L., Connelly, J.N., Dalziel, I.W.D., 2004, An Orphaned Basement Block: The Arequipa-Antofalla Basement of the Central Andean margin of South America: *Geol. Soc. Am. Bull.*, v. 116, p. 171-187.

- López-Escobar, L., Frey, F., Vergara, M., 1977, Andesites and high-alumina basalts from central-south Chile High Andes: Geochemical evidence bearing on their petrogenesis: *Contrib. Mineral. Petrol.*, v. 63, p. 199-228.
- Lork, A., Bahlburg, H., 1993, Precise U-Pb ages of monazites from the Faja Eruptiva de la Puna Oriental and the Cordillera Oriental, NW Argentina: XII Congreso Geológico Argentino y II Congreso de Exploración de Hidrocarburos Actas, v. IV, p. 1-6.
- Lucassen, F., Fowler, C.M.R., Franz, G., 1996, Formation of magmatic crust at the Andean continental margin during early Mesozoic: a geological and thermal model of the North Chilean Coast Range: *Tectonophysics*, v. 262, p. 263- 279.
- Lucassen, F., Franz, G., 1996b, Magmatic arc metamorphism: petrology and temperature history of metabasic rocks in the Coastal Cordillera of northern Chile/Region Antofagasta: *J. Metamorph. Geol. Rundsch*, v. 14, p. 249-265.
- Lucassen, F., Thirwall, M.F., 1998, Sm-Nd formation ages and mineral ages in metabasites from the Coastal Cordillera, northern Chile: *Geol. Rundsch*, v. 86, p. 767-774.
- Lucassen, F., Lewerenz, S., Franz, G., Viramonte, J., Mezger, K., 1999b, Metamorphism, isotopic ages and composition of lower crustal granulite xenoliths from the Cretaceous Salta Rift, Argentina: *Contributions to Mineralogy and Petrology*, v. 134, p. 325- 341.
- Lucassen, F., Becchio, R., Harmon, R., Kasemann, S., Franz, G., Trumbull, R., Wilke, H., Romer, R., Dulski, P., 2001, Composition and density model of the continental crust at an active continental margin-the Central Andes between 21°S and 27°S: *Tectonophysics*, v. 341, p. 195-223.
- Lucassen, F., Escayola, M., Romer, R.L., Viramonte, J., Koch, K., Franz G., 2002, Isotopic composition of the Late Mesozoic basic and ultrabasic rocks from the Andes (23-32°S) - Implications for the Andean mantle: *Mineral Petrologie*, v. 143, p. 336 - 349.
- Macfarlane, A.W., Marcet, P., LeHuray, A.P., Petersen, U., 1990, Lead isotope provinces of the central Andes inferred from ores and crustal rocks: *Economic Geology*, v. 85, p. 1857-1880.
- Mamani, M., Ibarra, I., Carlier, G., & Fornary, M., 2004, Petrología y geoquímica del magmatismo alcalino de la zona noroeste del Altiplano peruano (departamento de Puno): In: J. Jacay & T. Sempere (eds.), *Nuevas contribuciones del IRD y sus contrapartes al conocimiento geológico del sur del Perú*, Sociedad Geológica del Perú, Publicación Especial n° 5, p. 157-174.
- Marocco, R., Delfaud, J., Lavenu, A., 1985, Ambiente deposicional de una cuenca contanintal intramontaña andina: el Grupo Moquegua (sur de Perú) primeros resultados: *Bol. Soc. Geol. Perú*, v. 75, p. 73-90.
- Marrett, R., Allmendinger, R., Alonso, R., Drake, R., 1994, Late Cenozoic tectonic evolution of the Puna Plateau and adjacent foreland, northwestern Argentine Andes: *Journal of South America Earth Sciences*, v. 7, p. 179-207.
- McDonough, W.F., Sun, S.-s., Ringwood, A.E., Jagoutz, E., Hofmann, A.W., 1992, Potassium, rubidium and cesium in the Earth and Moon and the evolution of the mantle of the Earth: *Geochim. Cosmochim Acta*, v. 56, p. 1001-1012.
- McDonough, W.F., Sun, S.-S., 1995, The composition of the Earth: *Chem. Geol.*, v. 120, p. 223-253.
- McQuarrie, N., DeCelles, P., 2001, Geometry and structural evolution of the central Andean back thrust belt, Bolivia: *Tectonics*, v. 20, p. 669-692.

- McQuarrie, N., 2002, Initial plate geometry, shortening variations, and evolution of the Bolivian orocline: *Geology*, v. 30, p. 867-870.
- Miller, D.M., Goldstein, S.L., Langmuir, C.H., 1994, Cerium/lead and lead isotope ratios in arc magmas and the enrichment of lead in the continents: *Nature*, v. 368, p. 514-520.
- Mlynarczyk, M.S.J., Williams-Jones, A.E., 2005, The role of collisional tectonics in the metallogeny of the Central Andean tin belt: *Earth and Planetary Science Letters*, v. 240, p. 656-667.
- Morris, J.D., Leeman, W.P., Tera, F., 1990, The subducted component in island arc lavas: constraints from Be isotopes and B-Be systematic: *Nature*, v. 344, p. 31-36.
- Mpodozis, C., Hervé, F., Davidson, J., Rivano, S., 1983, Los granitoides de Cerros de Lila, manifestaciones de un episodio intrusivo y termal del Paleozoico inferior en los Andes del Norte de Chile: *Revista Geológica de Chile*, v. 18, p. 3-14.
- Mukasa, S.B., 1986, Common Pb isotopic compositions of the Lima, Arequipa and Toquepala segments in the Coastal Batholith, Peru: implication for magma genesis: *Geochim. Cosmochim. Acta*, v. 50, p. 771-782.
- Mukasa, S.B., Vidal, C.E., Injoke-Espinoza, J., 1990, Pb isotopes bearing on the Metallogenesis of sulfide ore deposits in central and southern Peru: *Economic Geology*, v. 85, p. 1438-1446.
- Müller, J.P., Kley, J., Jacobshagen, V., 2002, Structure and Cenozoic kinematics of the Eastern Cordillera, southern Bolivia (21°S): *Tectonics*, v. 21 (5)1037, doi:10.1029/2001TC001340.
- Myers, S., Beck, S., Zandt, G., Wallace, T., 1998, Lithospheric-scale structure across the Bolivian Andes from tomographic images of velocity and attenuation for P and S waves: *J. Geophys. Res.*, v. 103, p. 21233- 21252.
- Norambuena, E., Leffer-Griffin, L., Mao, A.; Dixon, T., Stein, S., Sacks, S.; Ocola, L., Ellis, M., 1998, Space geodetic observations of Nazca-South America convergence across the Central Andes: *Science* v. 279, p. 358-362.
- O'Hara, M.J., Mathews, R.E., 1981, Geochemical evolution in an advancing, periodically replenished, periodically tapped, continuously fractionating magma chamber: *Journal of Geological Society of London*, v. 138, p. 237-277.
- Oversby, V.M., 1978, Lead isotopes in Archean plutonic rocks: *Earth and Planetary Science Letters*, v. 38, p. 237-248.
- Pacci, D., Hervé, F., Munizaga, F., Kawashita, K., Cordani, U., 1980, Acerca de la edad Rb-Sr Precambrica de rocas de la Formación Esquistos de Belén, Departamento de Parinacota, Chile: *Revista Geológica de Chile*, v. 11, p. 43-50.
- Pardo-Casas, F., Molnar, P., 1987, Relative motion of the Nazca (Farallon) and South American plates since Late Cretaceous time: *Tectonics*, v. 6/3, p. 233-248.
- Pearce, J.A., 1983, Role of the sub-continental lithosphere in magma genesis at active continental margins: In C. Hawkesworth, Norry, MJ (Editor), *Continental basalts and xenoliths*. Shiva, Nantwich, p. 230-272.

- Petford, N., Atherton, M.P., Halliday, A.N., 1996, Rapid magma production rates, underplating and remelting in the Andes: isotopic evidence from northern-central Peru (9-11°S): *Journal of South American Earth Sciences*, v. 9, p. 69-78.
- Pichowiak, S., Buchelt, M., Damm, K.W., 1990, Magmatic activity and tectonic setting of early stages of the Andean cycle in northern Chile: *Geol. Soc. Am. Spec. Pap.*, v. 241, p. 127-144.
- Pichowiak, S., 1994, Early Cretaceous magmatism in the Coastal Cordillera and the central depression of North Chile: In Scheuber, E., Wigger, P.J. (eds) *Tectonic of the Southern Central Andes; structure and evolution of an active continental margin*. Springer Verlag, Berlin, p. 203-217.
- Pilger, R.H.J., 1984, Cenozoic plate kinematic, subduction and magmatism: South American Andes: *Journal of the Geol. Soc. London*, v. 141, p. 793-802.
- Plank, T., Langmuir, C.H., 1988, An evolution of the global variation in the major element chemistry of arc basalt: *Earth Planet. Sci. Lett.*, v. 90, p. 349-370.
- Potts, P.J., 1987, Inductively coupled plasma-mass spectrometry. In: *A Handbook of Silicate Rock Analysis*: Blackie, Glasgow, p. 575-586.
- Prinz, P., Wilke, H.G., Hillebrandt, A.V., 1994, Sediment accumulation and subsidence history in the Mesozoic marginal basin of northern Chile: In: K.J. Reutter, E. Scheuber and P.J. Wigger (Editors), *Tectonics of the Southern Central Andes*. Springer, Heidelberg, p. 219-232.
- Puig, A., 1988, Geological and metallogenic significance of the isotopic composition of lead in galenas of the Chilean Andes: *Economic Geology*, v. 83, p. 843-858.
- Ramos, V.A., Jordan, T.E., Allmendinger, R.W., Mpodozis, C., Kay, S.M., Cortes, J.E. and Palma, M., 1986, Paleozoic terranes of the Central Argentine-Chilean Andes: *Tectonics*, v. 5, p. 855-880.
- Ramos, V.A., 1988, Late Proterozoic-Early Paleozoic of South America - a collisional history: *Episodes*, v. 11, p. 168-174.
- Ramos, V.A., Kay, S.M., 1992, The Southern Patagonian plateau basalts: retroarc testimony of a ridge collision, Argentina: in Oliver, R.A., Vatin-Perignon, N. and Laubacher, G., eds, *Andean Geodynamics Symposium, Grenoble, Tectonophysics*, v. 205, p. 261-282.
- Ramos, V.A., 1999, Plate Tectonic Setting of the Andean Cordillera: *Episodes*, v. 22, p. 183-190.
- Ramos, V.A., Aleman, A., 2000, Tectonic evolution of the Andes. In: Cordani, U.G., et al. (Eds), *Tectonic Evolution of South America*. 31st Int. Geol. Cong., Rio de Janeiro, p. 635-685.
- Richards, J.P., Boyce, A.J., Pringle, M.S., 2001, Geologic evolution of the Escondida area, northern Chile: A model for spatial and temporal localization of porphyry Cu mineralization: *Economic Geology*, v. 96, p. 271-305.
- Rickwood, P., 1989, Boundary lines within petrologic diagrams which use oxides of major and minor elements: *Lithos*, v. 22, p. 247-263.
- Rodriguez, B.D., 1998, Regional crustal structure beneath the Carlin trend, Nevada based on deep electrical geophysical measurements, U.S. Geological Survey Open-File p. 15-19.
- Rogers, G., Hawkesworth, C.J., 1989, A Geochemical Traverse across the north Chilean Andes: Evidence for Crustal Generation from the Mantle Wedge: *Earth and Planetary Science Letters*, v. 91, p. 271-285.

- Roperch, P., Sempere, T., Macedo, O., Arriagada, C., Fornari, F., Tapia, C., García, M., Laj, C., 2006, Counterclockwise rotation of late Eocene-Oligocene fore-arc deposits in southern Peru and its significance for oroclinal bending in the central Andes: *Tectonics*, v. 25, TC3010, doi:10.1029/2005TC001882, 2006.
- Rousse, S., Gilder, S., Fornari, M., Sempere, T., 2005, Insight into the Neogene tectonic history of the northern Bolivian Orocline from new paleomagnetic and geochronologic data: *Tectonics*, v. 24, TC6007, doi:10.1029/2004TC001760, 2005.
- Salfety, J.A., Marquillas, R.A., 1981, Las unidades estratigráficas cretácicas del Norte de la República Argentina. In: Volkheimer, W., Musacchio, E. (Eds.): *Cuencas sedimentarias del Jurásico y Cretácico de America del Sur*, Comité Sudamericano del Jurásico y Cretácico, v. 1, p. 303-317.
- Scheuber, E., Bogdanic, T., Jensen, A., Reutter, K.J., 1994, Tectonic development of the north Chilean Andes in relation to plate convergence and magmatism since the Jurassic, in *Tectonics of the Southern Central Andes*: edited by K.-J. Reutter, E. Scheuber, and P. Wigger, pp. 121- 139, Springer-Verlag, New York.
- Schmitz, M., 1994, A balanced model of the southern central Andes: *Tectonic*, v. 13, p. 484-492.
- Schreiber, U., Schwab, K., 1991, Geochemistry of Quaternary shoshonitic lavas related to the Calama-Olacapato-El Toro lineament (NW Argentina): *J. South Am. Earth Sci.*, v. 4, p. 73-86.
- Schröder, W., Wörner, G., 1996, Widespread Cenozoic ignimbrites in N-Chile, W-Bolivia and S-Peru 17°-20°S/71°-68°W. Stratigraphy extension, correlation and origin: 3rd ISAG, St. Malo, Andean Geodynamics, ORSTOM Editions, Collection Colloques et Séminaires, p. 645-648.
- Schweller, W.J., Kulm, L.D., Price, R.A., 1981, Tectonics, structure and sedimentary framework of the Peru-Chile trench: in Kulm, L.D., Dymond, J., Desch, E.J., and Hussong, D.M., eds., *Nazca Plate. Crustal formation and Andean convergence*. Geological Society of America Memoir, v. 154, p. 323-351.
- Slater, J.G., Jaupart, C., Galson, D., 1980, The heat flow through oceanic and continental crust and the heat loss of the Earth: *Reviews of Geophysics and Space Physics*, v. 18, p. 269-311.
- Sébrier, M., Lavenu, A., Fornari, M., Soulas, J.P., 1988, Tectonic and uplift in Central Andes (Peru, Bolivia and northern Chile) from Eocene to present: *Géodynamique*, v. 3, p. 85-106.
- Sébrier, M., Soler, P., 1991, Tectonics and magmatism in the Peruvian Andes from Late Oligocene time to the present: in Harmon, R.S. and Rapela, C.W., eds, *Andean magmatism and its tectonic setting*, Geological Society of America Special Paper, v. 265, p. 259-276.
- Sempere, T., 1990, Cuadros Estratigráficos de Bolivia: propuestas nuevas: *Revista Técnica de Yacimientos Petrolíferos Fiscales Bolivianos*, v. 11, p. 215-227.
- Sempere, T., Marshall, L., Rivano, S., Godoy, E., 1994, Late Oligocene-Early Miocene compressional tectonosedimentary episode and associated Lan-Mammal Faunas in the Andes of Central Chile and adjacent Argentina (32-37°S): *Tectonophysics*, v. 229, p. 251-264.
- Sempere, T., Fornari, M., Acosta, J., Flores, A., Jacay, J., Peña, D., Roperch, P., Taipei, E., 2004, Estratigrafía, geocronología, paleogeografía y paleotectónica de los depósitos de antearco del sur del Perú: XII Congreso Peruano de Geología. Resúmenes Extendidos. Sociedad Geológica del Perú.
- Seyfried, H., Wörner, G., Uhlig, D., Kohler, I., 1995, Eine kleine Landschaftsgeschichte der Anden in Nordchile: *Wechselwirkungen*, Jahrbuch 1994 der Universität Stuttgart, p. 60-71.



Shackleton, R.M., Ries, A.C., Coward, M.P., and Cobbold, P.R., 1979, Structure, metamorphism and geochronology of the Arequipa Massif of coastal Peru: *Journal of the Geological Society, London*, v. 136, p. 195-214.

Siebel, W., Schnurr, W.B.W., Hahne, K., Kraemer, B., Trumbull, R.B., van den Bogaard, P., Emmermann, R., 2001, Geochemistry and isotope systematics of small- to medium-volume Neogene – Quaternary ignimbrites in the southern central Andes: evidence for derivation from andesitic magma sources: *Chemical Geology*, v. 171, p. 213– 237.

Sobolev, S., Babeyko, A., 1994, Modelling of mineralogical composition, density and elastic wave velocities in the unhydrous rocks: *Surveys in Geophysics*, v. 15, p. 515-544.

Soler, P., Bohomme, M., 1990, Relations of magmatic activity to plate dynamics in the Central Peru from Late Cretaceous to present: In *Plutonism from Antarctica to Alaska*, Kay and Rapela eds. Geological Society of America Special Paper, v. 241, p. 173-192.

Soler, P., Carlier, G., Fornari, M., Herail, G., 1992, An Alternative model for the origin and tectonic significance of the Neogene and Quaternary shoshonitic volcanism of the Andes (abstract): *Eos Trans. AGU 73 14 Spring Meeting Suppl.* , p. 341-342.

Somoza, R., 1998, Updated Nazca (Farallon)-South America relative motions during the last 40 My: implications for the mountain building in the central Andean region: *Journal of South American Earth Sciences*, v. 11, p. 211-215.

Spera, F.J., Bohron, W.A., 2001, Energy-constrained open-system magmatic processes; I, General model and energy-constrained assimilation and fractional crystallization (EC-AFC) formulation: *Journal of Petrology*, v. 42, p. 999-1018.

Stacey, J.S., and Kramers, J.D., 1975, Approximation of terrestrial lead isotope evolution by a two stages model: *Earth Planetary Science Letters*, v. 26, p. 207-221.

Stern, C., Killian. R., 1996, Role of the subducted slab, mantle wedge and continental crust in the generation of adakites from the Andean Austral Volcanic Zone: *Contributions to Mineralogy and Petrology*, v. 123, p. 263-281.

Stern, C., 2004, Active Andean volcanism: its geologic and tectonic setting: *Rev. geol. Chile*, v. 31, p. 161-206.

Stern, C.R., 1989, Pliocene to present migration of the volcanic front, Andean southern volcanic zone: *Revista Geológica de Chile*, v. 16, p. 145-162.

—, 1990, Comment on "A geochemical traverse across the North Chilean Andes: evidence for crust generation from the mantle wedge" by G. Rogers and C.J. Hawkesworth: *Earth Planet. Sci. Lett.*, v. 101, p. 129-133.

—, 1991, Role of subduction erosion in the generation of Andean Magmas: *Geology*, v. 19, p. 78-81.

Suarez, M.a.B., C.M., 1992, Triassic rift-related sedimentary basins in northern Chile (24°-29°S): *J. S. Am. Earth Sci.*, v. 6, p. 109-121.

Sweeney, J.F., 1982, Structure and development of the polar margin of North America , In *Scrutum*, R.A., ed., *Dynamics of passive margins: American Geophysical Union and Geological Association of America Geodynamics Series*, v. 6, p. 17-29.

- Swenson, J., Beck, S., Zandt, G., 2000, Crustal structure of the Altiplano from broadband regional waveform modeling: implications for the composition of thick continental crust: *Journal of Geophysical Research*, v. 105, p. 607-621.
- Tassara, A., 2006, Factors controlling the crustal density structure underneath active continental margins with implications for their evolution: *Geochemistry, Geophysics, Geosystems*, v. 7(1): doi: 10.1029/2005GC001040. issn: 1525-2027.
- Tassara, A., Götze, H.J., Schmidt, S., Hackney, R., 2006, Three-dimensional density model of the Nazca plate and the Andean continental margin: In press (August 23, 2006) by *Journal of Geophysical Research*.
- Taylor, S., Maclennan, S., 1985, *The continental crust; its composition and evolution*, Blackwell Scientific Publications, Oxford, England, 312 p.
- Tebbens, S.F., Cande, S.C., 1997, Southeast Pacific tectonic evolution from early Oligocene to present: *J. Geophys. Res.*, v. 102, p. 12061-12084.
- Thorpe, R., Francis, P., 1979, Variations in Andean andesite compositions and their petrogenetic significance: *Tectonophysics*, v. 57, p. 57-70.
- Thorpe, R., Francis, P., Harmon, R., 1981, Andean andesites and crustal growth: *Philos. Trans. Soc. London*, v. 301(A), p. 305-320.
- Thouret, J., Rivera, M., Wörner, G., Gerbe, MC., Finizola, A., Fornari, M., Gonzales, K., 2005, Ubinas: The evolution of the historically most active volcano in Southern Peru: *Bull. Volcanol.*, v. 67, p. 557-589.
- Tilton, G.R., Barreiro, B.A., 1980, Origen of lead in Andean calc-alkaline lavas, southern Peru: *Science*, v. 210, p. 1245-1247.
- Tosdal, R.M., Farrar, E., Clark, A.H., 1981, K-Ar geochronology of the late Cenozoic volcanic rocks of the Cordillera Occidental, southernmost Peru: *Journal of Volcanology and Geothermal Research*, v. 10, p. 157-173.
- Tosdal, R.M., and 15 others., 1993, Summary of Pb isotope compositions in epithermal precious-metal deposits, Orcopampa area of southern Peru, Berenguela area of western Bolivia, and Maricunga belt in north-central Chile, in *investigaciones de metales preciosos en el complejo volcanico Neogenico-Cuaternario de los Andes Centrales: La paz*, Servicio Geológico de Bolivia, Servicio Nacional de Geología y Minería, Chile, Instituto Geológico Minero y Metalurgico, Perú, and U.S. Geological Survey, p. 47-55.
- Tosdal, R.M., Gibson, P.C., Noble, D.C., 1995, Metal sources for Miocene precious-metal veins of the Orcopampa, Shila, Cailloma and Arcata mining districts, southern Peru: *Sociedad Geológica del Perú, Volumen jubilar Alberto Benavides*. Lima, p. 311-326.
- Tosdal, R.M., 1996, The Amazon-Laurentian connection as viewed from the Middle Proterozoic rocks in the central Andes, western Bolivia and northern Chile: *Tectonics*, v. 15, p. 827-842.
- Tosdal, R.M., Wooden, J.L., Bouse, R.M., 1999, Pb isotopes, Ore deposits, and Metallogenic Terranes: In *Application of radiogenic isotopes of ore deposits research and exploration*. Lambert, D.D., Ruiz, J. (eds). *Reviews in Economic Geology*, v. 12, p. 1-28.
- Trumbull, R.B., Wittenbrink, R., Hahne, K., Emmermann, R., Büsch, W., Gerstenberger, H., Siebel, W., 1999, Evidence for Late Miocene to Recent contamination of arc andesites by crustal melts in the

Chilean Andes (25°–26°S) and its geodynamic implications: *Journal of South American Earth Sciences*, v. 12, p. 135–155.

Viramonte, J.G., Kay, S.M., Becchio, R., Escayola, M., Novitski, I., 1999, Cretaceous rift related magmatism in central-western South America: *J. S. Am. Earth. Sci.*, v. 12, p. 109-121.

Vivallo, W., Henriquez, F., 1998, Génesis común de los yacimientos estratoligados y vetiformes de cobre del Jurásico Medio a Superior en la Cordillera de la Costa, Región de Antofagasta, Chile: *Rev. geol. Chile*, v. 25, p. 199-228.

Wasteneys, H.A., Clark, A.H., Farrar, E., Langridge, R.J., 1995, Grenvillian granulite-facies metamorphism in the Arequipa Massif, Peru: A Laurentia-Gondwana link: *Earth and Planetary Science Letters*, v. 132, p. 63-73.

Watts, A.B., Lamb, S.H., Fairhead, J.D., Dewey, J.F., 1995, Lithospheric flexure and bending of the Central Andes: *Earth Planet. Sci. Lett.*, v. 134, p. 9-21.

Whitman, D., Isacks, B., Kay, S., 1996, Lithospheric structure and along-strike segmentation of the Central Andean Plateau: seismic Q, magmatism, flexure, topography and tectonics: *Tectonophysics*, v. 259, p. 29-40.

Wilson, M., 1989, *Igneous Petrogenesis: A Global Tectonic Approach*, Chapman & Hall, 466 p.

Wooden, J.L., Stacey, J.S., Howard, K.A., Doe, B.R., Miller, D.M., 1988, Lead isotope evidence for the formation of Proterozoic crust in the southwestern United States, in Ernst, W.G., ed.: *Metamorphism and crustal evolution, western conterminous United States*; Rubey, Englewood Cliffs, New Jersey Prentice-Hall, v. 7, p. 68-86.

Wooden, J.L., DeWitt, E., 1991, Pb isotope evidence for the boundary between the Early Proterozoic Mojave and the Central Arizona crustal provinces in western Arizona: *Arizona Geological Society Digest*, v. 19, p. 27-50.

Wooden, J.L., Tosdal, R.M., Kistler, R.W., 1998, Pb-isotope mapping of crustal structure in the northern Great Basin and relationship to Au deposit trends: *U.S. Geological Survey Open-File Report 98-338*, p. 20-33.

Wörner, G., Harmon, R.S., Davison, J.D., Moorbath, S., Turner, T.L., McMillan, N., Nye, C., López-Escobar, L., Moreno, H., 1988, The Nevados de Payachata Volcanic Region 18°S/69°W, N. Chile. I. Geological, geochemical and isotopic observations: *Bulletin of volcanology*, v. 30, p. 287-303.

Wörner, G., Moorbath, S., Harmon, R.S., 1992, Andean cenozoic volcanics reflect basement isotopic domains: *Geology*, v. 20, p. 1103-1106.

Wörner, G., López-Escobar, L., Moorbath, S., Horn, S., Entenmann, J., Harmon, R.S., Davison, J.D., 1992, Variaciones Geoquímicas, locales y regionales, en el arco volcánico Andino del Norte de Chile (17°30'–22°00'S): *revista Geológica de Chile*, v. 19, p. 37-56.

Wörner, G., Moorbath, S., Entenmann, J., Harmon, R.S., Davison, J.D., López-Escobar, L., 1994, Large geochemical variation along the central Arc of northern Chile (17.5–22°S): In Reutter, K.J., Scheuber, E., Wigger, P.J., (editors). *Tectonics of the Southern Central Andes. Structure and evolution of an active continental margin*. Springer, Berlin, p. 77-92.

Wörner, G., Hammerschmidt, K., Hemjes-Kunst, F., Lezaun, J., Wilke, H., 2000, Geochronology (40 Ar-39Ar-, K-Ar-, and He-exposure-) ages of Cenozoic magmatic rocks from Northern Chile (18°–

22°S). Implications for magmatism and tectonic evolution of the central Andes: *Rev. Geol. Chile*, v. 27, p. 205-240.

Wörner, G., Lezaun, J., Beck, A., Heber, V., Lucassen, F., Zinngrebe, E., Rössling, R., and Wilke, H. G., 2000, Precambrian and Early Paleozoic evolution of the Andean basement at Belén (northern Chile) and Cerro Uyarani (western Bolivia Altiplano): *J. S. Am. Earth Sci. Rev.*, v. 13, p. 717-737.

Yañez, G., Cembrano, J., Pardo, M., Ranero, C., Selles, D., 2002, The Challenger-Juan Fernandez-Maipo major tectonic transition of the Nazca-Andean subduction system at 33 - 34°S: Geodynamic evidence and implications: *J. S. Am. Earth Sci.*, v. 15, p. 23-38.

Yuan, X., S. V. Sobolev, R., Kind, O., Oncken, and Andes Seismology Group, 2000, New constraints on subduction and collision processes in the central Andes from comprehensive observations of P to S converted seismic phases: *Nature*, v. 408, p. 958-961.

Yuan, X.S., S. V.; Kind, R., 2002, Moho topography in the central Andes and its geodynamic implication: *Earth and Planetary Science Letters*, v. 199, p. 389-402.

Zandt, G., Beck, S.L., Ruppert, S.R., Ammon, C.J., Rock, D., Minaya, E., Wallace, T.C., Silver, P.G., Anomalous crust of the Bolivian Altiplano, Central Andes; constraints from broadband regional seismic waveforms: *Geophysical Research Letters*, v. 23, p. 1159-1162.

Zartman, R.E., Doe, B.R., 1981, Plumbotectonics - The model: *Tectonophysics*, v. 75, p. 135-162.

Zartman, R.E., Haines, S.M., 1988, The plumbotectonic model for Pb isotope systematics among major terrestrial reservoirs-a case for bi-directional transport: *Geochimica et Cosmochimica acta*, v. 52, p. 1327-1339.

Zbar, B., 1991, Die Genese mafischer Einschluesse in den Andesiten der Zentralen Vulkanzone (Nordchile), Diploma thesis, Universtiät Bochum.

## Lebenslauf

Name Mamani-Huisa  
 Vorname Mirian-Irene  
 Geboren am 03-05-1975  
 in Cuyocuyo, Peru

### Schulbildung

1983-1986 Grundschule Santa Catalina de Siena, Juliaca-Peru.  
 1986-1992 Gymnasium Javier Heraud, Laberinto-Peru

### Universität Ausbildung

1993-1998 Bachelor in Geologie  
 San Antonio Abad del Cusco  
**Fakultät für Geowissenschaften und Geographie.**  
 Cusco, Peru

1998-2000 Diplom in Ing. Geologie  
 San Antonio Abad del Cusco  
**Fakultät für Geowissenschaften und Geographie.**  
 Cusco, Peru

2003 Beginn der Promotion an der Georg-August-Universität Göttingen  
**Fakultät für Geowissenschaften und Geographie.**  
 Göttingen, Deutschland

2006 Abschluss der vorliegenden Dissertation